Durham E-Theses

Active Management of Distributed Generation based on Component Thermal Properties

SAMUEL CHARLES EDWARD JUPE

How to cite:

JUPE, SAMUEL CHARLES EDWARD (2010) *Active Management of Distributed Generation based on Component Thermal Properties.* Doctoral thesis, Durham University.

Use policy

Active Management of Distributed Generation based on Component Thermal Properties

Samuel Charles Edward Jupe
M.Eng (Hons) Dunelm

A Thesis presented for the Degree of

Doctor of Philosophy

Durham
University

Energy Group
School of Engineering and Computing Sciences
Durham University
UK

January 2010

For my family—

past, present *and future*

I like work; it fascinates me.

I can sit and look at it for hours.

—Jerome K. Jerome

Active Management of Distributed Generation based on Component Thermal Properties

Samuel C. E. Jupe M.Eng (Hons) Dunelm

Submitted for the Degree of Doctor of Philosophy

January 2010

Abstract

Power flows within distribution networks are expected to become increasingly congested with the proliferation of distributed generation (DG) from renewable energy resources. Consequently, the size, energy penetration and ultimately the revenue stream of DG schemes may be limited in the future. This research seeks to facilitate increased renewable energy penetrations by utilising power system component thermal properties together with DG power output control techniques. The real-time thermal rating of existing power system components has the potential to unlock latent power transfer capacities. When integrated with a DG power output control system, greater installed capacities of DG may be accommodated within the distribution network. Moreover, the secure operation of the network is maintained through the constraint of DG power outputs to manage network power flows. The research presented in this thesis forms part of a UK government funded project which aims to develop and deploy an on-line power output control system for wind-based DG schemes. This is based on the concept that high power flows resulting from wind generation at high wind speeds could be accommodated since the same wind speed has a positive effect on component cooling mechanisms. The control system compares component real-time thermal ratings with network power flows and produces set points that are fed back to the DG for implementation. The control algorithm comprises: (i) An inference engine (using rule-based artificial intelligence) that decides when DG control actions are required; (ii) a DG set point calculator (utilising predetermined power flow sensitivity factors) that computes updated DG power outputs to manage distribution network power flows; and (iii) an on-line simulation tool that validates the control actions before dispatch. A section of the UK power system has been selected by ScottishPower EnergyNetworks to form the basis of field trials. Electrical and thermal datasets from the field are used in open loop to validate the algorithms developed. The loop is then closed through simulation to automate DG output control for increased renewable energy penetrations.

Declaration

The work in this thesis is based on research carried out within the Energy Group, School of Engineering and Computing Sciences, Durham University, United Kingdom. No part of this thesis has been submitted elsewhere for any other degree or qualification and it is all my own work unless referenced to the contrary in the text.

Reference is made to work that is confidential and commercially restricted.

Acknowledgements

I'd like to extend my sincere gratitude to those that have helped and inspired me on this research journey:

- Chang An, Graeme Lloyd, Gordon Millar and Tony Yip at AREVA T&D;

- Adam Berry, Dave Curry and Angela Morgan at Imass;

- Marc Bartlett, Ian Burdon and Bruce Stedall at PB Power; and

- Chris Berry, Mark Chamberlain, Jamie McWilliam and Dave Roberts at Scottish-Power EnergyNetworks.

- All my colleagues within the Energy Group;

- The undergraduate students: Daniel Abbott, Paul Edwards and Peter Davison;

- Padraig Lyons and Pavlos Trichakis— for passing on their experience;

- Andrea 'Dottore' Michiorri— an entertaining and dear companion on the research journey; and

- My supervisors: Professor Philip Taylor and Dr Neal Wade— for their guidance and encouragement.

- Dr Hendrik Nahler— for helping with the LaTeX quirks.

- Claire, my Mum and Dad, Hannah and Matt, and Charles and Judy— for their continuous love and support.

- Finally, Alfie the Cat— *for introducing any unspotted typos.*

Nomenclature

On occasions, context-specific symbols are used in the thesis. These symbols are not included in the nomenclature below but are explained in context.

Symbol	Definition	Unit
A	Conductor cross-sectional area	(m^2)
a	Initial condition of analysis	(no unit)
$C_{E(ROC)}$	Renewables obligation certificate sale price	(£/Wh)
$C_{E(wholesale)}$	Wholesale electricity price	(£/Wh)
C_{G_i}	Distributed generation installation cost	(£/W)
$C_{R(annual)}$	Annual net revenue of distributed generation developer	(£)
$C_{R(control)}$	Cost of distributed generation output control system	(£)
$C_{R(EY)}$	Annual income from active energy yield sales	(£)
$C_{R(inv)}$	Total investment cost for each developer	(£)
$C_{R(loss)}$	Annual cost of losses	(£)
$C_{R(OM)}$	Cost of annual operations and maintenance	(£)
$C_{R(real-time)}$	Cost of real-time thermal rating system	(£)
$C_{R(1,2,3)}$	Variable costs for financial analyses	(£)
$C_{Th(s)}$	Soil thermal capacitance	(J/kgK)
c	Component	(no unit)
D	External diameter of conductor	(m)
E_a	Annual energy yield	(Wh)
E_{loss}	Energy yield loss	(Wh)

Continued on next page

Symbol	Definition	Unit
$P_{i,k}$	Real power flow from node i to node k	(W)
P_{loss}	Real power loss	(W)
$P_{loss,i,k,m}$	Real power loss from node i to node k and apportioned to generator at node m	(W)
$P_{loss,i,k,total}$	Total real power loss from node i to node k	(W)
$PFSF$	Power flow sensitivity factor	(no unit)
PI	Profitability index	(no unit)
PV	Present value	(£)
Q	Reactive power	(VAr)
$'Q_{i,k}$	Initial reactive power flow from node i to node k before control actions take place	(VAr)
$''Q_{i,k}$	Final reactive power flow from node i to node k after control actions have taken place	(VAr)
Q_i	Reactive power demand at node i	(VAr)
q_{conv}	Heat loss by convection	(W/m)
q_{rad}	Heat loss by radiation	(W/m)
q_{sol}	Heat gain by solar radiation	(W/m)
R	Electrical resistance	(Ω)
R_{ac}	Electrical resistance to alternating current at maximum operating temperature	(Ω)
R_{Th}	Thermal resistance	(mK/W)
S	Apparent power	(VA)
S_{base}	Apparent power flow reference base	(VA)
$S_{i,k}^c$	Apparent power flow in component c from node i to k	(VA)
$'S_{i,k}$	Initial apparent power flow in component from node i to k before control actions take place	(VA)
S_{lim}	Thermal limit	(VA)
$S_{i,k(lim)}^c$	Thermal limit of power transfer in component c from node i to k	(VA)
$SSF_{i,k,m}^c$	Apparent power flow sensitivity factor of component c	(no unit)

Symbol	Definition	Unit
	between node i and k to a real power injection at node m	
T_a	Ambient temperature	(K)
T_c	Conductor temperature	(K)
T_s	Soil temperature	(K)
$T_{s(rated)}$	Rated soil temperature	(K)
$TVF^c_{i,k,m}$	Thermal vulnerability factor of component c	(no unit)
	between node i and k to a real power injection at node m	
t	Time	(s)
U	Component utilisation	(no unit)
$U^c_{i,k}$	Utilisation of component c between nodes i and k	(no unit)
U_{Tar}	Utilisation target for power flow control	(no unit)
V	Voltage	(V)
V_{L-L}	Line-to-line voltage	(V)
V_{ph}	Phase voltage	(V)
W	Solar radiation	(W/m^2)
X	Reactance	(Ω)
x	Integer	(no unit)
y	Integer	(no unit)
Φ	Egalitarian broadcast signal	(%)
α	Absorption coefficient	(no unit)
ϵ	Emission coefficient	(no unit)
θ_i	Voltage angle at node i	(rad)
θ_k	Voltage angle at node k	(rad)
λ	Air thermal conductivity	(W/mK)
ξ_T	Electric cable rating correction factor	(1/K)
ξ_ρ	Electric cable thermal resistivity correction factor	(W/mK)
$\rho_{Th(s)}$	Soil thermal resistivity	(mK/W)
$\rho_{Th(s,rated)}$	Rated soil thermal resistivity	(mK/W)
σ_{SB}	Stefan-Boltzmann constant	(W/m^{2}K^4)

Acronyms

Acronym	Definition
AAAC	All aluminium alloy conductor
AC	Alternating current
ACSR	Aluminium conductor steel reinforced
ADN	Active distribution network
AGC	Automatic generation control
ANM	Active network management
B	Busbar (identifier)
C	Component (identifier)
CHP	Combined heat and power
CI	Customer interruption
CIGRÉ	Conseil International des Grands Réseaux Électriques
	International Council on Large Electric Systems
CML	Customer minute lost
CSP	Constraint satisfaction problem
DC	Direct current
DER	Distributed energy resource
DG	Distributed generation
DIUS	Department for Innovation, Universities and Skills
DNO	Distribution network operator
DSO	Distribution system operator
EHV	Extra high voltage
ENA	Energy Networks Association

Continued on next page

Acronym	Definition
ESQCR	Electricity safety, quality and continuity regulations
ETR	Engineering technical recommendation
FACTS	Flexible AC transmission systems
GSF	Generation shift factor
GSP	Grid supply point
GUI	Graphical user interface
IEC	International Electrotechnical Commission
IEEE	Institute of Electrical and Electronics Engineers
L	Load (identifier)
LIFO	Last-in first-off
LTDS	Long term development statement
NPV	Net present value
OfGEM	Office of the Gas and Electricity Markets
OPF	Optimal power flow
pu	per unit
PC	Personal computer
PFSF	Power flow sensitivity factor
PI	Profitability index
PV	Present value
ROC	Renewables Obligation Certificate
RE	Renewable energy
RTTR	Real-time thermal rating
SCADA	Supervisory control and data acquisition
SOA	Service oriented architecture
T	Transformer (identifier)
TMA	Technically most appropriate
TVF	Thermal vulnerability factor
UKGDS	United Kingdom generic distribution system
WAsP	Wind Atlas Analysis and Application Program

Author's publication list

Journal papers

1. C. D'Adamo, P. C. Taylor, S. Jupe, B. Buchholz, F. Pilo, C. Abbey and J. Marti, "Active Distribution Networks: General features, present status of implementation and operational practices", *ELECTRA*, vol. 246, pp. 22-29, Oct., 2009;

2. A. Michiorri, P. C. Taylor, S. C. E. Jupe and C. J. Berry, "Investigation into the influence of environmental conditions on power system ratings", *Proc. IMechE Part A: J. Power and Energy*, vol. 277, no. A7, pp. 743-757, Nov., 2009;

3. S. C. E. Jupe and P. C. Taylor, "Distributed generation output control for network power flow management," *IET Renew. Power Gener.*, vol. 3, no. 4, pp. 371-386, Dec., 2009;

4. A. Michiorri, P. C. Taylor and S. C. E. Jupe, "Overhead line real-time rating estimation algorithm: description and validation", *Proc. IMechE Part A: J. Power and Energy*, In Press, 2009; and

5. S. C. E. Jupe, P. C. Taylor and A. Michiorri, "Coordinated output control of multiple distributed generation schemes", *IET Renew. Power Gener.*, (Accepted), 2010;

Book chapters

6. S. C. E. Jupe, A. Michiorri and P. C. Taylor, "Increasing the energy yield of generation from new and renewable resources, in *Renewable Energy*. Vienna, Austria: IN-TECH, 2009, ch. 4, pp. 37-62;

Conference papers

7. A. Neumann, P. C. Taylor, S. C. E. Jupe, A. Michiorri, A. Goode, D. Curry and D. A. Roberts, "Dynamic thermal rating and active control for improved distribution network utilization," in *Proc. PowerGrid*, Milan, Italy, 2008, (Accepted for oral presentation);

8. S. C. E. Jupe, P. C. Taylor, and C. J. Berry, "Assessing the value of active constrained connection managers for distribution networks," in *Proc. CIRED Seminar 2008: SmartGrids for Distribution*, Frankfurt, Germany, 2008, (Accepted for poster presentation);

9. P. C. Taylor, P. Trichakis, S. C. E. Jupe, A. Michiorri and P. Lyons, "Active management of MV and LV distribution networks", in *Proc CIGRÉ NGN*, Paris, France, 2008, (Accepted for poster presentation);

10. S. C. E. Jupe, P. C. Taylor, A. Michiorri, and C. J. Berry, "An evaluation of distributed generation constrained connection managers," in *Proc. 6th Mediterranean Conference on Generation, Transmission and Distribution*, Thessaloniki, Greece, 2008, (Accepted for oral presentation);

11. S. C. E. Jupe and P. C. Taylor, "Strategies for the control of multiple distributed generation schemes," in *Proc. 20th International Conference on Electricity Distribution*, Prague, CZ, 2009, (Accepted for poster presentation);

12. C. D'Adamo, S. C. E. Jupe, and C. Abbey, "Global survey on planning and operation of active distribution networks - update of CIGRÉ C6.11 working group activities," in *Proc. 20th International Conference on Electricity Distribution*, Prague, CZ, 2009, (Accepted for oral presentation);

13. H. T. Yip, C. An, G. Lloyd, P. C. Taylor, A. Michiorri, S. C. E. Jupe and M. Bartlett, "Dynamic thermal rating and active control for improved distribution network utilisation", *10th IET International Conference on Developments in Power System Protection*, Manchester, UK, 2010, (Accepted for oral presentation); and

14. —, "Dynamic thermal rating and active control for improved distribution network utilisation", *Protection, Automation and Control World Conference*, Dublin, Ireland, 2010, (Accepted for oral presentation).

Contents

List of Figures

List of Tables

Chapter 1

Introduction

1.1 Background

Growing concern regarding the carbon intensity of fossil fuel electricity generation prompted the Kyoto Protocol to be created and, in an attempt to reduce carbon emissions, agreements have been signed by countries across the globe. The impetus of governments, on an international scale, to move towards low-carbon economy targets has brought about the proliferation of distributed electricity generation, particularly from new and renewable energy (RE) resources [1,2]. In order for the UK to make the transition towards a low-carbon economy, as set out in the government's Energy White Paper [3] (sourcing 20% of the UK's electricity demand from renewable energy by 2020 and 60% by 2050) participation is required on many levels from policy makers and regulators within the political arena, through electricity generators, power system equipment manufacturers and network operators, right down to industrial, commercial and domestic energy consumers.

At present the UK distribution network tends to be operated as a passive entity with bulk power generation at centralised locations being transmitted at voltage levels of 400kV and 275kV in England and Wales (132kV in Scotland) to feed lower voltage load customers through the distribution network. The power output of significant capacities of distributed generation (DG), installed at sub-transmission network voltage levels (132kV and below) may, at times, exceed local load demands and cause power flows to reverse within the distribution network. This, coupled with increasing consumer energy demands, has caused distribution network operators (DNOs) to seek methods of increasing the utilisation of their existing power system assets. The increased utilisation of assets must be realised cautiously such that the security of supply to customers is not reduced, particularly when the age of distribution network assets is taken into account.

A developer that is seeking to connect DG of significant capacity may be offered a firm connection by the DNO on the condition that an investment is made (by the developer) in the necessary network reinforcements. However, the developer may not be able to justify the expense of the required reinforcement and may negotiate a non-firm or 'constrained' connection agreement, whereby the DG scheme is tripped off or constrained back under certain network operating conditions. Furthermore, difficulties may be encountered when attempting to gain permission to build network infrastructure, in order to accommodate new DG schemes, due to planning problems and environmental objections [4]. One potential solution or means of deferring these problems is the adoption of real-time thermal rating systems which have the potential, in certain circumstances, to be both less invasive and more cost effective when compared to network reinforcement options. Non-firm DG connections are expected to occur more frequently as network power flow congestion occurs. Therefore the deployment of a power output control system, informed by real-time thermal ratings, may be required to increase the energy yield of generation from new and RE resources.

1.2   Active management of DG project

1.2.1   Project overview

The research detailed in this thesis forms part of a UK government-sponsored project which aims to develop and deploy an on-line power output control system for DG installations through the exploitation of power system real-time thermal ratings [5]. The control system compares component real-time thermal ratings with network power flows and produces set points that are fed back to the DG scheme operator for implementation, as shown in Figure 1.1.

Through the Technology Strategies Board, the UK Department for Innovation, Universities and Skills (DIUS) has part-sponsored research into the "Active management of distributed generators based on component thermal properties", Project No: TP/4/EET/6/1/ 22088. Throughout the thesis this is referred to as the "DIUS Project". The DIUS Project research consortium comprises AREVA T&D (the power systems equipment manufacturer), Imass (an information technology consultancy firm), Parsons Brinckerhoff (the international consultancy firm), Durham University (the UK research institution) and ScottishPower EnergyNetworks (the UK DNO).

The consortium provides the complete route to market for the control system (i.e. the design, development, prototyping, testing and eventual commercialisation of the product)

Figure 1.1: DG output control informed by component real-time thermal ratings

with ScottishPower EnergyNetworks acting as the customer, AREVA T&D as the product supplier and Durham University, Imass and PB Power as the product development and management team.

The deliverables of the project were: (i) The development power system component thermal models; (ii) the identification of a site within ScottishPower EnergyNetworks' distribution network that would be suitable for hosting field trials; (iii) the design of the overall architecture of the DG output control system; (iv) the development of thermal state estimation techniques whereby the rating of components, which are not directly monitored within the power system, may be assessed; (v) the development of control algorithms such that thermal state estimations may be used for the output control of DG; (vi) the development of electro-thermal simulations to model the sections of the UK power system; (vii) the integration of thermal state estimation and control algorithms within AREVA's industrial

hardware platform, thus creating a prototype control system; (viii) the commissioning and installation of electrical and thermal monitoring equipment within the field trial network; (ix) the assessment of prototyped DG output control system performance through open-loop field trials; and (x) the closed-loop output control of a DG scheme based on component thermal properties.

The time-bound nature of the DIUS Project meant that negotiations to operate a DG scheme in closed loop were limited. Moreover, the DG scheme present within the field trial network was not of sufficient size (in terms of installed capacity) to cause the violation of thermal constraints within the power system. Therefore the closed-loop operation of the prototype control system was demonstrated in the simulation environment.

The research presented in this thesis pertains to the the following specific phases of the DIUS Project: (i) The architecture design; (ii) the control algorithm development; (iii) the development of electro-thermal simulation tools; (iv) the field trial installation and commissioning; (v) the open loop testing of the algorithms; and (vi) the closed loop testing of the algorithms. The control algorithms and electro-thermal simulation tools were extended beyond the practical limitations of the field trial implementation to develop both control strategies and evaluation techniques for the coordinated output control of multiple DG schemes based on component thermal properties.

1.2.2 Project perceived benefits

The development of a DG output control system based on component thermal properties was perceived to facilitate the widespread and cost-effective connection of DG from RE resources, thus allowing the associated environmental benefits to be captured. From the original funding application, environmental and social impacts of the project expected to be positive and included [6]:

1. The increase in utilisation of power system assets which will delay the need for network reinforcement, also avoiding the unnecessary replacement of assets and requirements for new wayleaves. Thus the environmental impact associated with new construction, disposal and replacement of assets will be reduced;

2. The maintenance and potential improvement in the quality and security of supply to consumers, particularly in remote parts of the network where enhanced automation of the network equipment may assist "islanded" operation;

3. The integration of distributed renewable generators into networks will reduce connection costs which may have a beneficial impact on electricity prices;

4. Increasing the annual energy yield from renewable generators will improve the revenue and therefore cost effectiveness of these schemes. Thus the amount of energy delivered to the UK power system from non-polluting sources will lead to reductions in carbon emissions to the atmosphere;

5. The project will contribute to the transformation of the UK electricity industry into a more sustainable one; and

6. This work will enhance the competitive position of a major UK manufacturer, UK consultancy, IT company and University thus creating and preserving jobs.

1.3 Research scope

The scope of the research presented in this thesis is outlined below:

- Algorithms will be developed for the output control of single DG schemes and the coordinated output control of multiple DG schemes, based on static, seasonal or real-time thermal ratings of the power system components, in order to manage distribution network power flows. The simulation of wind-based DG schemes is of particular interest in the DIUS project;

- the algorithms developed for DG output control will be evaluated in simulation through United Kingdom Generic Distribution Systems and the field trial network, with single DG output control techniques implemented within the prototype control system for evaluated in field trials;

- it is assumed that there will be full SCADA access to provide the electrical inputs to the DG output control system. However, for development purposes, electrical state estimation techniques may be used because full SCADA access is limited in the DIUS Project.

- the DG output control system will be implemented as a stand-alone system and not integrated within the SCADA system of the DNO;

- the DG output control system functions for a system intact topology. Therefore it is assumed that there are no outages [planned or unplanned] present within the electrical power system;

- other methods of relieving thermal overloads such as load shedding, network reconfiguration, adjusting transformer tap positions[1] are deemed beyond the thesis research scope;

- since the primary aim of DG operators is to maximise the active energy yield of DG schemes, as this directly affects the revenue stream of DG owners, it is assumed that DG schemes are operated at, or close to, unity power factor. Therefore DG schemes are controlled through the adjustment of real power outputs;

- the DG output control system functions with constrained (non-firm) DG connections whereby DG schemes may have an installed capacity beyond the firm capacity of the network;

- the DG output control system is reactive and triggered by a thermal violation. Any voltage issues that occur and are not coincident with a thermal violation are assumed to be dealt with outside the jurisdiction of the control system. The development of a proactive DG output control system control system, utilising generation, load and real-time thermal rating forecasts, is deemed to be beyond the scope of the thesis and DIUS Project research; and

- the DG output control system is developed for real-time decision support in the operational control room of the DNO. Therefore the decision-making process in identifying control actions must be transparent and should gracefully degrade if communications signals are lost.

1.4 User and functional requirements

The key user requirements, relevant to the research in this thesis, were specified as:

1. Increase the thermal exploitation of the power system through the intelligent management of constrained DG connections in non-contingent [electrical] situations without violating:

   (a) Voltage requirements; and

   (b) equipment thermal ratings;

---

[1]For the same power transfer an increase in operating voltage reduces the operating current and may mitigate the thermal overload

2. Provide real power set points to DG schemes connected to the network under control;

3. Provide a method for selection of measured thermal quantities and locations;

4. Be cost effective with respect to network reinforcement and present constrained connection techniques;

5. Provide easy integration of the control system with power system components and SCADA, minimising interruptions to supply;

6. Utilise transparent decision making processes to facilitate performance evaluation;

7. Be tolerant of communication faults and degrade in a graceful manner; and

8. Ensure safe power system operation;

This led to the specification of functional requirements as outlined below:

1. Calculate real power output signals for single and multiple DG schemes;

2. Utilise power system static, seasonal or real-time thermal ratings (available to the control system through the doctoral research of Andrea Michiorri, also participating within the DIUS Project);

3. Utilise load flow routines based on electrical network models and a power systems equipment database;

4. Obtain electrical measurements [such as voltage, current, power flow and circuit breaker status], interfacing with SCADA [in the commercialised product];

5. Provide decision support for the DNO control room engineers;

6. Be self-diagnostic; and

7. Utilise an appropriate software architecture, allowing for modularity, flexibility, maintainability and openness;

1.5   Research objectives

Through the critical review of work in relevant areas (provided in Chapter 2), together with the research scope and specifications outlined in Sections 1.3 and 1.4, a number of research objectives were identified. The research objectives which are the focus of this thesis are:

1. The proposal of a methodology for the development of DG output control systems;

2. The development of techniques for the on-line output control of single and multiple DG schemes, based on power system static, seasonal and real-time thermal ratings;

3. The validation of the techniques and assessment of gains through simulation; and

4. The practical implementation of a prototype DG output control system.

1.6   Thesis overview

An overview of the thesis structure is provided in Figure 1.2 together with the author's published work, as relevant to each chapter, and listed in the preamble of the thesis. Published journal papers are given in Appendix A.

The thesis is structured in the following way: Chapter 2 provides a review of present literature which is relevant to, and informs, the research objectives of this thesis (as presented in Section 1.5). Chapter 3 describes preliminary analysis work which includes the selection of case study networks to be used as test-beds for algorithm simulation and validation throughout the thesis. Chapter 4 proposes a methodology for the development of DG output control systems.

The first stage of the methodology requires an assessment of the location of thermally vulnerable components within distribution networks. This is achieved through the off-line calculation of thermal vulnerability factors that relate power flow sensitivity factors (the change in network power flows that result from the change in DG power outputs) to power system thermal limits. The theoretical background for this work is presented in Chapter 5 and applied to the case study networks in Chapter 6.

The identification of thermally vulnerable components within distribution networks directly informs stages two and three of the DG output control system development methodology. Namely, network thermal characterisation and the development of power system real-time thermal rating systems. These topics are discussed in Chapter 7 and, whilst these stages are integral to the proposed DG output control system development methodology, the research presented in Chapter 7 was the primary research focus of the author's PhD colleague, Andrea Michiorri.

In the fourth and final stage of the methodology, as presented in Chapters 8 and 9, control algorithms are developed for the active exploitation of power system thermal ratings in order to inform and manage the power output of DG schemes.

Chapter number		Author's relevant publications
2	Literature review	**{1, 12}**
3	Preliminary network investigations	
4	Methodology for developing DG output control system	**{3, 7, 9}**
5	Theory of thermally vulnerable component identification assessments	**{3}**
6	Application of thermally vulnerable component identification assessments → Assessment of power flow sensitivity factors (PFSFs)	**{3}**
7	Network thermal characterisation and real-time thermal rating system development	**{2, 4}**
8	DG output control algorithm development	**{5}**
9	ETR 124-based output control of single DG schemes ← DG output control algorithm evaluation techniques → PFSF-based output control of multiple DG schemes	**{5, 8, 11}**
10	Simulation of ETR 124-based output control of single DG schemes	**{8, 10}**
11	Simulation of multiple DG scheme control with single thermal constraint	**{6, 11}**
12	Simulation of multiple DG scheme control with multiple thermal constraints	**{5}**
13	Practical implementation of prototype DG output control system	**{13, 14}**

Figure 1.2: Thesis overview

Techniques based on Engineering Technical Recommendation 124 are developed for the output control of single DG schemes and the power flow sensitivity factors, derived in the first stage of the control system development methodology, are incorporated into strategies for the output control of multiple DG schemes. Chapter 9 also proposes a number of parameters for the evaluation of the control algorithms developed. The next three chapters focus on the off-line open loop simulation of the control algorithms, deployed with static, seasonal and real-time thermal ratings systems. Chapter 10 considers the case of a single DG scheme, the power output of which is controlled as a result of a single power flow-constraining component. Chapter 11 considers the power output control of multiple DG schemes as a result of a single power flow-constraining component within the distribution network. Chapter 12 considers the case of multiple DG scheme control as a result of multiple power flow-constraining components within the distribution network.

Chapter 13 describes the practical implementation of a prototype DG output control system, installed within a section of ScottishPower EnergyNetworks' distribution network for field trial evaluation. The control algorithm described in Chapter 10 was developed for use within an industrial hardware platform, manufactured by AREVA T&D and, informed by the real-time thermal rating system, was used in open and closed loop trials for the active management of DG based on component thermal properties. Chapter 14 evaluates the conducted research against the research objectives. Chapter 15 concludes the thesis with a summary of key findings and the avenues identified for further work.

Chapter 2

Literature Review

This chapter provides a detailed review of literature to date that informed the research objectives summarised in Chapter 1. The review intends to provide a brief synopsis of the literature, summarising key points that inform the current research. Where relevant, a critical analysis of the literature is presented to assess its limitations and identify openings for innovative research areas. The research openings have been summarised at the end of this chapter together with concluding remarks. In the literature review the following areas are considered: Active distribution networks; component thermal rating systems; distributed generation (DG) connection capacity assessments; DG output control research and development projects; candidate DG output control techniques; the evaluation of techniques against user and functional specifications; and regulatory incentives.

2.1 Active distribution networks

The proliferation of DG together with load growth, energy storage technology enhancements and increased consumer expectations have significantly changed the approach to planning [7–9] and operation of distribution networks. Around the globe, distribution companies, equipment manufacturers, electrical engineering consultants, research institutions, regulators and other stakeholders are dealing with the transition of distribution networks from passive to active entities. Part of this new paradigm includes the possibility for distribution network operators (DNOs) / distribution system operators (DSOs) to control, operate and thereby integrate distributed energy resources (DERs) into the network under their responsibility. The CIGRÉ C6 Study Committee [10] is specifically focused on the "development and operation of active distribution networks" and has produced the following shared global definition of active distribution networks (ADNs) [11]:

Active distribution networks are distribution networks that have systems in place to control a combination of distributed energy resources such as generators, loads and storage. Distribution System Operators have the possibility of managing the electricity flows using a flexible network topology. Distributed Energy Resources take some degree of responsibility for system support, which will depend on a suitable regulatory environment and connection agreements.

The main UK-based active network management (ANM) research activities are summarised in [12] as concentrating on voltage, power flow and fault level limitations. International projects relating to ANM are given in [13] which provides a comprehensive register of research activities upto, and including, 2006.

A Long Term Development Statement (LTDS) [14] is prepared by ScottishPower Plc to provide information regarding planned changes and operation of the distribution network. The report summarises distribution code regulations within which the system is operated and component-specific electrical data such as resistance and reactance parameters, and component seasonal thermal ratings. In terms of frequency and voltage, the following regulations are summarised as a direct distillation from the Electricity Safety, Quality and Continuity Regulations [15]:

1. That system frequency should not deviate by more than $\pm 1\%$ of the declared value of 50Hz;

2. At voltages of 132kV the deviation must be less than $\pm 10\%$;

3. Between 132kV and 1kV voltages must be maintained between $\pm 6\%$ of nominal; and

4. Below 1kV voltages may deviate to the extent 10% above and 6% below the nominal value.

The purpose of these regulations is to ensure that load customers have a quality of supply that does not damage any electrical equipment connected to the distribution network.

2.2 Component thermal rating systems

Real-time thermal ratings are a *hot topic* of research for the following institutions: EPRI in the USA for increased security and capacity of transmission networks [16], NUON in the Netherlands for coping with load growth and delaying infrastructure investment [17], E.ON and Central Networks in the UK to facilitate the non-firm (or constrained) connection

of DG [18] and the Energy Networks Strategy Group within the UK, as a solution for the accommodation of DG from the Distributed Generation Coordinating Group in Work Stream 3 [19].

Significant research has been carried out at the transmission level for real-time thermal rating applications. Research tends to focus on overhead lines which, due to their exposure to the environment, exhibit the greatest rating variability. A description of the cost and suitability of different uprating techniques for overhead lines is described in [20], taking into account different operating conditions. This work shows how real-time thermal ratings can be a more appropriate solution than network reinforcement when connecting new customers to the network who are able to curtail their generation output or reduce their power demand requirement at short notice. Similarly, experience regarding thermal uprating in the UK is reported in [21] where it was suggested that real-time thermal ratings could give overhead lines an average uprating of 5% for 50% of the year. An example of an real-time thermal rating application for transmission overhead lines of Red Eléctrica de España is described in [22] where a limited number of weather stations are used to gather real-time data. The data is then processed using a meteorological model based on the Wind Atlas Analysis and Application Program (WAsP) [23], taking into account the effect of obstacles and ground roughness, and finally the rating is calculated. A similar system was developed in the USA by EPRI in the late 1990s which considered overhead lines, power transformers, electric cables and substation equipment. The system is described in [24] and preliminary results of field tests are given in [25]. At the distribution level, a real-time thermal rating project carried out by the Dutch companies NUON and KEMA is described in [17] which demonstrates the operating temperature monitoring of overhead lines, electric cables and power transformers.

The advantages of real-time thermal rating systems for the connection of DG, especially wind power, are reported in various sources, each of which considers only single power system components. It is demonstrated in [26] that the rating of transformers positioned at the base of wind turbines may presently be oversized by up to 20%. Moreover, in [27] the power flowing in an overhead line close to a wind farm is compared to the real-time thermal rating using WAsP. In this research it was highlighted that high power flows resulting from wind generation at high wind speeds could be accommodated since the same wind speed has a positive effect on the line cooling. This observation makes the adoption of real-time thermal rating systems relevant in applications where strong correlations exist between the cooling effect of environmental conditions and electrical power flow transfers. The ther-

mal models, used to estimate real-time thermal ratings for different types of power system components, are fundamental to this research as the accuracy of the models influence the accuracy of real-time thermal ratings obtained. Particular attention was given to industrial standards because of their wide application and validation both in industry and academia. For overhead lines, the model is described in [28, 29] which has been developed into industrial standards by the IEC [30], CIGRÉ [31] and IEEE [32]. Static seasonal ratings for different standard conductors and for calculated risks are provided by the Energy Networks Association (ENA) in [33]. Thermal model calculation methods for electric cable ratings are described in [34] and developed into an industrial standard by the IEC [35]. The same models are used by the IEEE in [36] and the ENA in [37] to produce tables of calculated ratings for particular operating conditions. Power transformer thermal behaviour is described in [38] with further models described in industrial standards by the IEC [39], IEEE [40] and ENA [41].

A technique for identifying the thermally vulnerable span of an overhead line is given by Berende *et al.* in [42]. The team from the Netherlands used imagery from helicopter flights to record and time-stamp the sag of overhead lines. The power system operating conditions corresponding to the time stamp of the sag images were identified and then, together with an off-line algorithm, used to simulate the sag for other operating conditions. The technique was appropriate for that particular application because the vulnerable section of the network had been predetermined through operational experience.

2.3   DG connection capacity assessments

DG connection capacity assessments are the current research focus of numerous institutions in order to determine the impact of voltage regulations, operational economics, fault levels, losses and thermal limits as constraining parameters. Dinic *et al.* [43] consider voltage limitations and installed DG capacity, relative to the system fault level, in 33kV networks and conclude that capacitive compensation can allow capacity maximisation within operational limits. The economics of DG connections are considered by Currie *et al.* [44] with a methodology that facilitates greater DG access for multiple generators by exploiting operating margins with an active power flow management technique termed 'trim then trip'. Vovos *et al.* [45] develop an optimal power flow (OPF) technique along with an iterative procedure to calculate DG allocations at nodes based on fault level limitations. Mendez Quezada *et al.* examine the impact of increased DG penetration on electrical losses within

the IEEE 34-node test network [46] and conclude that losses follow a U-shaped trajectory when plotted as a function of DG installed capacity. Within [47] Harrison and Wallace present an OPF formulation to determine the maximum connection capacity of DG based on thermal limits and statutory voltage regulation. The 'reverse load-ability' methodology coupled with OPF software modelled generators as loads with a fixed power factor and created an analysis tool that could allow additional constraints (such as fault-level limitations) to be incorporated into the formulation if necessary. It was also suggested that Lagrangian relaxation of constraint coefficients may be developed to simulate changes in component ratings although this was not demonstrated. It is acknowledged that technical barriers such as voltage rise [48] and fault levels [49] may limit DG connection capacities. However, the research presented in this thesis focuses on the connection capacities and operation of DG as determined by power flow constraints. Therefore it is assumed that power system thermal ratings are the limiting factor that is breached before voltage and fault level constraints.

2.4 DG output control research and development projects

In the UK, strategies for the power flow management of single DG schemes have been proposed by the ENA [50] as a direct distillation of a report by the Distributed Generation Coordinating Groups Technical Steering Group [19] that considers a spectrum of ANM solutions. Four solutions are presented to facilitate the connection of increased DG capacities and the necessary power flow management requirements are illustrated. Network availability assessments (i.e. how much power may be injected by DG into the network) are made by considering the capacity of network assets under normal operation and following a first circuit outage, the maximum and minimum load demand at the DG connection busbar and the potential utilisation of short-term component thermal ratings. The power output of generators is controlled through tripping (disconnection) and a demand-following technique with auxiliary tripping. Additionally, Roberts [51] considers the feasibility of incorporating the proposed solutions within a supervisory, control, and data acquisition (SCADA) system for DNOs. The advantages of using SCADA were given as:

1. SCADA infrastructure is already installed throughout the distribution network for monitoring and protection purposes;

2. SCADA systems have been developed and tested on robust hardware platforms;

3. Communication protocols are already established; and

4. SCADA software is logic-based and therefore the functionality could be adapted for ANM purposes.

However, a number of disadvantages to adapting SCADA were given as:

1. Hardware limitations, in terms of methods of operation, speeds of operation, reliability and robustness could occur if SCADA systems are adapted;

2. A resilient communications infrastructure, particularly in rural parts of the UK, is presently lacking;

3. Reprogramming and maintaining the logic software could result in large overhead costs; and

4. The culture change required by the DNO workforce to accept the movement to a SCADA system with ANM functionality could take a number of years to propagate.

The commercial implications of adapting SCADA systems for ANM functionality were not discussed. A key limitation of using SCADA was identified as utilising the system for a purpose other than for which it was designed with the potential of leading to unforeseen operational ramifications.

The design and commissioning of an active DG constraint system for an offshore wind farm is presented by Liew and Moore [52]. In this application an intelligent control system is developed to allow an offshore wind farm to utilise additional power transfer capacity for system intact operation and to constrain the wind farm output during fault conditions. This system avoids network reinforcement and provides the lowest cost solution to allow the wind farm to export up to 76 MW of power. 'Down turn' signals are dispatched to the wind farm to constrain the power output in discrete intervals of 25%.

Research by the University of Strathclyde in conjunction with the DNO Scottish Hydro Electric Power Distribution Ltd [53] investigates the constrained connection of multiple DG schemes on the island of Orkney. The resulting control strategy utilises a 'trim and trip' philosophy embedded in programmable logic control [54]. In this strategy DG is categorised as firm generation, non-firm generation, and regulated non-firm generation. Firm generation is able to operate freely at its maximum rated output under normal conditions and following a first circuit outage. Non-firm generation is able to operate freely under normal conditions but is tripped during first circuit outage conditions. Regulated non-firm generation is trimmed and/or tripped depending on the prevailing network conditions. In order to reflect

present operational practices in the UK, as embodied in commercial agreements between the generator owners and the DNO, a last-in first-off strategy is adopted to define the order in which regulated non-firm generators are controlled. Although it is suggested that an extension to the work could be to incorporate short-term thermal ratings in the assessment of trimming and tripping margins, this aspect of the work is not demonstrated.

A consortium of UK universities and DNOs is currently researching and developing an autonomous regional active network management system (AuRA-NMS) to offer real-time voltage, restoration, and thermal control solutions for distribution networks. As part of this continuing project, Dolan *et al.* [55] present two techniques for the management of power flows within static thermal constraints: an artificial intelligence technique which formulates and ranks solutions to constraint satisfaction problems (CSPs), and a current-tracing algorithm which allows DG curtailment to be apportioned according to the individual contributions of generators towards a thermal violation. The techniques are illustrated through the control of two DG schemes within an 11kV radial/ring distribution network and are assessed in terms of algorithm computational times and impact on DG real power output curtailments. It is shown for the particular case study that the current-tracing technique marginally achieves the least DG real power curtailment but that the CSP technique is more computationally efficient and allows contractual constraints to be considered.

Kabouris and Vournas [56] demonstrate the on-line development of interruptible wind farm contracts in order to manage the power flow through a congested corridor of the Hellenic Interconnected System in Greece. When security constraints are violated, the control of multiple generation schemes is achieved through the proportional reduction of the generators' power output or by distributing generator curtailments according to a continuously updated priority list. Both proactive (pre-outage) and reactive (post-outage) control concepts are developed and illustrated based on a static security assessment of the available transfer capacity through the congested corridor. It is shown that proactive control has the potential to increase wind energy penetration by 206% from 125 GWh/annum to 383 GWh/annum in the case of wind farms with guaranteed contracts (firm connections) and interruptible contracts (non-firm connections). If interruptible contracts are applied to all generators and a proactive control approach is adopted this has the potential to unlock a further 38 GWh/annum. Moreover, the potential for a 900 GWh/annum wind energy penetration could be achieved through the reactive control of wind farms with interruptible contracts. However, this strategy would require very reliable control equipment such as telecommunications, protection devices and robust software as well as changes to the Greek

Grid Code to allow for security assessment criteria violations.

The concept of a delegated dispatch control centre has been developed in Spain to act as a mediator between the transmission system operator and a collection of wind farms connected to the same injection node [57]. Using a proactive control approach based on 15-minute operational forecasts, the delegated dispatch responds to system operator constraints imposed on the injection node. An optimization problem is formulated that considers active and reactive power outputs of the generators, generator profit, busbar voltages, and component thermal limits. In meeting the system operator constraints at the injection bus, the objective function of the optimization problem aims to maximize the aggregated profit of the generators.

Makarov *et al.* [58] investigate the operational impacts of increased wind generation within the Californian power system. Case study scenarios are modeled for the years 2006 (with 2.6 GW installed capacity of wind generation) and 2010 (with anticipated 6.7 GW installed capacity of wind generation). In particular, the paper focuses on the forecasted difference between generation and load demand, and the required ramp rates of the generators to balance the power in real-time. Power flow congestion is managed using a proactive control approach whereby hour-ahead and five-minute-ahead load and wind generation forecasts inform the California Independent System Operator Balancing Authority. This allows the system operator to schedule and dispatch conventional generation to maximize the wind generation penetration.

The incorporation of overhead line real-time thermal ratings for the power output control of wind farm connections in the UK is presently being considered by Yip *et al.* [18]. In this application the wind farm is sent a power output reduction signal if a power flow violation beyond the real-time thermal rating occurs. With auxiliary functionality, the wind farm is tripped to protect the overhead line if the power output is not reduced by the designated amount within the designated time-frame.

A key aspect of the implementation of DG output control systems is the controllability of generators to achieve the desired set points. The methods of control of various DG types are given in [59] for wind power, photovoltaic power, hydro power, landfill gas schemes and combined heat and power (CHP) plants. In general terms the most basic DG output control implementation could be to trip-off the entire generation plant through the opening of the connecting circuit breaker [50]. A slightly more sophisticated approach would be to curtail the DG output in discrete intervals e.g. full output – 66% full output – 33% full output – trip-off. This could be achieved through the switching off of individual turbines within the

DG plant [51]. A disadvantage to tripping DG output control methods (whether they be all-off or discrete interval) is that the DG output is not necessarily matched to the capability of the network and thus the overall generation plant is potentially curtailed more than necessary. This could impact on the annual energy yield of DG schemes and ultimately their revenue streams. With the maturing of generation technologies it is becoming more common for DG schemes to have the capability to limit maximum power outputs to specific MW set points at times of DG output control. The work presented in this thesis particularly relates to wind generation, where wind turbine technologies have matured over the past decade and automatic generator control (AGC) techniques are now developed and operational [60]. The power output of a wind turbine is proportional to the cube of wind velocity since the wind velocity affects the angular velocity of the blades [61]. Automatic generator control methods can feather the turbine blades by altering their pitch angle and capturing different proportions of the potential maximum power output. Thus an independence is achieved between the wind speed and generator output with the turbines responding to dispatched set point changes within a 5 s time frame [62]. Supplementary relevant work in given in [63] for hydro turbines where the real power output of the generator is related to the water velocity and valve position. The simulation and experimental validation of the penstock-governed Francis turbine showed that an active power set point change from 6.4 MW to 4.8 MW could be achieved within 12 s.

2.5 Candidate DG output control techniques

From the review of DG output control research and development projects, a number of candidate DG output control techniques were identified. In addition, a number of other candidate DG output control techniques were identified in literature. These are explained below and a summary of the candidate DG output control techniques is provided at the end of this section.

Through the use of Tellegen's theorem Director and Rohrer developed generalised expressions for the sensitivity coefficients that relate nodal voltages and branch currents in two adjoint networks [64]. This work was built upon by Ejebe and Wollenberg to give the general form of relationships between perturbations in a base network and the changes seen in an adjoint network for the automatic ranking and assessment of worst case network contingencies [65]. As an adjustable variable is changed (e.g. a generator's real power output) it is assumed that the power system reacts so as to satisfy the complete set of power flow

equations. Some sensitivity coefficients may change rapidly as the adjustment is made and the power flow conditions are updated. This is because some system quantities (e.g. voltages and MVAr flows) vary in a non-linear relationship with the adjustment and resolution of the power flow equations. Sensitivities such as the variation of component real power flows with respect to changes in generator real power outputs are linear across a wide range of operating conditions. This resulted in the development of generation shift factors and line outage distribution factors that relate changes in component power flows to changes in generation or network configurations in DC approximations of AC networks [66]. Ng developed generalised generation distribution factors to replace generation shift factors. The model relates component power flows with generator outputs for a given network topology and is in integral form to allow the new flows in components to be calculated without running a new load flow when total system generation changes [67]. Sensitivity coefficients within power systems are used extensively to solve a variety of problems. Examples include optimal power flow formulations for the economic dispatch of generators to solve congestion management issues at the transmission level [68, 69] and flexible AC transmission systems for power flow management [70] as well as more recent voltage rise issues at the distribution level [71, 72]. The work describing voltage rise issues is of particular relevance to the research presented in this thesis as it is concerned with the control of multiple DG power outputs as determined by voltage sensitivity factors.

OPF is a complex and difficult mathematical problem to solve since the goal is to find an optimal solution to the complete set of non-linear power flow equations within many (sometimes conflicting) power system and economic constraints. A large number of different techniques have been employed to solve OPF problems, the classic approaches being linear programming, interior point methods and Lagrangian relaxation [66]. With the increase in available computational power has come the application of artificial intelligence techniques such as genetic algorithms, artificial neural networks and ant colony search methods to solve economic dispatch and generator scheduling for congestion management problems [73].

Much research was carried out in the 1990s to solve congestion management issues in transmission networks through the development of flexible AC transmission systems (FACTS) [70]. In this research, series components such as capacitors are used to alter component power flows such that the transfer of real power is maximised and the rescheduling of generation is not required.

Recent power system unbundling and deregulation has led to the solution of transmission congestion management issues through the development of competitive electricity market

models [74]. Two such models involve bilateral contracts between suppliers and consumers and a bidding pool structure utilising a central pool operator. Bilateral models involve the independent arrangement of power transactions between suppliers and consumers and competition is encouraged by consumers trading with the cheapest generators. This does not provide a mechanism for incorporating transmission system constraints within the model, neither does it facilitate and attribution of system losses to generators or consumers, nor does it provide a mechanism for ancillary services provided by the generator to secure supplies to consumers. In the pool model a central pool operator receives bids from generators and through nodal spot pricing and a locational adjustment to account for losses is able to supply consumers in the most efficient way whilst satisfying transmission system constraints.

The candidate DG output control techniques to manage network power flows were identified as:

- Tripping (disconnection);

- demand-following;

- control in discrete intervals;

- trimming and tripping;

- formulation and solution of constraint satisfaction problems;

- current tracing;

- interruptible contracts [with a ranked DG curtailment list or proportional output control];

- creation of a 'delegated dispatch';

- offsetting of conventional generation (economic dispatch);

- power flow sensitivity factors;

- optimal power flow formulation and solution;

- flexible AC transmission systems adapted for distribution network usage; and

- competitive market models at the distribution network level.

2.6   Evaluation of candidate DG output control techniques

Given the candidate DG output control techniques identified in Section 2.5 this section evaluates the possible techniques against the DIUS Project user and functional specifications. This facilitated the selection of appropriate techniques, to be taken forward for development, in order to achieve the active management of DG based on component thermal properties.

DG output control through tripping (disconnection) is suggested in Engineering Technical Recommendation (ETR) 124 [50] as a technique to manage the power flows associated with a single DG scheme, based on component static, seasonal or real-time thermal ratings. It has also been implemented by AREVA T&D in the MiCOM protection relay cubicle [18]. Whilst the complete disconnection of DG at times of power flow management would be expected to impact on the revenue stream of DG developers, the use of this technique could provide the DG output control system auxiliary functionality if communications signals are lost and sustained high currents could put the power system at risk of damage. This would fulfil the user requirement of ScottishPower EnergyNetworks to ensure safe power system operation, provide the DG output control system with credibility for commercial exploitation by AREVA and provide a datum by which gains from alternative DG output control techniques could be measured.

DG output control through a load demand-following technique is also suggested in ETR 124 as a technique to manage the power flows associated with a single DG scheme, based on component static, seasonal or real-time thermal ratings. On the basis of ETR 124, the DG output control system would have credibility for commercial exploitation by AREVA T&D, particularly if this technique is coupled with the afore mentioned auxiliary DG tripping technique discussed above. Whilst the demand-following technique is described in ETR 124 for a single DG scheme, it is suggested (although not demonstrated) that the technique could be developed to provide demand-following capabilities for multiple DG schemes based on local and, potentially, global network availabilities.

DG output control in discrete intervals represents the intermediate step between the complete disconnection and demand-following techniques proposed in ETR 124. The technique has the potential to be deployed with power system static, seasonal or real-time thermal ratings. This could provide an alternative datum against which other, more sophisticated, control techniques are evaluated.

The 'trim and trip' DG output control technique developed by the University of Strathclyde for the deployment on the Island of Orkney is a hard-wired and bespoke solution

which might not, at present, be readily adapted for use in alternative locations. Although it is suggested in [54] that an extension to the research could be to incorporate short-term thermal ratings in the assessment of trimming and tripping margins, this aspect of the work is not demonstrated.

The identification of solutions to CSPs requires the employment of artificial intelligence techniques. Such techniques may be perceived by DNOs as 'black box' technology whereby there is questionable transparency in the decision-making process. A key user and functional requirement is that the control algorithms, for use in the DIUS Project, are developed with transparent decision-making capabilities.

Current- and flow-tracing techniques have been developed to trace the flow of active (and possibly reactive) power from generators (sources) to loads (sinks). For a particular operating condition the algorithms give an approximation of the active (and reactive) power flowing in network components that can be attributed to particular generators or load customers. This may then be used, off-line, to assign losses to generators or load customers for transparent market and charging mechanisms in unbundled power systems. Since power flow-tracing and current-tracing algorithms were developed at transmission level for the off-line allocation of losses (and to inform use-of-system charges) the real-time use of such algorithms on distribution networks has not yet been extensively demonstrated.

The interruptible contract techniques described in [56] lead to a number of alternative operational contracts for multiple wind-based generators, such as the distribution of power reductions in a proportional manner to the generators' present power outputs. Whilst the interruptible contract techniques do not incorporate power system real-time thermal ratings in the assessment of generator power output constraints, there is scope for the proposed interruptible contract techniques to inform control algorithm development, particularly related to multiple DG scheme control.

The creation of a 'delegated dispatch' is based on a pro-active control technique for DG output control. The utilisation of such a technique in the DIUS Project would require the forecast of power system real-time thermal ratings. In terms of incremental control system development, and with concerns raised by the DIUS Project consortium regarding the uncertainty associated with meteorological condition forecasts, it was agreed by the research consortium that the control system should make use of monitored data to estimate power system thermal ratings for the reactive control of DG power outputs.

The reduction in power output of centralised conventional generation power plants to accommodate DG from renewable resources is feasible in vertically integrated power systems

where the system operator is able to schedule and control all the generation schemes. However, in the UK, where the field trial prototype control system is hosted, the power system is unbundled and therefore generation is scheduled at transmission level to meet UK load demands with DG tending to be unscheduled.

The solution to OPF problems is a trade-off between the speed, accuracy and robustness of the algorithm. Therefore optimisation techniques lend themselves to planning tool applications where the time taken for the algorithm to converge to a solution is not a critical feature and it is not critical if the tool, on occasions, fails to converge. However, in a real-time decision-making environment the formulation and solution of the optimisation problem may not be robust, particularly if the solution method is sensitive to input errors. In addition (and as with CSPs), artificial intelligence techniques which are required to solve complex constraint problems, are perceived by DNOs as 'black box' technology whereby there is questionable transparency in the decision-making process.

Sensitivity factors provide the underlying control derivatives by which OPF problems are solved. If used in a transparent manner, power flow sensitivity factors could be coupled with power system thermal rating systems to achieve DG power output control. When comparing the concept of flow-tracing to sensitivity factors it can be shown that, for a particular operating condition, the flow-tracing algorithm provides the assignation of flows to generators whereas the sensitivity factors relate the change of flows to changes in generator outputs. Thus, for sensitivity factor derivation the flow-tracing algorithms would require two solutions: once with the present operational state and once with a perturbation of the DG scheme(s). Thus by employing the flow-tracing algorithm, additional information is gained (as to the approximate composition of power flows in lines) and this is of benefit for loss allocation applications.

The installation of FACTS devices can cost millions of pounds, which may be economically viable at the transmission system level but not, presently, at distribution network level. Furthermore, the maximisation of real power transfers requires the alteration of reactive power transfers. This could be constrained by the thermal limit of the power system.

Whilst congestion management at the transmission level is well understood, the historical passive nature of distribution networks means that congestion management practices by DNOs are rare [71] and competitive market-driven mechanisms for congestion management have not been brought down to distribution network levels.

Based on the evaluation above, the following techniques were selected for development to achieve the active management of DG based on component thermal properties:

- Tripping (disconnection) [for single and multiple DG scheme control];

- demand-following [for single DG scheme control];

- discrete interval adjustments [for multiple DG scheme control];

- ranked lists to prioritise the constraint order of DG schemes [for multiple DG scheme control];

- proportional adjustments [for multiple DG scheme control]; and

- power flow sensitivity factors [for multiple DG scheme control].

2.7 Regulatory incentives

The present regulatory incentives for DG developers and for DNOs to accommodate DG developments are considered by Harrison *et al.* in [75]. Regulatory incentives are embodied in connection agreements, electrical losses and network reinforcement deferral. In addition, the strategic benefits of DG ownership for DNOs is discussed by Siano *et al.* in [76] and the authors conclude that incentives need to be put in place to encourage DG deployment for the benefit of the distribution network.

In the UK, loss targets are set by the regulator OfGEM to encourage DNOs to increase the efficiency of their networks. Following the distribution price control of 2004, losses were valued at £48/MWh with DNOs being rewarded for achieving losses below OfGEM's target and penalised for losses above. Whilst modest amounts of DG can be shown to reduce network losses, significant penetrations of DG could lead to increased distribution network losses with ensuing penalties for DNOs. The DNO is likely to assess the impact of DG on losses at the planning stage and reflect any additional charges for losses in the connection agreement. However, no formal mechanism exists at present to reward DG developers for reducing network losses. A mechanism is in place in Spain [46] for DSOs to recover the deficit in revenue caused by losses in their network. This is done by applying a 'standard loss coefficient' to the consumer electricity sale price. If the network is then made more efficient the DSO makes a profit, whereas if increased losses occur the DSO makes a loss. This revenue deficit is then charged to the DG developer as a penalty by the DSO.

Current- and flow-tracing methodologies have been developed to trace the flow of active (and possibly reactive) power from generators (sources) to loads (sinks) to assign losses to generators or load customers for transparent market and charging mechanisms in unbundled

power systems. Bialek proposed upstream-looking and downstream-looking algorithms for the tracing of power flows back to respective generators and loads [77]. The proposed power flow tracing methodology requires the assumption that the network is lossless or the introduction of an additional node, for every component, to balance losses. This may be feasible to implement in transmission networks with a limited number of power system components. However, it could be non-trivial to implement in distribution networks with complex topologies and large numbers of power system components. Kirschen and Strbac developed techniques for tracing active and reactive power flows through real and imaginary currents [78]. In this case the methodology may be readily implemented in radial networks but not in meshed or looped networks which is the prevalent topology of ScottishPower EnergyNetworks' distribution system.

DNOs are obliged by law to report to the regulator OfGEM on an annual basis their performance in maintaining the security, availability and quality of supply to customers [79]. The quality of service of a DNO is measured through customer interruptions (CIs), customer minutes lost (CMLs) and the quality and speed of telephone response. On this basis, DNOs are set quality of service targets and are rewarded or penalised by the regulator depending on their performance against the targets.

Two regulatory mechanisms have been implemented in the UK to encourage the active involvement of DNOs in research and development. These are the Innovation Funding Initiative where turnover is made available to DNOs for research and Registered Power Zones where DNOs may test new technologies on registered portions of their network outside of normal regulatory limitations [80].

2.8 Conclusion

This literature review has surveyed research in the areas of active distribution networks, component thermal rating systems, DG connection capacity assessments, DG output control research and development projects, DG output control techniques and regulatory incentives.

A number of techniques were identified for the off-line assessment of DG connection capacities. However, as DG proliferates there is an emerging requirement to manage non-firm DG connections in an on-line manner. Therefore, the following techniques have been selected for development to achieve the active management of DG based on component thermal properties:

- Tripping (disconnection) [for single and multiple DG scheme control];

- demand-following [for single DG scheme control];

- discrete interval adjustments [for multiple DG scheme control];

- ranked lists to prioritise the constraint order of DG schemes [for multiple DG scheme control];

- proportional adjustments [for multiple DG scheme control]; and

- power flow sensitivity factors [for multiple DG scheme control].

The advantages of a real-time thermal rating system for the connection of DG, especially wind power, are reported in various sources. The real-time thermal rating of existing power system components has the potential to unlock latent power transfer capacities. When integrated with a DG power output control system, greater installed capacities of DG may be accommodated within the distribution network. Moreover, the safe and secure operation of the network is maintained through the constraint of DG power outputs to manage distribution network power flows.

Considering the candidate DG output control techniques listed above, current practices tend to trip off generators in order to protect power system assets and maintain the security of supply to customers. A disadvantage of DG tripping methods (whether they be all-off or discrete interval) is that the DG output is not necessarily matched to the capability of the network and thus the overall generation plant is potentially curtailed more than necessary. This impacts on the annual energy yield of generation schemes and ultimately their revenue streams. With the maturing of generation technologies it is becoming more common for DG schemes to have the capability to match power outputs to specific MW set points at times of DG output control. Single DG output control techniques have been combined with component real-time thermal ratings although very few projects are presently in existence which actually implement these techniques. The techniques for controlling the output of multiple DG schemes are based on static thermal limit assessments of single components. Therefore development of techniques to control multiple DG schemes based on the thermal properties of multiple power system components could be of benefit. Furthermore, the process of coupling power system (multiple component) real-time thermal ratings with DG output control techniques to comprise a DG output control system could be of even greater benefit.

Chapter 3

Preliminary network analysis

3.1 Introduction

In this chapter the preliminary network analysis work, carried out in the early stages of the doctoral research, is presented and discussed. The basis of the present power system ratings used by DNOs for planning and operating distribution networks is presented in Section 3.2. The case study networks selected for analysis throughout the thesis are described in Section 3.3. The aims of the preliminary network investigations are given in Section 3.4 and a first-pass methodology for identifying the location and hierarchy of thermally vulnerable components within distribution networks is presented, and applied to the case study networks, in Section 3.5. The preliminary methodology is discussed in Section 3.6 and improvements to the methodology are suggested.

3.2 The basis of present power system ratings

In a balanced three-phase power system the total power transferred between nodes is related to the phase voltages and phase currents as in (3.1) [61]

$$S = 3V_{ph}I_{ph} \tag{3.1}$$

where S is the apparent power flow, V_{ph} is the phase voltage and I_{ph} is current in a single phase of the system. Since the nominal operating voltage of power system components is often quoted as a line-to-line value, the relationship between phase voltages and line-to-line voltages is given in (3.2)

$$V_{L-L} = \sqrt{3}V_{ph} \tag{3.2}$$

where V_{L-L} represents the line-to-line voltage. Substituting (3.2) into (3.1) gives a useful relationship for the maximum allowable apparent power through a component as a function of the phase current and line-to-line operating voltage (3.3)

$$S_{lim} = \sqrt{3}V_{L-L}I_{max} = |P + jQ|_{lim} \tag{3.3}$$

where S_{lim} is the maximum allowable apparent flow or thermal limit of a component, I_{max} is the steady-state current carrying capacity of the conductor and $|P+jQ|_{lim}$ represents the real and reactive components of the maximum apparent power flow.

The Long-Term Development Statement of ScottishPower EnergyNetworks [14] provides three classes of seasonal ratings for summer, spring/autumn and winter operating conditions. The ratings are sourced from UK-specific standards developed by the Energy Networks Association for overhead lines [33], electric cables [37] and power transformers [41]. In operational practice, difficulties associated with the maintenance of accurate seasonal rating databases often result in summer static ratings being utilised throughout the year [51].

3.3 Case study network selection

A key deliverable of the DIUS Project was to identify a site in which field trials of the prototype DG output control system could be hosted. In parallel with this, a number of United Kingdom generic distribution systems (UKGDSs) were selected to provide additional development and evaluation test-beds for the thermal state estimation and control algorithms. This was because the field trial network selected by ScottishPower EnergyNetworks was expected to contain a subset of the thermal issues present within distribution networks. Through the development of a simulation environment in which to analyse the case study networks it was hoped that a wider variety of thermal issues would be identified. This was achieved by selecting networks with different electrical component types, voltage levels and topologies to those exhibited by the field trial network.

3.3.1 Field trial network

The distribution network selected for the DIUS Project field trials has a meshed topology, with a prevalence of Lynx $175\,\mathrm{mm}^2$ overhead lines at the 132kV voltage level. Indoor and outdoor transformers rated at $45\,\mathrm{MVA}$, $60\,\mathrm{MVA}$ and $90\,\mathrm{MVA}$ convert the voltage between 132kV and 33kV levels. There are also four supergrid transformers at the grid supply
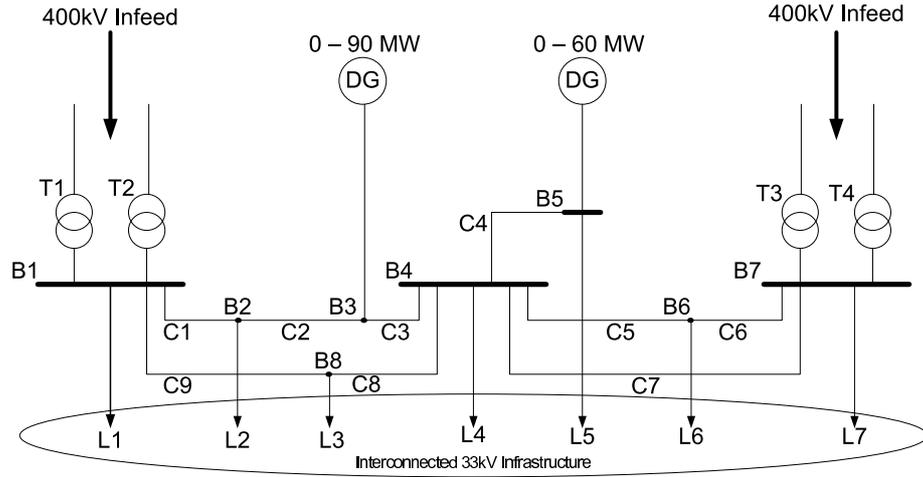
Figure 3.1: Field trial network

points rated at 240 MVA. A schematic diagram of the network is shown in Figure 3.1. A
60 MW offshore wind farm is connected at B5 and a further 90 MW of DG is expected to be
connected at B3, teeing into a 132kV overhead line feeder. The power system static ratings
together with minimum and maximum network loading levels were supplied by Scottish-
Power EnergyNetworks from their Long Term Development Statement [14]. By analysis
of load duration curves, the minimum loading level was found to be 35% of the maximum
loading level. For preliminary investigations the network was simplified by reducing sub-
stations to a single node with power flows and nodal voltages validated against those in the
original model. A full list of network parameters may be found in Appendix B.

3.3.2   United Kingdom generic distribution systems

UKGDS 'EHV3' [81] was selected and divided into three case study networks for analysis
purposes. Figure 3.2 displays UKGDS A which has a predominantly meshed topology. Fig-
ures 3.3 and 3.4 respectively represent UKGDS B and UKGDS C, which are predominantly
radial in topology. The network diagram representations have been kept in their original
format with busbars symbolised by circles containing the node identification number. For
simulation purposes the tie-lines between the sub-networks were modelled using the IPSA
load flow package with a load-equivalent to the power flow seen in the line during the full
network simulation. The interconnector in UKGDS A was modelled by maintaining the
voltage at node 345 at 1pu. The electrical parameters for the UKGDS case studies, includ-
ing component ratings and maximum and minimum loading conditions, are given in [81].
A full list of network parameters may be found in Appendix C.

Figure 3.2: UKGDS A Network
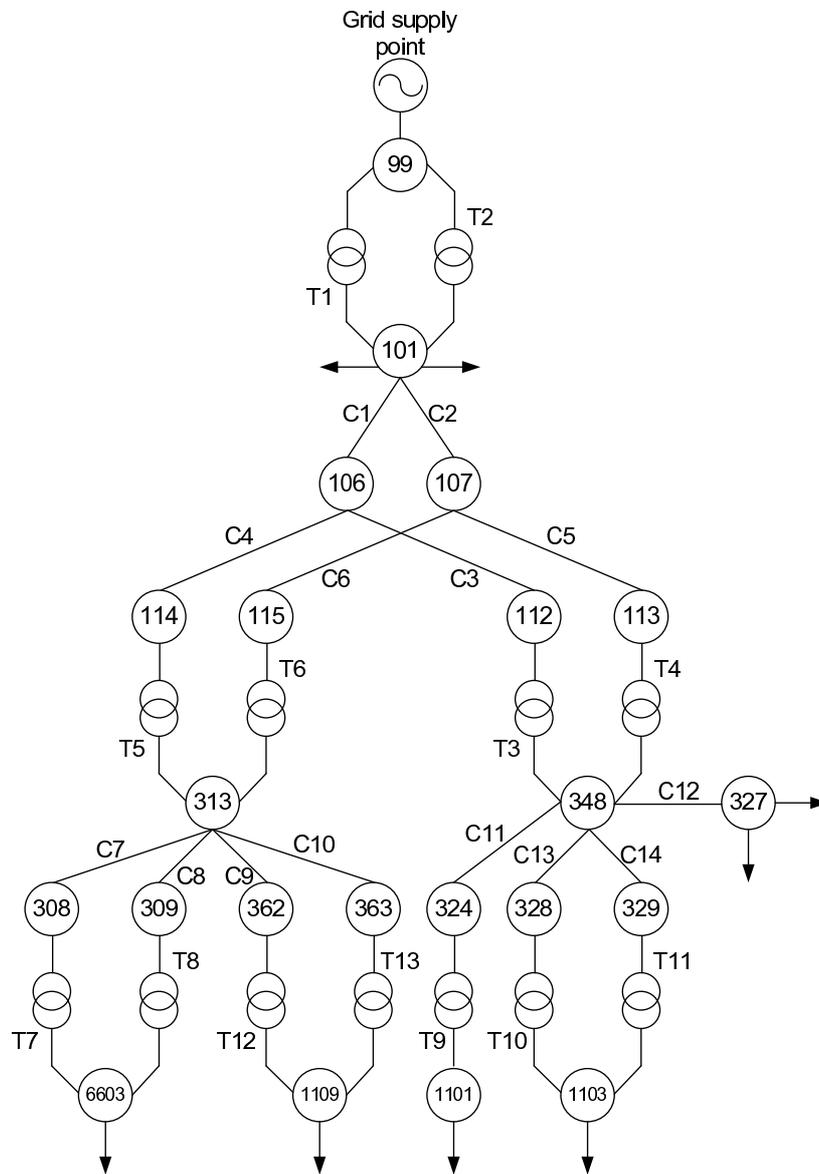
Figure 3.3: Topological representation of UKGDS B
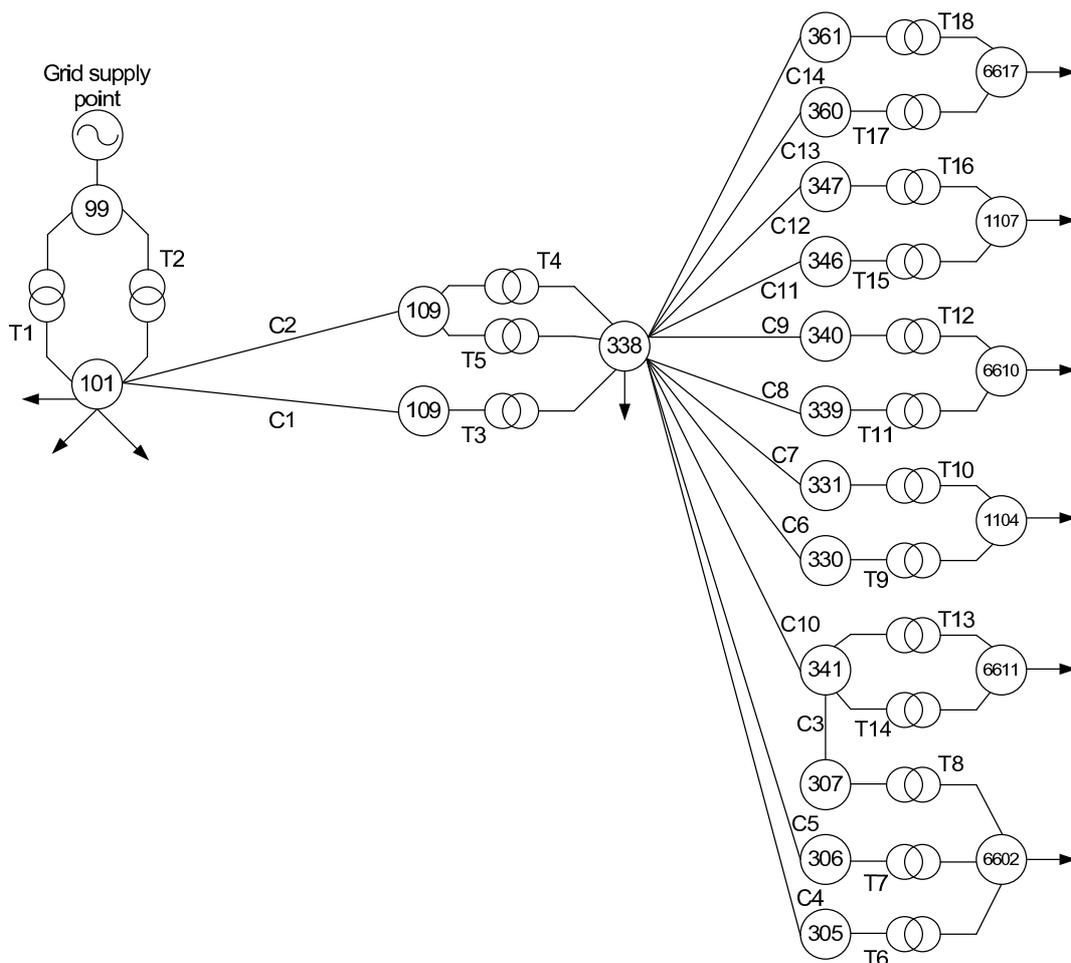
Figure 3.4: Topological representation of UKGDS C

3.4   Preliminary investigation of network behaviour

Preliminary investigations were conducted using the IPSA load flow simulation environment in order to gain an understanding of the electrical and thermal behaviour of the case study networks. In particular, the focus at this stage was to (i) understand the impact of DG on network power flows; (ii) identify the hierarchy and location of thermally vulnerable components within the distribution networks as a result of DG real power injections; and (iii) to identify the particular operating conditions (i.e. DG output and load demand combinations) that would lead to components becoming thermally vulnerable with no electrical outages present. As DG outputs were increased, busbar voltages were monitored through the capability of IPSA to colour-code the voltage levels. This gave an indication of when voltage limits were exceeded before thermal limits. The preliminary investigations were purely technical power flow studies and did not take into account limitations on DG connection capacities such as fault levels and economic considerations.

3.5   Thermally vulnerable component identification through numerical analysis

A summary of the initial analysis methodology, employed to investigate the case study networks, is outlined below:

1. The base case scenario was set up to provide a datum against which the thermal vulnerability of components could be measured;

2. The initial conditions for the particular operating condition were set up;

3. The DG power output was stepped-up in $2\,\mathrm{MW}$ intervals (reflecting the additional peak export resulting from the connection of an additional turbine within the DG scheme);

4. The IPSA load flow package was run in AC mode to simulate the real and reactive power flows, and busbar voltages within the distribution network; and

5. A rating violation summary table was automatically generated by IPSA and this was analysed to assess thermal and voltage violations brought about by operating the distribution network in the simulated condition.

Initially, the impact of increasing each DG scheme separately was simulated for both maximum and minimum network loading conditions. This was then extended to analyse the thermally vulnerable components resulting from multiple DG scheme interactions.

3.5.1   Numerical analysis applied to UKGDSs

The hierarchy of thermally vulnerable components resulting from the numerical analysis of UKGDS A is given in Figure 3.5. Node 316 (33kV) was selected to accommodate DG due to the large number of components attached to it. Component C15 was identified as the first thermally vulnerable component for DG power outputs in excess of 34 MW. Component C18 was identified as the second thermally vulnerable component for DG power outputs in excess of 60 MW. No further components became thermally stressed for increased DG outputs at node 316 before the load flow algorithm failed to converge.
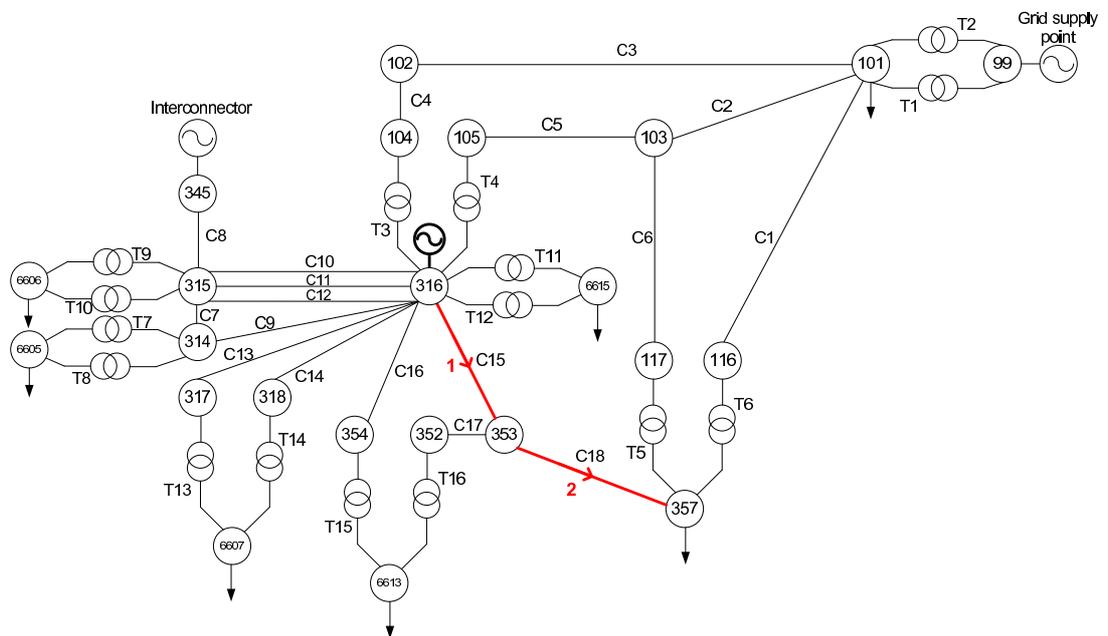
Figure 3.5: Hierarchy of thermally vulnerable components in UKGDS A due to DG connected at node 316

The hierarchy of thermally vulnerable components resulting from increased DG installed capacities at node 348 (33kV) within UKGDS B is given in Figure 3.6 and were found to be:

1. Component T4 (132/33kV transformer) with $G_{P,348} = 124\,\text{MW}$.

2. Component T3 (132/33kV transformer) with $G_{P,348} = 126\,\text{MW}$.

3. Component C5 (132kV line) with $G_{P,348} = 224\,\text{MW}$.

4. Component C3 (132kV line) with $G_{P,348} = 232\,\text{MW}$.

The hierarchy of thermally vulnerable components resulting from increased DG installed capacities at node 115 (132kV) within UKGDS B is given in Figure 3.7 and found to be:

1. Component C2 (132kV line) with $G_{P,115} = 154\,\text{MW}$.

2. Component C6 (132kV line) with $G_{P,115} = 230\,\text{MW}$.

In this case it was of interest to note that the first component to become thermally vulnerable was not directly attached to the DG connection busbar. The behaviour was attributed to the relative magnitudes of the component thermal ratings: C2 has a static rating of 100 MVA whereas C6 has a static rating of 190 MVA.

Since two separate nodes were selected in an attempt to tease out thermal issues in UKGDS B, the interaction of the two DG schemes was investigated. This was done by (a) setting $G_{P,348}$ to the maximum power output before the first thermal overload occurred (in the single DG scheme investigations detailed above) and increasing the power output of $G_{P,115}$ until a thermal violation occurred; and (b) repeating the procedure by setting $G_{P,115}$ to the maximum power output before first thermal overload occurred and increasing the power output of $G_{P,348}$ until a thermal violation occurred. The results are presented in Figure 3.8. Considering the superposition of power flows it was found that only 60 MW of $G_{P,115}$ could be accommodated at node 115 with $G_{P,348}$ set to 124 MW before component C2 became thermally overloaded. It was of note that the thermal violation occurred in the same network location as with the individual investigation of $G_{P,115}$ above. Setting $G_{P,115}$ to 154 MW and increasing the output of $G_{P,348}$ led to the first thermal violation occurrence in component T3 (for $G_{P,348} = 126\,\text{MW}$). This was attributed to a net reduction in power flow through T4 as power outputs from $G_{P,348}$ interact with power outputs from $G_{P,115}$ through components C6 and C5 and power is pushed into T3.
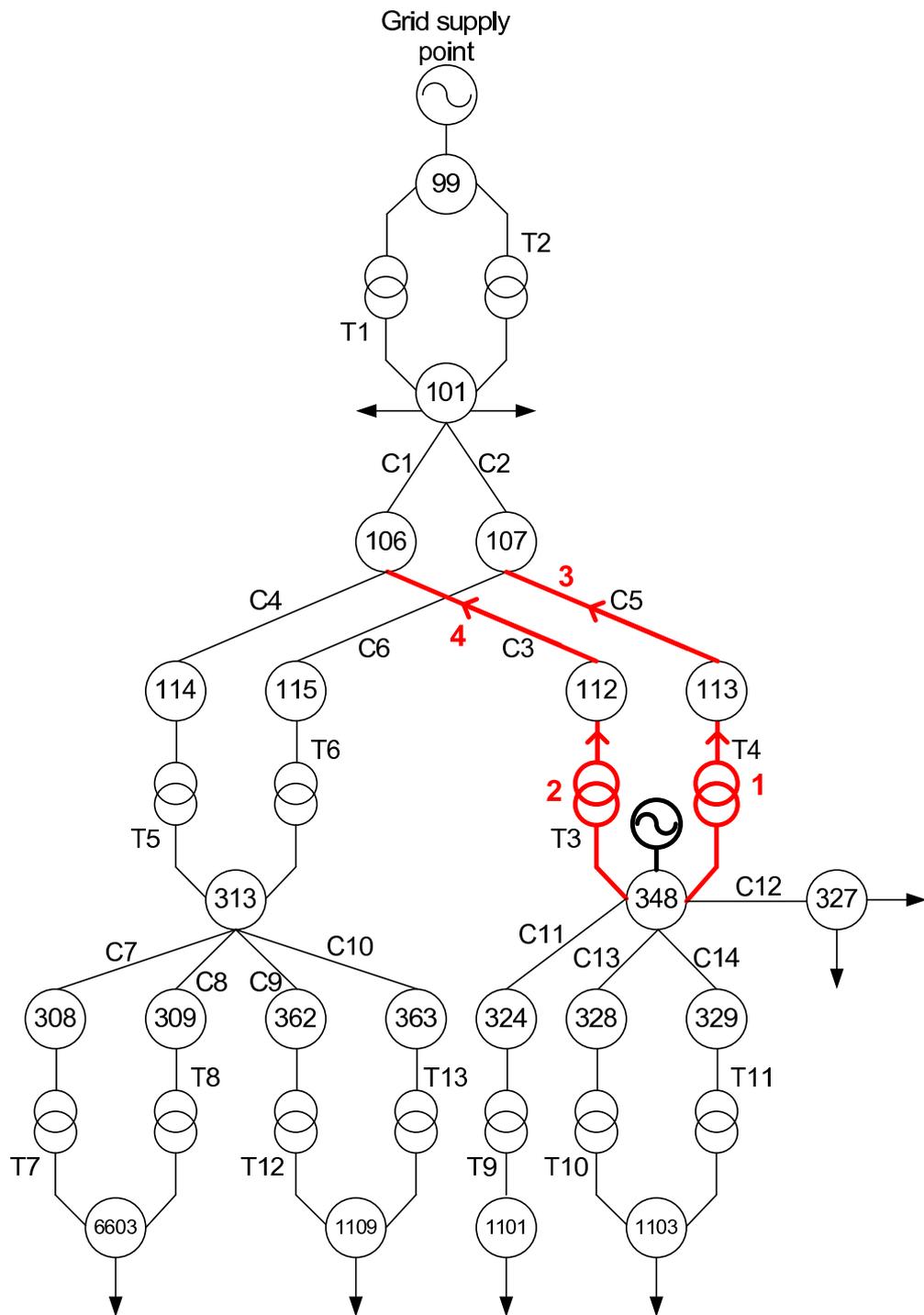
Figure 3.6: Hierarchy of thermally vulnerable components in UKGDS B due to DG connected at node 348
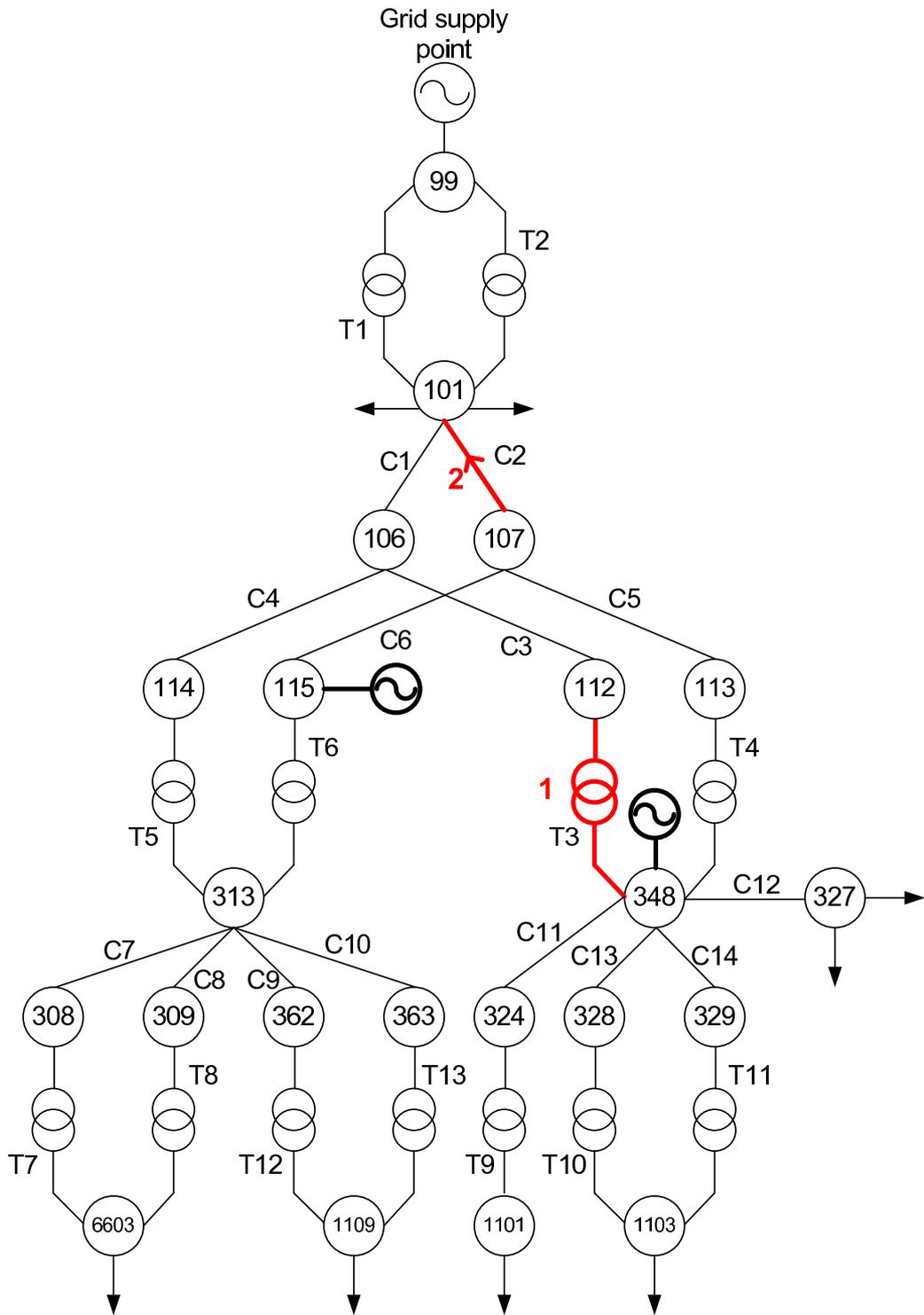
Figure 3.7: Hierarchy of thermally vulnerable components in UKGDS B due to DG connected at node 115
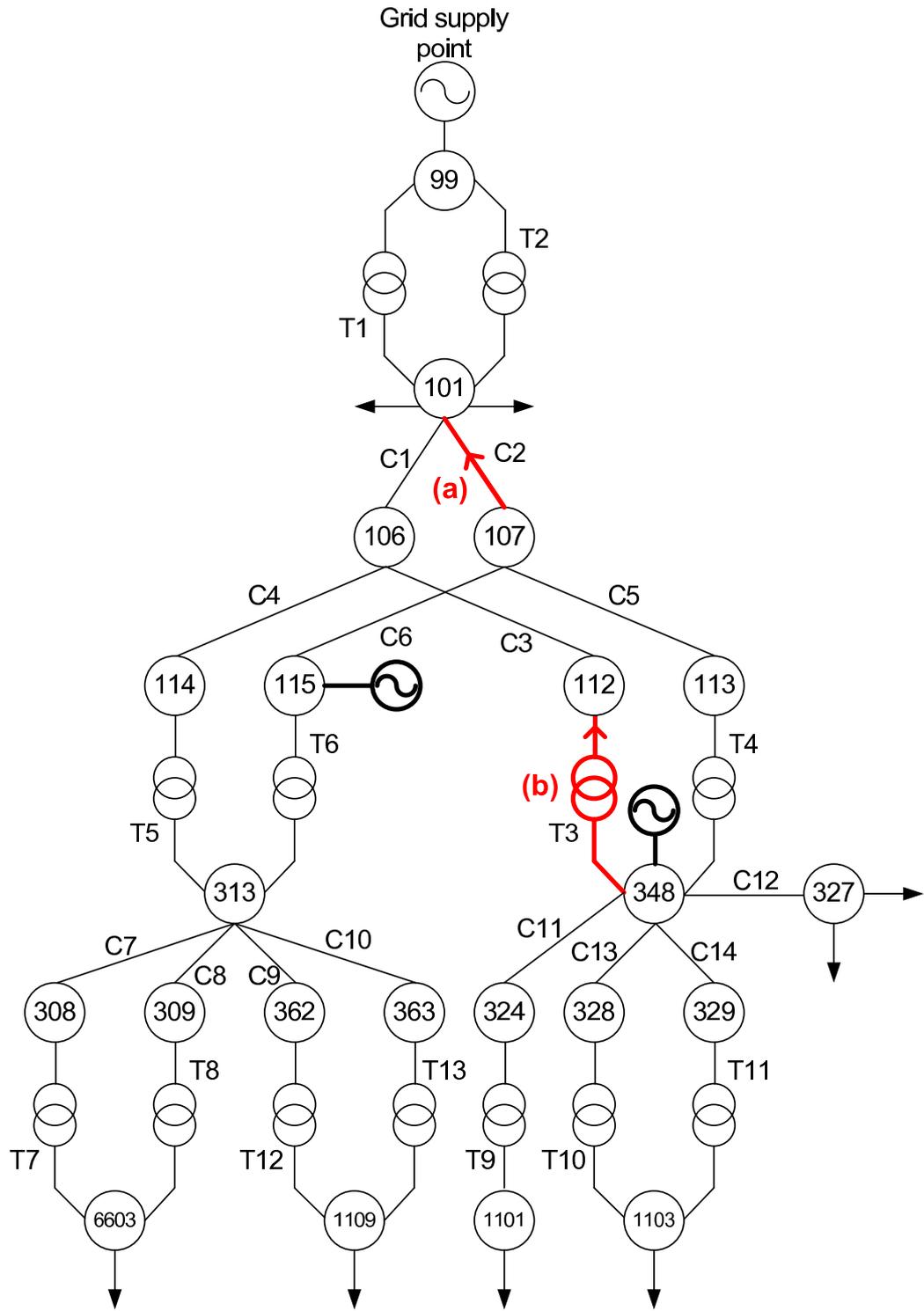
Figure 3.8: Hierarchy of thermally vulnerable components in UKGDS B due to DG interactions

The hierarchy of thermally vulnerable components resulting from increased DG connection capacities at node 338 (33kV) within UKGDS C is given in Figure 3.9 and were found to be:

1. Components T3 and T4 (132/33kV transformers) with $G_{P,338} = 268\,\text{MW}$.

2. Component T5 (132/33kV transformer) with $G_{P,338} = 272\,\text{MW}$.

3. Component C2 (132kV line) with $G_{P,338} = 284\,\text{MW}$.
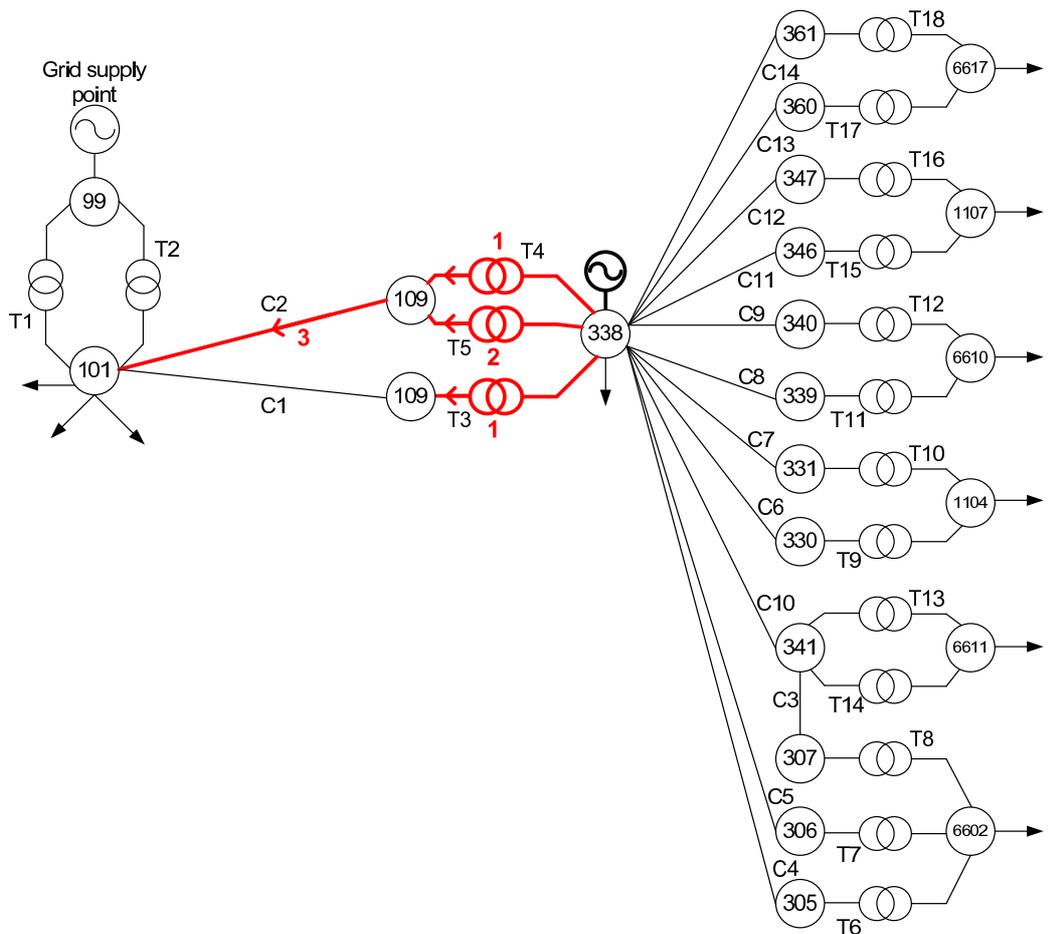
Figure 3.9: Hierarchy of thermally vulnerable components in UKGDS C due to DG connected at node 338

3.5.2   Numerical analysis applied to field trial network

The application of the numerical analysis methodology for identifying thermally vulnerable components within the field trial network is summarised in Figure 3.10 for single DG scheme impacts and Figure 3.11 for multiple DG impacts.
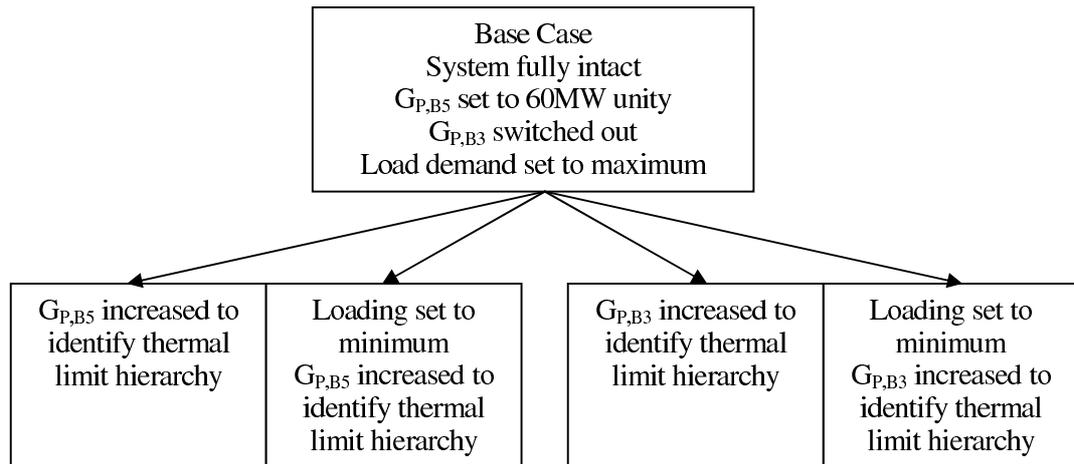
Figure 3.10: Application of numerical analysis to identify thermally vulnerable components within field trial network due to single DG schemes
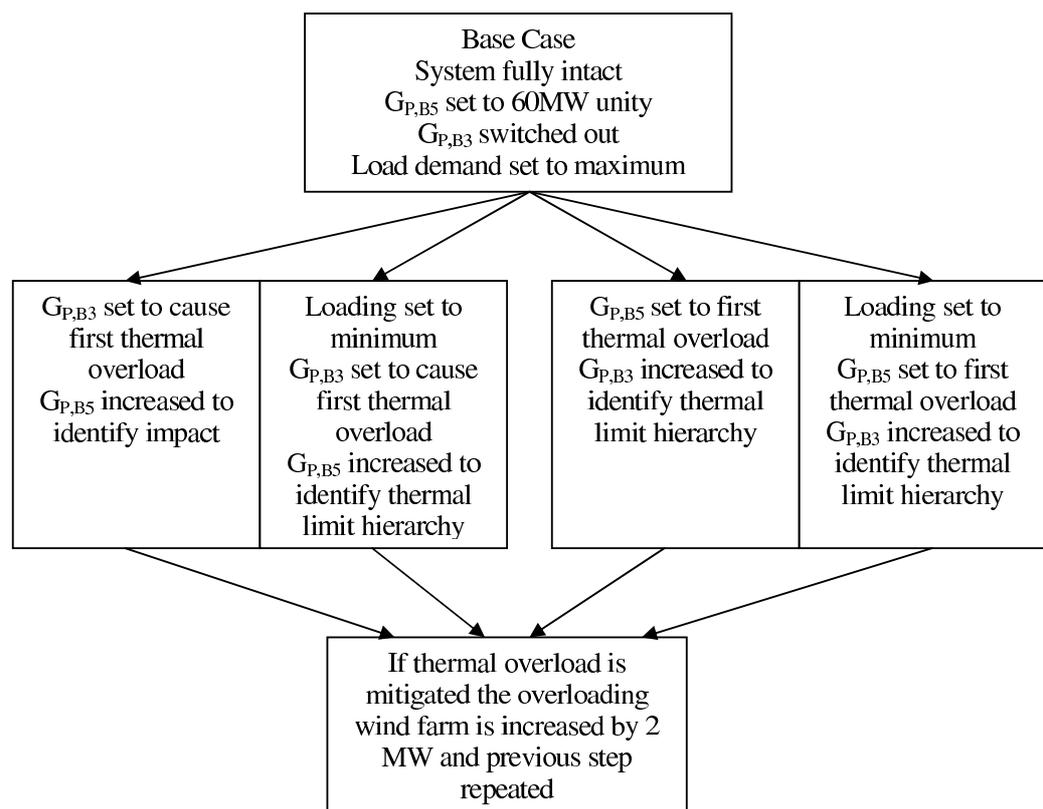
Figure 3.11: Application of numerical analysis to identify thermally vulnerable components within field trial network due to multiple DG schemes

The hierarchy of thermally vulnerable components resulting from increased DG connection capacities at node B5 within the field trial network is given in Figure 3.12. It was found that increasing the output of $G_{P,B5}$ caused the 132kV overhead line feeder, C4, to become thermally vulnerable under maximum and minimum loading conditions for connection capacities of 116 MW and 108 MW respectively. No other components became thermally vulnerable before the load flow algorithm failed to converge (beyond an installed capacity of 170 MW).

The hierarchy of thermally vulnerable components resulting from increased DG connection capacities at node B3 is given in Figure 3.13. For maximum network loading conditions it was found that the 132kV overhead line component C3 became thermally vulnerable for $G_{P,B3}$ power outputs beyond 118 MW. No further components were identified as being thermally vulnerable before the load flow algorithm failed to converge at DG connection capacities beyond 188 MW. For minimum network loading conditions it was found that DG connection capacities beyond 112 MW caused C3 to become thermally vulnerable, DG connection capacities beyond 186 MW caused the 132kV overhead line component C5 to become thermally vulnerable and DG connection capacities beyond 188 MW caused 132kV overhead line component C7 to become thermally vulnerable. Beyond 188 MW, in the minimum loading condition, the load flow algorithm failed to converge.

Figure 3.14 summarises the effect of DG power output interactions considering components C3 and C4 which represented the first components to become thermally vulnerable in the single DG scheme investigations. The area in which the DG may export power without causing a thermal overload within the field trial network is given for both maximum and minimum loading conditions. It is interesting to note the counter-flow relationship that means that export capacity of $G_{P,B3}$ can be unlocked by increasing the export of $G_{P,B5}$. This is a particular feature of meshed network topologies and arises due to voltage gradients and the impedance of power flows to local loads. An increase in $G_{P,B5}$ causes more of the local load to be met in that vicinity of the network and less power is needed from $G_{P,B3}$ to meet this loading condition. As a result the power exported from $G_{P,B3}$ along feeder C3 is reduced and the thermal limit is mitigated.
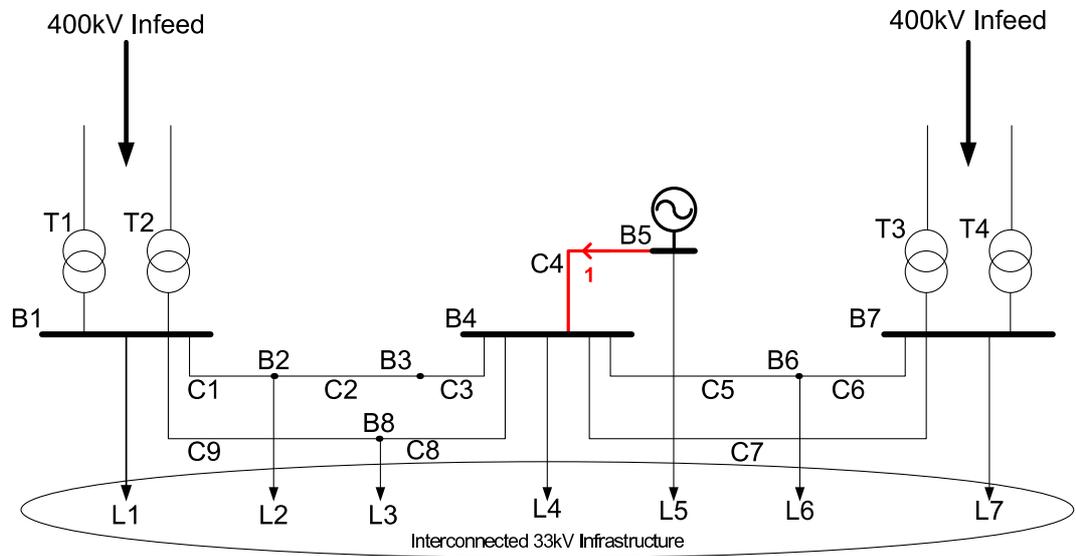
Figure 3.12: Hierarchy of thermally vulnerable components in field trial network due to DG connected at node B5
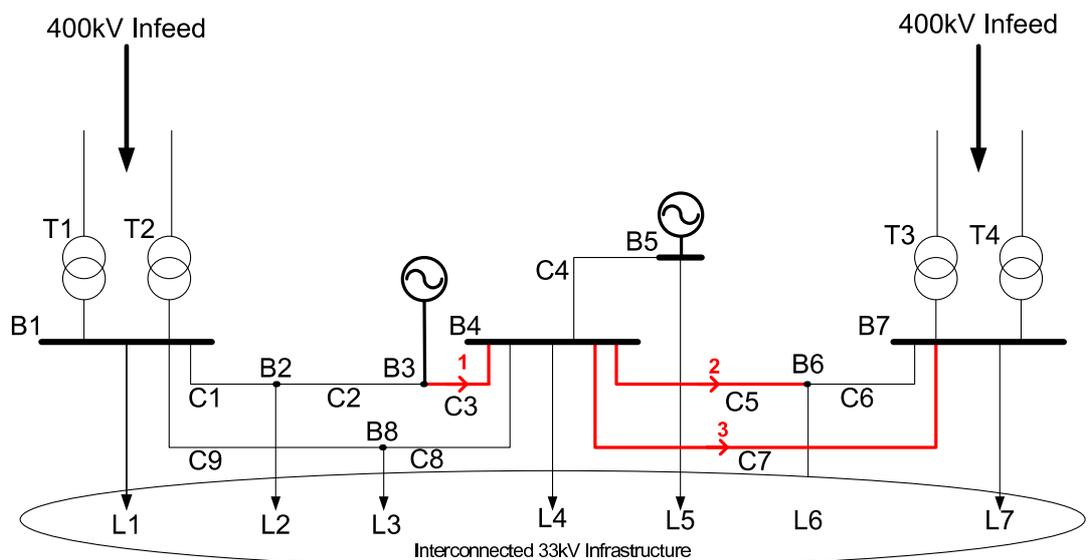
Figure 3.13: Hierarchy of thermally vulnerable components in field trial network due to DG connected at node B3
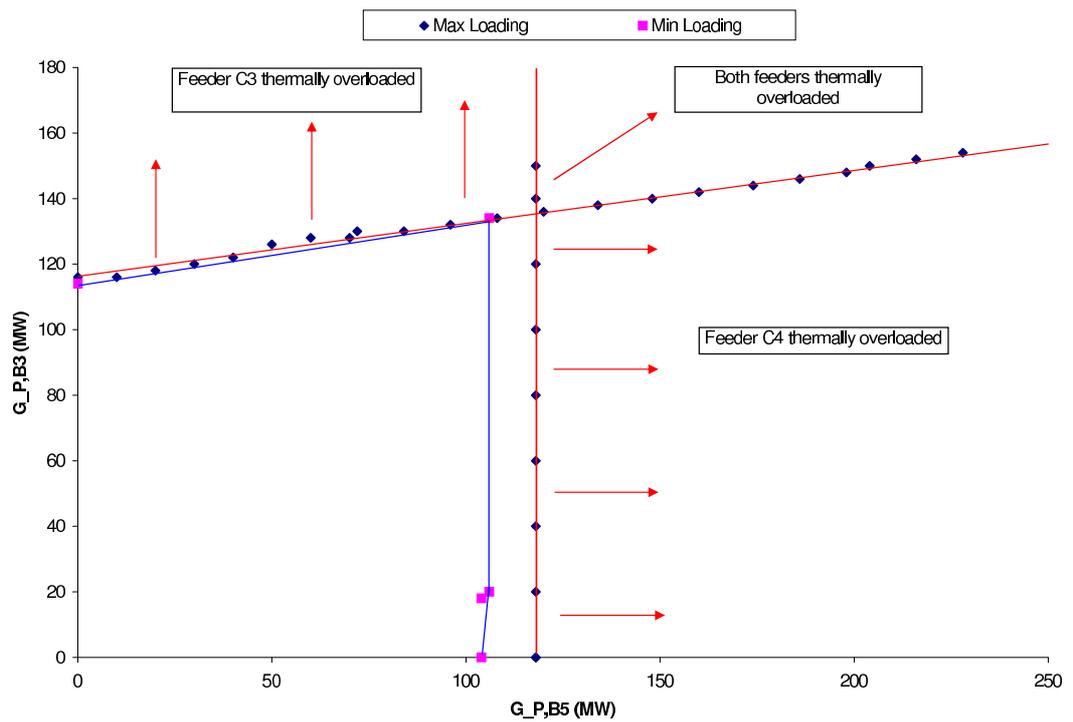
Figure 3.14: Thermal limit solution space in the field trial network

3.5.3   Discussion of numerical analysis applied to case study networks

The aim of the numerical analysis methodology was to identify the hierarchy of thermally vulnerable components as increased capacities of DG were connected within the case study distribution networks. The application of the methodology to UKGDSs aimed to tease out a wider set of thermally vulnerable components to those identified within the field trial network. The set of thermally vulnerable components identified through the case study analyses is given in Table 3.1.

In teasing out thermal issues relating to a variety of components and nominal voltage levels, it was found that the majority of the selected nodes in the UKGDSs could accommodate significant levels of DG relative to nominal voltage level of connection. This was because the selected nodes had a large number of components connected to them, providing many different power flow paths for the DG real power injection. The theoretical DG connection capacities at these nodes are likely to be limited before the first thermal limit of the power system is reached by other factors such as (i) security of supply compliance; (ii) economics for connecting DG at different voltage levels; and (iii) requisite planning permission.

Table 3.1: Thermally vulnerable component types resulting from case study analyses

Case study network	DG connection node	Subset of thermally vulnerable components
Field trial network	B5	132kV overhead line
Field trial network	B3	132kV overhead line
UKGDS A	316	33kV electric cables
UKGDS B	348	132/33kV transformers
		132kV overhead line
UKGDS B	115	132kV overhead lines
UKGDS C	338	132/33kV transfomers
		132kV overhead line

3.6   Discussion

At this preliminary stage, and without automating the analysis, the methodology was applied empirically. Thus it was found to be time-intensive, particularly when the incremental size of the DG capacity was small relative to the technical connection capacity which could be accommodated. However, the methodology resulted in a good indication of the maximum technical DG connection capacity that could be accommodated within distribution networks before thermal overloads occurred and was effective in identifying the hierarchy of thermally vulnerable components.

In order to reduce the analysis time required in applying the numerical methodology the 'bisection' numerical method [82] was utilised as follows:

1. Initial lower $(^{a}G_{i(LL)})$ and upper $(^{a}G_{i(UL)})$ bounds for the DG capacity search space were specified, where G_i corresponds to the size of the DG installed capacity, LL corresponds to the lower limit of the solution space (initially specified as $0\,\mathrm{MW}$), UL corresponds to the upper limit of the solution space and $a = 0$ represents the initial conditions of the analysis.

2. A load flow solution was run and any thermal violations present within the distribution network were identified through the exception-reporting capabilities of IPSA.

3. If a thermal violation was detected the solution space was narrowed by specifying $^{a+1}G_{i(LL)} = {}^{a}G_{i(LL)}$ and $^{a+1}G_{i(UL)} = \frac{{}^{a}G_{i(LL)} + {}^{a}G_{i(UL)}}{2}$. This halved the size of the solution search space.

4. If no thermal violations were detected the bounds of the solution space were adjusted by specifying $^{a+1}G_{i(LL)} = {}^{a}G_{i(UL)}$ and $^{a+1}G_{i(UL)} = \frac{^{a-1}G_{i(UL)} + {}^{a}G_{i(UL)}}{2}$, where, under initial conditions, $^{a-1}G_{i(UL)} = 2 \times {}^{a}G_{i(UL)}$ to expand the solution space until thermal violations were encountered.

5. Steps 2–4 were repeated until the DG connection capacity was found to a specified degree of accuracy (2 MW in the initial analysis and 0.1 MW in the validation analysis in Chapter 6).

Whilst the numerical methodologies outlined above are effective in identifying the location and hierarchy of thermally vulnerable components, the iterative nature of techniques, requiring multiple load flow runs, could potentially be time-intensive when compared to possible analytical techniques, utilising the underlying Jacobian matrix of the load flow solution. Moreover, the numerical techniques do not lend themselves, readily, to adaptation for the control of DG power outputs. Furthermore, the incorporation of updated component thermal ratings (resulting from up-ratings delivered by a real-time thermal rating system) would require completely new analysis to be carried out. Therefore an analytical methodology for identifying thermally vulnerable components within distribution networks, which has the potential to overcome the drawbacks associated with numerical analysis, is likely to be more attractive to DNOs or DG developers. A proposed analytical methodology for identifying thermally vulnerable components within distribution networks was developed and is presented in Chapter 5.

3.7   Conclusion

In this chapter the preliminary network analysis work, carried out in the early stages of the doctoral research, was presented and discussed. The basis of the present power system ratings used by DNOs for planning and operating distribution networks was presented and the case study networks selected for analysis throughout the thesis were described. The aims of the preliminary network investigations were to understand the electrical behaviour of the case study networks and identify thermal vulnerable components. A first-pass methodology for achieving the preliminary aims was presented and applied to the case study networks. The preliminary methodology was discussed and improvements to the methodology were suggested.

Chapter 4

Proposed methodology for DG output control system development

4.1 Introduction

This chapter proposes a methodology for the development of DG output control systems based on component thermal properties, as published by the author in [83]. In particular the role of power flow sensitivity factors within the proposed methodology is highlighted. power flow sensitivity factors are derived from a full AC load flow solution and define the mathematical relationship between changes in network component power flows due to changes in DG power outputs. This provides the direct mathematical link to the power flows in any component of the distribution network (not just the components electrically local to the DG scheme) and the DG scheme itself. The power flow sensitivity factors may be combined with power system thermal limits to identify, analytically, thermally vulnerable components within the distribution network. In addition, the derived power flow sensitivity factors may be utilised for the power output control of DG schemes. The main development stages in the DG output control system methodology are summarised below:

- Stage 1: Conduct an off-line assessment to identify areas of the distribution network that are thermally vulnerable to the penetration of DG. This may be achieved through the calculation of component thermal vulnerability factors by aggregating power flow sensitivity factors and component thermal ratings.

- Stage 2: Thermally characterise the vulnerable sections of the distribution network to quantify headroom gains that may be exploited through the use of a real-time thermal rating system. This may be achieved by the off-line analysis of directly monitored

conductor operating temperatures or by monitoring meteorological conditions that are then used to populate component steady-state thermal models.

- Stage 3: In situations where it is assessed to be viable, a system needs to be developed to allow the real-time exploitation of component thermal ratings.

- Stage 4: The component real-time thermal rating system could then be used to inform the power output control of DG for network power flow management. One means of achieving this is through the use of power flow sensitivity factors.

To reflect the key aspects of the proposed methodology, this chapter is structured in the following way: Section 4.2 discusses methods for the identification of thermally vulnerable components within distribution networks. Section 4.3 discusses the thermal characterisation of distribution networks (in light of the identified thermally vulnerable components). Section 4.4 outlines the development of real-time thermal rating systems through (i) the population of component steady-state thermal models with monitored meteorological conditions and (ii) the use of more sophisticated thermal state estimation techniques whereby a limited number of meteorological station installations may be used to assess the thermal status of wide areas of the distribution network. Section 4.5 describes DG output control for network power flow management based on component thermal properties. In addition, Section 4.6 describes the service oriented architecture (SOA) adopted (by recommendation of the consultancy firm, Imass) for the software architecture of the DG output control system.

4.2 Identification of thermally vulnerable components

The proposed first stage, in developing a DG output control system for network power flow management, is to identify the location of thermally vulnerable components within the distribution network. It is assumed that thermal violations will be relieved through the power output constraint of the DG scheme(s) causing components to become thermally vulnerable. By quantifying the severity of thermal vulnerability, a hierarchy of components can be identified, allowing the targeted development of component thermal models and informing network instrumentation investment decisions.

A preliminary set of off-line network analyses were conducted, to understand the behaviour of the distribution network, which involved the incremental increase in DG power outputs to cause component thermal violations and identify a hierarchy of thermally vul-

nerable components. The techniques adopted at this stage may be categorised as numerical methods and were described and discussed in Chapter 3.

In Chapter 5 an analytical methodology is proposed for the off-line calculation and assessment of thermal vulnerability factors [83]. Thermal vulnerability factors relate component power flow sensitivity factors (which can be derived from the Jacobian matrix in a full AC load flow solution) to component thermal limits. Thermal vulnerability factors are a measure of the change in component utilisations for a given injection of real power from a DG scheme. Thermal vulnerability factor assessments are not confined to a specific topology type and may be used to identify the thermal impacts of planned individual DG schemes, or in a more strategic way, to assess longer term and more widespread DG growth scenarios.

The identification of thermally vulnerable components within distribution networks may directly inform investment decisions regarding the installation of thermal monitoring equipment and/or for network reinforcement. If the monitoring equipment installation approach is adopted, the distribution network may be thermally characterised to assess the potential gains in developing a real-time thermal rating system for the thermally vulnerable component(s).

4.3   Network thermal characterisation

In the second stage of the DG output control system development methodology, distribution networks are thermally characterised by modelling the vulnerable sections of the power system identified in the previous methodology stage. This work was carried out at Durham University by a research colleague, Andrea Michiorri, also contributing towards the DIUS Project.

4.3.1   Component thermal models

In order to assess, in a consistent manner, power system real-time thermal ratings due to the influence of environmental conditions, thermal models were developed at Durham University based on IEC standards for overhead lines [30], electric cables [35] and power transformers [39]. Steady-state models were selected in preference to dynamic models since this would provide a maximum allowable rating for long term power system operation. Moreover, the estimation of final steady-state component temperatures after a transient has occurred is influenced by the initial conditions which must also be estimated. With the

resolution of data available (comprising hourly averaged environmental conditions) it would be extremely difficult to obtain an acceptable precision for dynamic models, particularly for overhead lines with time constants of less than an hour. The IEC component thermal models are described in detail in Chapter 7.

4.3.2   Instrumentation location selection

In order to select appropriate locations for network instrumentation a set of generic and field trial network-specific measurement requirements were developed. Measurements were categorised as electrical, thermal and meteorological and pertained to those needed for the DG output control system to function as well as verification measurements. Verification measurements were not input directly to the control system but used with an off-line tool to verify the accuracy of the algorithms within the DG output control system. This entailed the over-instrumentation of the field trial network for characterisation and prototype testing purposes. As a general rule the measurement equipment was to be placed at the most vulnerable and thermally sensitive points where it is difficult to estimate the thermal behaviour of the power system and failure to accurately predict the thermal limit would have severe consequences. Details of the network instrumentation process are provided in Chapters 7 and 13.

4.4   Real-time thermal rating system development

In the third stage of the methodology, real-time thermal rating systems are developed to exploit the potential headroom available in component power transfers, based on environmental conditions. This work was also carried out at Durham University by Andrea Michiorri. Real-time thermal rating systems, based on the direct population of component thermal models with environmental conditions and thermal state estimation techniques, are outlined below and described in detail in Chapter 7.

4.4.1   Direct population of thermal models with environmental conditions

In [84] research is presented which seeks to assist distribution network operators (DNOs) in the adoption of real-time thermal rating systems. The exploitation of power system rating variations is challenging due to the complex nature of environmental conditions such as wind speed. The adoption of a real-time thermal rating system may overcome this challenge and offers perceived benefits such as increased DG accommodation and avoidance of

component damage or premature ageing. Simulations, using lumped parameter component models, were used to investigate the influence of environmental conditions on overhead line, electric cable and power transformer ratings. Key findings showed that the average rating of overhead lines, electric cables and power transformers ranged from 1.70 to 2.53, 1.00 to 1.06 and 1.06 to 1.10 times the static rating, respectively. Since overhead lines were found to have the greatest potential for rating exploitation, the influence of environmental conditions on four overhead line types was investigated and it was shown that the value of a real-time thermal rating system is location dependent. Furthermore, the additional annual energy yield from DG that could be accommodated through a real-time thermal rating system deployment was quantified for a specific case and found to be 54%.

4.4.2   Thermal state estimation

In order to reduce network instrumentation requirements, deal with communication signal losses and in an attempt to make real-time thermal rating system deployments financially viable, research is presented in [85] which aims to realise a real-time thermal rating system for power system components based on thermal state estimation techniques. The solution developed by Andrea Michiorri at Durham University involves the use of a limited number of meteorological stations and a series of analytical models for estimating component ratings. The effect of data uncertainty is taken into account by an estimation algorithm based on the Monte Carlo method. Estimations of conductor temperature and environmental conditions were validated against measured data in five different network locations within the field trial network. Average errors of -2.2 °C, -1.9 °C, -1.2 °C, -1.9 °C and 1.4 °C were found for the five different network locations over a period of 71 days when comparing estimates to measured results. Results analysis identified that the IEC models used were the main source of error. The estimation of wind direction and solar radiation were the most sensitive to errors in the models.

4.5   DG output control using component thermal properties

The fourth stage of the methodology is the on-line (real-time) control of DG schemes based on component thermal properties. This entails the development of techniques for the control of single DG schemes and also the development of strategies for the control of multiple DG schemes based on power system static thermal ratings, seasonal thermal ratings or real-time thermal ratings.

As identified in Chapter 2, the control techniques documented in Engineering Technical Recommendation (ETR) 124 [50] could be implemented to fulfil the requirement of managing the power output of single DG schemes based on component thermal properties. Due to the wide acceptance of ETR 124 within the electrical power systems community, the implementation of the proposed techniques could provide credibility the DG output control system as it is developed into a commercialised product. The main drawback of ETR 124 is that it considers only single DG schemes and deals with the specific case of thermally vulnerable components local to the DG connection busbar.

The limitations of the techniques proposed in ETR 124 may be overcome through the development of control strategies for the output control of multiple DG schemes based on power flow sensitivity factors. In this case DG schemes may be controlled based on local and non-local thermal constraints where the power flows would be non-trivial to model algebraically. Since no techniques were identified in literature, at the time of conducting research, that adequately fulfilled the requirements for the output control of multiple DG schemes based on real-time thermal ratings, the theory of power flow sensitivity factors was extended to meet this need. The identified methods of DG output control, which are the focus of research presented in this thesis, are outlined in Sections 4.5.1 and 4.5.2 below.

4.5.1 Single DG scheme control using ETR 124 techniques

Based on ETR 124, the techniques for controlling the power output of a single DG scheme to manage network power flows include (i) the tripping of the DG scheme based on a static assessment of network availability; (ii) the tripping of the DG scheme based on seasonal thermal ratings; (iii) the demand-following output control of the DG scheme based on a static thermal rating; and (iv) the demand-following output control of the DG scheme based on real-time thermal ratings. The time-series simulation of these control techniques is described in detail in Chapter 10 and compared to the unconstrained connection of the DG scheme through network reinforcement.

4.5.2 Multiple DG scheme control using power flow sensitivity factors

Three candidate strategies for the output control of multiple DG schemes are investigated: (i) Last-in first-off (reflecting present contractual obligation practices); (ii) egalitarian (whereby a single percentage reduction signal is broadcast to all DG schemes); and (iii) technically most appropriate (whereby the most appropriate DG scheme to manage network power flows is selected to do so). In the author's publications, [86–88], the above

mentioned candidate strategies for the coordinated output control of multiple DG schemes are presented. The proposed strategies are underpinned by power flow sensitivity factors and allow real-time knowledge of power system thermal ratings to be utilised. This could be of value in situations where distribution network power flows require management as a result of DG proliferation. Through off-line open-loop time-series simulations, using historical data from a section of the UK distribution network, the candidate strategies are evaluated against a benchmark DG tripping control solution in terms of annual energy yields, component losses and voltages. Furthermore, the individual DG scheme annual energy yields and DG-apportioned losses are used to assess the net present values of candidate control strategies to DG scheme developers. These analyses are described in detail in Chapter 11 for the output control of multiple DG schemes arising from a single thermal constraint within the distribution network and in Chapter 12 for the control of multiple DG schemes in light of multiple thermal constraints within the distribution network.

4.6 Control system software architecture

Drawing on the expertise of consultants at Imass, the DG output control system was developed using a SOA [5] that can be implemented using web services [89]. A SOA is an information technology approach in which software applications make use of services available within a network (such as the world wide web). Each service may provide a single function or multiple functions to a client (another software application). An application is exposed to other applications as a service which means that it has a standard interface and data is passed between services using standard protocols. This allows the implementation of the service to be independent (in terms of language and/or platform) from other services within the network. Web services are an implementation of the SOA approach which allow the services to be geographically dispersed in terms of hardware platforms. This also allows the services to be accessed by remote graphical user interfaces (a feature which was deemed to be particularly beneficial in the DIUS Project since ScottishPower EnergyNetworks are based in the North-West of England, Parsons Brinckerhoff, Imass and Durham University in the North-East of England and AREVA in The Midlands). The specific benefits arising from the adoption of a SOA are [89]:

1. Re-usability of applications which run on different operating systems, are coded in different languages and use different programming interfaces and protocols;

2. Interoperability of applications through standard communication protocols that facil-
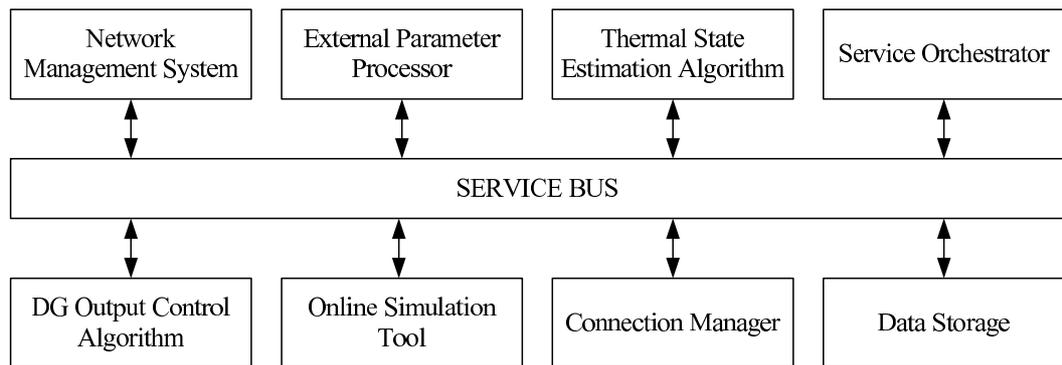
Figure 4.1: Service oriented architecture of controller software

itate cross-platform and/or cross-language interactions;

3. Scalability of the entire software architecture as new services are identified, developed and implemented;

4. Flexibility of the architecture to allow services to evolve without having to change the interface requirements; and

5. Cost efficiency through the integration of legacy systems and new software applications where the development of multiple application interfaces is prohibitively expensive in the long term.

The SOA of the DG output control system is outlined in Figure 4.1. A description of the services is given below and comprise the network management system interface service, a data storage service, an external parameter processing service, a thermal state estimation service, a DG output control service, an on-line simulation tool service, a DG connection manager service and a control system orchestration service.

4.6.1   Network management system

The network management system service is responsible for extracting the required electrical and thermal monitoring data from the distribution network and passing it to the data storage service. In the algorithm development phase of the research the electrical monitoring of the distribution network was provided through historical SCADA data, acquired by querying the DNO's PI database and extracting the required information as a series of Microsoft Excel spreadsheets. The data for characterising the network thermally was provided by (i) the MetOffice in the form of Microsoft Access database reports and (ii) the

data polled from FMCTech installations (described in Chapter 7) and available to download from a web browser as Microsoft Excel spreadsheets. In the field trial implementation phase of the research the electrical and thermal parameters were monitored using a series of AREVA's MiCOM relays. Since the relays have been developed to provide real-time protection functionality the software has been implemented using the C programming language. The harvested data is then polled back to a MySQL database.

4.6.2 Data storage

The data storage service is responsible for providing the control algorithm and on-line simulation tool services with electrical data, and the external parameter processor and thermal state estimation services with meteorological data. In the development phase of the research electrical data was stored as tab delimited text files to remove unnecessary data formatting associated with Microsoft Excel spreadsheets for memory efficiency. The thermal data was stored in a Microsoft Access database. In the field trial implementation phase of the research both the electrical and meteorological datasets were stored in a MySQL database.

4.6.3 External parameter processor

As a client the external parameter processor requests the meteorological information from the data storage service. As a service the external parameter processor is responsible for interpolating environmental conditions (such as wind speed, wind direction, air and soil temperatures and solar radiation) harvested from a limited number of meteorological measurement units. The adopted approach allows environmental conditions to be estimated, corrected and interpolated to represent more accurately the actual environmental operating conditions in areas of the distribution network. The inverse distance interpolation technique [90] allows environmental conditions to be determined over a wide geographical area using a reduced set of inputs. This is attractive for situations where a large amount of installed measurements may be financially unattractive to the distribution network operator (DNO) or DG scheme developer. The technique is also computationally efficient and allows the input locations to be readily adapted. The external parameter processor service was developed and implemented using the Visual Basic programming language.

4.6.4   Thermal state estimation

As a client the thermal state estimation service requests meteorological interpolations from the external parameter processor service. As a service the thermal state estimator is responsible for assessing the rating of components which are not directly monitored within the power system. Thermal state estimations facilitate the precise and reliable assessment of environmental conditions whereby a limited number of meteorological monitoring installations facilitate the computation of component thermal ratings within a wide area. This may then be validated through the carefully selected monitoring of component operating temperatures. The algorithm provides a reliable estimation of power system component thermal ratings described by an appropriate cumulative probability function. A state estimation technique based on the Monte Carlo method is used, giving a more complete description of the possible states of the system. The minimum, maximum, average and standard deviation of component ratings may be calculated according to the local meteorological conditions. As necessary for overhead lines and electric cables, each component is divided into sections to take into account different thermal operating conditions such as overhead line orientations and changes in electric cable installation conditions. The section resulting in the lowest rating values is then used to provide a rating for the entire component. Furthermore, the deployment of a real-time thermal rating system underpinned by thermal state estimation techniques has the potential to reduce the necessity of auxiliary communications infrastructure whilst simultaneously increasing the reliability of the system if measurement or communication failures occur. The thermal state estimation service was developed and implemented in Visual Basic for the field trial prototype control system.

4.6.5   Control algorithm

As a client the control algorithm requests electrical data from the data storage service and power system thermal ratings from the thermal state estimation service. As a service the control algorithm calculates DG output adjustments for network power flow management. As appropriate the updated DG output set points are passed to the on-line simulation tool service for validation. The control algorithm is described in more detail in Chapter 8. In the algorithm development phase of the research the control algorithm was developed using the Python programming language due to its rapid prototyping benefits and capability to automatically run the IPSA load flow package. For the field trial implementation the control algorithm was developed in the Java programming language due to its web-service

benefits, robustness and the software support available for this language from Imass.

4.6.6   On-line simulation tool

As a client the on-line simulation tool requests electrical information from the data storage service and updated DG output set points from the control algorithm. As a service the on-line simulation tool aids in validating the integrity of the control actions by running load flows with the present electrical information and the updated DG set points. The service returns updated component power flows and updated busbar voltages to the control algorithm. This then verifies that all power flows are within thermal limits and no voltage violations are present in the network (resulting from the control actions). If, through the on-line simulation tool, the control algorithm detects a thermal violation is still present in the network the DG is constrained further until no thermal violations are present. The on-line simulation tool was developed and implemented using IPSA with a Python 'wrapper' (or scripted interface)[1].

4.6.7   Connection manager

As a client the connection manager requests updated DG output set points from the control algorithm, which have been validated through the on-line simulation tool. As a service the connection manager is responsible for dispatching the updated real power set points to various DG operators within the jurisdiction of the DG output control system. This will be done, initially, through the decision support of control engineers within the DNO control room. However, as confidence in the control system grows, it is possible that closed-loop automatic active generation control could be achieved [60].

4.6.8   Control system orchestrator

As a client the control system orchestrator is triggered by an updated signal from a real-time system clock. As a service the control system orchestrator is responsible for coordinating the other services [89] to achieve the overall objectives of the DG output control system (i.e. DG output control for network power flow management based on component thermal properties).

---

[1]In the commercialised solution it is possible that the DG output control system could be installed without the on-line simulation tool if the DNO or DG developer is satisfied with the integrity of the control system without this feature.

4.7   Conclusions

This chapter has outlined a proposed methodology for DG output control system development in order to manage power flows within distribution networks. The first stage requires an assessment of the location of thermally vulnerable components within the distribution network. This is achieved through the off-line calculation of thermal vulnerability factors that relate component power flow sensitivity factors to component thermal limits. This directly informs Stage 2 – the targeted development of component thermal models and investment in equipment monitoring installations for network thermal characterisation. In Stage 3, steady-state component thermal models are populated with real-time environmental information from the meteorological stations to generate power system real-time thermal ratings. In Stage 4, the power flow sensitivity factors calculated in Stage 1 are embedded within a network power flow management system which, together with the component real-time thermal ratings calculated in Stage 3, is used to control the power output of DG schemes.

Whilst the role of power flow sensitivity factors is highlighted, particularly, since the factors may be used in Stages 1 and 4 of the methodology, clearly the methodology could be implemented with totally different techniques. For example optimal power flow (OPF) tools could be used to identify thermally vulnerable components within distribution networks, thermal imagery cameras could be used to inform instrumentation investment decisions, the thermal rating system could be based on numerical (not analytical) component thermal models and DG output control could be achieved through a 'trim and trip' approach. If different techniques are used to implement the stages in the methodology to those proposed in this thesis, this would demonstrate the potential flexibility (and hence value) of the methodology in providing a framework for the development of DG output control systems.

A description of the software services within the SOA were given and comprise the network management system interface service, a data storage service, an external parameter processing service, a thermal state estimation service, a DG output control service, an on-line simulation tool service, a DG connection manager service and a control system orchestration service. Adopting an SOA for the DG output control system allows algorithm implementation in different programming languages and across a number of hardware platforms in a fully centralised, fully decentralised or partially centralised / decentralised manner.

Chapter 5

Identification of thermally vulnerable components within distribution networks: Theory

5.1 Introduction

This chapter describes the analytical theory of power flow sensitivity factors, the formulation of thermal vulnerability factors and an empirical procedure for assessing power flow sensitivity factors and thermal vulnerability factors. The research presented in this chapter was published by the author in [83]. In addition, the off-line use of power flow sensitivity factors for sizing the installed capacity of non-firm distributed generation (DG) connections and preliminary investigations into the on-line use of power flow sensitivity factors for real-time DG output control are also described. Power flow sensitivity factors are integral to the work presented in this thesis and are related to the governing power flow equations for AC electrical networks in Section 5.2. Power flow sensitivity factors facilitate the identification of thermally vulnerable components by combination with power system steady-state thermal limits to formulate thermal vulnerability factors (as described in Section 5.3). Moreover, power flow sensitivity factors may be incorporated within strategies for the power output control of multiple DG schemes to manage power flows within distribution networks. An empirical procedure for the assessment of power flow sensitivity factors and thermal vulnerability factors is given in Section 5.4. The use of power flow sensitivity factors together with component thermal limits for the sizing of non-firm DG connections is described in Section 5.5. The preliminary use of power flow sensitivity factors together with component thermal ratings for real-time DG output control is described in Section

5.6. In Chapter 6, the analytical techniques presented in this chapter are applied to the case study networks that were detailed in Chapter 3.

5.2   Power flow sensitivity factors

The work presented in this thesis uses the Newton-Raphson method for solving power system load flows [66]. Changes in real and reactive power flows are related to the change nodal voltage magnitudes and voltage angles, as given in (5.1)

$$
\begin{bmatrix} \Delta P_i \\ \Delta Q_i \\ \Delta P_k \\ \Delta Q_k \\ \vdots \end{bmatrix} = \begin{bmatrix} J \end{bmatrix} \begin{bmatrix} \Delta \theta_i \\ \dfrac{\Delta |V_i|}{|V_i|} \\ \Delta \theta_k \\ \dfrac{\Delta |V_k|}{|V_k|} \\ \vdots \end{bmatrix} \tag{5.1}
$$

where θ_i and θ_k represent voltage angles at nodes i and k respectively, $|V_i|$ and $|V_k|$ represent nodal voltages, P_i and P_k represent real power injections at nodes i and k respectively, Q_i and Q_k represent reactive power injections at nodes i and k respectively and J is the Jacobian matrix, as given in (5.2).

$$
\begin{bmatrix} J \end{bmatrix} = \begin{bmatrix} \dfrac{\partial P_i}{\partial \theta_i} & \dfrac{\partial P_i}{\partial |V_i|} & \cdots \\[2ex] \dfrac{\partial Q_i}{\partial \theta_i} & \dfrac{\partial Q_i}{\partial |V_i|} & \cdots \\[2ex] \vdots & \vdots & \ddots \end{bmatrix} \tag{5.2}
$$

Once the inverse Jacobian has been evaluated in the full AC power flow solution, perturbations about a given set of system conditions may be calculated as in (5.3). This gives the changes expected in bus voltage angles and voltage magnitudes due to injections of real or reactive power.

$$
\begin{bmatrix}
\Delta\theta_i \\
\dfrac{\Delta|V_i|}{|V_i|} \\
\Delta\theta_k \\
\dfrac{\Delta|V_k|}{|V_k|} \\
\vdots
\end{bmatrix}
=
\begin{bmatrix} J \end{bmatrix}^{-1}
\begin{bmatrix}
\Delta P_i \\
\Delta Q_i \\
\Delta P_k \\
\Delta Q_k \\
\vdots
\end{bmatrix}
\tag{5.3}
$$

The work presented in this thesis is specifically concerned with calculating the effect of a perturbation of ΔP_m that is an injection of power at unity power factor (real power) into node m. Since the generation shifts, the reference (slack) bus compensates for the increase in power. The $\Delta\theta$ and $\Delta|V|/|V|$ values in (5.4) are thus equal to the derivative of the bus angles and voltage magnitudes with respect to a change in power at bus m.

$$
\begin{bmatrix}
\Delta\theta \\
\dfrac{\Delta|V|}{|V|}
\end{bmatrix}
=
\begin{bmatrix} J \end{bmatrix}^{-1}
\begin{bmatrix}
\Delta P_m \\
\Delta Q_m \\
\vdots \\
\Delta P_{ref} \\
\Delta Q_{ref}
\end{bmatrix}
\tag{5.4}
$$

Thus the sensitivity factors for a real power injection at node m are given in (5.5)-(5.8)

$$
f(\theta) : \frac{dP^c_{i,k}}{dG_{P,m}} = \left(\frac{\partial P}{\partial\theta}\right)_{i,k} \left(\frac{d\theta_k}{dG_{P,m}} - \frac{d\theta_i}{dG_{P,m}}\right)
\tag{5.5}
$$

$$
f(|V|) : \frac{dP^c_{i,k}}{dG_{P,m}} = \left(\frac{\partial P}{\frac{\partial|V|}{|V|}}\right)_{i,k} \left(\frac{\frac{d|V_k|}{|V_k|}}{dG_{P,m}} - \frac{\frac{d|V_i|}{|V_i|}}{dG_{P,m}}\right)
\tag{5.6}
$$

$$
f(\theta) : \frac{dQ^c_{i,k}}{dG_{P,m}} = \left(\frac{\partial Q}{\partial\theta}\right)_{i,k} \left(\frac{d\theta_k}{dG_{P,m}} - \frac{d\theta_i}{dG_{P,m}}\right)
\tag{5.7}
$$

$$
f(|V|) : \frac{dQ^c_{i,k}}{dG_{P,m}} = \left(\frac{\partial Q}{\frac{\partial|V|}{|V|}}\right)_{i,k} \left(\frac{\frac{d|V_k|}{|V_k|}}{dG_{P,m}} - \frac{\frac{d|V_i|}{|V_i|}}{dG_{P,m}}\right)
\tag{5.8}
$$

where $f(\theta)$ and $f(|V|)$ represent functions of voltage angles and voltage magnitudes respectively, $(\partial P/\partial\theta)_{i,k}$, $(\partial P/\partial|V|)_{i,k}$, $(\partial Q/\partial\theta)_{i,k}$ and $(\partial Q/\partial|V|)_{i,k}$ represent elements within the Jacobian matrix and $d\theta_i/dG_{P,m}$, $d|V_i|/|V_i|$, $d\theta_k/dG_{P,m}$ and $d|V_k|/|V_k|$ represent elements corresponding to the vector (5.9) evaluated in (5.4).

$$
\begin{bmatrix}
\Delta\theta \\
\dfrac{\Delta|V|}{|V|}
\end{bmatrix}
\tag{5.9}
$$

This gives an overall (apparent) power flow sensitivity ($SSF_{i,k,m}^c$) of component c, from node i to node k, due to an injection of real power, at node m, as in 5.10.

$$
SSF_{i,k,m}^c = \left\{ \left[\left(\frac{\partial P}{\partial \theta} \right)_{i,k} \left(\frac{d\theta_k}{dG_{P,m}} - \frac{d\theta_i}{dG_{P,m}} \right) \right] + \left[\left(\frac{\partial P}{\frac{\partial |V|}{|V|}} \right)_{i,k} \left(\frac{\frac{d|V_k|}{|V_k|}}{dG_{P,m}} - \frac{\frac{d|V_i|}{|V_i|}}{dG_{P,m}} \right) \right] \right\}
$$

$$
+ j \left\{ \left[\left(\frac{\partial Q}{\partial \theta} \right)_{i,k} \left(\frac{d\theta_k}{dG_{P,m}} - \frac{d\theta_i}{dG_{P,m}} \right) \right] + \left[\left(\frac{\partial Q}{\frac{\partial |V|}{|V|}} \right)_{i,k} \left(\frac{\frac{d|V_k|}{|V_k|}}{dG_{P,m}} - \frac{\frac{d|V_i|}{|V_i|}}{dG_{P,m}} \right) \right] \right\}
$$

$$(5.10)$$

Simplified versions of the power flow sensitivity factor theory (focusing on the $P - \theta$ sensitivity) are used at the transmission level for real power flow sensitivity analyses. The generation shift factor (GSF) technique proposed by Wood and Wollenburg [66] is acceptable for use in DC representations of AC systems where the network behaviour is approximated by neglecting MVAr flow and assuming voltage to be constant. However, in distribution networks those assumptions do not always hold since, in some cases, the ratio of $\frac{X}{R} \simeq 1$ and reactive power flow may contribute to a significant portion of the resultant power flowing in components. Thus it is important that both real and reactive power flows are considered when assessing the locations of thermally vulnerable components and developing techniques for the on-line power output control of DG.

The phenomenon of bi-directional power flow is becoming increasingly more common in distribution networks. Particularly, in situations when DG power outputs meet local load demands and power is exported in the opposite direction through feeders or back through transformers into higher voltage levels. Thus it is important to be aware of the reverse power flow capability of transformers [91]. Since the connection of DG may cause power flows to reverse through components under certain load-generation patterns, a frame of reference must be established whereby power flow sensitivities can be related to power flow directions and directional limits. Only by doing this is it possible to assess whether the power flow sensitivities of components to concurrent nodal injections will cause power flows to aggregate through the components or oppose one another, creating counter-flows and finding different impedance routes through the network. Pantos and Gubina describe this phenomenon in a simple diagram that displays the four possible power flow combinations of real and reactive power flow flowing to and from nodes in the same reference frame [92].

5.3 Thermal vulnerability factors

Equation (5.10) may be combined with power system thermal limits (3.3), as detailed in Chapters 3 and 7, and the resulting thermal vulnerability factor, as seen in (5.11), is standardised by conversion to a per unit term on the base MVA

$$TVF_{i,k,m}^c = \frac{SSF_{i,k,m}^c}{S_{i,k(lim)}^c} \; on \; S_{base} \tag{5.11}$$

where $TVF_{i,k,m}^c$ represents the thermal vulnerability factor of component c, from node i to node k due to a real power injection at node m, $SSF_{i,k,m}^c$ represents the overall (or apparent) power flow sensitivity factor of component c, from node i to node k, due to a real power injection at node m, $S_{i,k(lim)}^c$ represents the thermal limit of component c from node i to node k and S_{base} is a predefined MVA base.

This gives a consistent measure of component thermal vulnerabilities, relative to one another and accounts for different nodal real power injections, for a particular network operating condition. It can also be seen in (5.12) that the apparent power flow sensitivity factor relative to the component rating is equivalent to the change in utilisation of a particular component c from node i to node k, due to an injection of real power at node m

$$\frac{SSF_{i,k,m}^c}{S_{i,k(lim)}^c} = \frac{\Delta S_{i,k}^c}{\Delta G_{P,m} \times S_{i,k(lim)}^c} \equiv \frac{\Delta U_{i,k}^c}{\Delta G_{P,m}} \tag{5.12}$$

where $SSF_{i,k,m}^c$ represents the apparent power flow sensitivity factor of component c, from node i to node k, due to a real power injection at node m, $S_{i,k(lim)}^c$ represents the thermal limit of component c from node i to node k, $\Delta S_{i,k}^c$ represents the change in apparent power flow in component c from node i to node k, $\Delta G_{P,m}$ represents the change in real power injection at node m and $\Delta U_{i,k}^c$ represents the change in capacity utilisation of component c from node i to node k.

Power flow sensitivity factors indicate the extent to which power flow changes within components due to nodal power injections. However, a large change in power flow, indicated by high sensitivity, does not necessarily mean a component is thermally vulnerable unless its rating is taken into account. A large power flow change in a component with a large thermal rating ($S_{i,k(lim)}^c$) could be less critical than a small power flow change in a component with a small rating. By calculating the apparent power sensitivity relative to rating for each component, the thermally vulnerable components are identified and can be ranked for single nodal power injections or accumulated for multiple injections.

The physical meaning of the thermal vulnerability factor has been described in 5.12 as the change in a component capacity utilisation due to a per unit DG injection at a particular node. Depending on the status of the original power flow before DG is connected, an excursion relative to rating of 100% (or $TVF_{i,k,m}^{c} = 1$), does not necessarily mean a component is thermally overloaded. By definition the maximum possible $TVF_{i,k,m}^{c}$ without overload occurring could be just below 200%, recognising that a power flow utilising almost 100% of thermal capacity in one direction may be reversed by a DG injection to become 100% utilisation with power flowing in the opposite direction.

5.4 Power flow sensitivity factor and thermal vulnerability factor assessments

The procedure used to assess power flow sensitivity factors and generate lists of thermally vulnerable components for different network topologies is shown in Figure 5.1.

Initially a 'base case' AC load flow was run in the power system simulation package, IPSA [93], to establish initial real, reactive and apparent power flows for each component. The procedure iterated by injecting 1 pu of real power (in this case on 100 MVA base) at each node of interest and recording the new component power flows. In the United Kingdom generic distribution systems, new DG connections have been assumed at existing nodes in the network. However, in the field trial application the two nodes selected for thermal vulnerability assessments (and resulting DG power output control) correspond to existing DG connection points where DG may be replanted with larger installed capacities due to future planning applications. The initial flow, final flow and thermal rating of each component were used to relate component power flow sensitivity factors to nodal injections and ratings. The resulting power flow sensitivity factors and thermal vulnerability factors were efficiently stored in matrix form and, with the thermal vulnerability factors represented graphically, a visual identification of the most thermally vulnerable components was given. This also allowed negligible thermal vulnerability factors to be filtered out by inspection. Assessments were made at maximum generation-maximum loading and maximum generation-minimum loading conditions to identify the worst-case operating scenario for the critical components. Voltage limits in accordance with [15] and [94] were not directly formulated as constraints within the assessments but were constantly monitored in simulation runs through the functionality in IPSA to colour-code the network diagram according to voltage excursions.
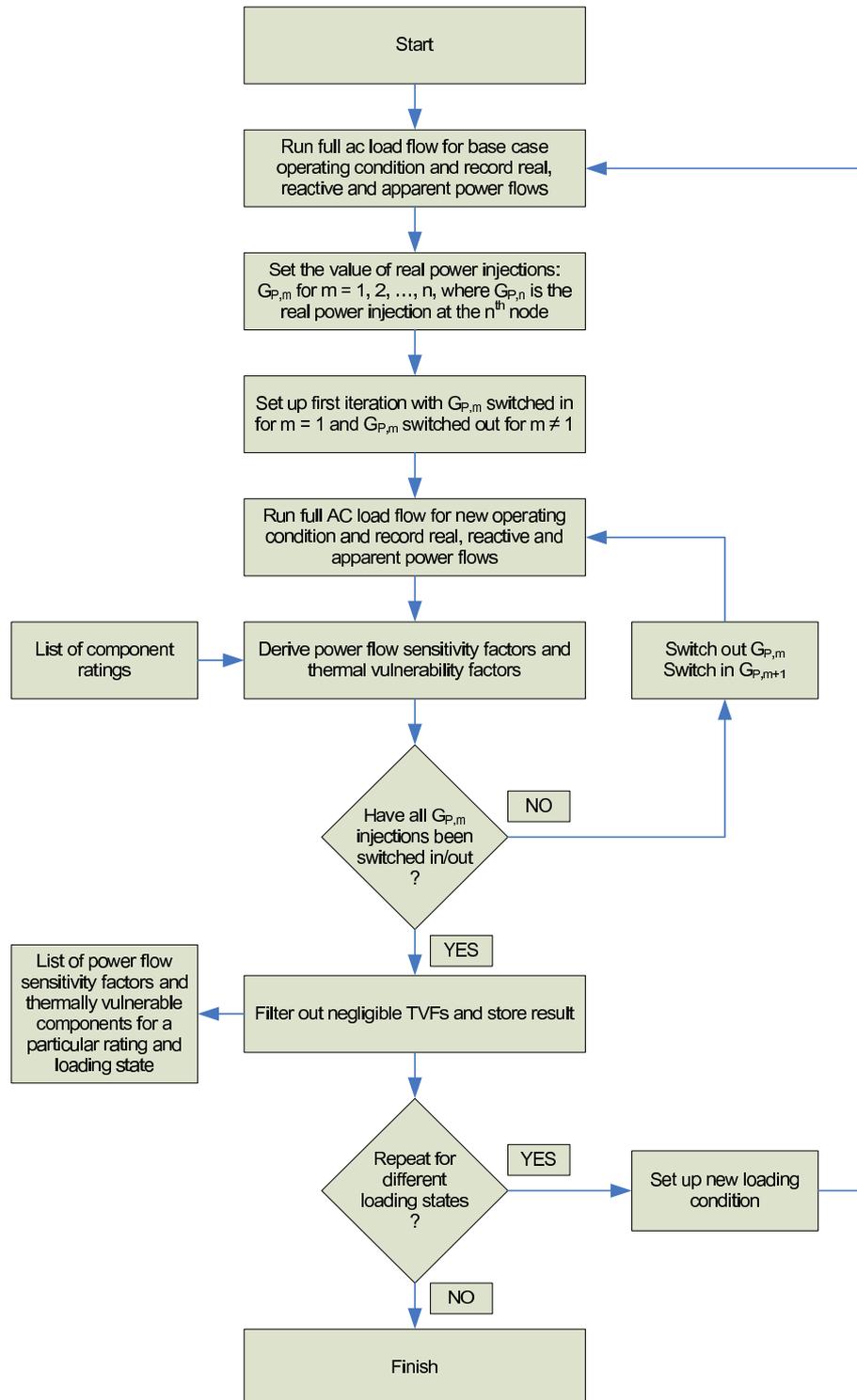
Figure 5.1: Flow chart for the assessment of power flow sensitivity factors and thermal vulnerability factors

The thermal vulnerability factor assessments presented in this thesis complement network characterisation, such as that carried out in [42] by first identifying the type (overhead line, underground cable, power transformer) and geographical location of thermally vulnerable components. The assessments may be used to give a holistic network view of the impact of multiple DG schemes in concurrent operation on accumulated power flows and hence vulnerable component locations.

5.5 Sizing the potential capacity of non-firm DG connections through power flow sensitivity factors

In order to identify thermally vulnerable components within distribution networks, the connection capacity of DG schemes was increased and the DG technical connection capacity was assessed at the first thermal limit of the power system. In Chapter 3, the technical connection capacity of DG schemes was assessed through a numerical method by incremental increases in DG power output. This method could have been adapted for single and multiple DG scheme power output control by developing an algorithm that incrementally ramped up or ramped down DG scheme outputs depending on network availability or power flow constraints. However, depending on the increment size and the magnitude of the DG constraint or constraint relaxation, and given the real-time control application to which this research was contributing, this technique (at the time of consideration) was deemed to be computationally-intensive and time-intensive.

By utilising the real component of the power flow sensitivity factors (already derived through the thermal vulnerability factor assessment applications), the analytical equation given in (5.13) may be used to linearise the power flow problem and predict DG technical connection capacities, at nodes of interest within the distribution network, as the first thermal limit of the power system (corresponding to a DG real power injection at the relevant node) is reached.

$$G_{P,m(max)} = \frac{\sqrt{(S^c_{i,k(lim)})^2 - ('Q_{i,k})^2} - 'P_{i,k}}{\frac{dP_{i,k}}{dG_{P,m}}} \qquad (5.13)$$

Where $G_{P,m(max)}$ is the maximum technical connection capacity of a DG scheme at node m, assuming real power export at unity power factor, $S^c_{i,k(lim)}$ is the thermal limit of the component between nodes i and k which is most thermally vulnerable component to DG real power injections at node m (as identified through thermal vulnerability factor

assessments), $'Q_{i,k}$ is the reactive power flow in the most thermally vulnerable component, $'P_{i,k}$ is the real power flow in the most thermally vulnerable component and $\frac{dP_{i,k}}{dG_{P,m}}$ is the power flow sensitivity factor that relates the change in nodal real power injection at node m with the change in real power flowing from node i to node k.

5.6 Single DG scheme control using power flow sensitivity factors

At times of power flow management within the distribution network, the amount an individual DG scheme is required to be constrained may be calculated (5.14)-(5.15) based on power flow sensitivity factors

$$\Delta G_{P,m} = \frac{\Delta P_{i,k}}{\frac{dP_{i,k}}{dG_{P,m}}} \tag{5.14}$$

where $\Delta G_{P,m}$ is the required change in real power output of the DG scheme at node m; $\frac{dP_{i,k}}{dG_{P,m}}$ is the power flow sensitivity factor that relates the change in nodal real power injection at m with the change in real power flowing from node i to node k; and $\Delta P_{i,k}$ is the required change in real power flowing from node i to node k in order to manage network power flows, as evaluated in (5.15)

$$\Delta P_{i,k} = \sqrt{(U_{Tar} \times S^c_{i,k(lim)})^2 - ('' Q_{i,k})^2} \\ -\sqrt{('S_{i,k})^2 - ('Q_{i,k})^2} \tag{5.15}$$

where U_{Tar} is the target utilisation of the thermally vulnerable component after control actions have been implemented; $S^c_{i,k(lim)}$ is the thermal limit of the thermally vulnerable component; $'S_{i,k}$ is the apparent power flowing from node i to node k before control actions are implemented and, $'Q_{i,k}$ and $''Q_{i,k}$ respectively represent the reactive power flowing from node i to node k before and after the control actions have been implemented. The theory leading to these equations is explained in Appendix D.

5.7   Conclusion

This chapter has outlined the analytical theory of power flow sensitivity factors, the formulation of thermal vulnerability factors, an empirical procedure for assessing power flow sensitivity factors and thermal vulnerability factors, the use of power flow sensitivity factors for sizing the installed capacity of non-firm DG connections and the preliminary use of power flow sensitivity factors for real-time DG output control. Power flow sensitivity factors are integral to the work presented in this thesis and it was demonstrated how the factors are related to the governing power flow equations for AC electrical networks. The power flow sensitivity factors facilitate the off-line identification of thermally vulnerable components by combination with power system steady-state thermal limits to formulate thermal vulnerability factors. Furthermore, power flow sensitivity factors may also be incorporated within techniques for the on-line power output control of DG to manage power flows within distribution networks. An empirical procedure for the assessment of power flow sensitivity factors and thermal vulnerability factors was suggested and the use of power flow sensitivity factors together with component thermal limits for the sizing of non-firm DG connections was also described.

Chapter 6

Identification of thermally vulnerable components within distribution networks: Application

6.1   Introduction

This chapter describes the application of the first stage of the distributed generation (DG) output control system development methodology (described in Chapter 4) to a number of case study networks, as published by the author in [83]. In order to assess the impacts of DG schemes on the location and thermal vulnerability of components within a range of distribution network topologies, the following assessments were conducted:

- Single DG schemes in a radial topology;

- single DG schemes in a meshed topology;

- multiple DG schemes in a radial topology; and

- multiple DG schemes in a meshed topology.

The results of the thermal vulnerability factor assessments are presented and discussed in Section 6.2. In Section 6.3 the application of assessments for sizing the installed capacity of non-firm DG connections is presented and discussed. In Section 6.4 preliminary DG output control investigations are conducted to assess the feasibility of using power flow sensitivity factors for the on-line control of DG outputs. This section also forms the link between thermal vulnerability factor assessments for the off-line identification of thermally vulnerable components, power flow sensitivity factors for the installed capacity-sizing of

Table 6.1: Application of TVF assessments to case study networks

	Single DG scheme	Multiple DG schemes
Radial	UKGDS C	UKGDS B
Meshed	UKGDS A	Field trial

non-firm DG connections in light of real-time thermal ratings and power flow sensitivity factors for the on-line (i.e. real-time) output control of DG schemes.

As a direct result of the thermal vulnerability factor assessments presented, and with validation from ScottishPower EnergyNetworks' engineers, instrumentation investment decisions were made to characterise the field trial network, both electrically and thermally. This work is described in Chapter 7.

6.2 Application of thermal vulnerability factor assessment to case study networks

In Chapter 3, nodes were selected intuitively to tease out thermal issues in the United Kingdom generic distribution systems (UKGDSs). In this chapter, the thermal vulnerability factor assessment, described in Chapter 5, was strategically applied to each 33kV node in UKGDS A, UKGDS B, UKGDS C and the 132kV nodes of interest in the field trial network. This led to the identification of thermally vulnerable component locations for both meshed and radial network topologies due to single-nodal and multiple-nodal real power injections. In validating the assessments, a full AC power flow simulation also yielded the DG capacity that could be connected before thermal issues arose. In each case it was found that the first technical limit met was a thermal constraint, with voltages close to nominal and within the regulations prescribed in [15] ($\pm 10\%$ at 132kV and $\pm 6\%$ at 33kV). Table 6.1 summarises the selection of test networks in order to analyse the different topology and DG scheme combinations. A 100 MVA base was used in each thermal vulnerability factor assessment.

6.2.1 Thermal vulnerability factor assessment with single DG schemes in a radial network topology

The thermal vulnerability factor assessment was applied to UKGDS C and used to establish the relationship between single DG real power injections and the location of thermally vulnerable components within a radial distribution network. The network topology for UKGDS C is given in Figure 3.4 of Chapter 3. Illustrative vulnerability correlations are
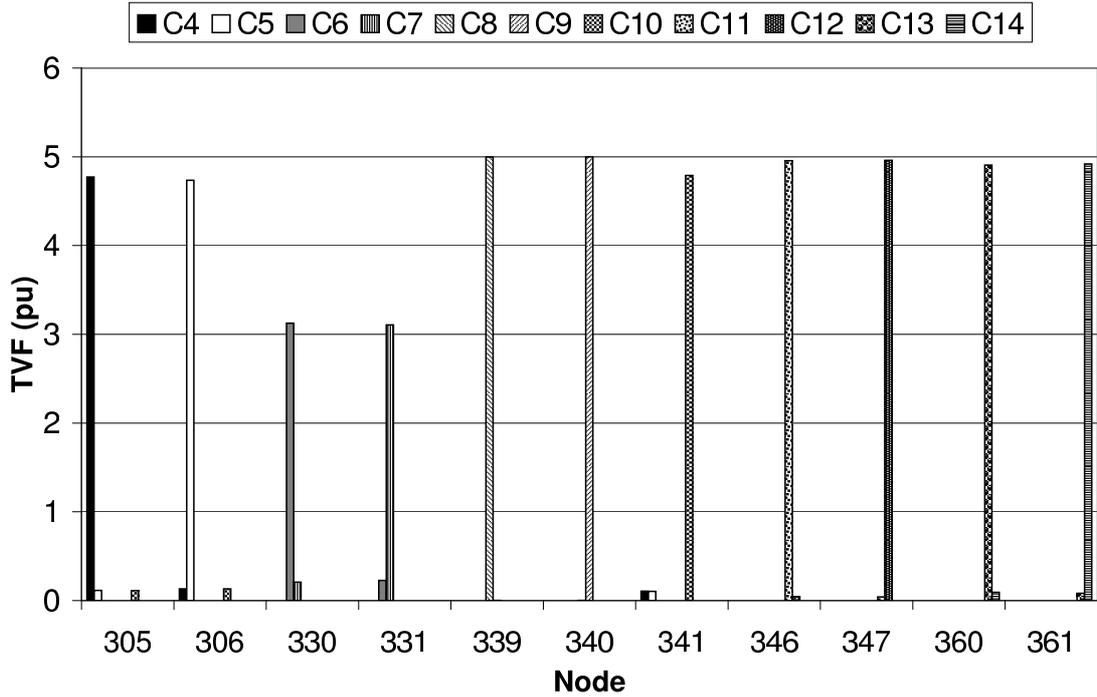
Figure 6.1: Vulnerable component identification for single DG injections in a radial distribution network (UKGDS C in Figure 3.4)

shown in Figure 6.1 and the simulated DG connection capacities at these nodes have been summarised in Table 6.2.

Figure 6.1 is interpreted by relating the magnitude of component thermal vulnerability factors to nodal locations via the network diagram in Figure 3.4. The DG connection capacities given in Table 6.2 correspond to a summer minimum loading condition when components C4–C14 would be most thermally at risk for large DG power outputs. This is because for a given quantity of DG, for example at node 305, the power exported through feeder C4 to the rest of the network would be greatest in summer when, typically, demand through T6 is at a minimum. Inspecting the results, it can be seen that single DG injections at each of the nodes listed in Table 6.1 have a vulnerable component local to the point of injection. This is a fairly intuitive finding as there is only one power flow path for DG outputs after local load demands have been met.

6.2.2 Thermal vulnerability factor assessment with single DG schemes in a meshed network topology

The thermal vulnerability factor assessment was applied to UKGDS A and used to establish the relationship between single DG real power injections and the location of thermally

Table 6.2: Vulnerable component hierarchies at different nodes in UKGDS C (All values are given in pu on 100 MVA base)

DG injection node	Simulated DG connection capacity at unity power factor	Thermally vulnerable component	Standard rating
305	0.268	C4	0.2
306	0.270	C5	0.2
330	0.355	C6	0.3
331	0.355	C7	0.3
339	0.283	C8	0.2
340	0.283	C9	0.2
341	0.335	C10	0.2
346	0.265	C11	0.2
347	0.265	C12	0.2
360	0.288	C13	0.2
361	0.288	C14	0.2

vulnerable components within a meshed distribution network. Illustrative vulnerability correlations are shown in Figure 6.2 and the simulated DG connection capacities at these nodes have been summarised in Table 6.3.

Figure 6.2 is interpreted by relating the magnitude of component thermal vulnerability factors to nodal locations via the network diagram in Figure 3.2 (Chapter 3). The DG connection capacities given in Table 6.3 correspond to a summer minimum loading condition when components C13–C18 would be most thermally at risk for large DG power outputs. This is because for a given quantity of DG, for example at node 317, the power exported through feeder C13 to the rest of the network would be greater in summer when demand through T13 is at a minimum.
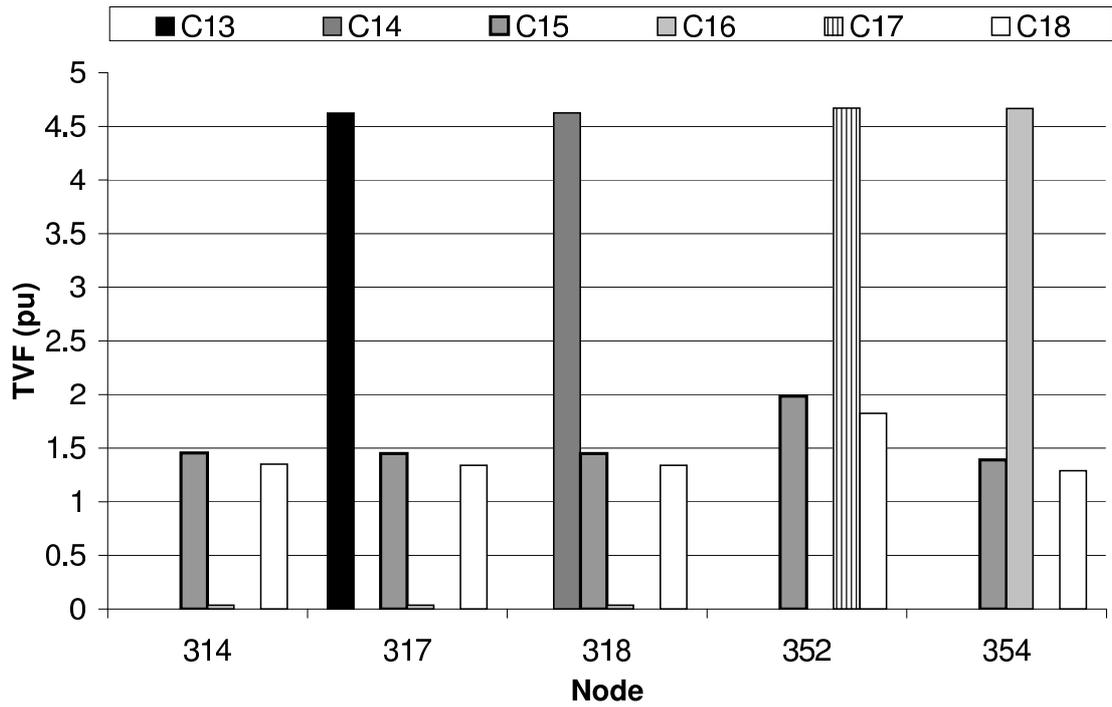
Figure 6.2: Vulnerable component identification for single DG injections in a meshed distribution network (UKGDS A in Figure 3.2)

Table 6.3: Vulnerable component hierarchies at different nodes in UKGDS A (All values are given in pu on 100 MVA base)

DG injection node	Simulated DG connection capacity at unity power factor	Thermally vulnerable component	Standard rating
314	0.511	C15	0.2
	0.567	C18	0.2
317	0.236	C13	0.2
318	0.236	C14	0.2
352	0.226	C17	0.2
	0.390	C15	0.2
	0.414	C18	0.2
354	0.228	C16	0.2
	0.466	C15	0.2
	0.501	C18	0.2

Inspecting the results, it can be seen that single DG injections at nodes 317, 318, 352 and 354 each have a vulnerable component local to the point of injection. Topologically, these nodes are in a more radial portion of the network. However, power injection at the meshed node, 314, causes components C15 and then C18 to become thermally vulnerable, which are non-local to the point of DG injection.

6.2.3 Cumulative thermal vulnerability factor assessment with multiple DG schemes in a radial network topology

The thermal vulnerability factor assessment was applied to UKGDS B to identify accumulated power flows due to the wide-spread injection of real power from DG schemes in a radial distribution network. The network diagram in Figure 3.3 (Chapter 3) together with the graph in Figure 6.3 show that, whilst strong local-overload correlations do exist for some nodes, if small contributions from nodes 324, 327, 328, 329 and 348 are accumulated then transformers T3 and T4 could potentially be at risk.
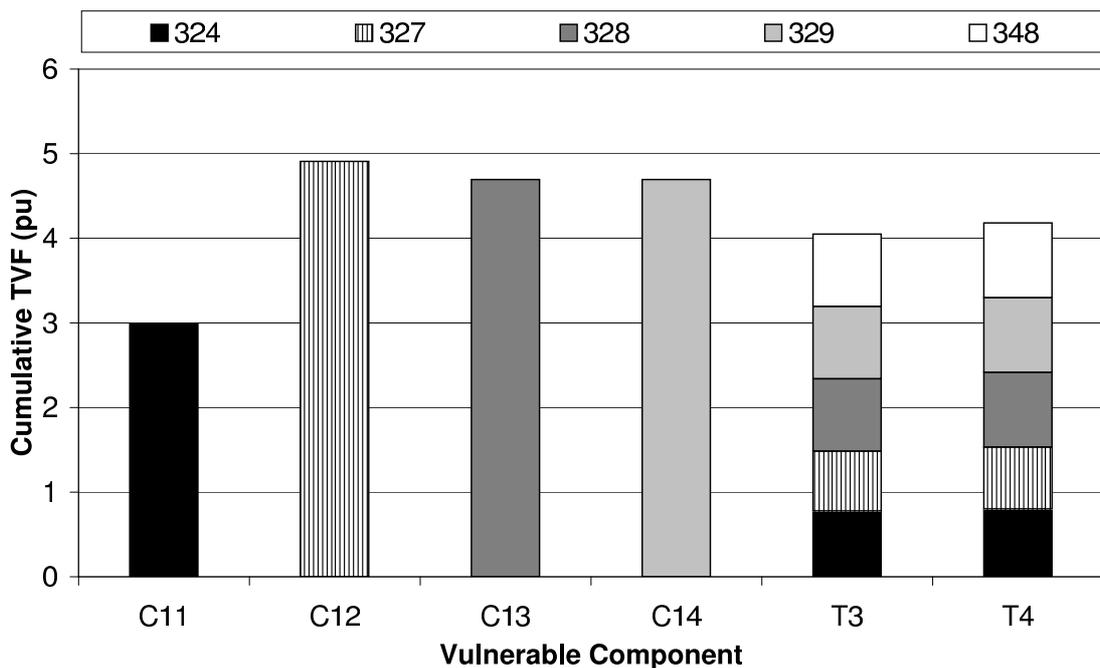
Figure 6.3: Assessing the location of vulnerable components through cumulative TVFs in radial distribution network (UKGDS B in Figure 3.3)

Table 6.4 illustrates six cases with a DG scheme switched out in turn (Cases 1-5) and all the DG schemes switched in (Case 6). In the last case, transformer T4 is thermally vulnerable from the accumulation of power flows.

Table 6.4: Accumulation of DG injections producing an overload in UKGDS B (All values are given in pu on 100 MVA base)

	$G_{P,324}$	$G_{P,327}$	$G_{P,328}$	$G_{P,329}$	$G_{P,348}$	$G_{P,Total}$	T4 rating	T4 power flow
Case 1	-	0.15	0.25	0.25	0.20	0.85	0.45	0.26
Case 2	0.40	-	0.25	0.25	0.20	1.10	0.45	0.37
Case 3	0.40	0.15	-	0.25	0.20	1.00	0.45	0.33
Case 4	0.40	0.15	0.25	-	0.20	1.00	0.45	0.33
Case 5	0.40	0.15	0.25	0.25	-	1.05	0.45	0.36
Case 6	0.40	0.15	0.25	0.25	0.20	1.25	0.45	0.47

6.2.4 Cumulative thermal vulnerability factor assessment with multiple DG schemes in the meshed field trial network topology

The thermal vulnerability factor assessments were applied to the field trial network given in Figure 3.1 of Chapter 3 at nodes B3 and B5. The purpose of examining the thermal vulnerability factors for node B5 was to assess the implications of the DG being re-planted with a greater installed capacity in the future. It can be seen in Figure 6.4 that circuit C4 is the most thermally vulnerable to a DG injection at node B5 whilst component C3 is the most thermally vulnerable to a DG injection into node B3. The assessment also revealed a counter-flow sensitivity relationship in component C3 where real power injection at node B5 caused a power flow increase from B4 to B3 and real power injection at node B3 caused a power flow increase from B3 to B4. The net effect is that in certain situations, DG injected at B5 could be used to allow greater power export from the DG scheme at B3 through component C3. In this particular case the phenomenon exists because injection at B5 meets more of the local demand in the 'right-hand' portion of the network and thus the power from B3 is diverted into component C2.

In conjunction with ScottishPower EnergyNetworks, a series of full AC power flow simulations demonstrated that potentially up to 115 MW of generation, at unity power factor, could be accepted at node B5 in the wintertime, reducing to 100 MW in the summertime. Similarly, 113 MW of generation, at unity power factor, could potentially be accepted at node B3, reducing to 100 MW during the summer months. These results are summarised in Table 6.5.
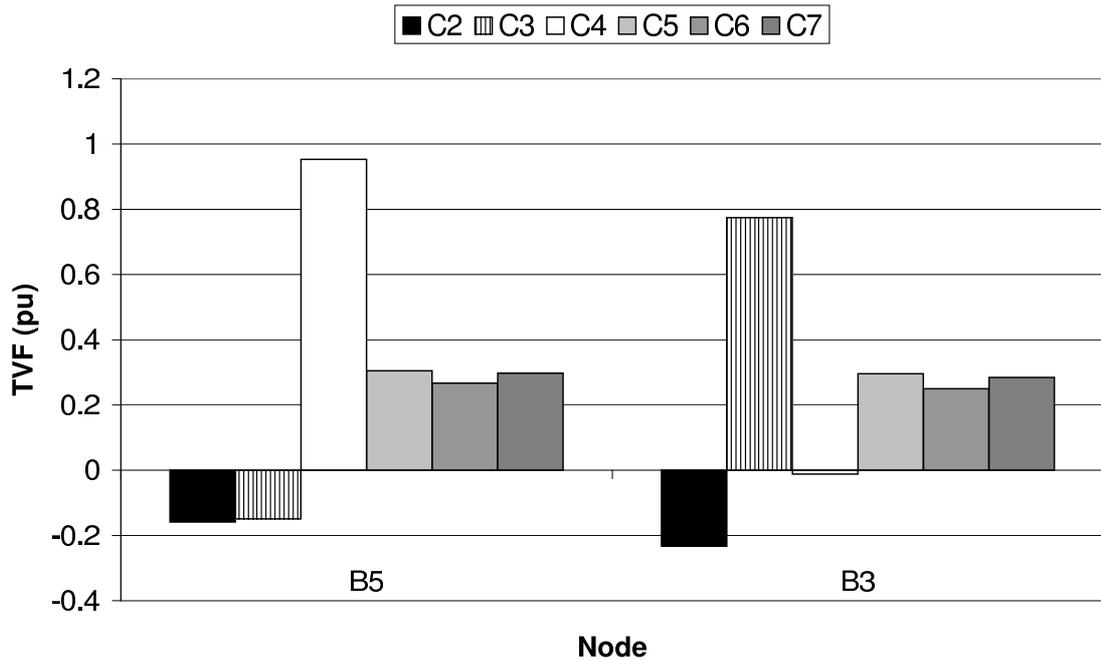
Figure 6.4: TVF analysis of the field trial network (in Figure 3.1)

Table 6.5: Simulated DG connection capacities in the field trial network (All values are given in per unit form on 100 MVA)

Node	Component	Loading Condition	$\frac{dP_{i,k}^c}{dG_{P,m}}$	$\frac{dQ_{i,k}^c}{dG_{P,m}}$	$\lvert\frac{\partial P}{\partial Q}\rvert$	Simulated DG connection capacity (at unity power factor)
B5	C4	Winter peak	0.947	-0.001	$\gg 100$	1.155
B5	C4	Summer min.	0.954	0.003	$\gg 100$	1.005
B3	C3	Winter peak	0.778	-0.018	52.3	1.134
B3	C3	Summer min.	0.778	0.003	$\gg 100$	1.001

6.2.5 Discussion of thermal vulnerability factor assessment applied to case study distribution networks

By analysing thermal vulnerability factors for single and multiple DG power injections, strategic locations for meteorological stations and conductor temperature monitoring equipment may be chosen. In the case of single DG injections at radial nodes it was found that components local to the point of DG injection may become thermally vulnerable. However, in the case of a single DG injection at a meshed node it was found that components non-local to the point of injection may become thermally vulnerable. In the case of multiple DG injections it was observed that wide-spread power injections may lead to an accumulation

of power flows, causing thermal problems on a more global scale.

Considering the field trial network with both DG schemes exporting power concurrently, the net result of vulnerability factors in C3 is lower when DG at B5 is exporting than when it is not. This result is based on counter-flow power flow sensitivity factors that show a greater amount of power could be exported from DG at B3 when DG at B5 is exporting. The thermal vulnerability factor assessment effectively identified components C3 and C4 as potentially being the power flow constraining components in the field trial network in the future. These results informed an instrumentation meeting with ScottishPower EnergyNetworks' engineers and resulted in the decision to thermally instrument components C3 and C4 to provide more detailed thermal characterisation, as suggested in Stages 2 and 3 of the DG power output control system development methodology.

Through the constant monitoring of maximum nodal voltage excursions, the analysed networks were found to reach thermal limits before voltage constraints for both meshed and radial topologies when considering static thermal ratings.

6.3 Assessment of non-firm DG connection capacities through power flow sensitivity factors

DG technical connection capacities were assessed (5.13) within the case study networks at the same nodes that were used to illustrate the nodal-component thermal vulnerability correlations. The results are presented in Table 6.6. The technical DG connection capacities were validated through full AC load flow simulations using the bisection numerical method described in Chapter 4.

Considering Table 6.6, the DG technical connection capacity assessments provide a good prediction of the DG technical capacity that can be connected to nodes before components become thermally vulnerable. The maximum error between predicted and simulated connection capacities was found to be 0.864% at node 352 in UKGDS A (corresponding to an under-prediction by the tool of 0.2 MW in real terms). The maximum error between predicted and simulated connection capacities was found to be -1.263% at node 331 in UKGDS C (corresponding to an over-prediction by the tool of 0.45 MW in real terms). In these cases the changes in real power injections at the particular node influence changes in reactive power flows and the linearity assumption must be applied with caution.

Table 6.6: Prediction and validation of DG technical connection capacities

Network	Node	Component causing power flow constraint	Rating (MVA)	$\frac{dP^c_{i,k}}{dG_{P,m}}$	$\frac{dQ^c_{i,k}}{dG_{P,m}}$	$\left\|\frac{\partial P}{\partial Q}\right\|$	Predicted DG connection capacity (MW at unity power factor)	Simulated DG connection capacity (MW at unity power factor)	% Error
UKGDSA	317	C13	20.0	0.997	-0.007	143.1	23.56	23.60	0.190
	318	C14	20.0	0.998	-0.007	147.7	23.55	23.60	0.200
	352	C17	20.0	0.978	-0.059	16.7	22.60	22.80	0.864
	354	C16	20.0	0.982	-0.039	25.2	22.81	22.80	-0.043
UKGDSC	305	C4	20.0	0.955	0.079	12.0	27.01	26.80	-0.793
	306	C5	20.0	0.947	0.093	10.2	27.20	27.00	-0.725
	330	C6	30.0	0.939	0.127	7.4	35.73	35.40	-0.927
	331	C7	30.0	0.933	0.137	6.8	35.95	35.50	-1.263
	339	C8	20.0	0.999	0.001	$\gg 100$	28.26	28.30	0.127
	340	C9	20.0	0.999	0.001	$\gg 100$	28.26	28.30	0.149
	341	C10	20.0	0.959	0.065	14.7	33.84	33.50	-1.002
	346	C11	20.0	0.991	0.021	46.3	26.48	26.50	0.064
	347	C12	20.0	0.992	0.061	16.3	26.47	26.50	0.115
	360	C13	20.0	0.981	0.044	22.2	28.78	28.80	0.058
	361	C14	20.0	0.983	0.057	17.3	28.75	28.80	0.189

6.3.1   Limitations of technical connection capacity assessment

The DG technical connection capacity assessments exhibiting the greatest error between predicted and simulated values were analysed further to understand the sources of error. In order to do this the DG technical connection capacity assessment equation, as given in (5.13), was inverted to predict the apparent power flow as a function of the DG connection capacity.

Figure 6.5 displays the variation of real, reactive and apparent power flows in component C17 (between node 352 and 353) due to increasing real power injections at node 352 in UKGDS A. Whilst the variation of real power flow ($P_{i,k}$) is linear with the real power injection, the reactive power flow ($Q_{i,k}$) reduces in magnitude from node 352 to 353 and reverses direction in a non-linear manner as the real power injection increases. This leads to a non-linear variation of the apparent power flow ($S_{i,k}$) resulting from the real power injection. The simulated apparent power flow and predicted apparent power flow (from the DG technical connection capacity assessment tool) were plotted as functions of the DG technical connection capacity in Figure 6.6. Considering Figure 6.6, where the predicted and apparent power flows reach the thermal limit of the component, it can be seen that, by not accounting for the reverse in direction of the reactive power flow, the DG technical connection capacity assessment overestimates the apparent flow (compared to the simulated flow) and therefore slightly underestimates the DG technical connection capacity.

Figure 6.7 displays the variation of real, reactive and apparent power flows in component C7 (between node 331 and 338) due to increasing real power injections at node 331 in UKGDS C. Whilst the variation of real power flow ($P_{i,k}$) is linear with the real power injection, the reactive power flow ($Q_{i,k}$) increases in magnitude from node 338 to 331 in a non-linear manner as the real power injection increases. This leads to a non-linear variation of the apparent power flow ($S_{i,k}$) resulting from the real power injection. The simulated apparent power flow and predicted apparent power flow (from the DG technical connection capacity assessment tool) were plotted as functions of the DG technical connection capacity in Figure 6.8. Considering Figure 6.8, where the predicted and apparent power flows reach the thermal limit of the component, it can be seen that, by not accounting for the increase in reactive power flow, the DG technical connection capacity assessment tool underestimates the apparent flow (compared to the simulated flow) and therefore slightly overestimates the DG technical connection capacity.
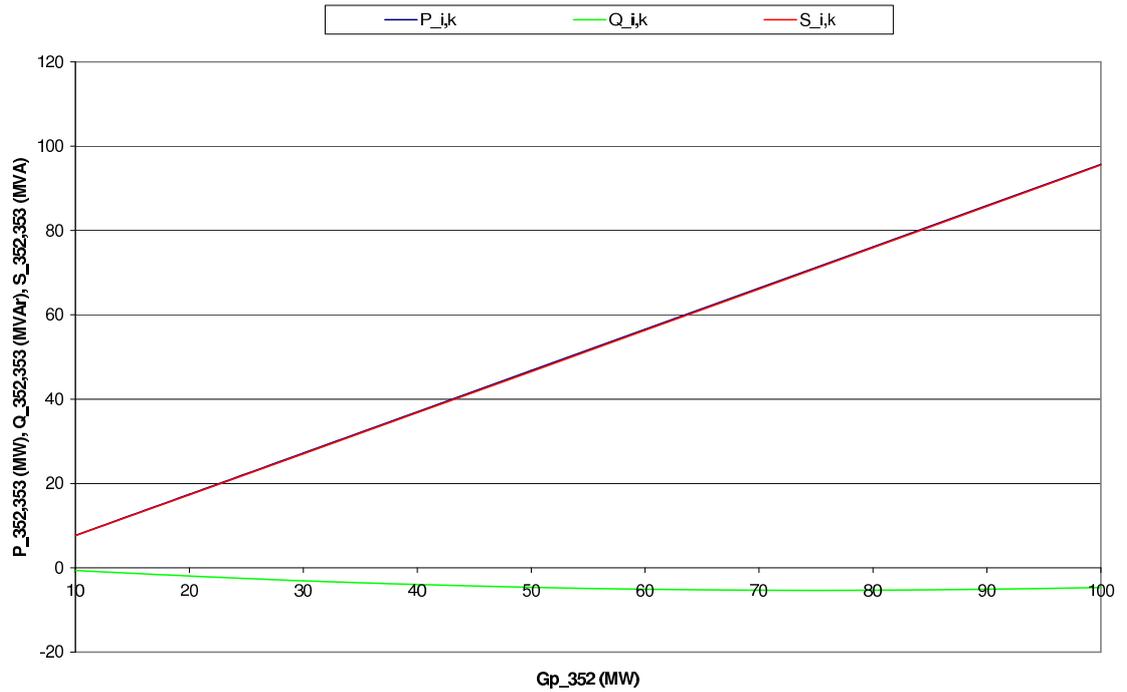
Figure 6.5: Variation of power flows from node 352 to node 353 due to real power injection at node 352 in UKGDS A
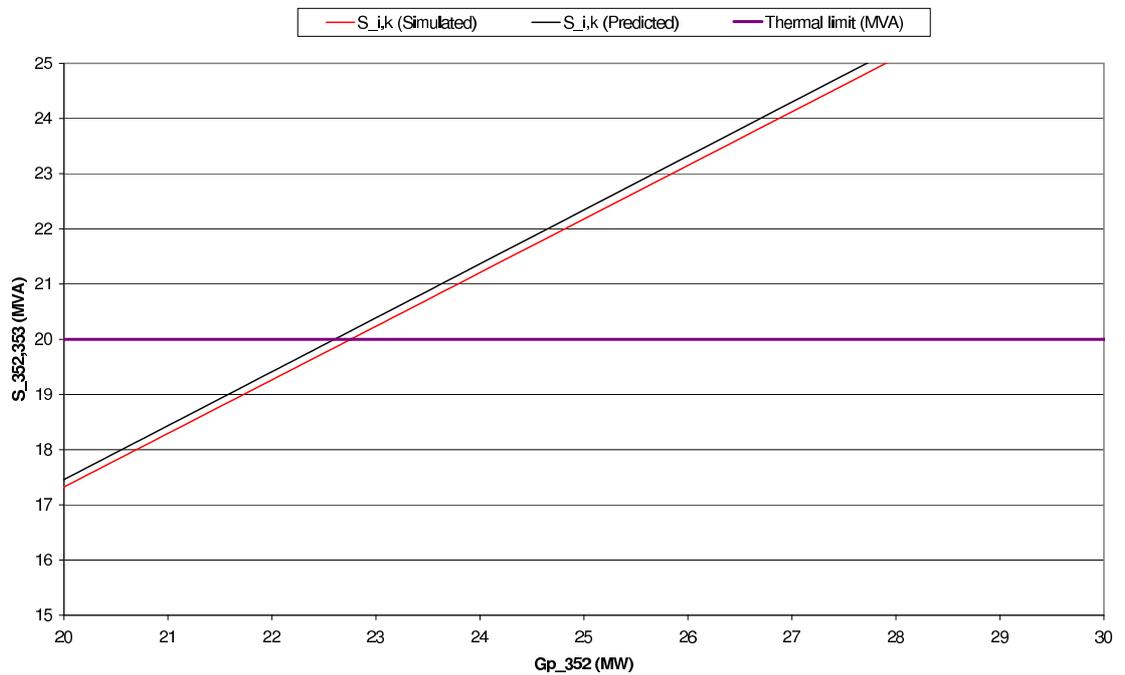
Figure 6.6: Predicted and simulated power flows from node 352 to node 353 due to real power injection at node 352 in UKGDS A
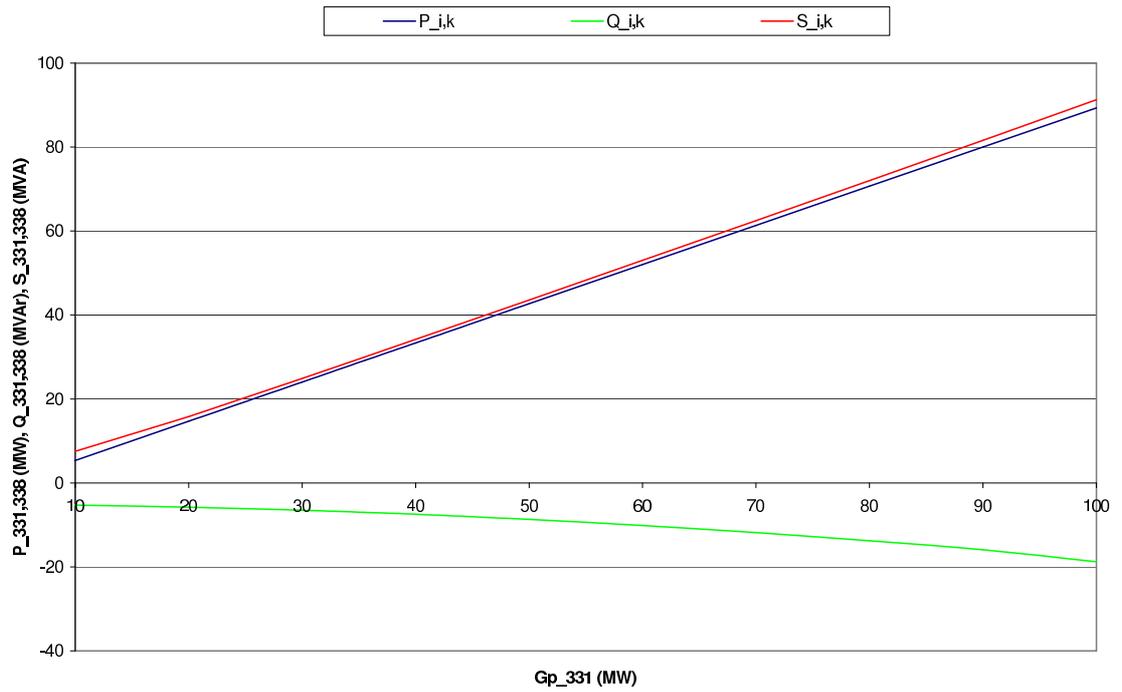
Figure 6.7: Variation of power flows from node 331 to node 338 due to real power injection at node 331 in UKGDS C
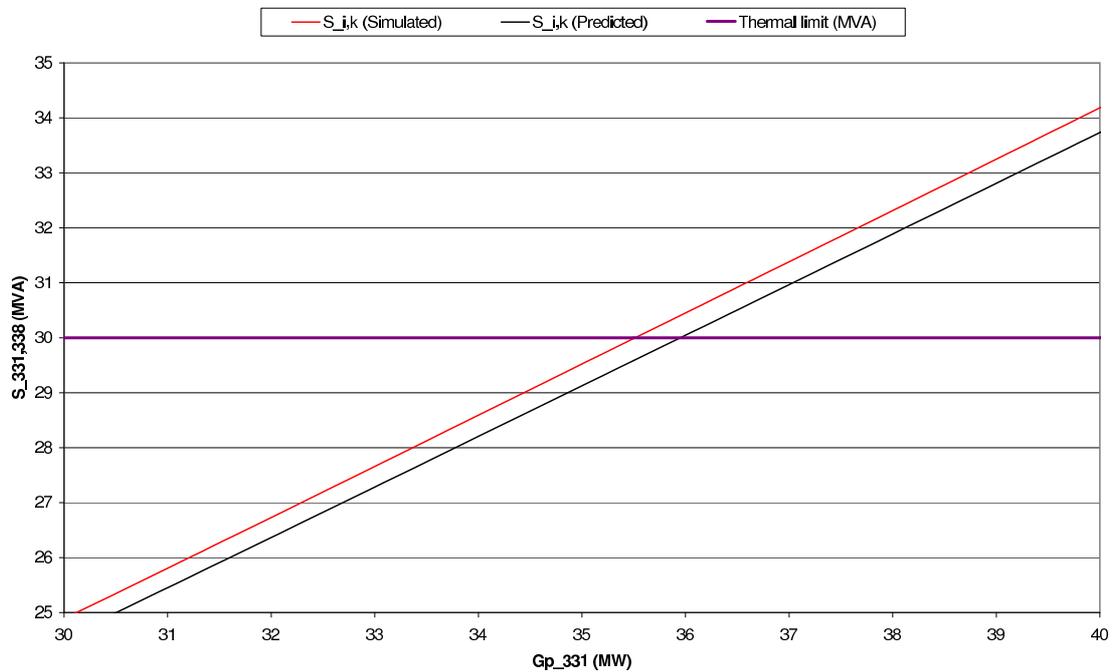
Figure 6.8: Predicted and simulated power flows from node 331 to node 338 due to real power injection at node 331 in UKGDS C

6.4 Preliminary DG output control investigations

This section provides the link between thermal vulnerability factor assessments for the off-line identification of thermally vulnerable components, the use of power flow sensitivity factors for the off-line assessment of DG technical connection capacities and the on-line use of power flow sensitivity factors for the real-time output control of DG schemes.

6.4.1 DG output control in a generic distribution system

Through a full AC power flow simulation an assessment was made of the maximum connection capacity of DG that could be individually accommodated at each 33kV node in UKGDS C with summer (minimum) load demand and static thermal rating operating conditions. These values are given in Table 6.6. DG capacities in excess of these thermal limits (but still within voltage and fault-level limits) were installed to emulate the management of non-firm DG connections. It was assumed that the circuits in the network were overhead lines with the potential to be up-rated by at least 50% - this is not unreasonable given Aeolian (wind) cooling of the line could produce increased capacities from 20% to as much as 100% [27]. With components up-rated individually (representing an incremental investment in meteorological station installations) and with target utilisation of 100% (i.e. $U_{tar} = 1$), the maximum possible adjustment in DG real power output was calculated, at each node, using (5.14)–(5.15) in Chapter 5 and validated with a full AC power flow simulation. A comparison was made of the increased DG output that could be achieved due to the increased component rating and a summary of these findings is given in Table 6.7.

From the full AC load flow assessments of technical DG connection capacities in UKGDS C, (as shown in Table 6.7) it can be seen that the greatest DG capacity could be accommodated at nodes 331 and 330. Furthermore, the components that thermally limit DG power output at these nodes (C7 and C6 respectively) would also facilitate the greatest increase in DG power output for a 50% uprating of the lines. A comparison of increased line rating versus increased DG power output shows that a 50% increase in rating will not necessarily allow a 50% increase in DG power output to be achieved. This is a topology-specific conclusion and relates to the magnitude of power flow sensitivity factors.

Table 6.7: Application of DG output control system to UKGDS C (All values are given in per unit form on 100 MVA)

Node	Component causing power flow constraint	Rating	$\frac{dP^c_{i,k}}{dG_{P,m}}$	$\frac{dQ^c_{i,k}}{dG_{P,m}}$	$\left|\frac{\partial P}{\partial Q}\right|$	Simulated DG connection capacity (at unity power factor)	ΔDG output through power output control system, %	ΔDG output through full ac load flow simulation, %
361	C14	0.20	0.983	0.057	17.3	0.288	35.4	35.4
360	C13	0.20	0.981	0.044	22.2	0.288	35.5	35.5
347	C12	0.20	0.992	0.061	16.3	0.265	38.2	38.2
346	C11	0.20	0.991	0.021	46.3	0.265	38.3	38.3
340	C9	0.20	0.999	0.001	$\gg 100$	0.283	36.0	36.0
339	C8	0.20	0.999	0.001	$\gg 100$	0.283	36.1	36.1
331	C7	0.30	0.933	0.137	6.8	0.355	45.1	44.6
330	C6	0.30	0.939	0.127	7.4	0.355	45.1	44.8
341	C10	0.20	0.959	0.065	14.7	0.335	31.8	31.5
306	C5	0.20	0.947	0.093	10.2	0.270	39.1	38.8
305	C4	0.20	0.955	0.079	12.0	0.268	38.6	38.2

Table 6.8: Application of DG power output control system to the field trial network (Where relevant, values are given in pu on 100 MVA base)

Node	Component causing power flow constraint	Rating	Simulated DG connection capacity (at unity power factor)	Δ DG output through power output control system, %	Δ DG output through full AC load flow simulation, %
B5	C4	0.89	1.155	40.9	41.0
B3	C3	0.89	1.134	50.7	50.8

6.4.2 DG output control in the field trial network

To illustrate the application of the DG power output control system in the field trial network, it was assumed that DG was installed in excess of the winter values, simulated in Table 6.5, in order to emulate non-firm DG connections. As before, (5.14)–(5.15) were used to predict potential DG power output adjustments for a 50% increase in the real-time thermal rating of the power flow-constraining components [84]. In conjunction with ScottishPower EnergyNetworks, the predicted power output adjustments were validated through a full AC power flow and a comparison of the results is given in Table 6.8. In this case the control system slightly under-predicted the potential power output adjustments. This is attributed to a negative $\frac{dQ_{i,k}^c}{dG_{P,m}}$ that means an increase in real power injection reduces the MVAr flow.

6.4.3 Discussion

Through the constant monitoring of maximum nodal voltage excursions, the analysed networks were found to reach thermal limits before voltage constraints for both meshed and radial topologies when considering static thermal ratings and, in the illustration of the DG power output control system, with the assets up-rated by 50%. The DG power output control system makes use of an on-line simulation tool that has the capability of validating operational voltages against operational voltage limits. If voltage limits were to become a constraining factor this would currently need to be dealt with outside of the jurisdiction of the DG power output control system using active voltage measures such as demonstrated in [95]. Alternatively, the functionality of the control system could be extended to make use of voltage sensitivity factors [71, 72].

In making the assumption that $\frac{dP_{i,k}^c}{dG_{P,m}} \gg \frac{dQ_{i,k}^c}{dG_{P,m}}$ and the simplification in Equation (5.15) that $''Q_{i,k}^c \simeq {}'Q_{i,k}^c$, the largest % error between the DG power output adjustment from the

control system and the full ac load flow power output adjustment for validation was 1.12% at node 331. In this case $|\frac{\partial P}{\partial Q}| = 6.8$. The slight discrepancies between adjustments will be accommodated in the control system by designing an error margin into the utilisation target limit, U_{tar}.

6.5   Conclusion

The identification of thermally vulnerable components within distribution networks was illustrated through the use of UKGDSs and the field trial network being considered in the DIUS Project. Through system simulations, in conjunction with ScottishPower EnergyNet-works, the components identified through the assessment of thermal vulnerability factors were validated. This formed the basis for instrumentation investment decisions that characterised the electrical and thermal behaviour of the field trial network (stage two of the DG output control system development methodology) and provided basis for the development of a real-time thermal rating system (stage three of the DG output control system development methodology). These two stages are described in Chapter 7.

The purpose of the thermal vulnerability factor assessment was to identify thermally vulnerable components within distribution networks. As demonstrated through the UKGDS applications, the thermal vulnerability factor assessment is not confined to a specific topology type. It can be applied to predominantly radial, predominantly meshed or mixed topologies with equally valid results. It has been shown that the thermal vulnerability factor assessment is appropriate for use in identifying the thermal impacts of planned individual DG schemes or, in a more strategic way, to assess longer term and more wide-spread DG growth scenarios. Therefore the thermal vulnerability factor assessment procedure would be valuable for DNOs looking to develop long-term DG accommodation strategies for areas of their network. The results of the thermal vulnerability factor assessments could be used to inform instrumentation investment decisions for the installation of monitoring equipment in thermally vulnerable sections of the network. The thermal vulnerability factor assessment identifies those components that would most benefit from being thermally monitored to unlock latent power flow capacity through a real-time thermal rating system, the off-line analysis of which may be used for sizing the installed capacity of non-firm DG connections. Alternatively, the thermal vulnerability factor assessment could be used to locate sections of the distribution network that would benefit from strategic reinforcement to accommodate planned future DG scheme connections.

Chapter 7

Network thermal characterisation and real-time thermal rating system development

7.1   Introduction

The work presented in this chapter relates to Stages 2 and 3 of the distributed generation (DG) output control system development methodology as described in Chapter 4. This was the primary research focus of Andrea Michiorri, a colleague at Durham University employed as a doctoral researcher within the DIUS Project. This chapter focuses on the thermal characterisation of the distribution network and development of power system real-time thermal rating systems. Network thermal characterisation involves the development of component thermal models and environmental condition interpolation techniques which can be used together with meteorological information for the off-line simulation of real-time thermal ratings. The off-line analysis of the simulation results allows the potential benefits of power system real-time thermal rating systems to be quantified. In situations where it is assessed to be viable, a system may then be developed to exploit power system real-time thermal ratings for on-line operational usage.

Section 7.2 discusses component thermal models and failure modes. In Section 7.3, methods to estimate power system environmental operating conditions are presented. In Section 7.4, off-line simulations are used to assess the potential benefits of real-time thermal rating system adoption. Section 7.5 focuses on network instrumentation for the DG output control system. Sections 7.6 and 7.7 consider the development of on-line real-time thermal rating systems through direct-population and thermal state estimation techniques.

7.2 Power system component thermal models

Due to the variability and unpredictability of meteorological conditions, fixed seasonal assumptions are used to determine power system ratings which can be a conservative representation of the actual operating conditions [84]. This potentially results in a conservative constraints on power flows. Difficulties associated with the maintenance of accurate seasonal rating databases often result in the use of summer static rating throughout the year for power system operation [51]. Moreover, the seasonal rating approach bears the latent risk of an anomalous 'hot day' where the prevailing meteorological conditions mean that power system components may be rated higher than they should be.

For the purposes of the research presented in this thesis, real-time thermal ratings are defined as a time-variant rating which can be practically exploited without damaging components or reducing their lifetime. It is assumed that actual environmental parameter measurements are available and can be used as the input to the steady-state thermal models. Short term transients, taking into account the thermal capacitance of power system assets, are not included within the real-time thermal rating assessment since this was not expected to affect, materially, the MWh/annum throughput of energy within the electrical power system.

In order to assess, in a consistent manner, component real-time thermal ratings due to the influence of environmental conditions, thermal models were developed at Durham University based on IEC standards for overhead lines [30], electric cables [35] and power transformers [39]. Where necessary, refinements were made to the models using [31] and [37]. Steady-state models have been used in preference to dynamic models since this would provide a maximum allowable rating for long term power system operation. The thermal models, used for real-time thermal rating calculations, are presented in detail in the paper "Investigation into the influence of environmental conditions on power system ratings" in Appendix A.

For calculating the conductor operating temperature of an overhead line at a given current, or the maximum current for a given operating temperature, it is necessary to solve the energy balance between the heat dissipated in the conductor by the current, and the thermal exchange on its surface, as given in (7.1)

$$I_{max} = \sqrt{\frac{q_{rad} + q_{conv} + q_{sol}}{R_{ac}}} \tag{7.1}$$

where I_{max} is the steady state current carrying capacity, q_{rad} is the heat loss by radiation

of the conductor, q_{conv} is the convective heat loss through wind cooling, q_{sol} is the solar heat gain by the conductor surface and R_{ac} is the AC electrical resistance of the conductor at its maximum operating temperature. The proposed formulae in [30] were used for the calculation of the contribution of solar radiation, radiative heat exchange and convective heat exchange as given in (7.2)–(7.4) respectively

$$q_{sol} = \alpha DW \tag{7.2}$$

$$q_{rad} = \epsilon \sigma_{SB} \left(T_c^4 - T_a^4 \right) \pi D \tag{7.3}$$

$$q_{conv} = \pi N u \lambda \left(T_c - T_a \right) \tag{7.4}$$

where α represents the absorption coefficient, D represents the diameter of the conductor and W represents solar radiation, ϵ represents the emission coefficient, σ_{SB} represents the Stefan-Boltzmann constant and T_c and T_a represent the respective conductor and ambient temperatures, Nu represents the Nusselt number and λ represents the air thermal conductivity.

The conductor temperature of an electric cable in steady-state conditions is modelled to account for the heat balance between the power dissipated in the conductor by the Joule effect, $I^2 R_{ac}$, and the heat dissipated in the environment through the thermal resistance, R_{Th} of the insulation and the soil, due to the temperature difference ΔT as shown in (7.5).

$$I^2 R_{ac} = \frac{\Delta T}{R_{Th}} \tag{7.5}$$

The electrical current rating, I, may then be calculated (7.6) [35].

$$I = \sqrt{\frac{\Delta T}{R_{ac} R_{Th}}} \tag{7.6}$$

The model given in (7.6) requires detailed knowledge of the electric cable installation in order to calculate R_{Th}. However, this information may not always be available and therefore it is difficult to make practical use of the model. In these circumstances an alternative model may be used (7.7) [37]. The rated current of electric cables, I_0, is given in tables depending on the nominal voltage level, V, the standardised cable cross-sectional area, A, and laying conditions (trefoil, flat formation; in air, in ducts or directly buried). The dependence of the cable ampacity on the actual soil temperature, T_s, away from the rated soil temperature, $T_{s(rated)}$, as well as the actual soil thermal resistivity, $\rho_{Th(s)}$, away

from the rated soil thermal resistivity, $\rho_{Th(s,rated)}$, is made linear through the coefficients ξ_T and ξ_ρ respectively.

$$I = I_0(A, V, laying) \times \left[\xi_T(T_s - T_{s(rated)})\right] \times \left[\xi_\rho(\rho_{Th(s)} - \rho_{Th(s,rated)})\right] \qquad (7.7)$$

The thermal model for power transformers is given in the paper "Investigation into the influence of environmental conditions on power system ratings" in Appendix A.

The following component-specific failure modes exist that can cause dangerous electrical faults to occur. Severe penalties may ensue, in terms of human fatalities and fines issued by the regulator, OfGEM, due to the loss of supply to customers:

1. Overhead lines: The first failure mode is the sag of the line. Overhead lines are tensioned to operate at a maximum temperature (for example 50 °C in the case of the Lynx 132kV lines in the field trial network). If the current carried by a line causes heating in excess of its maximum operating temperature the line could sag below statutory limits. If this happens over a road, and a vehicle collides with the line, the result may be the loss of human life. The second mode of failure can occur when the overhead line reaches a temperature high enough to melt lubricating grease contained within the strands of the line. It is possible that this grease could drip from the line causing injury to humans and the anticipated performance life of the line to be reduced. Thirdly, if the line reaches temperatures of 110 °C, and has aluminium or aluminium alloy construction, the mechanical properties of the line will change from elastic to plastic deformation. Therefore the line will be elongated from its original length upon cooling.

2. Electric cables: The primary thermal limitation of cables is the rate of ageing that could eventually lead to a breakdown in the electrical insulation around the conductor core. When the insulation breaks down or melts as a result of the core conductor temperature, the current being carried is discharged and a line-to-ground fault occurs. It is unlikely that this type of fault will endanger human life but it is likely that the supply to customers will be interrupted and this could contribute to financial penalties resulting from customer minutes lost (CMLs).

3. Power transformers: In terms of failure modes, the ageing of the paper insulation in the transformer construction is the limiting factor. Secondly, as the temperature of the transformer increases a hotspot may occur that causes the formation of air

bubbles in the oil. These air bubbles have a lower electrical resistance than the oil and sparking may occur that ignites the oil and causes the transformer to explode.

7.3   Environmental conditions

This section describes, in brief, the approach adopted to estimate, correct and interpolate environmental conditions to represent, more accurately, the actual environmental operating conditions in the vicinity of power system components. A more in-depth description of environmental condition estimation techniques is given in the paper "Investigation into the influence of environmental conditions on power system ratings" in Appendix A.

The inverse distance interpolation technique [90] allows environmental conditions to be determined over a wide geographical area using a reduced set of inputs. This is attractive for situations where a large amount of installed measurements may be financially unattractive to the DNO. The technique is also computationally efficient and allows the input locations to be readily adapted. Wind direction, air temperature and solar radiation values (which influence the thermal rating of overhead lines) were directly interpolated and did not require the application of a correction factor. Wind speeds (which influence the convective heat exchange of overhead lines) and the soil temperature and thermal resistivity values (which influence the thermal rating of electric cables) were corrected. For example, in the case of wind speed correction the wind power profile law was used.

7.4   Off-line analysis of real-time thermal rating potential

In [84] research is presented which seeks to assist distribution network operators (DNOs) in the adoption of real-time thermal rating systems. The exploitation of power system rating variations is challenging due to the complex nature of environmental conditions such as wind speed. The adoption of a real-time thermal rating system may overcome this challenge and offers perceived benefits such as increased DG accommodation and avoidance of component damage or premature ageing.

In order to quantify the influence of environmental conditions on power system ratings, simulations were carried out using the UK generic distribution systems and field trial network as described in Chapter 3. Each distribution network was subjected to a range of UK climatic conditions based on Met Office datasets. For each scenario the minimum, maximum and average thermal rating values were calculated. Key findings showed: The average rating of overhead lines ranged from 1.70 to 2.53 times the static rating, with minimum and

maximum ratings of 0.88 and 4.23 respectively; the average rating of electric cables ranged from 1.00 to 1.06 times the static rating, with minimum and maximum value of 0.88 and 1.23 respectively; and the average rating of power transformers ranged from 1.06 to 1.10 times the static rating, with minimum and maximum ratings of 0.92 and 1.22 respectively.

7.5 Network instrumentation

The instrumentation of the field trial network within the DIUS Project took place in the following phases:

1. The development of an electrical and thermal measurement requirements list for the DG output control system;

2. The specification of instrumentation requirements within the field trial network for network characterisation;

3. The commissioning of the instrumentation (through FMC-Tech) for network characterisation;

4. The specification of instrumentation requirements for the prototype control system; and

5. The commissioning of instrumentation (through AREVA) for the prototype DG output control system.

This section of the thesis focuses on network instrumentation phases 1–3 which are related to the network characterisation aspects of the DG output control system development. The network instrumentation phases relating to the installation of the prototype DG output control system are described in Chapter 13.

7.5.1 Control system measurement requirements list

This phase initiated the development of generic and site-specific measurement requirements list for DG output control system. Measurements pertain to those needed for the DG output control system to function as well as verification measurements (not input directly to the control system) but used with an off-line tool to verify the accuracy of the algorithms within the DG output control system. This entailed the over-instrumentation of the field network trial network for characterisation and prototype testing purposes. Measurements

were categorised as either 'essential' or 'desirable' and at this stage no attempt was made to determine the actual transducers to be used to collect this data and the frequency at which the data needed harvesting. As a general rule the measurement equipment was to be placed at the most vulnerable and thermally sensitive point where it is difficult to accurately estimate the thermal behaviour and failure to accurately predict the thermal limit would have severe consequences.

The generic parameters for electrical, thermal and meteorological monitoring were listed as follows:

1. Electrical measurements

    (a) Overhead line: Real and reactive power flow, voltage and current;

    (b) electric cable: Real and reactive power flow, voltage and current;

    (c) power transformer: Real and reactive power flow, primary voltage and secondary voltage;

    (d) DG: Real and reactive power output.

    (e) grid supply points: Real and reactive power flow and voltage;

    (f) loads: Real and reactive power demand; and

    (g) circuit breakers: Operational status.

2. Thermal measurements

    (a) Overhead line: Core operating temperature and surface operating temperature;

    (b) electric cable: Core operating temperature and surface operating temperature; and

    (c) power transformer: Hotspot temperature, top oil temperature and bottom oil temperature;

3. Meteorological measurements

    (a) Overhead line: Wind speed, wind direction, ambient temperature and solar radiation;

    (b) electric cable: Ground temperature, ambient temperature, ground thermal resistivity and rainfall; and

    (c) power transformer: Ambient temperature, wind speed*, wind direction* and solar radiation*.

    *If transformer is located outside.

7.5.2 Field trial network instrumentation requirements

After the development of the instrumentation requirements wish list, the instrumentation requirements for the field trial network electrical and thermal characterisation took place. The purpose of this phase was to recommend electrical, thermal and meteorological instrumentation locations for the characterisation of the field trial network. A requirements specification was written to encapsulate the measurement requirements in order that the network behaviour could be understood both electrically and thermally. This was an essential process before decisions could be made about reducing the measurement set to prove the validity of the DG output control system. A key output of the network characterisation was to understand the best placement for a reduced instrumentation set in order to achieve adequate network thermal visibility. An attempt was made to ensure that the thermal and electrical measurements were at similar, if not the same, locations in the power system to assist with correlation between electrical and thermal behaviour. This was also expected to reduce the time required to install the measurement equipment on site and minimise any interruptions to supply. General guidelines were produced for the instrumentation installations which included:

1. Time stamping for measurement synchronisation–this allowed the temporal alignment of electrical, meteorological and thermal data;

2. Meteorological stations needed to be near some thermal measurements for correlation between the two;

3. All measurements should be polled with a frequency of 60 s, 30 s would be ideal. This is because the sample frequency for characterisation can then be reduced if necessary (but if a polling time of 30 minutes is used it is impossible to know the data variation in between time instants);

4. Measurements near DG would be of great interest to this project;

5. Enough instrumentation needed to be installed to provide clear information for network characterisation (That is enough electrical measurements to be able to run a load flow, and enough thermal and meteorological instrumentation of the same area to run thermal models); and

6. There needed to be regions where electrical, thermal and meteorological measurements all exist to validate the algorithms used.

Guidelines for electrical instrumentation were developed to be able to emulate the electrical data from the DNO's network management system and to validate the methodology used for simulating the power flows using IPSA. This led to the specification of measurements for full network characterisation and for control algorithm validation. Guidelines and instrumentation specifications were also developed for the thermal characterisation of the network through the monitoring of component operating temperatures and the monitoring of meteorological conditions. In order to use meteorological measurements to validate the meteorological models, redundancy of meteorological weather stations was required. This allowed the state of meteorological conditions to be estimated at a particular meteorological station location, based on meteorological measurements at other meteorological stations, and validated using the meteorological conditions measured at the particular meteorological station location by the meteorological station itself [85]. A maximum distance of 10km between weather stations was specified. All instrumentation requirements were categorised into 'required' or 'desired'. This led to the commissioning of monitoring equipment of the field trial network characterisation.

7.5.3 Network instrumentation commissioning

Figure 7.1 summarises the instrumentation locations for the field trial network characterisation. The instrumented components correspond to those identified through the thermal vulnerability factor assessment in Figure 6.4. Electrical measurements for network characterisation, as specified above, were provided as off-line datasets from the historical electrical data logged by ScottishPower EnergyNetworks' SCADA system. Only electrical current validation measurements were commissioned in this phase.

7.6 Population of models with environmental conditions

One potential means by which power system real-time thermal ratings could be exploited is the direct population of component thermal models with monitored environmental conditions. Since industrial standards exist for the thermal modelling of components, systems developed to exploit real-time thermal ratings, based on these standards, would be expected to have integrity. Uncertainties in the accuracy of monitored data could be dealt with by creating a rating probability distribution and selecting the minimum rating for a particular operating condition [84]. However, there would be onerous instrumentation requirements to allow the exploitation of power system real-time thermal ratings in wide
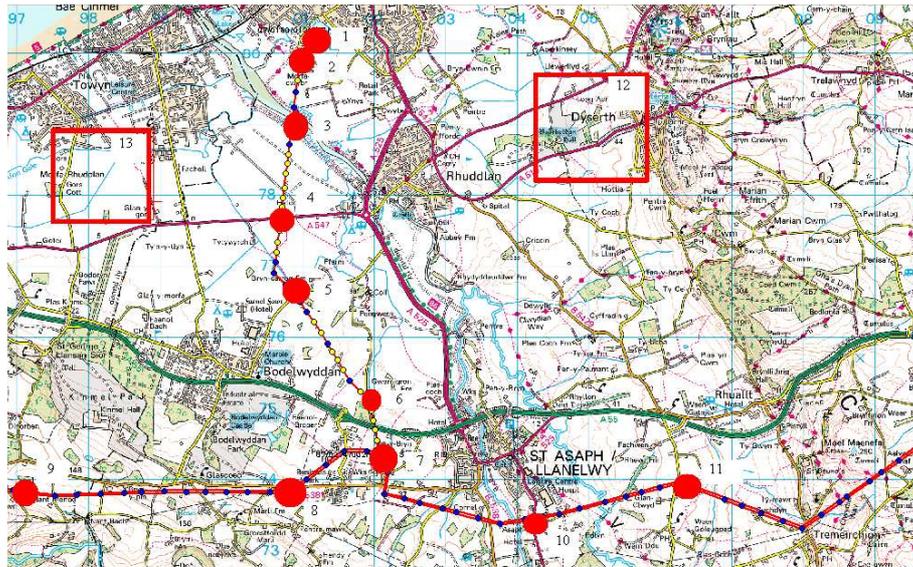
Figure 7.1: Location of monitoring equipment for network characterisation

areas of the distribution network. Furthermore, the real-time thermal rating system would require robust communications links to ensure thermal visibility at all times. Therefore this approach lends itself to situations where limited areas of the distribution network would require the real-time thermal rating to be exploited. This approach may also be used in protection relays to provide real-time thermal ratings for auxiliary power system security requirements [18].

7.7 Thermal state estimation

In this section the algorithm responsible for thermal state estimation is described [85]. The primary aim of the thermal state estimation algorithm is to allow the rating of components, which are not directly monitored within the power system, to be assessed. Thermal state estimations facilitate the precise and reliable assessment of environmental conditions whereby a minimal amount of meteorological monitoring installations facilitate the assessment of component thermal ratings within a wide area. This may then be validated through the carefully selected monitoring of component operating temperatures. The algorithm provides a reliable estimation of power system component thermal ratings described by an appropriate cumulative probability function. A state estimation technique based on the Monte Carlo method is used, giving a more complete description of the possible states of the system.

The Monte Carlo method consists of an iterative evaluation of results of deterministic

models relative to randomly selected input values. These inputs are randomly generated from probability density functions (PDF) describing parameter probabilistic structure. The results generated by the deterministic model in different trials can be represented in turn by probability distributions.

The minimum, maximum, average and standard deviation of component ratings may be calculated according to the variability of weather conditions. As necessary for overhead lines and electric cables, each component is divided into sections to take into account different thermal operating conditions such as overhead line orientations and changes in electric cable installation conditions. The section resulting in the lowest rating values is then used to provide a rating for the entire component. Furthermore, the deployment of a real-time thermal rating system which makes use of thermal state estimation techniques has the potential to reduce the necessity of auxiliary communications infrastructure whilst simultaneously increasing the reliability of the system if measurement or communication failures occur. This aids in fulfilling the functional requirement of the DG output control system to degrade, gracefully, in the presence of communications failures and data uncertainty.

7.8 Conclusion

This chapter described power system thermal limits and steady-state component thermal models, together with the use of meteorological information to populate component thermal models to provide component real-time thermal ratings. In addition, the use of thermal state estimation techniques whereby limited meteorological monitoring may provide power system real-time thermal ratings for wide areas of the distribution network were also described.

The control techniques that are described in Chapters 8 and 9 have been developed to utilise component thermal properties in making control decisions. Those thermal properties could be based on fixed meteorological assumptions or could be supplied by more sophisticated real-time thermal rating systems where they are available. Therefore the control techniques within the DG output control system may be deployed, equally applicably, with power system static thermal ratings, seasonal thermal ratings or real-time thermal ratings.

Chapter 8

DG output control algorithm development

8.1 Introduction

This chapter relates to the fourth and final stage of the distributed generation (DG) output control system development methodology as described in Chapter 4. In this chapter the control algorithm development is presented such that component thermal properties may be incorporated into on-line output control of DG schemes for network power flow management. Section 8.2 provides an overview of the control algorithm, including a functional specification for the control algorithm development. Section 8.3 provides details of the inference engine that allows the control algorithm to decide when DG output control is necessary for the management of network power flows. Section 8.4 describes techniques for DG set point calculation, the theory of which is presented in greater detail in Chapter 9. Section 8.5 describes the selection of a load flow package and its adaptation into a simulation tool for the off-line and on-line validation of control actions. Section 8.6 describes the data flow within the three control algorithm components (the inference engine, the DG set point calculator and the on-line simulation tool). Section 8.7 describes the evolutionary stages of the control algorithms and Section 8.8 discusses the functionality of the control algorithm to deal with partial data and data errors as inputs, as well as network topology changes.

8.2 Overview of control algorithm components

A decision flow chart was drawn up, as shown in Figure 8.1, to identify the specific functions of the control algorithm and simulation tool. This led to the following detailed functional specifications for the control algorithm and simulation tool development:

1. *Establish the present topology of the network:* As detailed in the scope of this research (Chapter 1) the DG output control system is designed to function with a 'system intact' network topology. Therefore the control system requires the functionality to be able to detect deviations in the network topology away from predetermined states. This information is provided by the status of circuit breakers within the distribution network;

2. *Detect if there is a thermal problem in the network:* The fundamental objective of this research is to develop a system to control the output of DG based on component thermal properties. Therefore the control system must be designed to detect the occurrence of thermal violations within the distribution network. This then acts as a trigger for the constraint of DG outputs in order to manage network power flows;

3. *Identify DG constraint solutions to solve thermal problems:* Candidate techniques for DG output control (as identified in Chapter 2) will be developed and assessed against present industry practices and network reinforcement options;

4. *Relax DG constraints if capacity headroom becomes available:* In the closed loop control system there needs to be functionality to relax DG constraints when power transfer headroom within the network becomes available;

5. *Validate solutions and refine as appropriate:* This may be achieved through a simulation tool which models the electrical behaviour of the distribution network; and

6. *Gracefully degrade in light of communication failures:* In order to fulfil this function the control system must be able to detect communication failures. A series of predetermined conservative default values may then be defined within the control algorithm to provide operational integrity in light of communication failures. It is envisaged that the DG output control system will behave in an increasingly conservative manner as an increasing number of communications signals are lost, defaulting eventually to the present industry practice of disconnecting DG schemes based on a static assessment of the network availability.

The six functional requirements detailed above were encapsulated within three software components: (i) an inference engine; (ii) a DG set point calculator; and (iii) an on-line simulation tool.
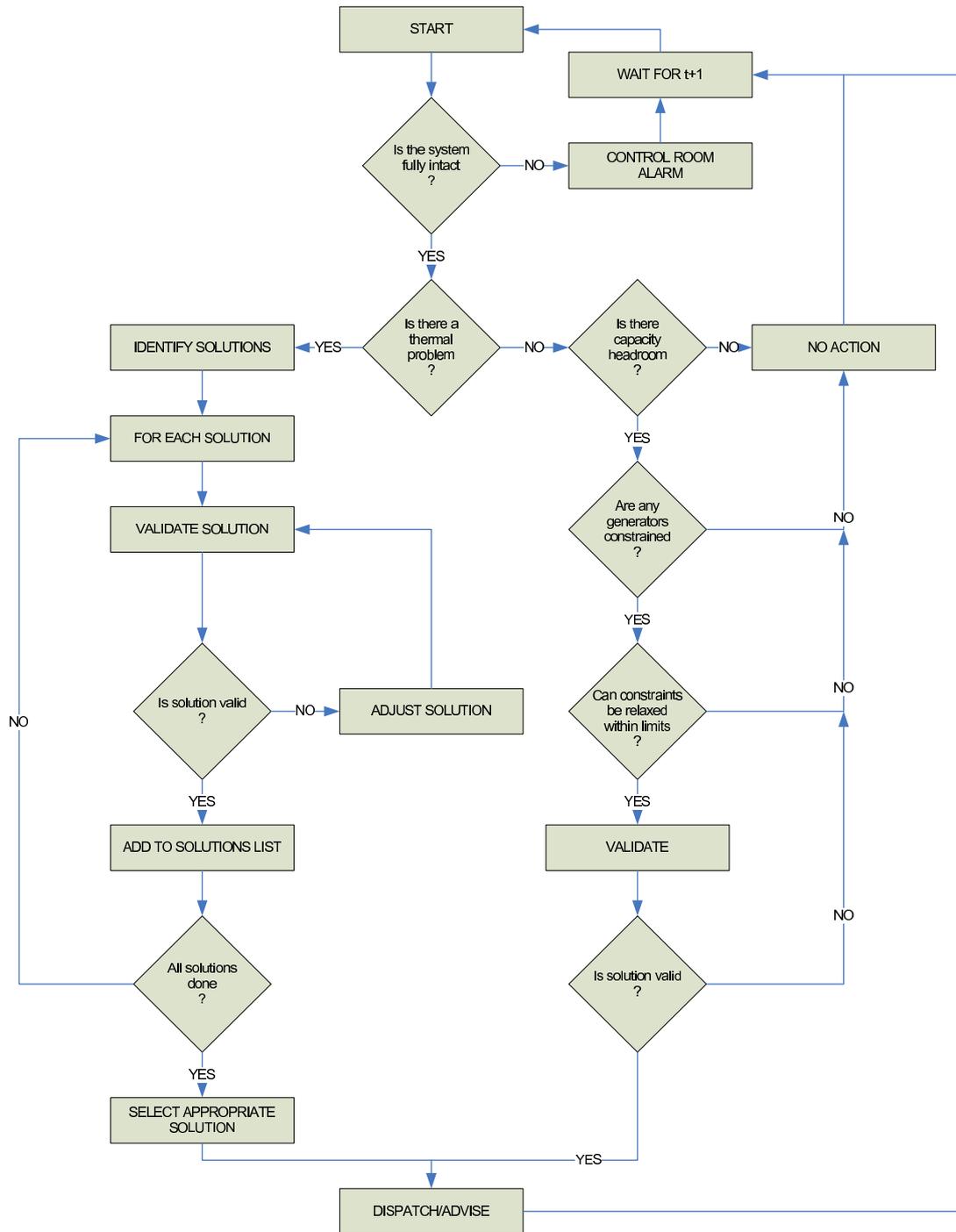
Figure 8.1: Control decision flow chart

The inference engine is deigned to emulate decision-making processes with artificial intelligence techniques. Therefore the functional requirements pertaining to decision-making (i.e. 'Is the system intact?', 'Is there a thermal problem?', 'Should DG be constrained or DG constraints be relaxed?, 'Is the control action valid?' and 'Are there any communica-

tions failures?') were assigned to this component. Whereas the inference engine is designed to establish if DG set point adjustments are required, the DG set point calculator compliments the inference engine by calculating the magnitude of the DG constraint or DG constraint relaxation. The on-line simulation tool is responsible for calculating updated network power flows and voltages based on the DG set point adjustments established by the DG set point calculator. This information is then passed back to the inference engine where the validation of power flow and voltage parameters can take place against thermal ratings and voltage limits. The development of the control algorithm and on-line simulation tool took place in two phases as seen in Figure 8.2. The third phase in this diagram relates to the integration of the control algorithm, the service orchestrator and connection manager within the service oriented architecture (as detailed in Chapter 4 for the practical implementation of the prototype DG output control system).

8.3 Inference engine

The fundamental purpose of the inference engine is to assess the operating state of the power system and make a control decision as appropriate. This may be done through rule-based decision-making with 'crisp' expected and actual operating states or through fuzzy decision-making in order to convert uncertainties in the actual operating state to 'crisp' values. Both of these techniques may be defined as 'artificial intelligence' techniques according to [96]. Some parameters within the system have 'crisp' states which means there is limited uncertainty about the actual operating state. For example, the status of a circuit breaker can be either opened or closed - it is not possible (in terms of electrical connectivity) to have a circuit breaker that is 'half' open or 'half' closed. Some parameters within an electrical network have uncertainty associated with them. For example the standard-based thermal rating of an overhead line is modelled based on a number of variables, such as wind speed, wind direction, ambient temperature and solar radiation, which are measured through monitoring equipment that may be non-local to the component. The accuracy of the calculated thermal rating is dependent on the accuracy of the model and also the monitoring equipment. Therefore, there is uncertainty regarding the extent to which the calculated thermal rating is representative of the 'actual' thermal rating. Moreover, since there is uncertainty associated with the thermal rating of a component this propagates to uncertainty regarding the extent to which a particular component is 'overloaded'. In this case the development of a fuzzy control system could help to deal with the uncertainties.
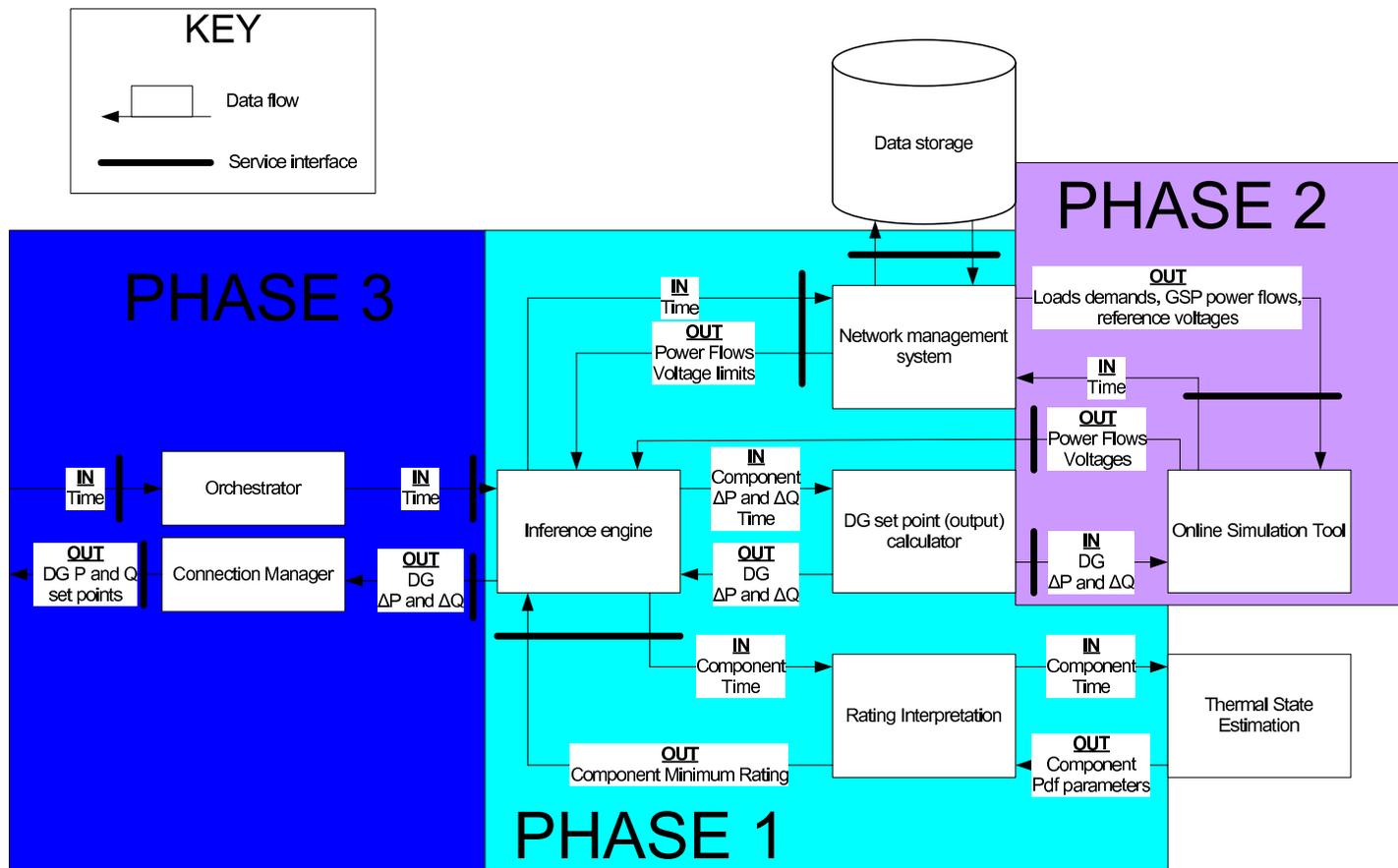
Figure 8.2: Development phases of DG output control system

The network topology is defined by the status of circuit breakers which have two 'crisp' boolean states - either opened or closed. Therefore, establishing the present network topology lends itself to rule-based decision making since a crisp set of expected circuit breaker states may be directly compared with the crisp set of actual circuit breaker states. Uncertainties may arise through loss of communications which may result in the actual status of a circuit breaker position being unknown. However, this could be dealt with by assuming worst case operating conditions (i.e. the actual circuit breaker status is in the opposite state to that which is 'expected') and taking control actions as appropriate.

In a similar way, uncertainties resulting from other communication failures may be dealt with using rule-based control techniques. For example any communication failures in the electrical parameters needed to operate the control system could result in conservative default values being used.

At this point it is necessary to define the utilisation of a power system component since this facilitates the control decision-making in terms of assessing the extent to which a component is 'over'-utilised or 'under'-utilised. Therefore DG constraints may be established when a component is assessed to be 'overloaded' and the relaxation of DG constraints may be established if component power transfer capacity headroom exists.

The utilisation of a particular power system component may be calculated as in (8.1)

$$U_{i,k}^c = \frac{S_{i,k}^c}{S_{i,k(lim)}^c} \tag{8.1}$$

where $U_{i,k}^c$ represents utilisation of component c between nodes i and k, $S_{i,k}^c$ represents the apparent power flow in component c from node i to node k and $S_{i,k(lim)}^c$ represents the thermal limit of component c.

Initially, although errors of $\pm 5\%$ exist within the monitoring of SCADA equipment [9] (this is discussed in Chapter 13), the monitored values recorded by the network management system were assumed to be representative of the 'actual' operating values. Real-time thermal ratings from the thermal state estimation algorithm are represented as a probability density function and the rating corresponding to the minimum probability was used to represent the real-time thermal rating of a particular power system component. Therefore, for the purposes of the research presented in this thesis, the component power flows and power system thermal ratings were assumed to have 'crisp' values. The 'crisp' component utilisation value can be used in rule-based inference as illustrated in Figure 8.3. In this diagram three utilisation values are specified: an upper utilisation limit (U-Constrain), a target utilisation limit (U-Target) and a lower utilisation limit (U-Relax). The variable util-
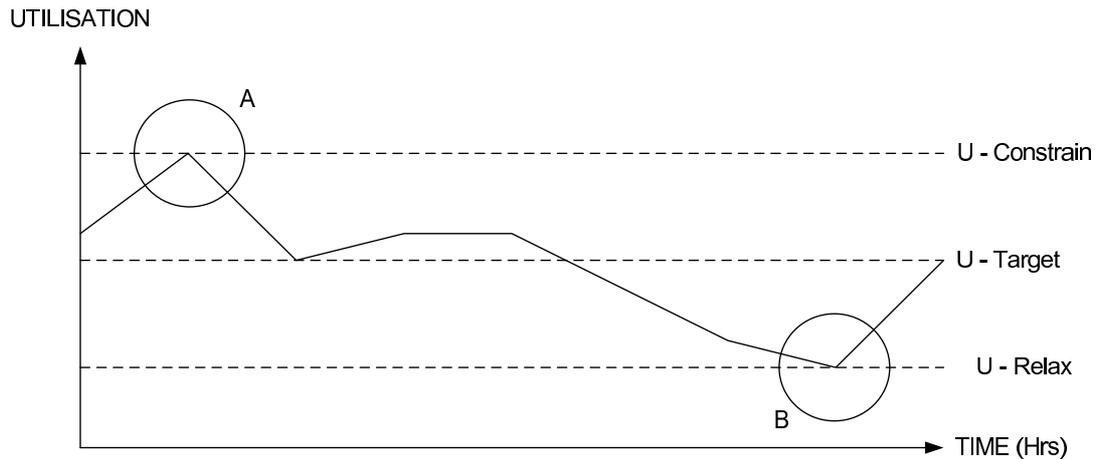
Figure 8.3: Three-rule inference engine

isation (illustrated by the unbroken line) represents the utilisation variation of a particular component with time. When a component utilisation occurs that is greater than (or equal to) the upper utilisation limit (denoted by region A) the resulting action is to constrain the output of the DG to achieve the target utilisation limit in order to protect the component from a sustained thermal overload. When a component utilisation occurs that is less than the lower utilisation target (denoted by region B) this triggers the control system to relax DG constraints back to the target utilisation limit. In the region between the upper and lower utilisation limits no control action is necessary.

8.4   DG set point calculator

Whilst the rule-based inference engine is responsible for determining whether or not a control action is necessary, the DG set point calculator is responsible for determining DG constraints or DG constraint relaxations that lead to the specified target utilisations of thermally vulnerable components. As detailed in the scope of this research, the primary aim of DG operators is to maximise the active energy yield of DG schemes and therefore wind farms tend to be operated at, or close to, unity power factor. Due to this driver the DG set point calculator determines updated real power outputs for the DG scheme(s) when control actions are necessary.

The DG set point calculator aims to reduce output constraints placed on DG schemes and hence increase annual active energy yield productions when compared to present operational practices. A number of candidate control techniques have been developed for both

single and multiple DG schemes and are described in detail in Chapter 9. The candidate control techniques for single DG schemes build on Engineering Technical Recommendation (ETR) 124 [50]. The multiple DG control strategies reflect (i) present last-in first-off contractual operating procedures; (ii) an egalitarian constraint strategy; and (iii) the most appropriate technical solution, based on power flow sensitivity factors. In addition, power output set points are established for multiple DG schemes in order to manage power flows in single and, if necessary, multiple components of the distribution network.

8.5 On-line simulation tool

ScottishPower EnergyNetworks own and operate a meshed electrical distribution network and, in all but the simplest of cases, a topological model combined with a load flow software package is required in order to solve component power flows and busbar voltages for the time-variant operation of the network. The top-level functionality of the on-line simulation tool is to produce updated component power flows and busbar voltages (based on updated outputs coming from the DG set point calculator) and pass these values back to the inference engine for validation against power flow and voltage limits. In order to select the most appropriate load flow package a number of sub-functions and user requirements were specified as follows:

1. Reliable and robust in terms of solution convergence for potential field application;

2. Efficient in terms of time taken to compute the load flow solution and computational memory requirements;

3. Accurate - allowing the user to specify the tolerance band of the convergence error;

4. Ease of building the electrical network in the simulation package and scalability for future network extensions;

5. Allow simulation inputs to be varied in real-time;

6. Allow inputs from SCADA to be readily incorporated;

7. Allow automation of simulations;

8. Return power flows and voltages in a format that facilitates comparison with operating limits;

9. Cost effective as a solution; and

10. Patent compatible.

An initial survey showed that a large number of commercially available load flow packages exist which offer a variety of functions. A short list of three packages was established, based on commercial exploitation, the availability of expert support for assessing the suitability of the load flow package against the criteria above, and the ease of integrating the load flow package into the service oriented architecture detailed in Section 4.6 of Chapter 4. The research findings are summarised below:

8.5.1 ScottishPower EnergyNetworks' network management system

The network management system installed in the control centre of ScottishPower EnergyNetworks contains an electrical state estimation algorithm and load flow algorithm for processing SCADA information monitored within the distribution network. However, the integration of these functions into the DG output control system was perceived by experts at ScottishPower EnergyNetworks to be prohibitively complex due to data access through security encryptions and the possible risk of network management system disruption.

8.5.2 AREVA's eterra*distribution* application

AREVA T&D have developed a suite of software tools for electrical network management system applications under the collective title of eterra*control*. Within this suite eterra*distribution* was identified as having the potential functionality required for the DG output control system. However, the load flow algorithm within the eterra*distribution* package could not easily be decoupled from large amounts of additional software which were superfluous to this particular application. Therefore, for the prototype control system development this option was disregarded.

8.5.3 IPSA

The assessment of the IPSA load flow package against the functional specifications showed that it could be adapted for incorporation in the DG output control system by the development of a scripting interface in the Python programming language. In the live multi-million pound AuRA-NMS project, involving seven top UK research institutions, IPSA was identified for use as an on-line simulation tool for validating control solutions. Therefore it was felt that there could be functionality overlap and scope for collaborative research in automating the operation of IPSA.

IPSA is a well-established steady-state load flow package within the electrical industry, being used by distribution network operators (DNOs), equipment manufacturers and consultants such as PB Power. The software tool was originally developed by researchers at the University of Manchester: Institution of Science and Technology (now the University of Manchester) with sponsorship from ScottishPower EnergyNetworks. Software development support was available through experts at TNEI with the provision of guidance and support in extending the functionality of IPSA to meet the requirements specified above.

Python is an open-source programming language that may be used for rapid prototyping applications. Many of the software fields and functions that are normally accessible to the user through IPSA's graphical user interface are mapped to software objects and software methods (in Python) within IPSA's scripted interface. Listed below are the principal advantages of using IPSA with a scripted interface:

- The development of Python scripts allows the functionality of the IPSA load flow package to be user-defined;

- load flows can be automated which means that a series of snapshots can be used to represent the steady-state operation of the network in real-time; and

- repetitive computations with minor network changes can be efficiently performed.

Four specific applications of scripted IPSA were developed in this project three of which were off-line and one of which was on-line:

1. Off-line simulation for parameter estimation at the 'front end' of the control system;

2. Off-line determination of power flow sensitivity factors;

3. Off-line simulation tool to validate updated DG set points; and

4. On-line simulation tool to validate updated DG set points.

Front end parameter estimation

As defined in the scope of this research (Section 1.3) the commercialised DG output control system will be integrated to receive electrical signals directly from SCADA monitoring equipment through the DNO's network management system. This decision has been taken since instrumentation and state estimation techniques for monitoring the electrical behaviour of power systems are already well-established. However, in developing the prototype DG output control system access to component power flow monitoring information

and circuit breaker status information was limited. For planning purposes ScottishPower EnergyNetworks have a complete model of their distribution network in the load flow package IPSA [93]. With the functionality provided by 'scripting' IPSA through the Python programming language [97] (whereby electrical datasets from ScottishPower EnergyNetworks' historical PI database can be input to the package, load flows automatically carried out and electrical dataset reports automatically generated) the operation of the distribution network (in terms of power flows and voltages) was able to be modelled by knowing the network topology, the generation into the system, the load demand from the system and voltage reference values at the grid supply points. This is illustrated in Figure 8.4.

Power flow sensitivity factor calculation

The functionality of scripted IPSA for the off-line calculation of power flow sensitivity factors is shown in Figure 8.5. Theory of power flow sensitivity factors is given in Chapter 4.

Off-line / on-line simulation tool

This application has the same functionality and is therefore a replication of the front-end parameter estimation application. The difference being that the front-end parameter estimation application represents the present network operating condition whereas the simulation tools use updated DG set points within the load flow algorithm in order to establish updated component power flows and busbar voltages as a result of control actions. The off-line simulation tool utilises off-line data whereas the on-line simulation tool utilises on-line data. These differences are shown in Figure 8.6.

8.6 Component inputs and outputs

Figure 8.7 displays the data flows within the DG output control system which specifically relate to the control algorithm and on-line simulation tool services developed and presented in this thesis.
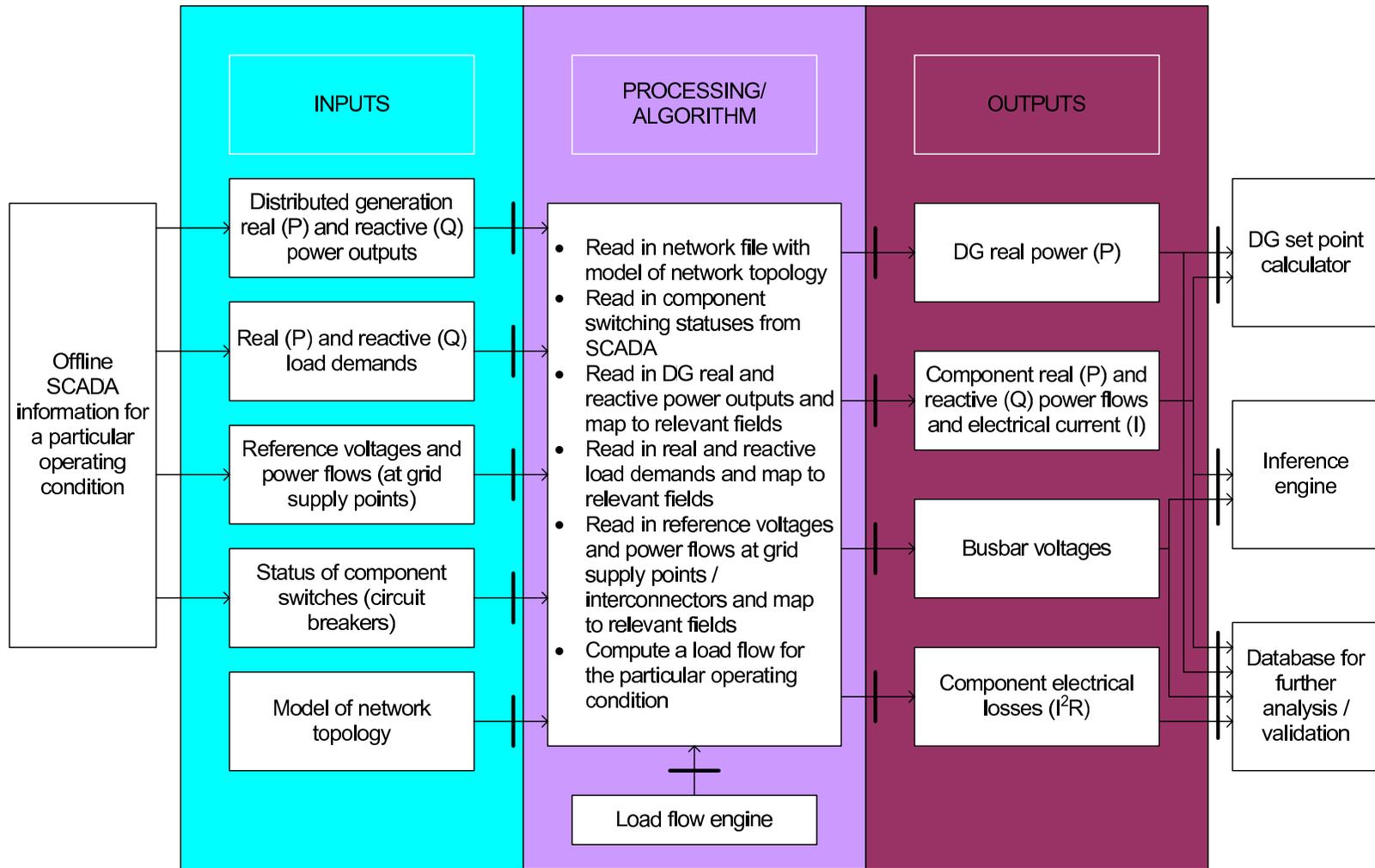
Figure 8.4: 'Front end' IPSA scripting for parameter estimation
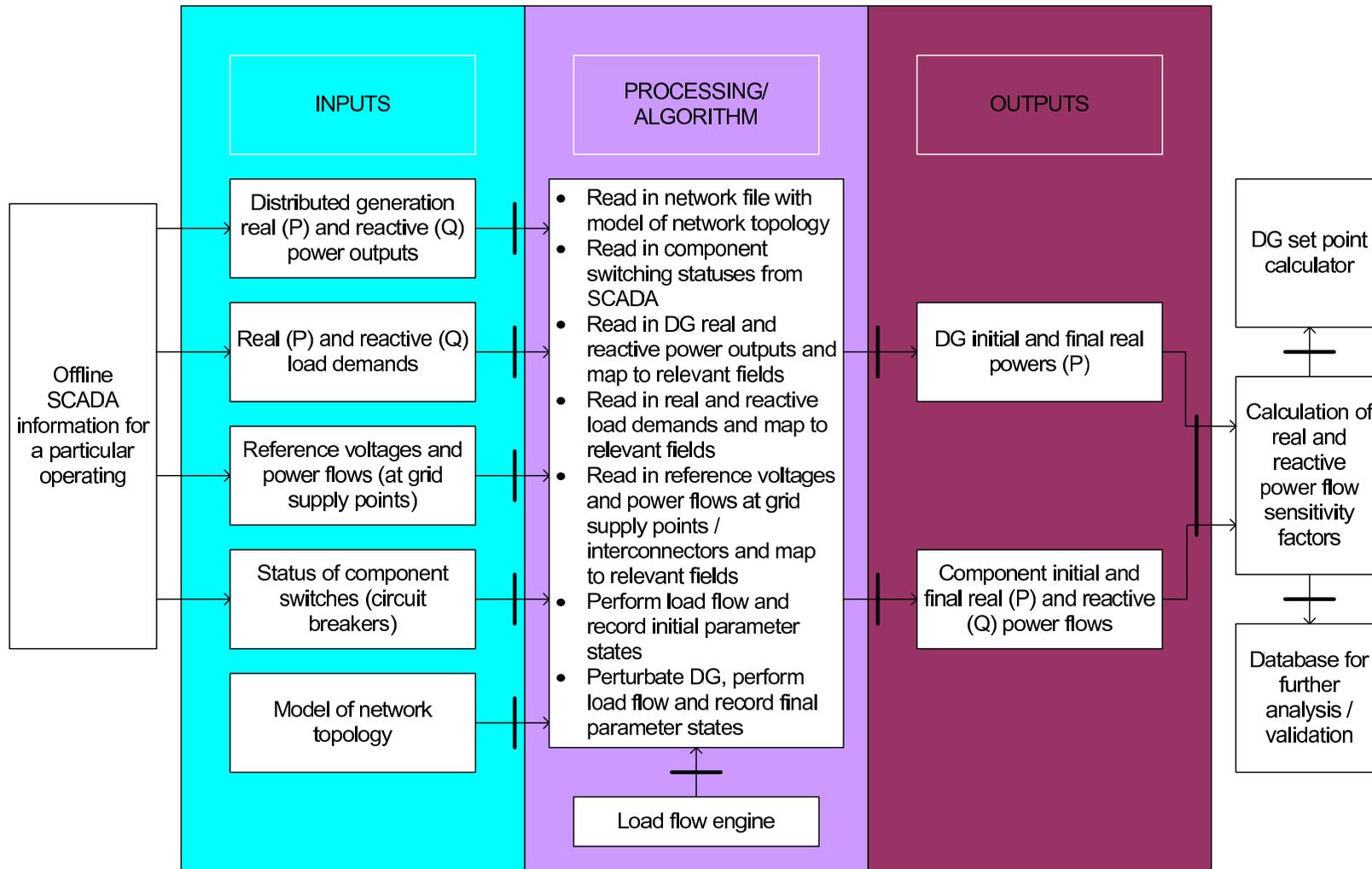
Figure 8.5: IPSA scripting for power flow sensitivity factor calculation
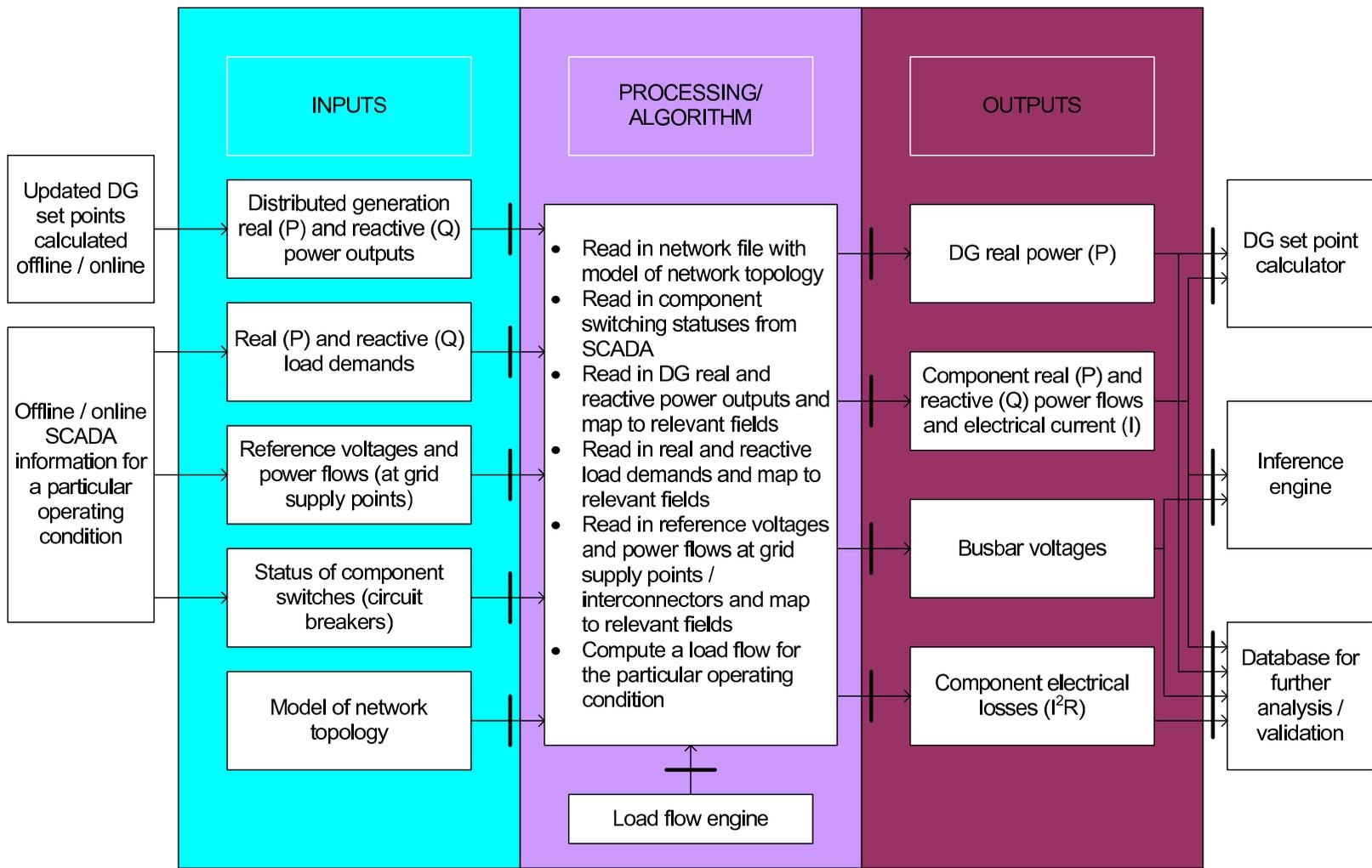
Figure 8.6: IPSA scripting for off-line and on-line simulation tool

SCADA

Present status of circuit breakers

DG Output Control

Alternative DG set point change solution strategies

Pre-calculated / Online Sensitivity Factors

$\Delta G_{p1}, \Delta G_{q1}, ...$ $\Delta G_{pn}, \Delta G_{qn},$

Online Simulation Tool

Java/Python Wrapper

IPSA (Load flow engine)

Present load demands, GSP power flows and reference voltages

SCADA

Electrical Network Model

P and Q Mismatches

Updated P and Q flows and busbar voltages

SCADA

Present P and Q flows

Inference Engine

A set of inference rules

Connection Manager Dispatch/Advise

Historical Database

Past P and Q flows and ratings

$\Delta G_{p1}, \Delta G_{q1}, ...$ $\Delta G_{pn}, \Delta G_{qn},$

Probability Density Function of Ratings

Thermal and Meteorological Measurements

External Parameter Processor

Thermal State Estimation Algorithm

Thermal Component Models

| Power Transformer | Underground Cable | Overhead Line |

KEY

Service within the architecture of the DG output control system

Component of a Service

Electrical / thermal network monitoring

Database

Data

Figure 8.7: Data flow within the DG output control system

8.7   Control algorithm evolution

The control algorithm within the DG output control system evolved in the following four stages:

1. Open-loop control with off-line data inputs;

2. Closed-loop control with off-line data inputs;

3. Open-loop control with on-line data inputs; and

4. Closed-loop control with on-line data inputs.

8.7.1   Off-line control loops

The off-line open and closed control loops, for the time-series analysis of the control system, are shown in Figure 8.8. In the open loop, normalised historical generation and load datasets are multiplied by peak scaling values which are fed into the network power flow emulation tool to produce a complete set of network power flows. The peak scaling factor(s) of the generation real power output profile(s) equal the installed capacity of the DG scheme(s). The inference engine utilises a rule-base with two rules to decide if 'DG constraint' or 'no action' is necessary. After the control algorithm has computed the necessary control actions and the DG set points have been validated, the new DG set points, busbar voltages, component utilisations and component losses are logged in a database for further off-line analysis. In the closed loop (represented in Figure 8.8 by the dotted line) the updated DG real power set point replaces the peak scaling factor (installed capacity) of the normalised historical generation profile. Therefore a third rule is introduced to the inference engine to relax DG constraints when the headroom in power transfer capacity leads to an 'under-utilisation' of the component. As before, DG set points, busbar voltages, component utilisations and component losses are logged in a database for further off-line analysis.

8.7.2   On-line control loops

The on-line open and closed control loops are shown in Figure 8.9. The network power flow emulation tool is replaced by electrical measurements which come directly from the distribution network. In the open loop, the DG real power output is multiplied by a scaling factor to represent a constrained connection and, as with the off-line open-loop control
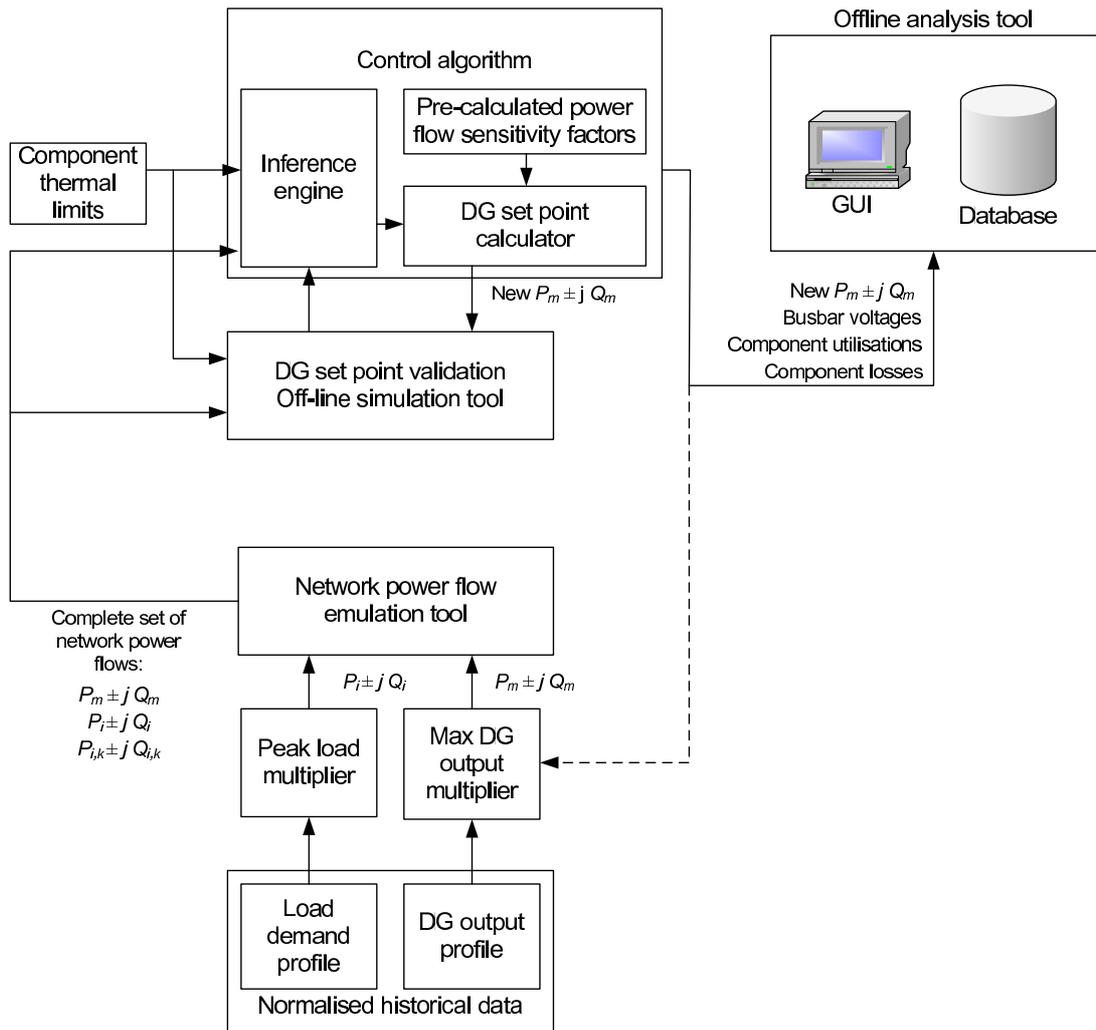
Figure 8.8: Off-line control in open and closed loops

system, the inference engine utilises a two-rule rule-base to decide if 'DG constraint' or 'no action' is necessary. After the control algorithm has computed the necessary control actions and the DG set points have been validated, the new DG set points, busbar voltages, component utilisations and component losses are logged in a database for further off-line analysis. In the closed loop, represented in Figure 8.9 by the dotted line leading to the decision support graphical user interface (GUI) in the DNO control room, the updated DG real power set points are dispatched to the DG scheme via the DNO control room. In this project this step was carried out in the simulation environment. As with the off-line closed-loop control system, a third rule is introduced to the inference engine to relax DG constraints when the headroom in power transfer capacity leads to an 'under-utilisation' of the component and DG set points, busbar voltages, component utilisations and component losses are logged in a database for further off-line analysis.
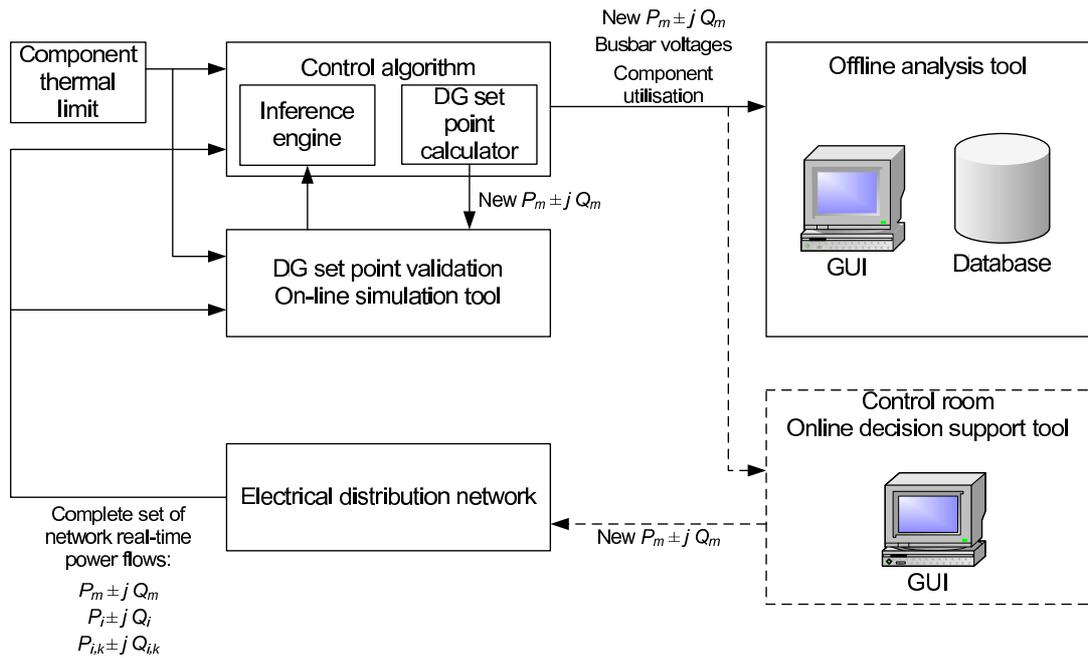
Figure 8.9: On-line control in open and closed loops

8.8   Data errors and network topology changes

This section proposes methods for dealing with input data errors and network topology changes. Data errors may arise (i) from partial datasets as a result of communications failures; and/or (ii) from the accuracy of monitoring equipment. Network topology changes could result from temporary electrical faults, scheduled maintenance work, as a result of a network reconfiguration action, network extensions or from new DG connections.

8.8.1   Dealing with partial data and data errors

In the event of communication failures, and in absence of auxiliary communication systems, the control algorithm may, at times, receive a partial dataset of input parameters. It is anticipated that the DG output control system, if deployed commercially, will receive inputs from the SCADA system which is likely to have electrical state estimation functionality and therefore be able to provide a complete electrical signal set to the DG output control system. As a back-up, a set of default values may be programmed into the 'front end' of the control algorithm. These default values represent conservative operating conditions and are selected to populate the missing parameter values if a partial dataset is input to the control algorithm. Thus the DG output control system is provided with graceful

degradation functionality. This is illustrated in Section 10.9 of Chapter 10.

Data errors may arise from the accuracy of monitoring equipment, installed to provide inputs to the control algorithm. In order to deal with data errors, assessments of the possible sources and magnitudes of errors are required and inputs to the control algorithm need to modified to account for the errors. Data errors and their impact on the DG output control system are discussed in detail in Section 13.5 of Chapter 13.

8.8.2 Dealing with network topology changes

Distribution network topology changes have the potential to impact on the continued operation of the DG output control system particularly, in the case of multiple DG scheme control, if the magnitude of power flow sensitivity factors is affected. This could require the adaptation of the control algorithm and on-line simulation tool within the control system to deal with the topology change. The cause of network topology changes may be broadly categorised as follows, each of which would require the control algorithm and simulation tool to be adapted in a slightly different manner:

- As a result of a temporary electrical fault in the network;

- as a result of network reconfiguration;

- as a result of scheduled maintenance in the network;

- as a result of network extensions; and

- as a result of new DG connections.

The potential ways in which the control system could be adapted to deal with network topology changes are outlined:

Electrical faults

Electrical faults could be detected through the unexpected opening or closing of circuit breakers i.e. circuit breakers that are not related to network reconfiguration actions. This could be achieved through the constant comparison of monitored circuit breaker signals with default values embedded within the control algorithm. It is outside the scope of this research to develop a DG output control system to function in electrical contingency scenarios and it is likely that the DG scheme will automatically be disconnected through control actions of the DNO's protection system.

Network reconfiguration

In the case of multiple DG scheme output control, the derived power flow sensitivity factors are network configuration-specific and assume that the network configuration will not be frequently changing. It is feasible, however, to develop an on-line control system that makes use of alternative sets of the above mentioned predetermined power flow sensitivity factors based on network switch status information.

Scheduled maintenance, network extensions and new DG connections

Scheduled maintenance of the distribution network, network extensions and new DG connections are planned by the DNO many months in advance of the event occurrence. During scheduled maintenance it is likely that the DG scheme(s) will be disconnected or required to operate at a reduced peak output based on the available network capacity.

The methodology framework required to adapt the DG output control system to deal with scheduled maintenance, network extensions and new DG connections is provided in Chapter 4. An overview of the required DG control system adaptation steps is provided below:

1. Modify the topology of the network as appropriate in the analysis and on-line simulation tool models;

2. Conduct an updated off-line study to identify any new thermally vulnerable components within the distribution network that may result from the topology change;

3. Develop as appropriate a new real-time thermal rating system to incorporate any new power system components that have become thermally vulnerable as a result of the topology change; and

4. Specifically related to the control algorithm, the particular control strategy / strategies need to be updated to incorporate the network topology change:

   (a) Conduct a new off-line analysis to determine power flow sensitivity factors;

   (b) modify rule-bases in the inference engine as necessary to achieve the desired control functions;

   (c) incorporate additional terms in the DG set point calculator equations to account for the control of the new network topology; and

(d) update the on-line simulation tool model and simulation algorithm to incorporate and validate the power flows and voltages resulting from the new network topology.

It should be noted that some scheduled maintenance work, network extensions and new DG connections may have a negligible impact on the power flow sensitivity factors of thermally vulnerable components to DG schemes and therefore control system modifications may not be strictly necessary. In addition, the anticipated length of the scheduled maintenance period is likely to impact on the decision to update the control system.

8.9   Conclusion

In this chapter the development of the control algorithm within the DG output control system was presented. Rule-based decision-making was proposed for use within an inference engine to determine the need for control actions which may constrain DG outputs, take no action or relax DG output constraints. The magnitude of DG output constraints or DG output constraint relaxations are determined by a DG set point calculator which incorporates candidate strategies for single or multiple DG scheme output control. Control actions are validated through an on-line simulation tool. It was decided that the development of strategies for the coordinated output control of DG schemes could be of more benefit to DG scheme developers than the development of a fuzzy inference techniques (the latter also had the potential to reduce the transparency of the DG output control system for users not familiar with fuzzy control techniques). Therefore DG output control techniques were investigated in greater depth than rule-based and fuzzy logic-based decision-making techniques and form the basis for the research presented in Chapters 9–13.

Chapter 9

Techniques for DG output control and evaluation

9.1 Introduction

This chapter describes the techniques which may be utilised for the output control of single DG schemes and the proposal of strategies for the coordinated output control of multiple DG schemes. The research presented in this chapter was published by the author in [86, 88, 98]. Engineering Technical Recommendation (ETR) 124-based techniques are adapted for the output control of single DG schemes and are described in Section 9.2. Section 9.3 recaps the theory regarding DG output control based on power flow sensitivity factors. Section 9.4 extends this theory to propose three strategies for the output control of multiple DG schemes. These are: (i) A last-in first-off (LIFO) strategy (reflecting present DG contractual agreements) [54]; (ii) an egalitarian strategy (whereby the power output of multiple DG schemes is adjusted by an equal percentage of their current output using a single broadcast signal) [56]; and (iii) a technically most appropriate (TMA) DG constraint strategy (whereby the DG scheme with the best technical ability to manage network power flows is selected to be adjusted) [72]. In Section 9.5, parameters are proposed to evaluate the control algorithms in order to quantify potential DG output control system benefits. The techniques used to quantify the evaluation parameters are given in generic forms and include: Numerical integration to calculate annual energy yields and annual energy losses; a loss apportioning technique to attribute energy losses to particular DG schemes; the financial quantification of DG development net present values (NPVs) and profitability indices (PIs); and the summarising of component power transfers and busbar voltages through duration curves.

9.2   Single DG scheme control using ETR 124 techniques

For the management of power flows associated with the connection of a single DG scheme, the following techniques are proposed, based on ETR 124 [50]:

1. DG tripping based on a static assessment of network availability;

2. DG tripping based on component seasonal thermal ratings;

3. Demand-following DG output control based on component static thermal ratings; and

4. Demand-following DG output control based on component real-time thermal ratings.

Schematic diagrams for the DG tripping and demand-following DG output control techniques are respectively provided in Figures 10.3 and 10.4 of Chapter 10. The DG tripping technique is implemented using the algorithm given in (9.1).

$$
\begin{aligned}
If: & \quad Current > Rating \\
Then: & \quad Trip\ DG\ to\ Rating + Base\ load
\end{aligned}
\tag{9.1}
$$

When this algorithm is implemented with the static assessment of network availability, the DG output will be tripped to the static rating plus the base load if the power flow in the thermally vulnerable component exceeds the static rating. This corresponds to the implementation of Technique 1 in the list above. Similarly, in a seasonal rating implementation [51], such as Technique 2, the DG output will be tripped to the seasonal rating plus the base load if component power flow exceeds the seasonal rating. These techniques do not account for the variable nature of the load and thus they trip off individual generating units, rather than constraining them back.

Demand-following DG output control is implemented using the algorithm in (9.2) based on static, seasonal or real-time thermal ratings and monitoring of the variable load demand.

$$
\begin{aligned}
If: & \quad Current > Rating \\
Then: & \quad Control\ DG\ output\ to\ Rating + Load\ demand
\end{aligned}
\tag{9.2}
$$

The control algorithm given in (9.2) is implemented with static ratings to realise Technique 3 and real-time thermal ratings to realise Technique 4. The demand-following DG output control techniques are more sophisticated than the DG tripping techniques and have the potential to offer energy yield gains by taking into account the variable nature of power system thermal ratings and the load demand. To ensure the safe and secure operation of

the network assets, demand-following DG output control techniques require an auxiliary trip system, which utilises the same ratings as the control algorithm, to act as a backup in the case of control system operational failure.

ETR 124 describes techniques for the output control of single DG schemes and, although it is suggested that the proposed techniques may be extended to control multiple DG schemes, this aspect is not demonstrated. Due to the simple algebraic power flow algorithms given in ETR 123, the proposed techniques are appropriate for situations where the power output from a single DG scheme is being controlled as a result of a local thermal constraint. If power output control of the DG scheme is required to solve power flow constraint issues deeper into the network then the algebraic formulations provided in ETR 124 are not adequate. In this situation power flow constraints may be solved through the use of power flow sensitivity factors that relate changes in the output of DG schemes to changes in distribution network power flows. These concepts are described in Section 9.3 and in Appendix D.

9.3 Proposed techniques for DG control using power flow sensitivity factors

For a given operating condition the evaluated power flow sensitivity factors may be stored efficiently in matrix form (9.3).

$$
M_{PFSF} = \begin{bmatrix} \dfrac{dP_{1,2}}{dG_{P,1}} & \dfrac{dP_{1,3}}{dG_{P,1}} & \cdots & \dfrac{dP_{i,k}}{dG_{P,1}} \\[2em] \dfrac{dP_{1,2}}{dG_{P,2}} & \dfrac{dP_{1,3}}{dG_{P,2}} & \cdots & \dfrac{dP_{i,k}}{dG_{P,2}} \\[2em] \vdots & \vdots & \ddots & \vdots \\[2em] \dfrac{dP_{1,2}}{dG_{P,m}} & \dfrac{dP_{1,3}}{dG_{P,m}} & \cdots & \dfrac{dP_{i,k}}{dG_{P,m}} \end{bmatrix} \tag{9.3}
$$

When network power flow management is required, the amount an individual DG scheme is constrained may be calculated (9.4) using values from the power flow sensitivity factor matrix, M_{PFSF}, (9.3)

$$\Delta G_{P,m} = \frac{\Delta P_{i,k}}{\left(\dfrac{dP_{i,k}}{dG_{P,m}}\right)} \qquad (9.4)$$

where $\Delta G_{P,m}$ is the required change in real power output of the DG scheme connected at node m; $\frac{dP_{i,k}}{dG_{P,m}}$ is the power flow sensitivity factor that relates the change in nodal real power injection at m with the change in real power flowing from node i to node k; and $\Delta P_{i,k}$ is the required change in real power flowing from node i to node k in order to manage network power flows, as evaluated in (9.5)

$$\begin{aligned} \Delta P_{i,k} &= \sqrt{(U_{Tar} \times S_{i,k(lim)}^{c})^2 - ('' Q_{i,k})^2} \\ &\quad - \sqrt{('S_{i,k})^2 - ('Q_{i,k})^2} \end{aligned} \qquad (9.5)$$

where U_{Tar} is the target utilisation of the congested component after control actions have been implemented; $S_{i,k(lim)}^{c}$ is the thermal limit of the congested component; $'S_{i,k}$ is the apparent power flowing from node i to node k before control actions are implemented and, $'Q_{i,k}$ and $''Q_{i,k}$ respectively represent the reactive power flowing from node i to node k before and after the control actions have been implemented. Thus the updated DG scheme output is evaluated using (9.6)

$$'' G_{P,m} = \ 'G_{P,m} + \Delta G_{P,m} \qquad (9.6)$$

where $'G_{P,m}$ and $''G_{P,m}$ represent the respective real power outputs of the DG scheme connected at node m before and after control actions have been implemented.

9.4 Proposed strategies for multiple DG scheme control

This section presents the candidate strategies for power output control of multiple DG schemes and extends the theory for the control of individual DG schemes based on power flow sensitivity factors. The proposed strategies are:

- LIFO PFSF-based DG output control;

- DG output control using an egalitarian broadcast signal whereby DG schemes adjust their power output by the same percentage of their present power output; and

- DG output control by selecting the TMA DG scheme to adjust.

The LIFO PFSF-based strategy represents current operational practices with the addition of power flow sensitivity factor benefits i.e. matching DG power output adjustments to

the network availability. The egalitarian broadcast signal strategy was of particular interest to ScottishPower EnergyNetworks due to the anticipated ease of implementation. The TMA strategy represents the best technical option if contracts are in place to deal with arising commercial and regulatory issues. The strategies are outlined in greater detail in the sections that follow.

9.4.1   LIFO PFSF-based

DG power outputs are curtailed in a LIFO contractual order, defined within the matrix $\boldsymbol{M}_{LIFO}$ (9.7)

$$\boldsymbol{M}_{LIFO} = \begin{bmatrix} x_1^{G_{id}} & x_2^{G_{id}} & \cdots & x_{m_T}^{G_{id}} \end{bmatrix} \tag{9.7}$$

where the integer x, represents the ranked order of curtailment for the DG scheme, G, with a unique identifier (id), at nodes 1, 2, up to m_T respectively (m_T being the DG connection node with the highest index). The unique identifier aids clarity and is necessary for situations where multiple DG schemes have the same connection point to the distribution network but separate operating contracts. The generic form of this strategy is given in (9.8)–(9.11). A set point change is dispatched to relevant DG operators that match DG power outputs to the capability of the network. If, by implementing the required reduction, as calculated in (9.8), the signal is driven negative (9.9) the DG is tripped (9.10) and the next DG scheme, contractually, to be constrained is apportioned the required power output reduction (9.11). By adopting this approach, 'last-in' DG schemes are penalised if power flow excursions occur, even if they are not making a significant power output contribution at that time. Moreover, as DG proliferates there is an increased implementation complexity for DNOs in terms of dispatching the constraint signals to a series of DG scheme operators.

$$^{x}\Delta G_{P,m} = \frac{^{x}\Delta P_{i,k}}{^{x}\left(\dfrac{dP_{i,k}}{dG_{P,m}}\right)} \tag{9.8}$$

If:

$$^{x}G_{P,m} + {}^{x}\Delta G_{P,m} < 0 \tag{9.9}$$

Then:

$$^{x}G_{P,m} = 0 \tag{9.10}$$

and

$$^{x+1}\Delta P_{i,k} = {}^{x}\Delta P_{i,k} - {}^{x}G_{P,m} \times {}^{x}\left(\frac{dP_{i,k}}{dG_{P,m}}\right) \tag{9.11}$$

9.4.2 Egalitarian broadcast signal

The complexity of dispatch signals, associated with a LIFO control strategy could be overcome through an egalitarian percentage constraint signal that is simultaneously broadcast to all DG schemes. In this strategy a reduction signal, Φ, as calculated in (9.12)–(9.13), is broadcast to all the relevant DG schemes. When an assessment of the reduction signal is calculated, not only does this take into account the power output magnitudes of each DG scheme, it also considers the power flow sensitivity factors. The constraints required to manage the network power flows are shared by each DG scheme and those DG schemes making a significant power output contribution are constrained more, in terms of the absolute power output reduction (ΔG_P) than those DG schemes making a small contribution. The derivation of the egalitarian broadcast signal is given in Appendix D.

$$\Delta G_{P,m} = G_{P,m} \times \Phi \tag{9.12}$$

$$\Phi = \frac{\Delta P_{i,k}}{\sum\limits_{m=1}^{m=m_T} \left(G_{P,m} \times \left(\frac{dP_{i,k}}{dG_{P,m}} \right) \right)} \tag{9.13}$$

9.4.3 Technically most appropriate

The DG scheme are ranked for power output adjustment, in a technical priority order, by the relative magnitude of power flow sensitivity factors given in matrix $\boldsymbol{M}_{TMA}$ (9.14)

$$\boldsymbol{M}_{TMA} = \begin{bmatrix} x_1^{G_{id}} & x_2^{G_{id}} & \cdots & x_{m_T}^{G_{id}} \end{bmatrix} \tag{9.14}$$

where the integer x, represents the ranked order of DG curtailment for the DG scheme, G, with a unique identifier (id) at nodes 1, 2, up to m_T respectively, based on the relative magnitudes of power flow sensitivity factors given in (9.3). The generic form of this strategy implementation, as with the LIFO strategy, is given in (9.8)-(9.11). In this case the DG scheme with the best technical ability to manage network power flows is selected.

9.5 Proposed DG output control evaluation parameters

This section proposes a number of parameters for the time-series evaluation of DG output control techniques and suggests techniques that may be used to quantify the evaluation parameters. These include: (i) Numerical integration to calculate annual energy yields

and annual energy losses; (ii) a loss apportioning technique to attribute energy losses to particular DG schemes; (iii) the financial quantification of DG development NPVs and PIs; and (iv) the summarising of component power transfers and busbar voltages through duration curves. In the sections that follow the techniques used to quantify the evaluation parameters are given in generic forms.

9.5.1 Annual energy yields

The numerical technique used to integrate DG power outputs and hence quantify DG annual energy yields is given in (9.15)

$$E_a = t \times \left(\frac{^0G_P + {}^yG_P}{2} + \sum_{x=1}^{x=y-1} {}^xG_P \right) \tag{9.15}$$

where E_a represents the annual energy yield of the DG scheme, t represents the time-step of the integration, and $^{0,x,y}G_P$ represents the real power output of the DG scheme, G, at the initial (0), intermediate (x), and final (y) time-steps.

9.5.2 Loss apportioning

The technique used to apportion energy losses to individual DG schemes in a proportional manner, through a component connecting multiple DG schemes to the distribution network, is given in (9.16)-(9.17).

$$P_{loss,i,k,m} = P_{loss,i,k,total} \times \frac{G_{P,m}}{\sum G_{P,m}} \tag{9.16}$$

where $P_{loss,i,k,m}$ represents the real power lost in the component between node i and node k and apportioned to a particular DG scheme at node m; $P_{loss,i,k,total}$ represents the total real power lost as heat in the component between node i and node k due to the Joule effect (I^2R_{ac}); $G_{P,m}$ represents an individual DG scheme real power injection at node m; $\sum G_{P,m}$ represents the total real power injection at node m from multiple DG schemes and

$$E_{loss} = t \times \left(\frac{^0P_{loss} + {}^yP_{loss}}{2} + \sum_{x=1}^{x=y-1} {}^xP_{loss} \right) \tag{9.17}$$

where E_{loss} represents the apportioned annual energy loss, and P_{loss}, t, x and y retain their definitions as above. More complex loss apportioning techniques, looking deeper into the power system, are described by Bialek [77] for power flow tracing and by Kirschen and Strbac [78] for current tracing.

9.5.3 Economic assessment

The economic assessments focus, in particular, on wind farms as this was of most interest in the DIUS Project. Building on the work of Payyala and Green [99], the methodology used to evaluate the NPV of the wind farm investment to each DG developer, and therefore the PI, is presented. The total investment cost for each developer, $C_{R(inv)}$, is modelled as a sum of three variable costs, $C_{R(1-3)}$ (9.18)–(9.21)

$$C_{R(inv)} = C_{R(1)}(G_i) + C_{R(2)}(n_1) + C_{R(3)}(n_2) \tag{9.18}$$

where

$$C_{R(1)}(G_i) = G_i C_{G_i} \tag{9.19}$$

and G_i represents the installed capacity of the DG scheme and C_{G_i} represents the total wind farm installation costs including wind turbine generators, foundations, electrical infrastructure, and planning and development costs;

$$C_{R(2)}(n_1) = C_{R(control)}/n_1 \tag{9.20}$$

where the cost of the control system, $C_{R(control)}$, including development costs, installation costs, necessary communications links and the auxiliary trip system is shared amongst the number of stakeholder investors (n_1) and

$$C_{R(3)}(n_2) = C_{R(real-time)}/n_2 \tag{9.21}$$

where the cost of the real-time thermal rating system, $C_{R(real-time)}$, including development costs, thermal instrumentation costs, and the cost of necessary communications links is shared amongst the number of stakeholder investors, n_2.

The cost of the annual operations and maintenance, $C_{R(OM)}$, is modelled as a proportion, K_{OM}, of the wind farm installation cost (9.22)

$$C_{R(OM)} = K_{OM} G_i C_{G_i} \tag{9.22}$$

The annual net revenue, $C_{R(annual)}$, of each wind farm developer is modelled in (9.23)–(9.25) by subtracting the cost of losses, $C_{R(loss)}$, from the revenue generated through the metered active energy yield, $C_{R(EY)}$

$$C_{R(annual)} = C_{R(EY)} - C_{R(loss)} \qquad (9.23)$$

$$C_{R(EY)} = E_a \left(C_{E(wholesale)} + C_{E(ROC)} \right) \qquad (9.24)$$

$$C_{R(loss)} = E_{loss} \times C_{E(wholesale)} \qquad (9.25)$$

where E_a is the metered active annual energy yield of the wind farm development, E_{loss} is the active annual energy losses apportioned to each DG developer, $C_{E(wholesale)}$ represents the wholesale electricity price, and $C_{E(ROC)}$ is the sale price of Renewables Obligation Certificates (ROCs).

The NPV of each wind farm investment is quantified in (9.26) by assessing the present value (PV) of the annuity $(C_{R(annual)} - C_{R(OM)})$, discounted over the project lifetime, and subtracting the cost of the original investment.

$$NPV = PV \left(C_{R(annual)} - C_{R(OM)} \right) - C_{R(inv)} \qquad (9.26)$$

The PI for each wind farm development is defined as the ratio of the NPV to the initial investment (9.27) [99].

$$PI = \frac{NPV}{C_{R(inv)}} \qquad (9.27)$$

Clearly the results of financial evaluations are sensitive to wind farm installation costs, discount rates, project lifetimes, wholesale electricity prices and the sale price of ROCs. In addition, and particularly for financial analyses related to multiple DG schemes, the connection charging mechanism plays an important role [100]. If a deep charging mechanism is assumed then the DG developer pays for all the costs incurred within the distribution network that can be attributed to the DG scheme connection and operation. For example, the cost of the local circuit and any necessary uprating to switchgear equipment. This charging mechanism is presently applied to connections at the distribution network level. An alternative shallow charging mechanism is applied at transmission network level. In applying this charging mechanism the DG developer would pay directly only for the part of the power system which is solely used by the DG scheme. Other reinforcement costs are recovered through use-of-system charges. However, the development of a use-of-system charging mechanism at the distribution network is more complex than the use-of-system

charging mechanism at the transmission network level since the users are expected to change more frequently at the distribution network level.

9.5.4   Power transfers and busbar voltages

Load duration curves [14] are a planning tool used to summarise and analyse the power demand at supply points in the power system. The same technique was adapted to produce the power transfer curves of components and evaluate the performance of DG control strategies in utilising power system assets more effectively. Moreover, busbar voltage duration curves were produced to summarise and analyse the impact of candidate DG control strategies on busbar voltages across the year.

9.6   Conclusion

This chapter described techniques which may be utilised for the output control of single and multiple DG schemes. ETR 124-based techniques are adapted for the output control of single DG schemes. The theory of power flow sensitivity factors was developed to propose three strategies for the coordinated output control of multiple DG schemes. These included: (i) A LIFO strategy (reflecting present DG contractual agreements); (ii) an egalitarian strategy (whereby multiple DG schemes are adjusted by an equal percentage of their current output using a single broadcast signal); and (iii) a TMA strategy (whereby the DG scheme with the best technical ability to manage network power flows is selected to be adjusted). In order to quantify DG output control system benefits, techniques and parameters were proposed to evaluate the control algorithms. These included: Numerical integration to calculate annual energy yields and annual energy losses; a loss apportioning technique to attribute energy losses to particular DG schemes; the financial quantification of DG development NPVs and PIs; and the summarising of component power transfers and busbar voltages through duration curves. The proposed techniques and evaluation parameters may provide a comprehensive framework which facilitates the quantification of DG output control system benefits for DNOs and DG scheme developers.

Chapter 10

Case study 1: Output control of a single DG scheme based on a single thermal constraint

10.1 Introduction

This chapter describes the simulation of Engineering Technical Recommendation (ETR) 124-based control techniques in order to manage the power output of a single distributed generation (DG) scheme based on component thermal properties. The research presented in this chapter was published by the author in [98, 101]. The technical considerations and economics of a number of techniques that would allow a greater installed capacity of DG to be connected to, and operated within, the distribution network are presented. The techniques include: (i) The tripping-off of the DG scheme based on a static assessment of component ratings and minimum load demand at the DG connection busbar; (ii) the tripping-off of DG based on seasonal thermal ratings and minimum load demand at the DG connection busbar; (iii) the load demand-following output control of DG schemes based on a static thermal ratings; (iv) the load demand-following output control of DG schemes based on real-time thermal ratings (RTTRs); and (v) the provision of an unconstrained DG connection through network reinforcement.

The chapter is structured in the following way: Section 10.2 describes the case study network, Section 10.3 describes the real-time thermal rating assessment of the thermally vulnerable overhead line, Section 10.4 describes the power flow management techniques, Section 10.5 describes the time-series electro-thermal simulation approach, Section 10.6 describes the quantification methodology for the evaluation of the DG output control tech-

Table 10.1: Summary of ratings utilised

Conductor type	Rating condition	Rating (A)	Rating (MVA)
LYNX	Static / summer seasonal	390	89
LYNX	Spring/autumn seasonal	450	103
LYNX	Winter seasonal	485	111
LYNX	Real-time (average daily minimum)	695	159
UPAS	Static / summer seasonal	770	176

niques, Section 10.7 presents the simulated real-time changes in DG power outputs, Section 10.8 presents and discusses the results of the evaluation parameter quantification methodology and Section 10.9 demonstrates the graceful degradation of the control algorithm due to partial dataset inputs.

10.2 Case study description

The case study network shown in Figure 10.1 is derived from the section of ScottishPower EnergyNetworks' distribution network given in Figure 3.1 and formed the basis for the prototype DG output control system field trials in the DIUS Project. Considering Figure 10.1 in the context of Figure 3.1, B5 represents the DG connection busbar and B4 represents the slack busbar with static, seasonal and real-time thermal ratings applied to component C4. Although it is not displayed in Figure 10.1, Engineering Recommendation P2/6 [8] security of supply requirements are met for the connected load through an underlying meshed 33kV infrastructure. An installed wind capacity of 150 MW was selected to create a constrained connection.

10.3 Real-time thermal rating assessment

Table 10.1 displays the ratings used in the energy yield quantification analyses. The static and seasonal ratings were based on the SP Manweb Long Term Development Statement [14]. The average simulated daily minimum real-time thermal rating is also given in Table 10.1. Off-line analysis showed that a thermal constraint would be met in this section of the network before voltage or fault-level limitations.

In the first series of control algorithm simulations [98], a modest Aeolian up-rating of

Wind Farm
150 MW Installed Capacity
Injecting power at bus at unity power
factor

DG

132kV

LYNX 175 square-mm
ACSR conductor

LOAD
10 MVA $-$ 36 MVA
(44A $-$ 157A)
At an average power
factor of 0.97
(importing VArs)

Tensioned at
50 degrees Celsius

R + jX = 0.007+j0.0165 pu
on 100MVA base

132kV (Slack bus)
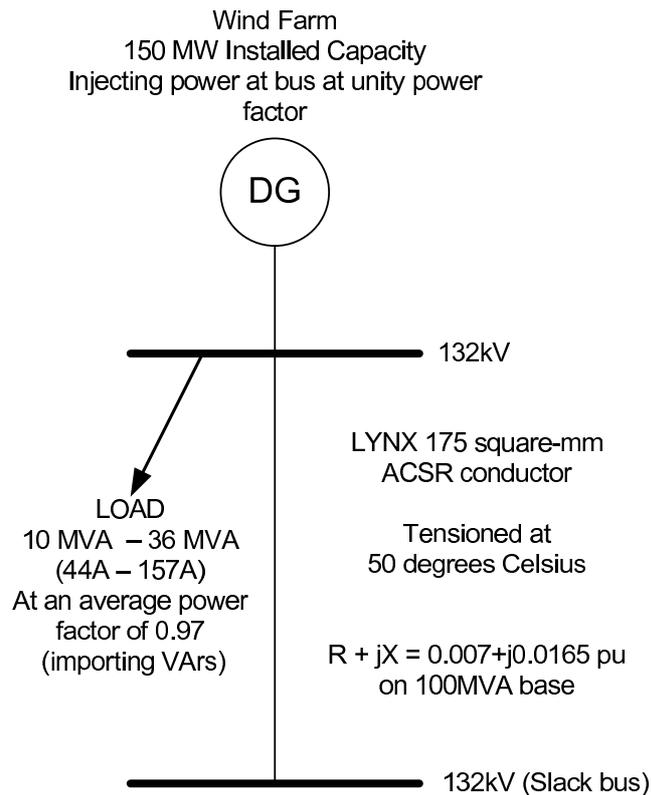
Figure 10.1: Field trial network with single DG connection

30% above the static thermal rating was used for the real-time thermal rating analysis [27]. This assumption was deemed appropriate as the up-rated line is geographically close to the wind farm site and thus at times of maximum power output from the DG scheme there would also be a maximum wind-cooling effect on the line.

In the second series of control algorithm simulations [101], the daily minimum real-time thermal ratings were calculated using the steady-state thermal model of the overhead line conductor populated with historical meteorological data for the relevant region of the UK (as described in Chapter 7). In addition, a more in-depth analysis of the various techniques was carried out by quantifying the losses introduced by the DG scheme and using these values to modify the financial evaluations.

The simulated daily real-time thermal rating of the Lynx conductor is given in Figure 10.2 for the calendar year 2005. The simulation used the overhead line model described by (7.1)–(7.4) in Section 7.2 and historical meteorological data for the 'Valley' area of Wales, UK [102]. As a comparison, the seasonal ratings for the conductor are also plotted in Figure 10.2. On occasions it can be seen that the real-time thermal rating drops below the
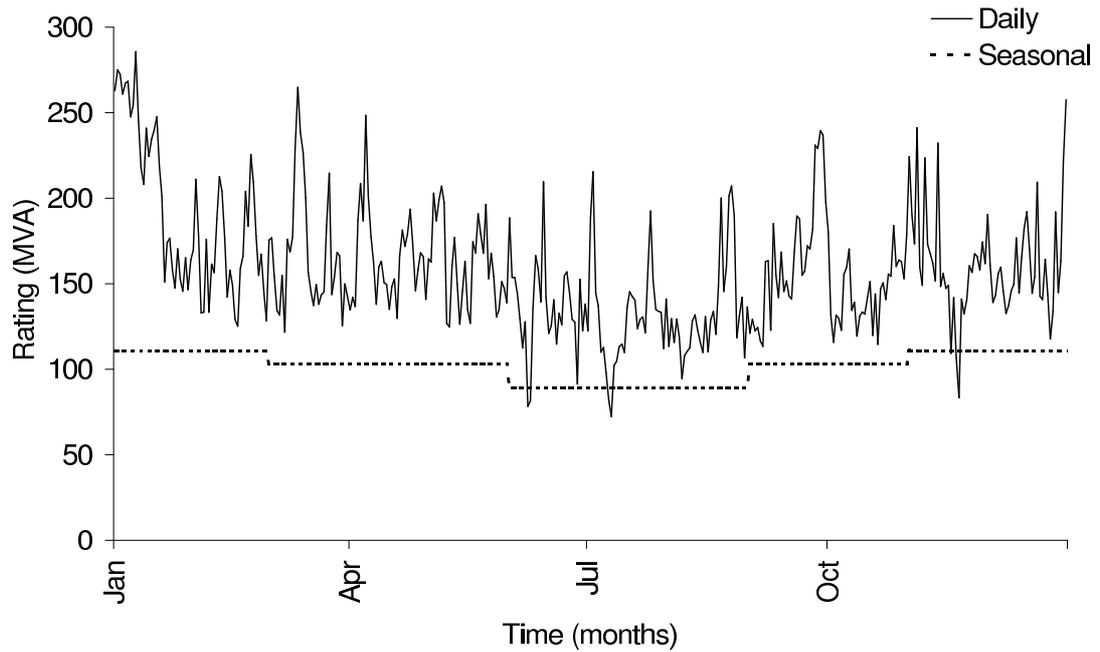
Figure 10.2: Rating variation of LYNX overhead line

seasonal thermal rating. This is due to the fixed meteorological assumptions that are used to calculate seasonal thermal ratings that may not be an accurate reflection of prevailing meteorological conditions.

10.4   Power flow management techniques

For the single DG connection within the field trial network the following techniques were simulated to manage power flows within the DG connection feeder:

1. DG tripping based on a static assessment of network availability;

2. DG tripping based on component seasonal thermal ratings;

3. Demand-following DG output control based on component static thermal ratings;

4. Demand-following DG output control based on component real-time thermal ratings (RTTRs); and

5. Network reinforcement to provide an unconstrained DG connection.

Each section below assesses the strengths and weaknesses of the particular power flow management technique. Where appropriate, the algorithm used to manage the DG connection is given, together with an approximate cost of the technique implementation.

10.4.1 DG tripping

The DG tripping schematic is shown in Figure 10.3 and implements the algorithm given in (10.1).

$$
\begin{aligned}
If: \quad & Current > Rating \\
Then: \quad & Trip\ DG\ to\ Rating + Base\ load
\end{aligned}
\tag{10.1}
$$

When this algorithm is implemented with the static rating of 390 A, the DG output will be tripped to 434 A at unity power factor (390 A rating + 44 A base load) if the current flow in the line exceeds 390 A. This corresponds to the implementation of Technique 1.

Similarly, with incorporation of a seasonal rating system [51], such as Technique 2, the DG output will be tripped back to the seasonal rating plus the base load if line flow exceeds the seasonal rating. These techniques are conservative as they do not account for the dynamic nature of the load and thus they trip-off generators rather than constraining them back. Furthermore, the seasonal rating approach bears the latent risk of an anomalous 'hot day' where the prevailing meteorological conditions may mean that assets are rated higher than they should be.

The cost of implementation of these techniques was estimated by considering software and hardware costs, communication link costs and labour costs. The DG tripping software was estimated to cost £1k, the relay hardware (based on an industrial PC) was estimated to cost £1k, a single communication link from the relay to the DG scheme to coordinate the opening of generator circuit breakers was estimated to cost £1k, labour costs were divided into system set-up and system maintenance costs with system set-up costs totalling £1k (based on 5 h SCADA access set-up, 10 h software installation and testing and 5 h relay installation, each costing £50/h) and system maintenance costing £1k. This produced a total of £5k which was doubled to £10k to account for cost estimation deviations and a profit margin.

10.4.2 Demand-following DG output control techniques

Figure 10.4 shows the schematic that allows the algorithm in (10.2) to be implemented to control the DG output based on static, seasonal or real-time network availabilities and a variable load demand at the DG connection busbar.

$$
\begin{aligned}
If: \quad & Current > Rating \\
Then: \quad & Control\ DG\ output\ to\ Rating + Load\ demand
\end{aligned}
\tag{10.2}
$$
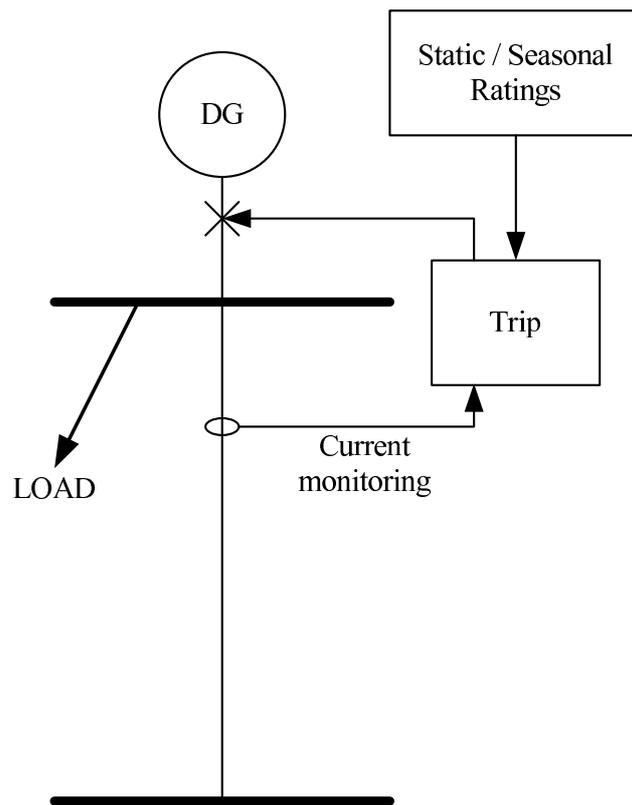
Figure 10.3: DG tripping with component static or seasonal thermal ratings

Control algorithm (10.2), implemented with a static rating of 390 A, corresponds to Technique 3. The DG output control techniques are more sophisticated than the DG tripping techniques and have the potential to offer energy yield gains by taking into account the dynamic nature of the load demand. Additional power flow monitoring equipment is required to facilitate demand-following DG output control.

In the case of the control system informed by component real-time thermal ratings (Technique 4), additional thermal and meteorological monitoring is also required. To ensure the safe and secure operation of the network assets, each demand-following DG output control technique requires an auxiliary trip system, which calculates the same ratings as the control system, to act as a backup in the case of control system operational failure.

The estimated cost of the demand-following DG output control technique deployed with component static / seasonal thermal ratings was £50k. This comprised £5k for the relay system described above, £5k for the DG output control software, £3k for an industrial PC hardware platform to host the DG output control software, £11k for two additional relay cubicles to provide stand-alone capability for the control system and monitor the electrical
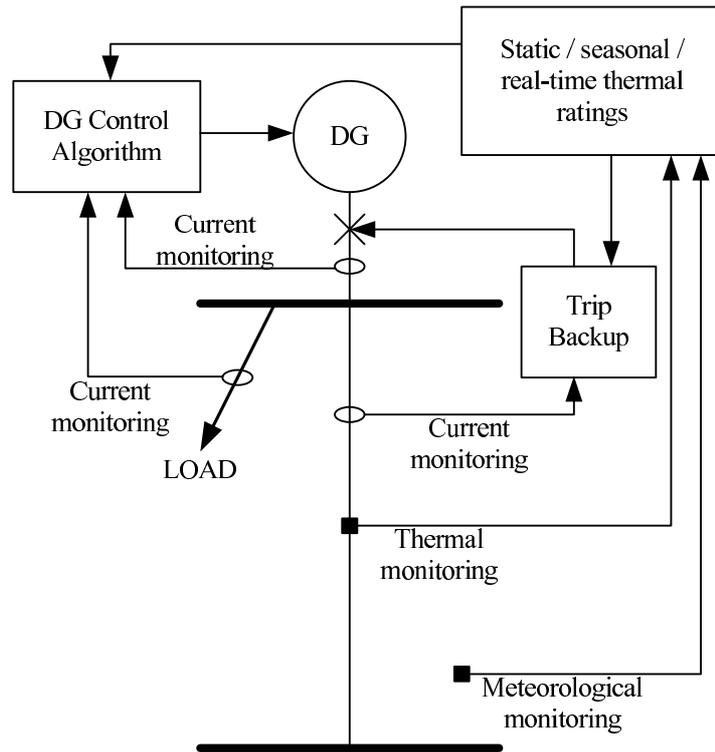
Figure 10.4: DG output control with static, seasonal or real-time thermal ratings

parameters (DG real and reactive power outputs and the real and reactive power load demands) with an additional communication link to control the DG power output, and an additional labour cost of £1k. The total cost (£25k) was doubled to account for estimation deviations and a profit margin.

The cost of the demand-following DG output control technique deployed with component real-time thermal ratings was estimated to be £100k. This comprised £5k for the real-time thermal rating software, £6k for two meteorological stations to monitor wind speed, wind direction, ambient temperature and solar radiation in the vicinity of the overhead line, £2k to provide the communication link between the meteorological stations and the relay cubicles and £37k for DG output control system described above with the modification to the system to integrate real-time thermal ratings into the host PC platform and relay cubicle. The total cost (£50k) was doubled to account for estimation deviations and a profit margin.

10.4.3   Network reinforcement

The network reinforcement option (Technique 5) would require a replacement 132kV overhead line to be constructed and the existing overhead line to be de-commissioned. It is assumed that the replacement line conductor is Upas $300\,\mathrm{mm}^2$ AAAC. If this conductor is tensioned to maintain statutory ground clearances [15] at an operational temperature of $75\,^\circ\mathrm{C}$, the rating would be sufficient to provide an unconstrained annual energy yield from the DG scheme. However, it requires the largest capital investment [103] and could take several years to be installed due to the lengthy environmental assessments, planning permission, commissioning and building processes. The estimated cost of the network reinforcement option, to install an up-rated $7\,\mathrm{km}$ 132kV line, was quoted by ScottishPower EnergyNetworks planning engineers as £2M.

10.5   Simulation approach

The constrained connection configurations were simulated through an off-line time-series analysis using the half-hourly regional loading and wind farm power output profiles for the complete calendar year 2005. Weather data from Valley (Wales, UK) was used to estimate weather parameter values along the length of the overhead line. These, in conjunction with the model described in Section 7.2, were used to calculate a series of daily thermal ratings for the studied line. Control algorithms (10.1) and (10.2) were applied to the case study network (with the relevant component thermal rating system) and the necessary constraints were implemented off-line.

10.6   Evaluation parameter quantification methodology

The annual energy yield at the DG connection busbar was calculated for each technique, by integrating the real power output of the DG scheme across the year in 30 minute intervals. The per unit electrical losses ($I^2 R_{ac}$) resulting from the simulation of each technique were calculated using the current flowing in the overhead line with per unit resistances of 0.0070 and 0.0041 for the Lynx and Upas conductors respectively. These were then summated across the year on a half-hourly basis to produce annual energy loss figures. For each technique, the net annual revenue was calculated by multiplying the annual energy yield at the DG connection bus by £101.43/MWh (£52.15/MWh wholesale electricity price [104] + £49.28/MWh Renewables Obligation Certificate sale price [105]) and making an adjustment

for the cost of the losses incurred by transferring this energy to the slack busbar (calculated as the annual energy losses multiplied by the wholesale electricity price).

The basic tripping scheme based on summer static ratings (Technique 1) was taken as the datum technique with a capital cost of £10k and net annual revenue of £42.35M (based an energy yield at the DG connection busbar of 418.1 GWh and 1.3 MWh lost through power transfer to the slack bus). The estimated marginal costs (due to additional network costs), predicted marginal revenues (due to additional energy yield) and marginal losses (resulting from electrical power transfer to the slack busbar and changes in electrical resistance of the line) were compared to this technique. This allowed a basic net present value (NPV) comparison of the alternative techniques, based on their relative marginal costs and marginal revenues. A 10% discount rate and 20 year economic life was assumed [106]. The capital cost of the wind farm itself was neglected as this would be constant for each technique. Furthermore, because the wind farm is connected to the distribution network via a single overhead line, any faults or scheduled maintenance on this line will cause it to shut down. Since such events have an equal constraint on the energy yield of each technique this effect was neglected. All the costs within the financial evaluations were estimates of equipment costs, provided by AREVA T&D based on the most appropriate data available at the time of consideration.

10.7   Real-time changes in DG power output

The real-time change in DG power outputs resulting from the various technique simulations are demonstrated in Figures 10.5–10.7 by the selection of illustrative days to represent summer, spring/autumn and winter operating conditions respectively. Considering Figure 10.5, the graph demonstrates the operation of the different control techniques for a 24-hour period during the illustrative time period in July. Techniques 1 and 2 result in the same real-time DG power output since the component seasonal rating in the summer months is equivalent to the component static thermal rating. For the time period considered, Techniques 1 and 2 produce the greatest constraint in the DG power output when compared to the other techniques. At times of constraint the DG scheme is tripped back to the static thermal rating of the overhead line plus the base load demand at the DG connection busbar. By taking into account the real-time variation of the load demand at the DG connection busbar, DG output control based on component static thermal ratings (Technique 3) leads to a greater DG power output during this time period than the DG tripping techniques.
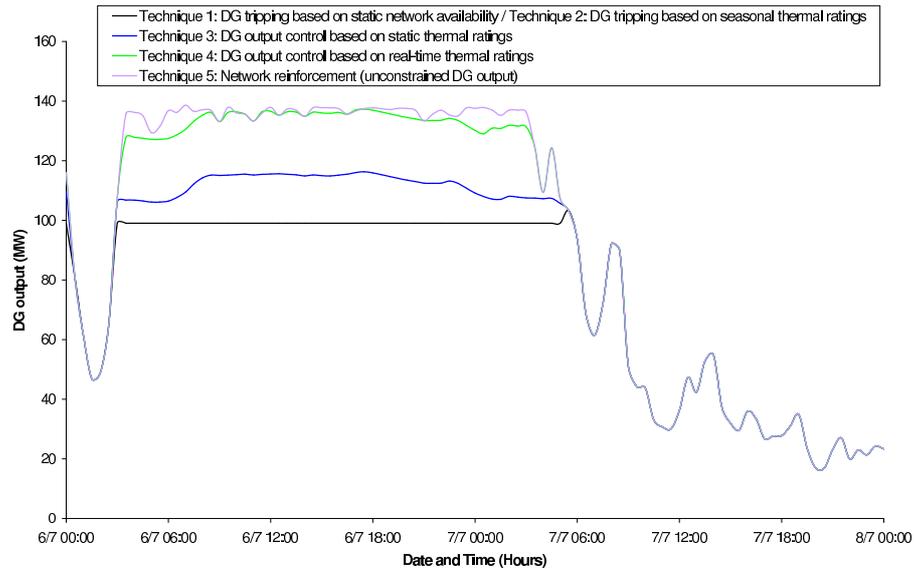
Figure 10.5: Illustration of real-time changes in DG output for summer operating conditions

This is because the DG power output is matched to the static thermal rating of the overhead line plus the time-varying load demand at the DG connection busbar. An additional power output from the DG scheme may be accommodated by the adoption of the demand-following DG output control technique deployed with component real-time thermal ratings. In this case the DG power output is matched to the time-varying thermal rating of the overhead line combined with the time-varying load demand at the DG connection busbar. For the time period selected it may also be seen that the unconstrained (and thus greatest) DG power output is facilitated by network reinforcement.

Considering Figure 10.6, two periods of DG constraint exist from 00:00 on 28/9 to 07:00 on 28/9 and from 10:30 on 28/9 to 15:30 on 29/9. Regarding the second DG output constraint period, and in comparison to Figure 10.5, it is possible to distinguish between the DG tripping technique based on component static thermal rating and the DG tripping technique based on the spring/autumn thermal rating since the latter results in a greater DG power output. Moreover, the demand-following nature of the DG output control technique based on the static thermal rating is apparent as the DG output follows a typical UK load demand profile. From 12:00 on 28/9 the load demand grows to a peak demand during the evening-time (reflected by the peak DG output for this technique during the time period considered). The load demand then reduces during the night-time hours from 00:00 on 29/9 to 06:00 on 29/9 (reflected by a reduction in the DG power output during the corresponding time period) and rises steadily through the morning from 06:00 on 29/9 to 08:30 on 29/9
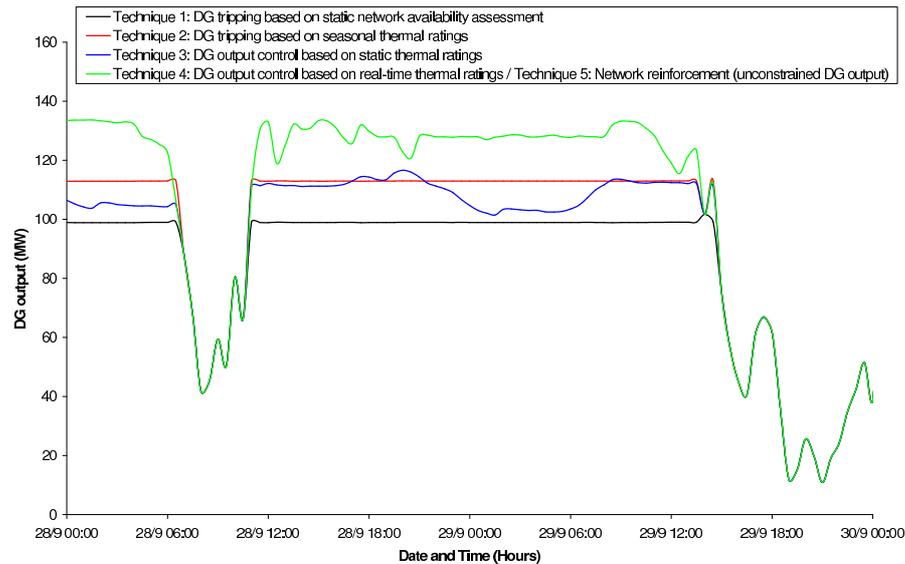
Figure 10.6: Illustration of real-time changes in DG output for autumn operating conditions

to reach a plateau during the day-time (as reflected by the DG power output). During the time period considered, the greatest DG power output is facilitated by the demand-following DG output control technique deployed with component real-time thermal ratings. The also corresponds to the unconstrained DG power output resulting from network reinforcement for the time period considered.

Figure 10.7 illustrates real-time changes in the power output of the DG scheme for the different control techniques applied in wintertime. Periods of DG constraint occur for different durations during the time period considered and it is possible to observe the impact of the thermal rating system and the method of DG power output constraint. DG tripping based on a static assessment of the component thermal rating and load demand produces the greatest constraint in the power output of the DG scheme. During the time period considered DG output control based on the component static thermal rating and variable load demand produces a greater constraint on the power output of the DG scheme than DG tripping based on the seasonal winter rating. During the time period considered, the greatest DG power output is facilitated by the demand-following DG output control technique deployed with component real-time thermal ratings. The also corresponds to the unconstrained DG power output resulting from network reinforcement. A period of DG constraint exists between 03:00 and 04:00 on 22/12 where the DG power output resulting from DG tripping based on seasonal thermal ratings is greater than DG output control based on component real-time thermal ratings. This highlights a situation where a potentially dangerous situation could arise due to anomalous weather conditions that produce a latent
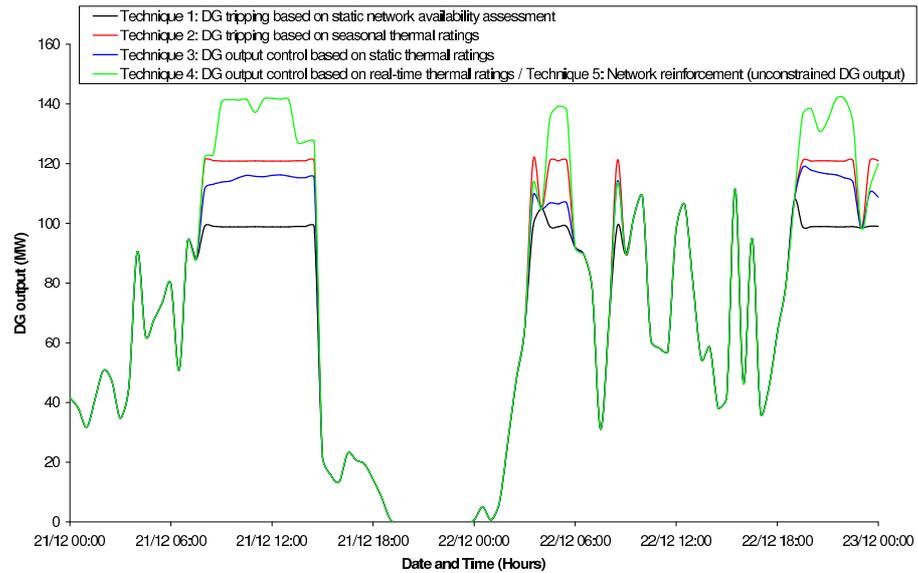
Figure 10.7: Illustration of real-time changes in DG output for winter operating conditions

risk of component thermal overloads. During this one-hour interval the overhead line is rated higher than it should be, based on assumed winter meteorological conditions. This detracts from the use of seasonal thermal ratings without adequate thermal monitoring systems to give the DNO control room visibility of the distribution network actual thermal operating conditions.

10.8 Evaluation parameters: Results and discussion

The results from the quantification methodology are summarised in Table 10.2. For this case study, it appears that controlling DG output to follow load demand based on the summer static rating (Technique 3) yields greater revenue for the DG developer than switching ratings on a seasonal basis and tripping DG as a result (Technique 2). DG tripping based on seasonal thermal ratings (Technique 2) requires a lower initial investment. However, the risk on the part of the DNO is greater if seasonal ratings are utilised. This is to due the possibility of an anomalous 'hot day' occurring when ratings have been relaxed. This risk may be mitigated by investment in a real-time thermal rating system to provide accurate knowledge of the current thermal status of the network.

Table 10.2: Quantification methodology results

Technique	Marginal cost (£k)	Marginal annual energy yield at DG connection bus (%)	Marginal annual energy losses (%)	Marginal net annual revenue (£M)	Marginal 20 Year NPV @ 10% discount factor (£M)
1: DG tripping based on a static assessment of network availability	0	0.00	0.00	0.00	0.00
2: DG tripping based on seasonal thermal ratings	0	4.93	18.41	2.08	17.71
3: Demand-following DG output control using static thermal ratings	40	5.24	18.99	2.21	18.76
4: Demand-following DG output control using RTTRs	90	10.75	43.39	4.53	38.46
5: Network reinforcement to provide an unconstrained connection	1990	10.76	-16.31	4.58	36.97

Economically, the most attractive technique to the developer is the DG output control based on component real-time thermal ratings and load demand (Technique 4). The annual revenue of the project is increased by £4.53M and shows the highest marginal NPV at £38.46M. For this case study, this technique appears to be more attractive than the alternative reinforcement option (Technique 5). This provides an unconstrained energy yield (and hence maximum annual revenue) but would require an extra capital investment of £1.99M to upgrade the overhead line. Network reinforcement (Technique 5) would reduce network losses relative to the other techniques since the larger cross-sectional area of the conductor would reduce the electrical resistance to power flow. However, despite increasing electrical losses through implementing a demand-following DG output control technique, the cost of capital for the DG developer is likely to make the active network management solutions, with lower upfront costs, a more attractive investment.

10.9 Graceful degradation

Rather than tripping-off the DG scheme if communications failures occur, the 'front-end' of the DG output control algorithm is configured with default values to allow continued operation of the control system, and graceful degradation, in the event of communication signal losses. The real power output of the DG scheme defaults to its maximum output (installed capacity value) if this signal is lost or corrupted. The reactive power output of the DG scheme is assumed to be negligible for the normal operating mode at unity power factor. Local load demands at the DG connection busbar default to zero and component real-time thermal ratings default to the standard static summer rating values. These values are selected to represent the worse case operating conditions if a communication failure occurs and are summarised in Table 10.3.

A methodology was employed to test the graceful degradation of the control algorithm as follows:

1. Initially, the DG power output was simulated for the condition with full communications visibility;

2. Considering the inputs to the control algorithm given in Table 10.3, each communication signal, in turn, was set to the default value whilst the other signals remained unchanged. This represented the loss of the particular communications signal and the replacement of the lost signal with the default value. For each contingency the simulation was re-run and the updated DG power output profile was recorded;

Table 10.3: Control algorithm default values

Input parameter	Default value
DG real power output (MW)	G_i
DG reactive power output (MVAr)	0
Real power load demand (MW)	0
Reactive power load demand (MVAr)	0
Component rating (MVA)	Summer static rating, S_{lim}

3. As a comparison of 'full visibility' and 'no visibility' behaviour the simulation was also run with complete signal losses as inputs to the control algorithm to establish the DG power output profile; and

4. The DG power outputs were plotted to understand the ranked order in severity of communication signals lost.

The governing equations for the updated DG power output, in the context of Figure 3.1 and as a function of the variables listed in Table 10.3 are given in (10.3) and (10.4)

$$''G_{P,B5} = \; 'G_{P,B5} + \Delta G_{P,B5} \tag{10.3}$$

where $''G_{P,B5}$ is the real power output of the DG scheme in the event of loss of communication signals; $'G_{P,B5}$ is the DG output before the loss of communication signals occurred; and $\Delta G_{P,B5}$ is the calculated change in DG output as a result of communication signals lost;

$$\Delta G_{P,B5} = \sqrt{(S_{B5,B4(lim)}^{C4})^2 - (G_{Q,B5} - Q_{B5})^2} - (G_{P,B5} - P_{B5}) \tag{10.4}$$

where $S_{B5,B4(lim)}^{C4}$ is the static, seasonal or real-time thermal limit of component C4; $G_{P,B5}$ and $G_{Q,B5}$ represent the respective real and reactive power flows from the DG scheme; and P_{B5} and Q_{B5} represent the real and reactive load demands at node $B5$. It should be noted that the terms given in (10.4) are replaced by the default values given in Table 10.3 in the event that the particular signal is lost. The graceful degradation of the control algorithm is illustrated in Figure 10.8 through the selection of a day in July to demonstrate the different DG power output profiles for different communication signals lost. The DG
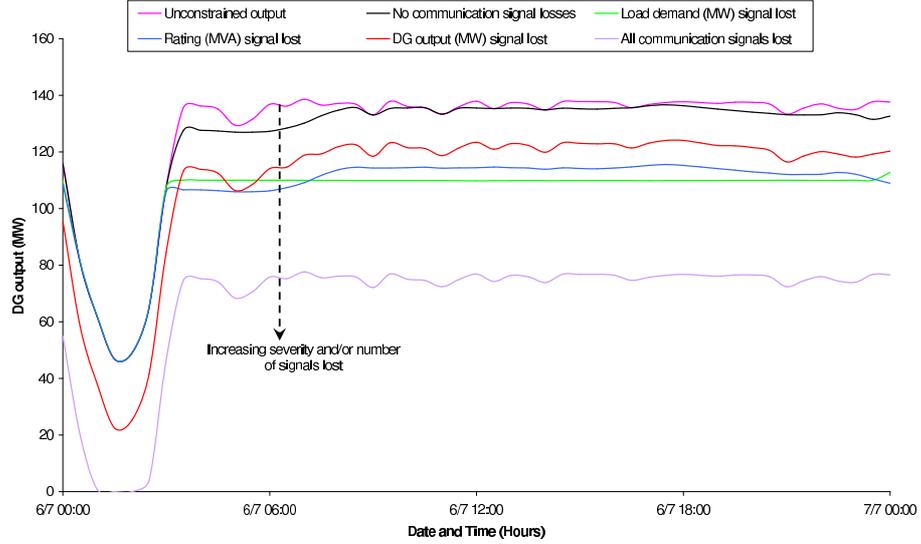
Figure 10.8: Graceful degradation of the control algorithm

installed capacity, as previously in this chapter, was set to 150 MW to create a constrained connection. As the severity of the communication signal lost increases, and/or number of communication signals lost increases, the DG output control algorithm makes increasingly conservative calculations regarding the maximum power output of the DG scheme.

The initial DG output, load demand and real-time thermal rating values (corresponding to the unconstrained DG scheme operation at 06:00 on 6/7/2006) are given in (10.5)–(10.7) respectively.

$$G_{P,B5} \; + \; jG_{Q,B5} = 136.8 \, \text{MW} \; - \; j0.1 \, \text{MVAr} \tag{10.5}$$

$$P_{B5} \; + \; jQ_{B5} = 17.3 \, \text{MW} \; + \; j2.4 \, \text{MVAr} \tag{10.6}$$

$$S^{C4}_{B5,B4,lim} = 110 \, \text{MVA} \tag{10.7}$$

These figures may be substituted directly into (10.3)–(10.4) to calculate the constrained DG output with full communication signal visibility as $''G_{P,B5}$ equal to 127.3 MW. If the DG real power output signal is lost, $G_{P,B5}$ is set to 150 MW (note that $'G_{P,B5}$ is still equal to 136.8 MW). Therefore $\Delta G_{P,B5}$ (10.4) is calculated to be -22.7 MW and thus $''G_{P,B5}$ (10.3) is equal to 114.1 MW. If the real power load demand signal is lost, P_{B5} is set to 0 MW (this represents the complete real power output of the DG scheme flowing directly into component C4). Therefore $\Delta G_{P,B5}$ (10.4) is calculated to be -26.8 MW and thus $''G_{P,B5}$

(10.3) is equal to 110.0 MW. If the real-time thermal rating signal is lost, $S^{C4}_{B5,B4(lim)}$ is set to 89 MVA. Therefore $\Delta G_{P,B5}$ (10.4) is calculated to be -30.5 MW and thus $''G_{P,B5}$ (10.3) is equal to 106.3 MW. For this particular illustration it was found that the loss of reactive power signals made negligible impact on the calculation of $''G_{P,B5}$. Clearly combinations of the above mentioned signals could be lost simultaneously. This would result in increasing conservatism from the DG power output control system. The most severe case would be the complete loss of communication signals which are input to the control algorithm. In this case $\Delta G_{P,B5}$ (10.4) is calculated to be -61.0 MW and thus $''G_{P,B5}$ (10.3) is equal to 75.8 MW. Assuming that signal dispatches to the DG scheme are not lost too, this would represent value to the DG developer in terms of the DG scheme not being tripped off.

10.10   Conclusion

This chapter described the simulation of ETR 124-based control techniques in order to manage the power output of a single DG scheme. The technical considerations and economics of a number of techniques that would allow a greater installed capacity of DG to be connected to, and operated within, the distribution network were presented. The techniques included (i) the tripping of the DG scheme based on a static thermal rating; (ii) the tripping of the DG scheme based on seasonal thermal ratings; (iii) the demand-following output control of the DG scheme based on a static thermal rating; (iv) the demand-following output control of the DG scheme based on real-time thermal ratings; and (v) the provision of an unconstrained DG scheme connection through network reinforcement.

The demand-following DG output control technique with real-time thermal ratings resulted in a marginal annual energy yield gain of 10.75% when compared to 418.1 GWh/annum resulting from a present industry practice of DG tripping based on static thermal ratings. Despite increasing electrical losses (which were quantified and charged back to the DG developer), the demand-following DG output control technique was found to have a marginal net present value to the DG developer of £38.46M, compared to £36.97M resulting from a network reinforcement option. The cost of capital for the DG developer is likely to make DG output control systems, with lower upfront costs, a more attractive investment.

Chapter 11

Case study 2: Output control of multiple DG schemes based on a single thermal constraint

11.1 Introduction

This chapter describes the simulated use of power flow sensitivity factors to control the power output of multiple DG schemes, based on a single thermal constraint, within United Kingdom Generic Distribution System (UKGDS) A. The research presented in this chapter was published by the author in [86, 87]. The case study network and description of DG schemes is given in Section 11.2, the thermal vulnerability factor assessment for the installed DG schemes is presented in Section 11.3, the real-time thermal rating assessment for the thermally vulnerable component, identified in Section 11.3, is described in Section 11.4, power flow sensitivity factor-based DG output control strategies are illustrated in Section 11.5 and the time series electro-thermal simulation approach is described in Section 11.6. As a result of the electro-thermal simulations, the real-time changes in DG power outputs are presented in Section 11.7 and the DG annual energy yields, quantified to assess the DG output control system benefits, are presented and discussed in Section 11.8.

Last-in first-off (LIFO) control strategies for multiple DG schemes have developed in the current regulatory framework of the UK. However, as the power transfer capacity of distribution networks becomes saturated, there is an economic disadvantage to 'last-in' DG schemes. This is because they are the first DG schemes to be disconnected or have their power output constrained in order to manage network power flows. The resulting annual energy yield of such schemes may be significantly curtailed and, based on the anticipated

Table 11.1: DG scheme properties

Generator node, m	Generator type	Installed capacity (MW)	Last-in first-off constraint order	$dP_{353,357}/dG_{P,m}$
352	Hydro	18	2	0.475
353	CHP	40	3	0.477
354	CHP	30	1	0.327

net present value of the investment, the DG development may not be economically viable. The candidate control strategies move away from piecemeal DG scheme control systems to coordinate the power outputs of multiple DG schemes in order to achieve aggregated benefits for power system stakeholders. Under certain conditions the proposed strategies (LIFO PFSF-based, egalitarian and technically most appropriate (TMA)) have the potential to facilitate improved individual and aggregated annual energy yields for separately owned DG schemes [86], when compared to a benchmark LIFO discrete interval DG control strategy. In such circumstances the coordinated output control of DG schemes could enhance the revenue streams of 'last-in' DG developers to an extent that the investment in the installation is economically viable. Moreover, cross-payments could be set-up between DG scheme developers to ensure that those developers that constrain the power output of their DG scheme to allow an aggregated annual energy yield gain are remunerated. However, there is no regulatory mechanism in the UK, at present, to encourage and support this operational framework.

11.2 Network description

The case study network, shown in Figure 11.1 was derived from a section of the UKGDS 'EHV3' network [81]. The network was modified for the output control of multiple DG by connecting a hydro generator and two combined heat and power (CHP) generators to the network at 33kV nodes. A summary of the DG scheme properties is given in Table 11.1.

11.3 Thermal vulnerability factor assessment

The most thermally vulnerable components within the case study network were identified using a thermal vulnerability factor assessment as given in Figure 11.2. From this assessment it may be seen that a DG real power injection at node 352 increases the thermal
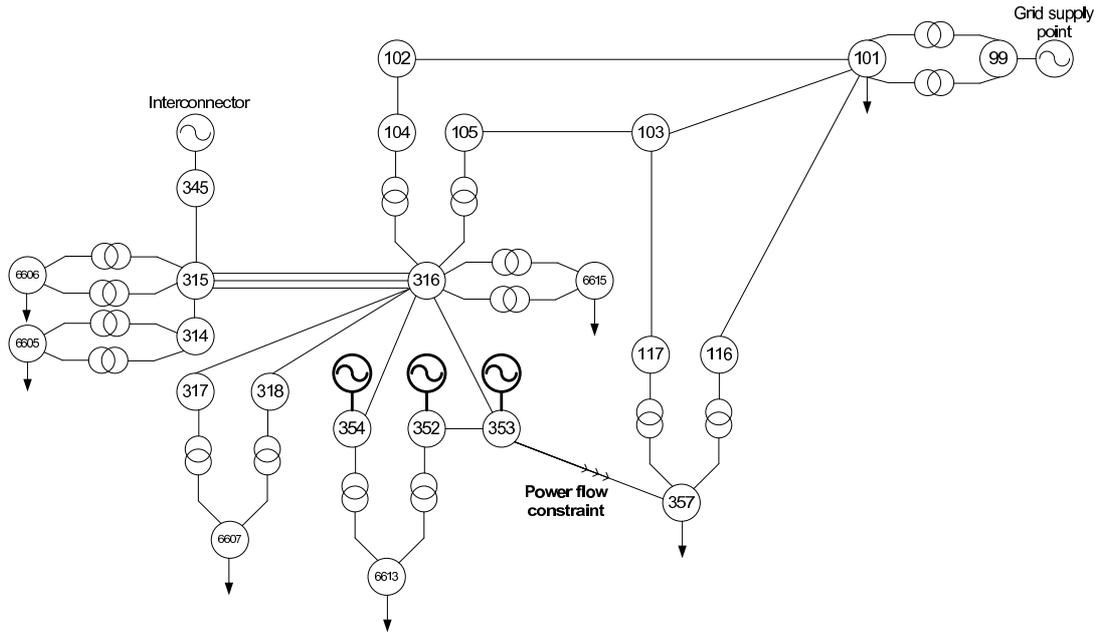
Figure 11.1: UKGDS A case study network with DG

vulnerability of the components between nodes 352 and 353, and between nodes 353 and 357 but reduces the thermal vulnerability of the component between nodes 316 and 353. Moreover, a DG real power injection at node 353 increases the thermal vulnerability of the component between nodes 353 and 357 but reduces the thermal vulnerability of the component between nodes 316 and 353. Furthermore, a DG real power injection at node 354 increases the thermal vulnerability of the components between nodes 316 and 353, 354 and 316, and 353 and 357. However, this injection has little impact on the thermal vulnerability of the component between nodes 352 and 353. In this particular case, multiple DG injections cause the thermal vulnerability factors to accumulate for the electric cable between nodes 353 and 357, making it the most thermally vulnerable component. Having identified this component as being a potential thermal pinch-point and requiring power flow management within the network, the targeted development of a real-time thermal rating system was informed.

11.4 Component real-time thermal rating assessment

A summary of the characteristics of the thermally vulnerable electric cable are given in Table 11.2. The 'Valley' UK MetOffice dataset [102] for the calendar year 2006 was used with the thermal state estimation technique described in Chapter 7 to estimate environmental operating conditions local to the electric cable [87]. This information was used by Andrea

Generator injection node:
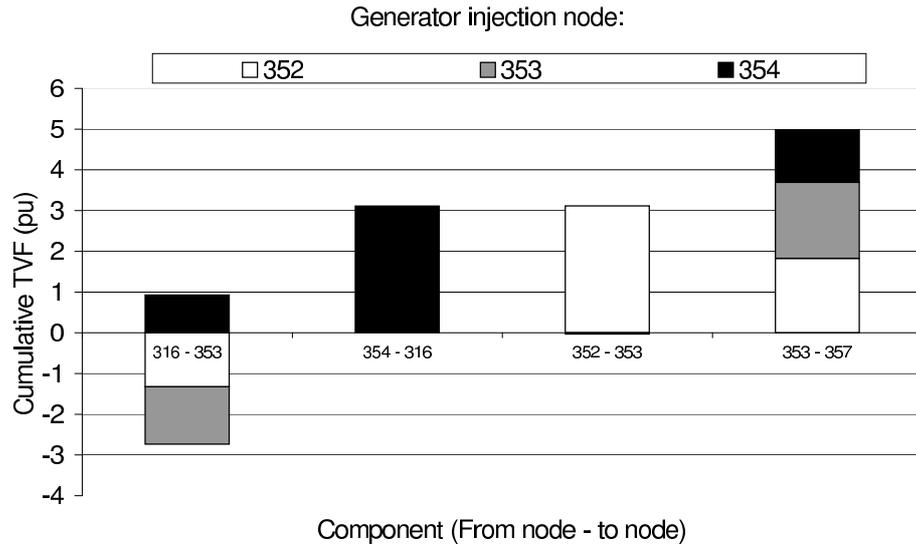
Figure 11.2: Cumulative TVF assessment of UKGDS A (in Figure 11.1)

Table 11.2: Electric cable characteristics

Electric cable characteristic	Value / category
Total resistance, R_{ac}	0.01489 pu
Total reactance, X	0.01296 pu
Cross-sectional area	150 mm^2
Standard rating, $S_{353,357,lim}$	30 MVA
Nominal line-to-line voltage	33kV
Standardised phase current rating	525 A
Installation conditions	Flat formation, buried in a duct

Michiorri to populate the electric cable steady-state thermal model described by (7.7) in Chapter 7. The resulting real-time thermal rating for the electric cable, together with the static rating, is given in Figure 11.3. It was found that the average uprating for the electric cable, based on minimum daily ratings was 6.0% across the year.

11.5   DG output control strategy illustrations

In implementing the DG set points, calculated using the different control strategies outlined below, it was assumed that CHP plants had the capability to regulate the real power injected into the distribution network. In addition it was assumed that the hydro scheme had the capability to regulate real power injections in a similar manner to the technique described in [63].
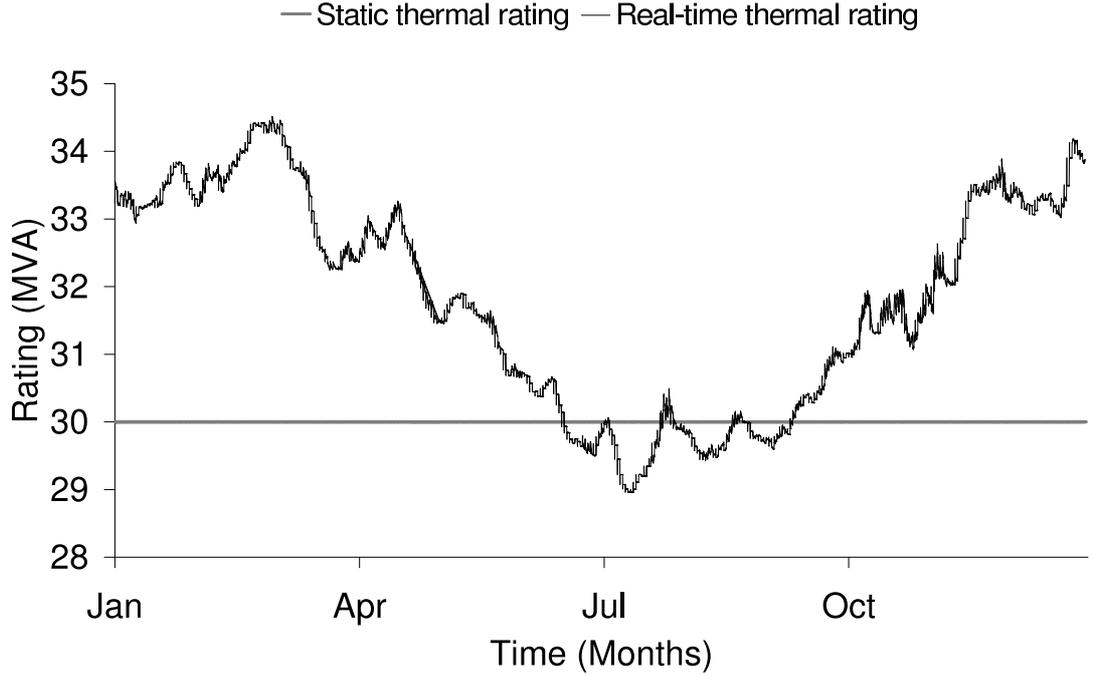
Figure 11.3: Electric cable static and real-time thermal rating variation

In the power flow sensitivity factor-based control strategies that are illustrated in Sections 11.5.2-11.5.4, the required real power reduction in the electric cable, $\Delta P_{353,357}$ in order to bring the resultant power flow back within the desired thermal limit was calculated using (11.1) with $U_{Tar} = 0.99$.

$$
\Delta P_{i,k} = \sqrt{(U_{Tar} \times S^c_{i,k,lim})^2 - (''Q_{i,k})^2} \\
- \sqrt{('S_{i,k})^2 - ('Q_{i,k})^2}
\tag{11.1}
$$

11.5.1 LIFO discrete interval

In order to manage network power flows and reflect present operational practices, the power output of the DG schemes was reduced in discrete intervals of 33% according to the contractual priority order given in Table 11.1. Thus, when a thermal violation was detected, the power output of the DG scheme at node 354 was reduced by 33%, then 66%, followed by complete disconnection. If the thermal violation was still present after the complete disconnection of the DG scheme at node 354, the output of DG scheme at node 352 was reduced by 33%.

11.5.2   LIFO PFSF-based

The required power output reduction of the first DG scheme (contractually) to be con-strained, $\Delta G_{P,354}$, was calculated using (11.2) for $G_{P,354} - \Delta G_{P,354} > 0$ and the output from $G_{P,352}$ and $G_{P,353}$ was unconstrained. On occasions when the required constraint of the DG scheme at node 354 would result in $G_{P,354} - \Delta G_{P,354} < 0$, the DG scheme was dis-connected and the necessary power flows were managed by the next DG scheme (at node 352) to be contractually constrained.

$$\Delta G_{P,354} = \frac{\Delta P_{353,357}}{0.327} \tag{11.2}$$

11.5.3   Egalitarian

The equal percentage reduction signal, Φ, broadcast to all DG schemes in order to manage network power flows was calculated and simulated using (11.3)-(11.6).

$$\Phi = \frac{\Delta P_{353,357}}{(0.475 \times G_{P,352}) + (0.477 \times G_{P,353}) + (0.327 \times G_{P,354})} \tag{11.3}$$

$$\Delta G_{P,352} = G_{P,352} \times \Phi \tag{11.4}$$

$$\Delta G_{P,353} = G_{P,353} \times \Phi \tag{11.5}$$

$$\Delta G_{P,354} = G_{P,354} \times \Phi \tag{11.6}$$

11.5.4   Technically most appropriate

Since, in this case, the DG scheme at node 353 has the greatest technical ability to manage network power flows (as assessed by the comparative magnitude of power flow sensitivity factors in Table 11.1), Equation (11.7) was implemented to reduce the aggregated DG scheme constraint and thus increase the aggregated annual energy yield of the DG schemes. On occasions when the required constraint of the DG scheme at node 353 would result in $G_{P,353} - \Delta G_{P,353} < 0$, the DG scheme was disconnected and the necessary network power flows were managed by the DG scheme with the next-greatest power flow sensitivity factor (in this case at node 352).

$$\Delta G_{P,353} = \frac{\Delta P_{353,357}}{0.477} \tag{11.7}$$

11.6 Electro-thermal simulation approach

This section describes the off-line time series electro-thermal simulation that was used to quantify the individual and aggregated DG scheme annual energy yields for the multiple DG scheme control strategies. A flow chart of the simulation procedure is given in Figure 11.4. UKGDS half-hour loading and generation profiles were utilised with the scripted IPSA load flow software tool to simulate network power flows and busbar voltages for a complete operational year. The open-loop control system compared network power flows to component static and real-time thermal limits for each half-hour interval within the simulated year. When power flow management was required (signified in this case by an electric cable utilisation, $U_{353,357} \geq 1$) each DG output control strategy was implemented and the updated individual DG scheme real power outputs were recorded. A validating load flow simulation was conducted as part of the control algorithm to ensure that the updated DG power outputs managed the power flows effectively and did not breach busbar voltage limits (set to $\pm 6\%$ of nominal) [15]. The individual and aggregated DG power outputs were integrated across the simulated year in order to estimate the annual energy yields resulting from the candidate multiple DG control strategies. Each control strategy was simulated with static and then real-time thermal rating systems.

11.7 Real-time changes in DG power outputs

The real-time change in DG power outputs resulting from the various strategy deployments with component static thermal ratings were analysed. Figures 11.5, 11.6, 11.7 and 11.8 represent the respective outputs of $G_{P,352}$, $G_{P,353}$, $G_{P,354}$ and the aggregated DG scheme outputs for an illustrative week of operation during May.

Considering Figure 11.5, $G_{P,352}$ is predominantly unconstrained for the time period considered for the LIFO and TMA control strategies. This is because the DG scheme at node 352 is, contractually, the second DG scheme to be constrained at times of network power flow management and therefore, if the first-off DG scheme (at node 354) manages the required network power flow constraint then $G_{P,352}$ is unconstrained. Considering Table 11.1, $G_{P,352}$ has the second-highest power flow sensitivity factor and is, technically, the second DG scheme to be constrained at times of network power flow management when

the TMA strategy is adopted. Therefore if the required network power flow constraint is managed by the TMA DG scheme at node 353, then $G_{P,352}$ is unconstrained. Considering the egalitarian control strategy, the output of $G_{P,352}$ is constrained.
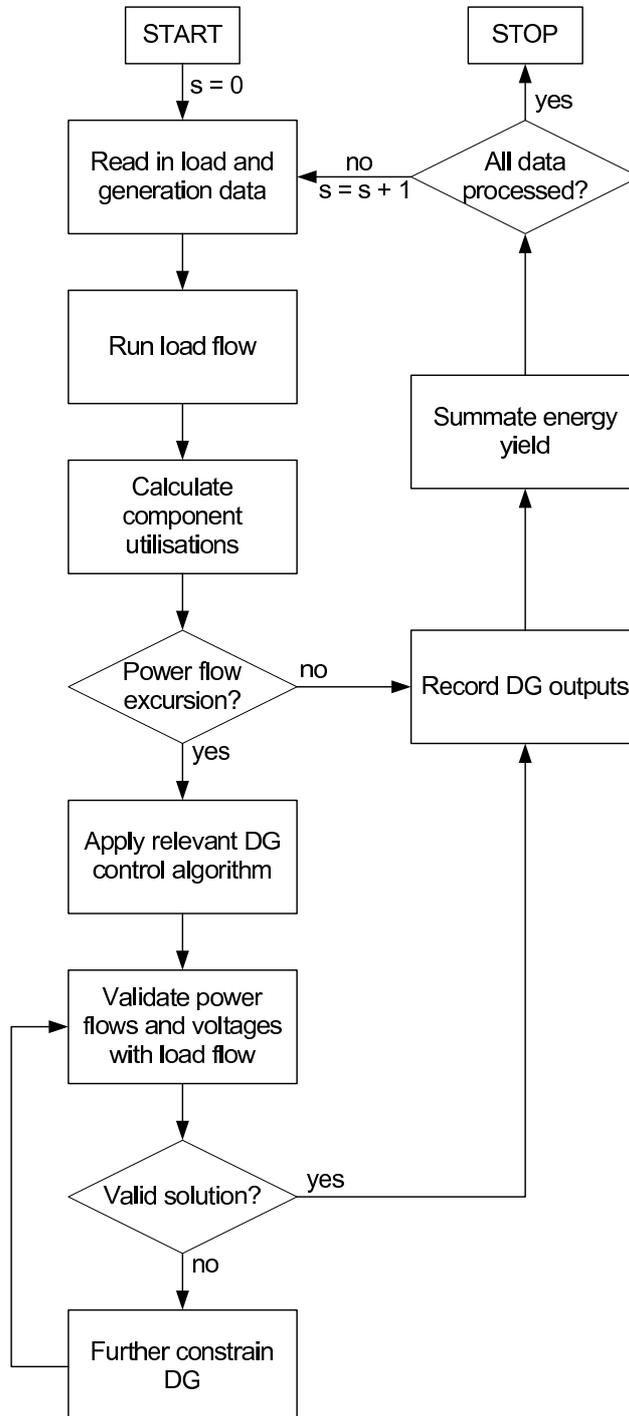
Figure 11.4: Simulation flow chart
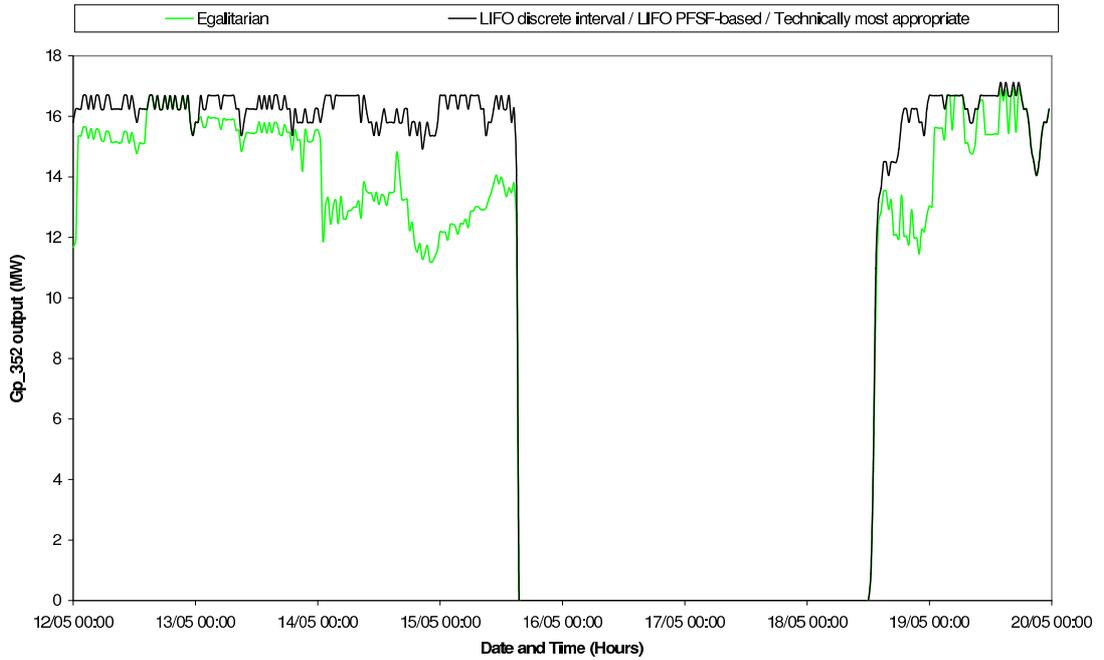
Figure 11.5: Illustration of real-time changes in DG output of $G_{P,352}$
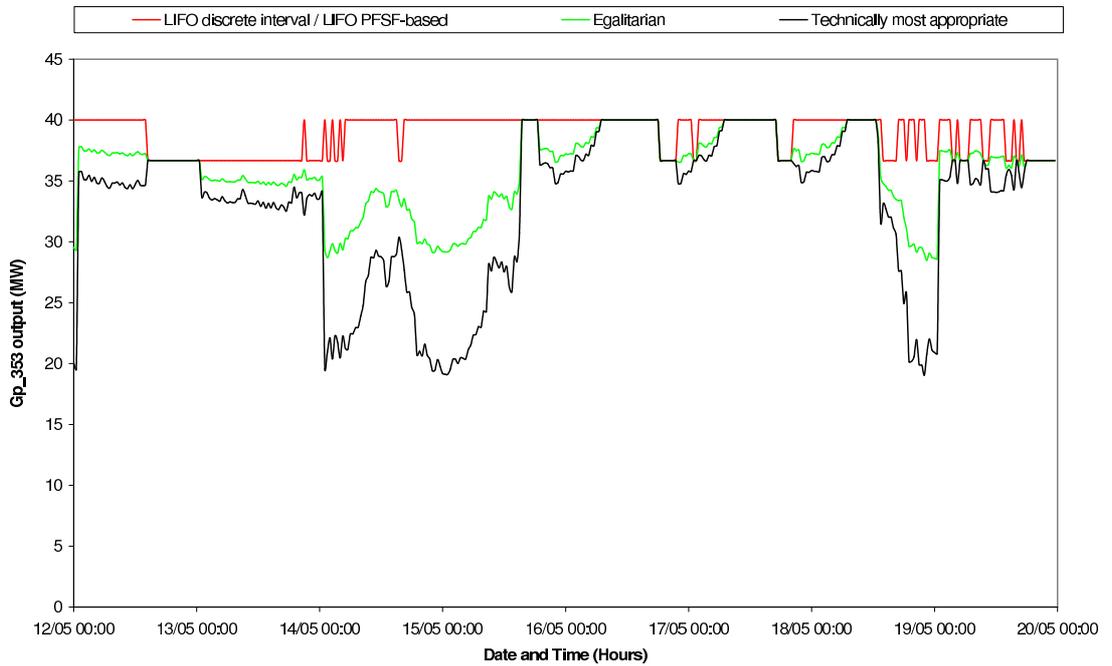
Figure 11.6: Illustration of real-time changes in DG output of $G_{P,353}$
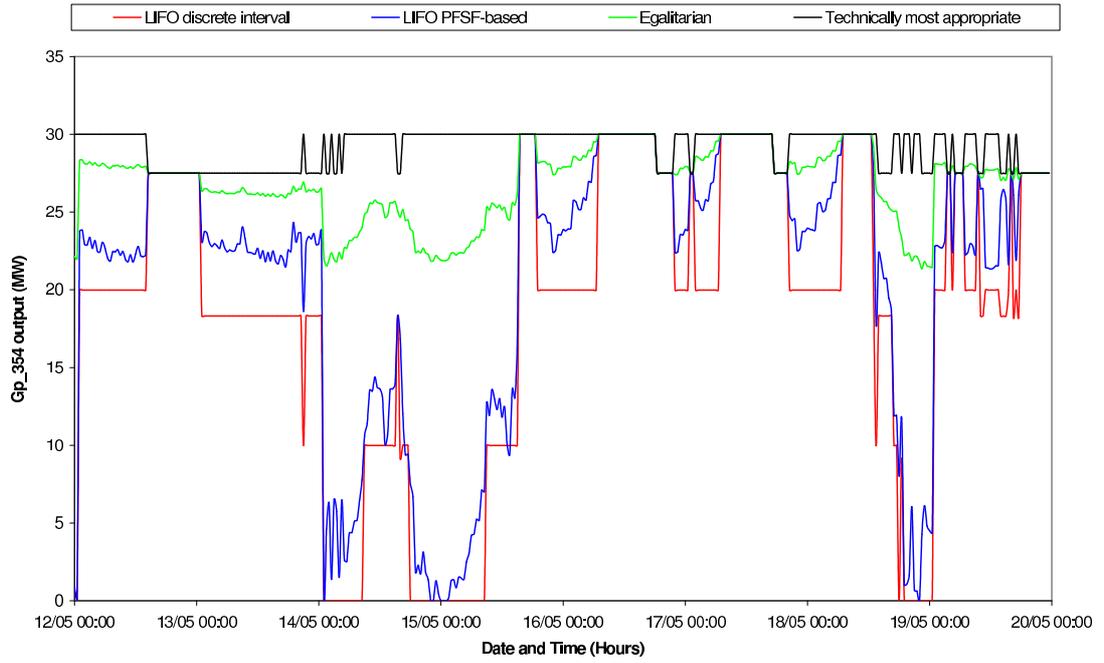
Figure 11.7: Illustration of real-time changes in DG output of $G_{P,354}$
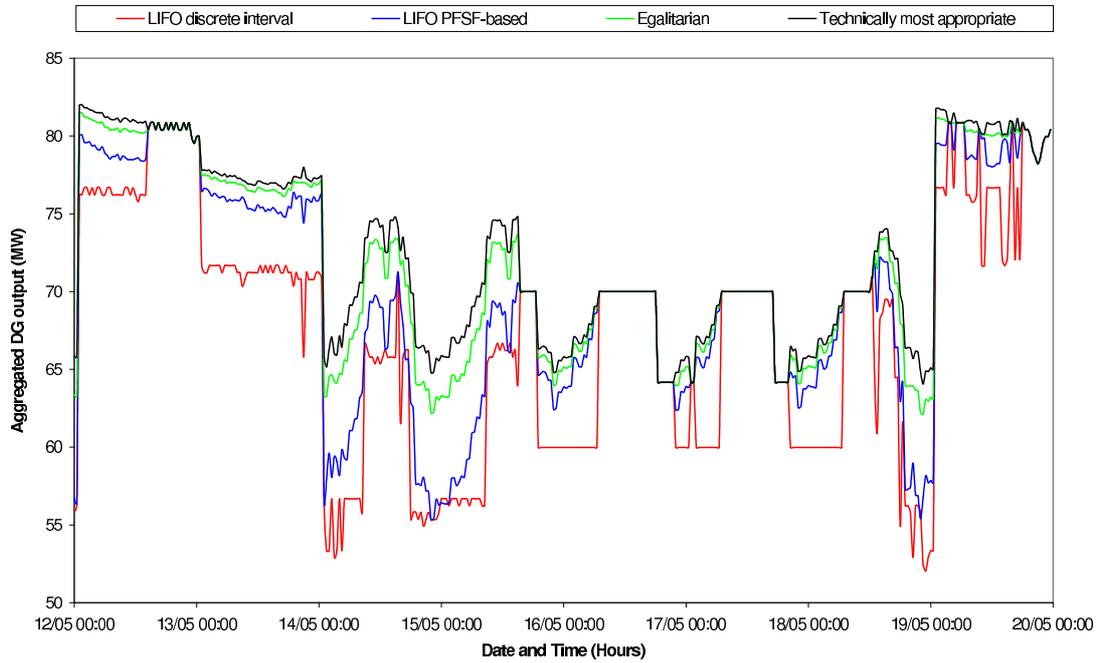
Figure 11.8: Illustration of real-time changes in the aggregated DG output of $G_{P,352}$, $G_{P,353}$ and $G_{P,354}$

This is because, for this particular strategy, all DG schemes participate in the management of network power flows. The period of negligible power output could be attributed to a lack of rainfall to power the hydro scheme or a period of scheduled maintenance.

Considering Figure 11.6, technically $G_{P,353}$ is the most appropriate DG scheme to constrain at times of DG output control since it has the highest power flow sensitivity factor (as seen in Table 11.1) and therefore has the greatest technical ability to manage network power flows. As a result, $G_{P,353}$ for the TMA strategy implementation is the lowest when compared to the other strategies. At times of power output constraint, $G_{P,353}$ tracks the available power transfer capacity which varies as a result of the continuously changing load demand in the network. As illustrated in (11.3)-(11.6), the egalitarian strategy requires participation by all DG schemes in order to manage network power flows. Therefore the output of $G_{P,353}$ is also constrained under this operating regime. In this case, all the DG schemes are tracking the variation in available power transfer capacity as a result of the continuously changing load demand in the network. Therefore the power output of $G_{P,353}$ follows the same general profile, but is less constrained than that of the TMA strategy. The LIFO strategies both produce the same (unconstrained) DG output.

Considering Figure 11.7, the impact of each control strategy on the power output of $G_{P,354}$ may be observed. Since $G_{P,354}$ is the first-off DG scheme (as given in Table 11.1), the LIFO discrete-interval control strategy leads to the greatest constraint of the DG output when compared to the other strategies. Illustrative time periods such as 02:00 to 12:00 on 12/05 and 09:30 to 15:00 on 15/05 represent the DG power output at 0.666 and 0.333 of maximum capacity respectively. The LIFO PFSF-based control strategy leads to an increase of $G_{P,354}$, relative to the LIFO discrete interval strategy, since the power output is matched to the available transfer capacity between nodes 353 and 357. The egalitarian control strategy employs all the DG schemes in the management of power outputs and therefore an additional increase in $G_{P,354}$ is facilitated. As discussed previously, $G_{P,353}$ is technically the most appropriate DG scheme to constrain in order to manage power flows in this case study network. Therefore $G_{P,354}$ is unconstrained for the TMA control strategy.

The aggregated DG power outputs are presented in Figure 11.8. This demonstrates that the TMA strategy facilitates the greatest aggregated DG output gains, followed by the egalitarian strategy, followed by the LIFO PFSF-based control strategies, when compared to the LIFO discrete interval control strategy.

Table 11.3: DG marginal annual energy yields (%) with component static thermal ratings

	Marginal	Annual	Energy	Yield (%)
DG Control Strategy	$G_{P,352}$	$G_{P,353}$	$G_{P,354}$	$G_{P,aggregated}$
LIFO (discrete intervals)	0.0	0.0	0.0	0.0
LIFO (PFSF-based)	1.1	0.0	16.8	4.1
Egalitarian percentage reduction of output	-9.7	-10.0	66.6	7.7
Technically most appropriate	1.7	-19.2	85.1	9.0

11.8 Annual energy yield results and discussion

The marginal annual energy yields resulting from the control strategies simulated with static and real-time thermal ratings are summarised in Tables 11.3 and 11.4 respectively. The LIFO discrete interval strategy deployed with static component ratings was used as a datum with annual energy yields of 106.38 GWh, 298.26 GWh, 120.84 GWh and 525.48 GWh for $G_{P,352}$, $G_{P,353}$, $G_{P,354}$ and $G_{P,aggregated}$ respectively.

11.8.1 Results with static thermal ratings

Considering Table 11.3, for the case study network it can be seen that power flow sensitivity factor-based approaches have the potential to unlock gains in the aggregated annual energy yield contribution of multiple DG schemes. Moving from a LIFO discrete interval to a LIFO PFSF-based control strategy has the potential to unlock an extra 4.1%. Moreover, a further 4.9% annual energy yield gain may be achieved by utilising the TMA DG scheme to reduce aggregated DG constraints. For the egalitarian control strategy, it can be seen that the relative annual energy yields of $G_{P,353}$ and $G_{P,352}$ are reduced in order to achieve an aggregated DG annual energy yield gain. This phenomenon is even more pronounced in the TMA strategy where annual energy yield gains of 1.7% and 85.1% for $G_{P,352}$ and $G_{P,354}$ respectively are facilitated by the 19.2% reduction in the annual energy yield of $G_{P,353}$.

Table 11.4: DG marginal annual energy yields (%) with component real-time thermal ratings

	Marginal	Annual	Energy	Yield (%)
DG Control Strategy	$G_{P,352}$	$G_{P,353}$	$G_{P,354}$	$G_{P,aggregated}$
LIFO (discrete intervals)	1.7	0.0	25.8	6.3
LIFO (PFSF-based)	1.7	0.0	41.9	10.0
Egalitarian percentage reduction of output	-5.5	-6.2	73.6	12.3
Technically most appropriate	1.7	-12.0	85.1	13.1

11.8.2 Results with real-time thermal ratings

Considering Table 11.4, for the case study network it can be seen that the adoption of both real-time thermal rating systems and power flow sensitivity factor-based control strategies have the potential to unlock gains in the aggregated annual energy yield contribution of multiple DG schemes. Moving from a static thermal rating system to a real-time thermal rating system has the potential to unlock an extra 6.3% aggregated annual energy yield for the LIFO discrete interval control strategy. If a LIFO contractual priority is retained but a power flow sensitivity factor-based control strategy is adopted this has the potential to unlock an extra 3.7% marginal aggregated annual energy yield. Moreover, a further 3.1% annual energy yield gain may be achieved by adopting the TMA strategy that reduces aggregated DG scheme constraints. In simulating the egalitarian control strategy, it can be seen that the relative annual energy yields of $G_{P,352}$ and $G_{P,353}$ are reduced in order to achieve an aggregated DG scheme annual energy yield gain. This phenomenon is even more pronounced in the TMA strategy where annual energy yield gains of 1.7% and 85.1% for $G_{P,352}$ and $G_{P,354}$ respectively are facilitated by the 12.0% reduction in the annual energy yield of $G_{P,353}$.

In this particular scenario, as seen by inspecting Table 11.1, each DG scheme has a similar power flow sensitivity factor for the thermally vulnerable component ($dP/dG_{P,352}$ = 0.475, $dP/dG_{P,353}$ = 0.477, $dP/dG_{P,354}$ = 0.327) and thus the aggregated annual energy yields resulting from the different power flow sensitivity factor-based control strategies are

of a similar magnitude. For new DG scheme developments, this is likely to favour the adoption of the egalitarian control strategy on the basis of operational simplicity (of DG set point dispatch) relative to the LIFO and TMA strategies. The risk of DG scheme non-compliance, in terms of achieving output constraints, is also distributed across a number of schemes, rather than a single DG scheme bearing sole responsibility for network power flow management. For existing DG scheme operation, there may be inertia to change from a LIFO control strategy to egalitarian or TMA strategies if the aggregated annual energy yields resulting from the different power flow sensitivity factor-based control strategies are of a similar magnitude.

In situations where the power flow sensitivity factors of DG schemes exhibit a significant variation relative to one another, and are not of a similar magnitude, it is possible that the TMA strategy would be favoured since the additional aggregated annual energy yield gains, and hence DG revenue stream enhancements, could warrant the adoption of a more operationally complex control system.

In order to embrace the multiple DG control strategies presented in this chapter, there clearly needs to be contractual mechanisms in place that give incentives to separately owned DG schemes to have their power output reduced in order to increase the overall DG annual energy yield contribution. One such mechanism could be to set up cross-payments between DG schemes whereby those DG schemes that are constrained to increase the aggregated energy yield are rewarded by payments from the other DG schemes.

11.9 Conclusion

This chapter has presented the simulated use of power flow sensitivity factors to control the power output of multiple DG schemes, based on a single thermal constraint, within UKGDS A.

The DG output control system development methodology, as described in Chapter 4 was demonstrated in simulation for multiple DG scheme control. This included (i) the identification of a thermally vulnerable component through a thermal vulnerability factor assessment that related DG power flow sensitivity factors to component thermal limits; (ii) the targeted development of an electric cable thermal model to allow latent capacity in the network asset to be unlocked through a real-time thermal rating system, (iii) the population of the electric cable steady-state thermal model with historical data from meteorological monitoring equipment to produce real-time thermal ratings; and (iv) the use of component

static and real-time thermal ratings together with power flow sensitivity factors to control the power output of multiple DG schemes.

Based on a datum value of 525.48 GWh/annum (corresponding to LIFO discrete-interval DG output control with static thermal ratings), non-LIFO-based control strategies led to DG aggregated annual energy yield gains of 7.7% and 9.0%. In addition, gains of 12.3% and 13.1% resulted from non-LIFO-based control strategies with component real-time thermal ratings.

In order to embrace the multiple DG control strategies presented in this chapter there clearly needs to be suitable connection agreements and contractual mechanisms in place that give an incentive to DG developers to have the power output of their DG scheme reduced in order to increase the aggregated energy yield penetration from new and RE resources.

Chapter 12

Case study 3: Output control of multiple DG schemes based on multiple thermal constraints

12.1 Introduction

This chapter describes the off-line simulation of the multiple DG scheme control strategies, implemented to manage power flows within multiple components of the field trial network, based on power flow sensitivity factors. The research presented in this chapter builds on previous work which described the methodology for DG output control system development (Chapter 4), the identification of thermally vulnerable components within the field trial network (Chapter 6), the thermal characterisation of the field trial network and development of a real-time thermal rating system (Chapter 7) and the control algorithm to exploit component thermal properties for the active management of multiple DG schemes (Chapters 8, 9 and 11). The research presented in this chapter was published by the author in [86–88].

In situations where it is assessed to be viable, power flows may be managed through the deployment of a DG power output control system coupled with power system real-time thermal ratings. The adoption of real-time thermal rating systems is particularly relevant in applications where strong correlations exist between the cooling effect of environmental conditions and electrical power flow transfers. For example where high power flows resulting from wind generation at high wind speeds can be accommodated since the same wind speed has a positive effect on overhead line or power transformer cooling [26, 27, 84].

The chapter is structured in the following way: Section 12.2 describes the field trial network and the location of thermally vulnerable components due to the planned installation

of additional DG schemes; Section 12.3 describes the approach adopted to control the output of the DG schemes in order to manage power flows within multiple components of the field trial network; Section 12.4 describes the approach adopted for the off-line time series simulation of the candidate control strategies; Section 12.5 describes the real-time changes in DG power outputs resulting from the simulation of the candidate control strategies; Section 12.6 presents the evaluation of the candidate control strategies (where appropriate, the results are expressed as marginal values based on a datum control strategy corresponding to a last-in first-off (LIFO) DG tripping approach deployed with component static ratings); and, in light of the findings as discussed in Section 12.7, recommendations are made regarding the suitability of the control strategies for deployment with different component thermal rating systems.

12.2   Network description

A section of the distribution network of ScottishPower EnergyNetworks, selected for field trials in the DIUS Project, is given in Figure 12.1 [14]. Additional generation was introduced at nodes B4 and B9 representing planned future DG connections [107]. A summary of DG types and installed capacities is given in Table 12.1, together with datum DG annual energy yield values which correspond to the benchmark LIFO DG tripping strategy deployed with component static ratings. An underlying meshed 33kV network was included in the network model for simulations but for simplicity is not presented. Through an off-line analysis of the network (which entailed the simulation of the DG with unconstrained outputs throughout the year), power flow management was required for components C3, C5, C6, C7, C8 and C9. These components have been highlighted in Figure 12.1. Meteorological station locations for the real-time thermal rating system have been represented with the symbol M.

12.3   Control Approach

Rule-based decision making (inference) may be described as an artificial intelligence technique [96] which has the potential to facilitate the automated control of systems in a transparent manner. In this case the rule-based inference engine has been designed to support the control decisions of distribution network operators (DNOs). For the field trial network operating in normal conditions, the power flow sensitivity factor matrix, $\boldsymbol{M}_{PFSF}$ (9.3), was found to be of the form (12.1). From left to right across the rows the elements in each column correspond to components C3, C5, C6, C7, C8 and C9 respectively. From top to
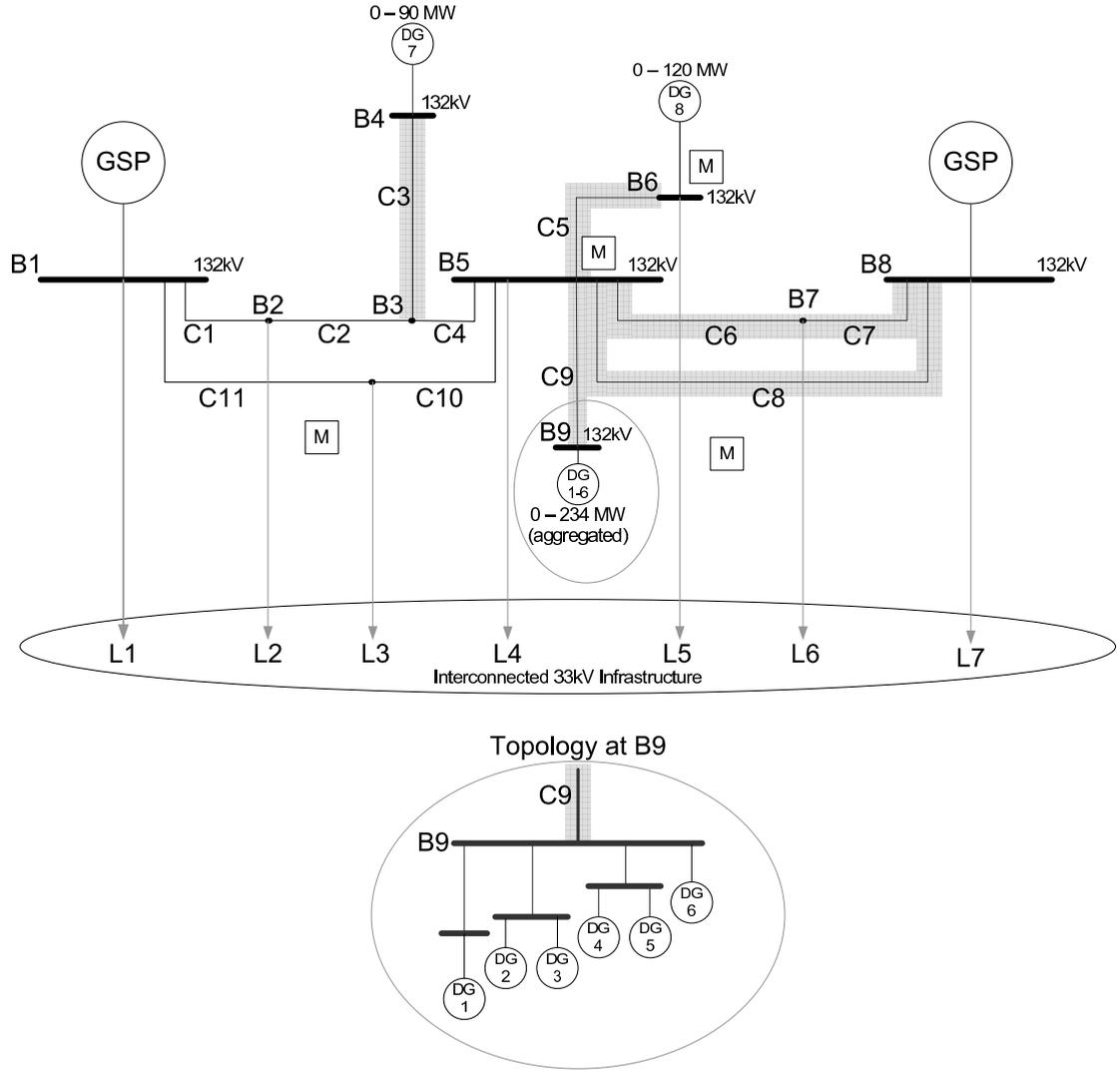
Figure 12.1: Field trial network topology

bottom the elements in each row correspond to DG7, DG8, DG1, DG2, DG3, DG4, DG5 and DG6 respectively.

M_{PFSF} was populated as given in (12.2) [83], corresponding to the lower of the power flow sensitivity factors assessed at maximum generation–maximum loading and maximum generation–minimum loading conditions. Furthermore, the LIFO DG constraint matrix (M_{LIFO}) and the technically most appropriate (TMA) DG constraint matrix (M_{TMA}) were found to be of the form (12.3). M_{LIFO} is given in (12.4), based on (9.7) and DG contractual mechanisms. In addition, M_{TMA} is given in (12.5), based on (9.14) and (12.2).

A series of 'If-Then' rules were created to establish the relationship between the thermally vulnerable components and the DG schemes that it would be necessary to constrain in order to manage network power flows.

Table 12.1: DG scheme details

G_{id}	DG type	Installed capacity (MW)	LIFO constraint order	Datum energy yield (GWh/annum)
DG1	Onshore wind	24	1st	30.9
DG2	Onshore wind	30	2nd	46.7
DG3	Onshore wind	39	3rd	71.5
DG4	Onshore wind	40	4th	87.9
DG5	Onshore wind	56	5th	114.6
DG6	Onshore wind	45	6th	113.9
DG7	Offshore wind	90	7th	205.5
DG8	Offshore wind	120	8th	272.2

$$M_{PFSF} = \begin{bmatrix} \frac{dP_{B3,B4}^{C3}}{dG_{P,B4}} & \frac{dP_{B5,B6}^{C5}}{dG_{P,B4}} & \frac{dP_{B5,B7}^{C6}}{dG_{P,B4}} & \frac{dP_{B7,B8}^{C7}}{dG_{P,B4}} & \frac{dP_{B5,B8}^{C8}}{dG_{P,B4}} & \frac{dP_{B5,B9}^{C9}}{dG_{P,B4}} \\[2em] \frac{dP_{B3,B4}^{C3}}{dG_{P,B6}} & \frac{dP_{B5,B6}^{C5}}{dG_{P,B6}} & \frac{dP_{B5,B7}^{C6}}{dG_{P,B6}} & \frac{dP_{B7,B8}^{C7}}{dG_{P,B6}} & \frac{dP_{B5,B8}^{C8}}{dG_{P,B6}} & \frac{dP_{B5,B9}^{C9}}{dG_{P,B6}} \\[2em] \frac{dP_{B3,B4}^{C3}}{dG_{P,B9}^{1}} & \frac{dP_{B5,B6}^{C5}}{dG_{P,B9}^{1}} & \frac{dP_{B5,B7}^{C6}}{dG_{P,B9}^{1}} & \frac{dP_{B7,B8}^{C7}}{dG_{P,B9}^{1}} & \frac{dP_{B5,B8}^{C8}}{dG_{P,B9}^{1}} & \frac{dP_{B5,B9}^{C9}}{dG_{P,B9}^{1}} \\[2em] \frac{dP_{B3,B4}^{C3}}{dG_{P,B9}^{2}} & \frac{dP_{B5,B6}^{C5}}{dG_{P,B9}^{2}} & \frac{dP_{B5,B7}^{C6}}{dG_{P,B9}^{2}} & \frac{dP_{B7,B8}^{C7}}{dG_{P,B9}^{2}} & \frac{dP_{B5,B8}^{C8}}{dG_{P,B9}^{2}} & \frac{dP_{B5,B9}^{C9}}{dG_{P,B9}^{2}} \\[2em] \frac{dP_{B3,B4}^{C3}}{dG_{P,B9}^{3}} & \frac{dP_{B5,B6}^{C5}}{dG_{P,B9}^{3}} & \frac{dP_{B5,B7}^{C6}}{dG_{P,B9}^{3}} & \frac{dP_{B7,B8}^{C7}}{dG_{P,B9}^{3}} & \frac{dP_{B5,B8}^{C8}}{dG_{P,B9}^{3}} & \frac{dP_{B5,B9}^{C9}}{dG_{P,B9}^{3}} \\[2em] \frac{dP_{B3,B4}^{C3}}{dG_{P,B9}^{4}} & \frac{dP_{B5,B6}^{C5}}{dG_{P,B9}^{4}} & \frac{dP_{B5,B7}^{C6}}{dG_{P,B9}^{4}} & \frac{dP_{B7,B8}^{C7}}{dG_{P,B9}^{4}} & \frac{dP_{B5,B8}^{C8}}{dG_{P,B9}^{4}} & \frac{dP_{B5,B9}^{C9}}{dG_{P,B9}^{4}} \\[2em] \frac{dP_{B3,B4}^{C3}}{dG_{P,B9}^{5}} & \frac{dP_{B5,B6}^{C5}}{dG_{P,B9}^{5}} & \frac{dP_{B5,B7}^{C6}}{dG_{P,B9}^{5}} & \frac{dP_{B7,B8}^{C7}}{dG_{P,B9}^{5}} & \frac{dP_{B5,B8}^{C8}}{dG_{P,B9}^{5}} & \frac{dP_{B5,B9}^{C9}}{dG_{P,B9}^{5}} \\[2em] \frac{dP_{B3,B4}^{C3}}{dG_{P,B9}^{6}} & \frac{dP_{B5,B6}^{C5}}{dG_{P,B9}^{6}} & \frac{dP_{B5,B7}^{C6}}{dG_{P,B9}^{6}} & \frac{dP_{B7,B8}^{C7}}{dG_{P,B9}^{6}} & \frac{dP_{B5,B8}^{C8}}{dG_{P,B9}^{6}} & \frac{dP_{B5,B9}^{C9}}{dG_{P,B9}^{6}} \end{bmatrix} \tag{12.1}$$

$$\boldsymbol{M}_{PFSF} = \begin{bmatrix} -0.99 & 0 & 0.46 & 0.46 & 0.47 & 0 \\ 0 & -0.95 & 0.46 & 0.47 & 0.47 & 0 \\ 0 & 0 & 0.41 & 0.41 & 0.42 & -0.91 \\ 0 & 0 & 0.42 & 0.43 & 0.43 & -0.92 \\ 0 & 0 & 0.42 & 0.42 & 0.43 & -0.92 \\ 0 & 0 & 0.43 & 0.43 & 0.44 & -0.94 \\ 0 & 0 & 0.43 & 0.43 & 0.44 & -0.94 \\ 0 & 0 & 0.45 & 0.45 & 0.46 & -0.98 \end{bmatrix} \tag{12.2}$$

$$\boldsymbol{M}_{LIFO,TMA} = \begin{bmatrix} x_{B4}^{DG7} & 0 & x_{B4}^{DG7} & x_{B4}^{DG7} & x_{B4}^{DG7} & 0 \\ 0 & x_{B6}^{DG8} & x_{B6}^{DG8} & x_{B6}^{DG8} & x_{B6}^{DG8} & 0 \\ 0 & 0 & x_{B9}^{DG1} & x_{B9}^{DG1} & x_{B9}^{DG1} & x_{B9}^{DG1} \\ 0 & 0 & x_{B9}^{DG2} & x_{B9}^{DG2} & x_{B9}^{DG2} & x_{B9}^{DG2} \\ 0 & 0 & x_{B9}^{DG3} & x_{B9}^{DG3} & x_{B9}^{DG3} & x_{B9}^{DG3} \\ 0 & 0 & x_{B9}^{DG4} & x_{B9}^{DG4} & x_{B9}^{DG4} & x_{B9}^{DG4} \\ 0 & 0 & x_{B9}^{DG5} & x_{B9}^{DG5} & x_{B9}^{DG5} & x_{B9}^{DG5} \\ 0 & 0 & x_{B9}^{DG6} & x_{B9}^{DG6} & x_{B9}^{DG6} & x_{B9}^{DG6} \end{bmatrix} \tag{12.3}$$

$$\boldsymbol{M}_{LIFO} = \begin{bmatrix} 1 & 0 & 7 & 7 & 7 & 0 \\ 0 & 1 & 8 & 8 & 8 & 0 \\ 0 & 0 & 1 & 1 & 1 & 1 \\ 0 & 0 & 2 & 2 & 2 & 2 \\ 0 & 0 & 3 & 3 & 3 & 3 \\ 0 & 0 & 4 & 4 & 4 & 4 \\ 0 & 0 & 5 & 5 & 5 & 5 \\ 0 & 0 & 6 & 6 & 6 & 6 \end{bmatrix} \tag{12.4}$$

$$\boldsymbol{M}_{TMA} = \begin{bmatrix} 1 & 0 & 2 & 2 & 2 & 0 \\ 0 & 1 & 1 & 1 & 1 & 0 \\ 0 & 0 & 8 & 8 & 8 & 6 \\ 0 & 0 & 7 & 7 & 7 & 5 \\ 0 & 0 & 6 & 6 & 6 & 4 \\ 0 & 0 & 5 & 5 & 5 & 3 \\ 0 & 0 & 4 & 4 & 4 & 2 \\ 0 & 0 & 3 & 3 & 3 & 1 \end{bmatrix} \tag{12.5}$$

Considering (12.2), the zero terms in the matrix represent a negligible power flow sensitivity factor and indicate that the power output of a DG scheme has negligible impact on the power flows in that particular component. By inspection of this matrix it is possible to see that the power flows in components C3 and C5 are affected only by DG at nodes B4 and B6 respectively. This agrees with intuition as these components are the feeder connections for the relevant DG schemes. Moreover, the power flow in component C9 is sensitive only to the DG connected at node B9. Considering components C6, C7 and C8 it can be seen from Figure 12.1 that this is where power flows from all the DG schemes accumulate. Therefore the power flows in these components are sensitive to outputs from each DG scheme connected. Having identified these relationships the necessary rule-bases were created for the candidate control strategies. An example rule-base is given in (12.6)–(12.9) for the implementation of the egalitarian control strategy.

$$\begin{aligned} If: \quad & U_{B5,B7}^{C6} \geq 1 \\ & Then: \quad Constrain\ DG1 - DG8 \end{aligned} \tag{12.6}$$

$$\begin{aligned} If: \quad & U_{B7,B8}^{C7} \geq 1 \\ & Then: \quad Constrain\ DG1 - DG8 \end{aligned} \tag{12.7}$$

$$\begin{aligned} If: \quad & U_{B5,B8}^{C8} \geq 1 \\ & Then: \quad Constrain\ DG1 - DG8 \end{aligned} \tag{12.8}$$

$$\begin{aligned} If: \quad & U_{B9,B5}^{C9} \geq 1 \\ & Then: \quad Constrain\ DG1 - DG6 \end{aligned} \tag{12.9}$$

where $U_{i,k}^{c}$ represents the utilisation of a particular component and is defined in (8.1) as the ratio of apparent power flow to the thermal limit ($S_{i,k}^{c}/S_{i,k(lim)}^{c}$). It should be noted

that $S_{i,k(lim)}^c$ could be the component static, seasonal or real-time thermal rating.

12.4   Simulation Approach

As a step towards the on-line control of multiple DG schemes, an off-line time series analysis was conducted in order to quantify the impact of the candidate control strategies on the evaluation parameters described in Chapter 9 for a complete operational year. The control system simulation, as shown in Figure 12.2, functions in the following manner:

1. Grid supply point (GSP) reference voltages and power flows are input to the 'distribution network simulator' and 'off-line simulation tool' both of which are load flow algorithms (a).

2. Normalised historical load demand and generation power output profiles are scaled through multiplication by peak values (b)–(c) respectively, which are also input to the 'distribution network simulator' and 'off-line simulation tool' (d)–(e).

3. Component static, seasonal and real-time thermal ratings are fed into the 'rule-based inference engine' (f) together with a full set of component power flows which have been computed by the 'distribution network simulator' (g). Based on the ranked magnitude of component utilisations together with embedded knowledge of the ability of DG to manage network power flows (signified by non-zero values in $\boldsymbol{M}_{PFSF}$), the 'rule-based inference engine' decides if a control action is necessary and which DG scheme(s) should be constrained. If a control action is required then the $\Delta P_{i,k}$ value, as calculated in (9.5), is passed to the 'DG set point calculator' (h). If no action is required then the 'off-line analysis tool' records the present DG power outputs, component losses, component utilisations and busbar voltages (k) and the control system reads in data for the next half hour interval.

4. The 'DG set point calculator' receives information from the 'rule-based inference engine' regarding the necessary real power flow reduction as well as an indication of which DG schemes have the ability to manage network power flows. Using a look-up table of predetermined power flow sensitivity factors ($\boldsymbol{M}_{PFSF}$), updated DG set points are calculated depending on the candidate control strategy selected.

5. New DG set point values are passed to the 'off-line simulation tool' (i) and together with GSP reference voltages, reference power flows and load demands, an updated load flow is computed.
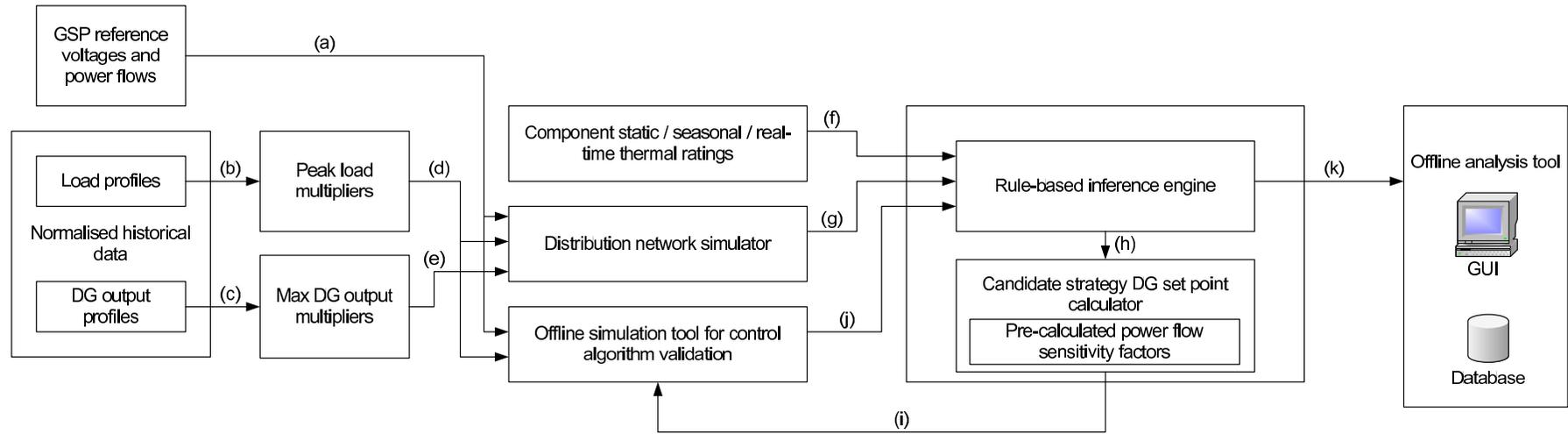
Figure 12.2: Power flow control block diagram

6. The updated sets of complete power flows and busbar voltages are passed back to the inference engine (j). This validates that all power flows and voltages are within designated limits. Steps 3–6 are repeated with the updated DG set point values to manage power flows within all the necessary components of the network.

In the simulated deployment of the candidate control strategies within the field trial network, the topology and DG installed capacities were assumed to be constants of the system. The component types and ratings used are summarised in Table 12.2 together with datum component energy losses corresponding to the benchmark LIFO DG tripping control strategy. Component real-time thermal ratings were computed with a half-hourly data resolution for the calendar year 2006 using the thermal models described in Chapter 7 [84] and historical meteorological data for the 'Valley' area of Wales, UK [102]. Simulations were conducted with a target utilisation, $U_{Tar} = 0.95$.

12.4.1   Limitation of the 'TMA' strategy

On certain occasions it was found that the simulation of the TMA strategy produced an aggregated energy yield result that was lower than the egalitarian and LIFO strategies. This apparently anomalous behaviour was investigated further and the following discovery was made which led to a refinement of the rule-base for the TMA strategy. Figure 12.3 shows a generic situation where multiple overloads occur in multiple components of the distribution network. Supposing $U_{i,k} > U_{m,i}$ and $\frac{dP_{i,k}}{dG_{P,n}} > \frac{dP_{i,k}}{dG_{P,m}}$ this would lead to a constraint of the DG scheme at node n in order to solve the most significant overload which, in this case, happens to occur between nodes i and k. However, the constraint of the DG scheme at node n does not solve the power flow issue between nodes m and i. Therefore the DG scheme at node m is required to be constrained and, in doing so, causes the power flow from node i to node k to reduce further. The inference rule-base was refined to select distributed generators to be constrained based on locality to the overloaded component when situations, described above, arose.

Table 12.2: Component thermal ratings

Component	Summer rating (MVA)	Spring/ autumn rating (MVA)	Winter rating (MVA)	Average real-time rating (MVA)	Component properties	Energy loss (GWh/annum)
C1	89	103	111	n/a	Lynx 175mm^2 50°C	3.17
C2	89	103	111	n/a	Lynx 175mm^2 50°C	1.48
C3	89	103	111	136.9	Lynx 175mm^2 50°C	0.41
C4	89	103	111	n/a	Lynx 175mm^2 50°C	0.48
C5	89	103	111	141.6	Lynx 175mm^2 50°C	0.12
C6	89	103	111	129.9	Lynx 175mm^2 50°C	3.30
C7	89	103	111	128.3	Lynx 175mm^2 50°C	2.58
C8	89	103	111	126.5	Lynx 175mm^2 50°C	4.75
C9	120	130	136	177.9	Poplar 200mm^2 75°C	4.66
C10	89	103	111	n/a	Lynx 175mm^2 50°C	1.98
C11	89	103	111	n/a	Lynx 175mm^2 50°C	2.88
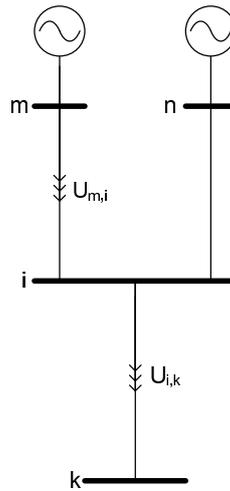
Figure 12.3: Limitation of the TMA strategy

12.5 Real-time changes in DG power outputs

For the case study network considered, it was found that the variation of DG outputs (and hence annual energy yields) resulting from the candidate control strategies deployed with component static thermal ratings was significantly greater than the variation of DG outputs resulting from control strategies deployed with component real-time thermal ratings. This was because the use of component real-time thermal ratings increased the power flow transfer capacity of thermally vulnerable components and reduced the necessity for DG output control in order to manage power flows. Therefore, illustrative graphs have been plotted to demonstrate the real-time changes in DG power outputs as a result of the candidate control strategy simulated with component static thermal ratings.

The real-time changes in DG power outputs resulting from the control strategy simulations are given in Figures 12.4, 12.5, 12.6 and 12.7 for DG1, DG6, DG7 and DG8 respectively. Since DG2, DG3 and DG4 displayed the same general trends as DG1, and DG5 displayed the same general trends as DG6, these power output profiles are provided in Appendix E.1. During the illustrative time period there were three extended periods when power flow management was required in component C9. These were 04:30 to 08:00, 10:30 to 13:00 and 18:30 to 22:00. There were also two periods when power flow management in component C6 was required. These were 01:30 to 04:00 and 09:30 to 10:30.

Considering Figure 12.4, DG1 is the first-off DG scheme (being the last to connect, historically). Therefore, the power output of DG1 is completely constrained for extended

periods of the day for the LIFO control strategy simulations. This affects the revenue stream of DG1 and leads to an undesirable power output profile because the DG scheme is continuously disconnected and reconnected. The maximum power output (12 MW) occurs at 09:30 which represents half of the installed capacity. The egalitarian broadcast signal strategy facilitates increased power outputs for DG1 since all the DG schemes participate in managing power flows and therefore DG1 is no longer 'first-off'. The TMA control strategy leads to greatest power output for DG1 since the scheme is not required to be constrained to manage power flows.

Considering Figure 12.5, the LIFO strategies, as expected, facilitate the highest power output since DG6 is the last-off DG scheme (having historically connected to the distribution network at node B9 first). The egalitarian strategy produces the least variable output with the DG output capped for periods of the day. The TMA strategy requires constraint of DG6 to manage power flows in component C9. Therefore for periods of the day when power flow management of component C9 is required, the DG scheme is completely constrained.

Considering Figure 12.6, DG7 is unconstrained for extended periods and therefore the LIFO and TMA strategies all produce the same simulated power output. From 01:30 to 04:00 and 09:30 to 10:30 power flow management in component C6 is required. When simulating the egalitarian control strategy, as given in (12.6), this requires the participation of all DG schemes to manage network power flows. Therefore, the power output of DG7 is reduced for the egalitarian strategy simulation when compared to the LIFO and TMA strategies.

Considering Figure 12.7, DG output constraints occur from 01:30 to 04:00 and 09:30 to 10:30 when power flow management in component C6 is required. In this case DG8 is the TMA DG scheme to constrain in order to manage power flows in C6. Therefore the output of DG8 is constrained the most when compared to the other power output control strategies. The egalitarian control strategy requires the output control of all the DG schemes to manage power flows in component C6. Since the power flow constraint is shared amongst all the distributed generators, the power output DG8 is constrained less than when the TMA strategy is simulated. For the LIFO strategy simulations, DG8 has an unconstrained power output during the time period considered. This is because DG8 was the first DG scheme to connect to the distribution network and is therefore the last DG scheme to be constrained when power flow management is required as a result of multiple DG scheme power flow accumulations.
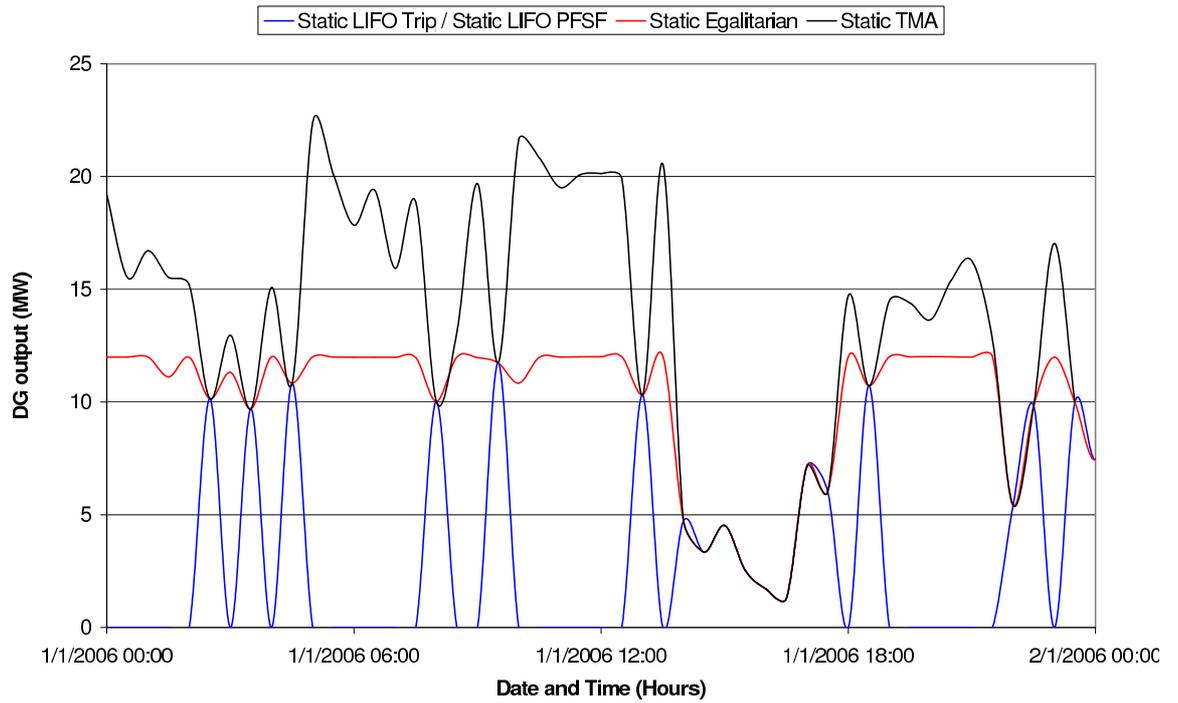
Figure 12.4: Illustration of real-time changes in DG1 output for candidate control strategy simulations
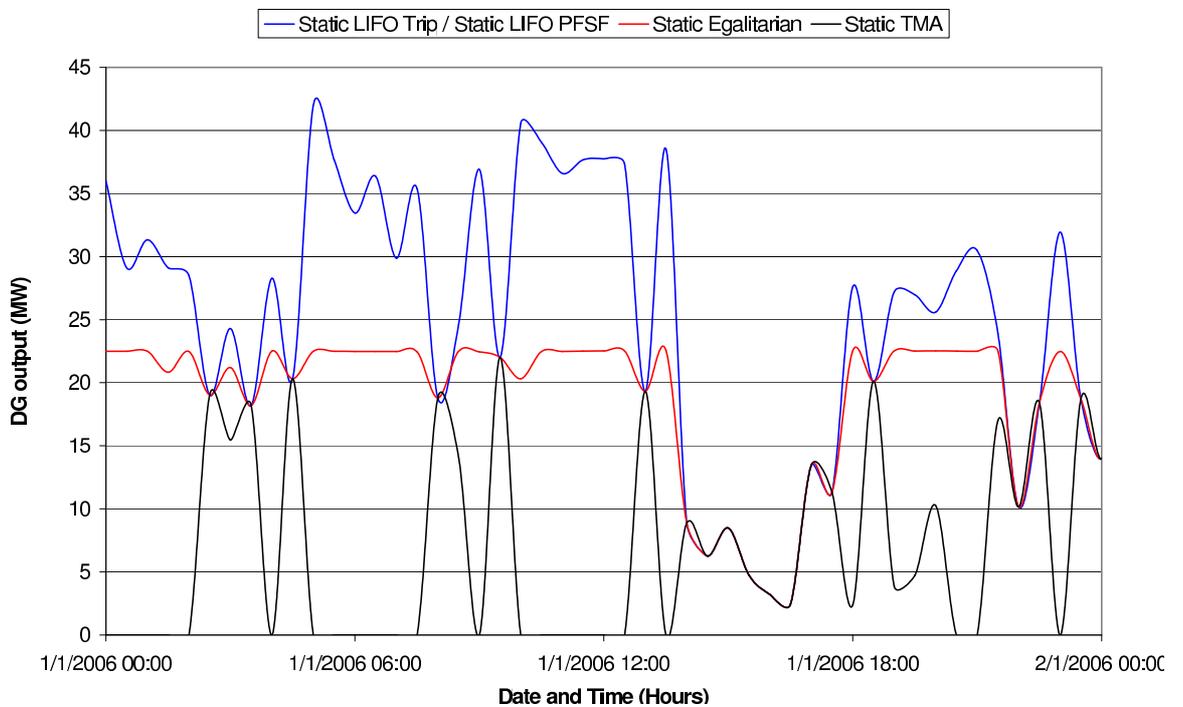
Figure 12.5: Illustration of real-time changes in DG6 output for candidate control strategy simulations
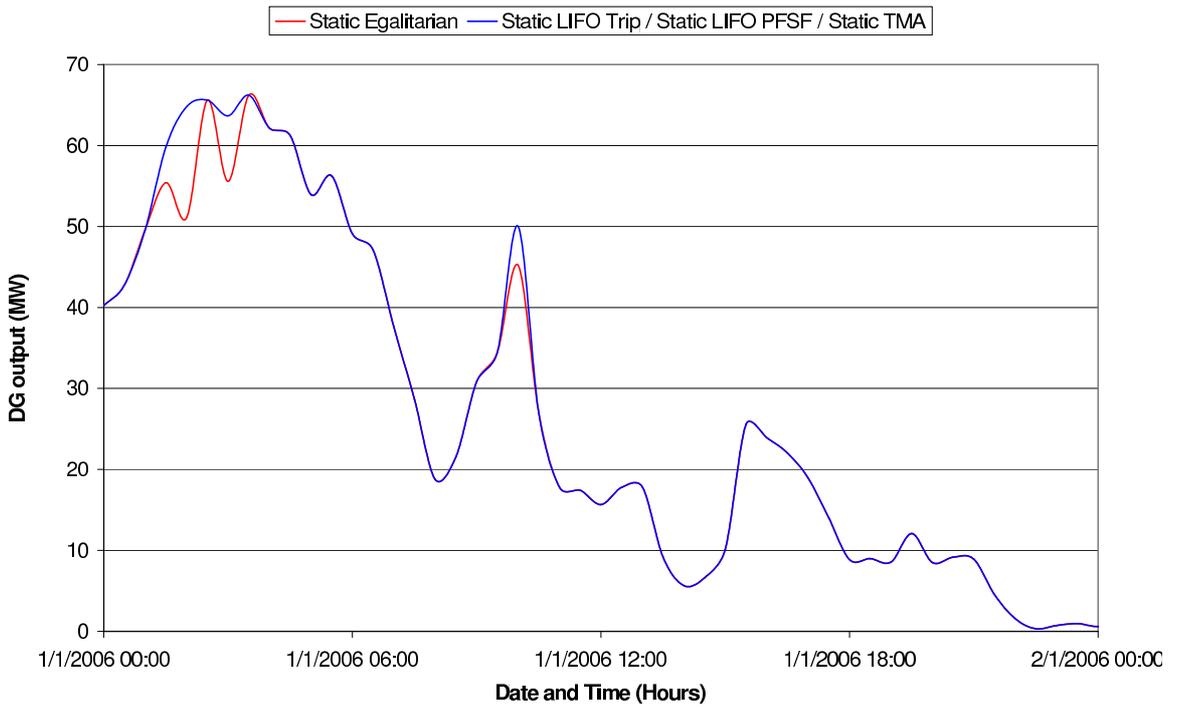
Figure 12.6: Illustration of real-time changes in DG7 output for candidate control strategy simulations
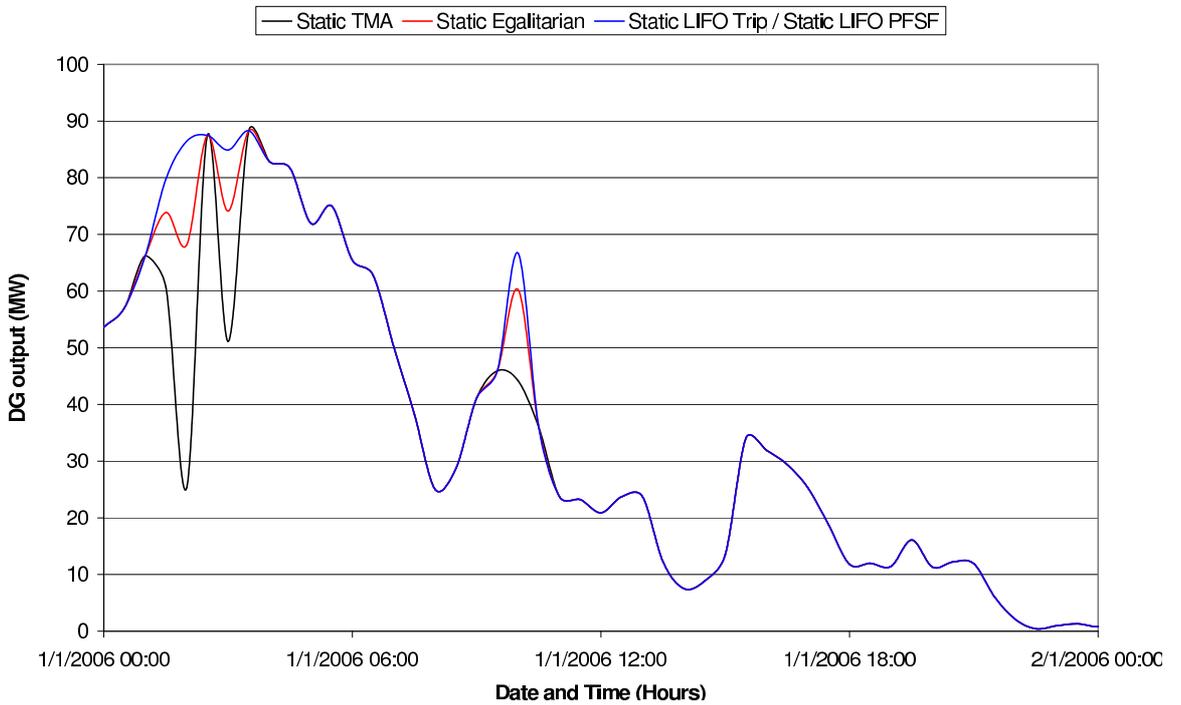
Figure 12.7: Illustration of real-time changes in DG8 output for candidate control strategy simulations

12.6   Evaluation parameters: Results and discussion

This section presents and discusses the quantification results of the control strategy evaluation parameters given in Chapter 9. In order to conduct a comprehensive evaluation of the proposed power flow sensitivity factor-based control strategies, each control strategy and thermal rating deployment was analysed by considering the impact on DG annual energy yields, DG apportioned losses, investment net present values (NPVs) and profitability indices (PIs), component power transfers and busbar voltages.

The simulation of the control strategies with seasonal thermal ratings represents an intermediate step between control system deployments with static and real-time thermal rating systems. Therefore the results analysis pertaining to an individual DG scheme focuses on static and real-time thermal rating system simulations. Supplementary results analyses, considering the impact of seasonal thermal rating systems on individual DG schemes, are provided in Appendix E.2.

The datum values of individual DG annual energy yields and individual component annual energy losses are presented in Tables 12.1 and 12.2 respectively. These values were obtained by simulating the LIFO DG tripping strategy with component static rating systems in the field trial network. This strategy was used to benchmark the performance of the candidate power flow sensitivity factor-based control strategies.

In quantifying the NPVs and PIs a discount factor of 10% was assumed for a 20-year operational lifetime of the wind farm [106], the wholesale electricity price was assumed to be £52.15/MWh [104], and the trading price of renewables obligation certificates (ROCs) was assumed to be £49.28/MWh [105]. The cost of the offshore wind farm installation was assumed to be £1000/kW and the costs of the onshore wind farm installations were assumed to be £800/kW [108]. Wind farm annual operations and maintenance costs were assumed to be 5% of the wind farm installation cost [109] and the value of the power flow control system was assumed to be £200k with the incorporation of component thermal monitoring equipment and £100k without.

12.6.1   Annual energy yields

Based on the datum values in Table 12.1, the marginal annual energy yields for each wind farm development resulting from the control strategy simulations with static thermal ratings and real-time thermal ratings are given in Figures 12.8 and 12.9 respectively. Considering Figures 12.8 and 12.9, the adoption of egalitarian and TMA control strategies is particularly

favourable for 'last-in' DG schemes DG1–4 in terms of increased annual energy yields and hence revenue stream enhancement.
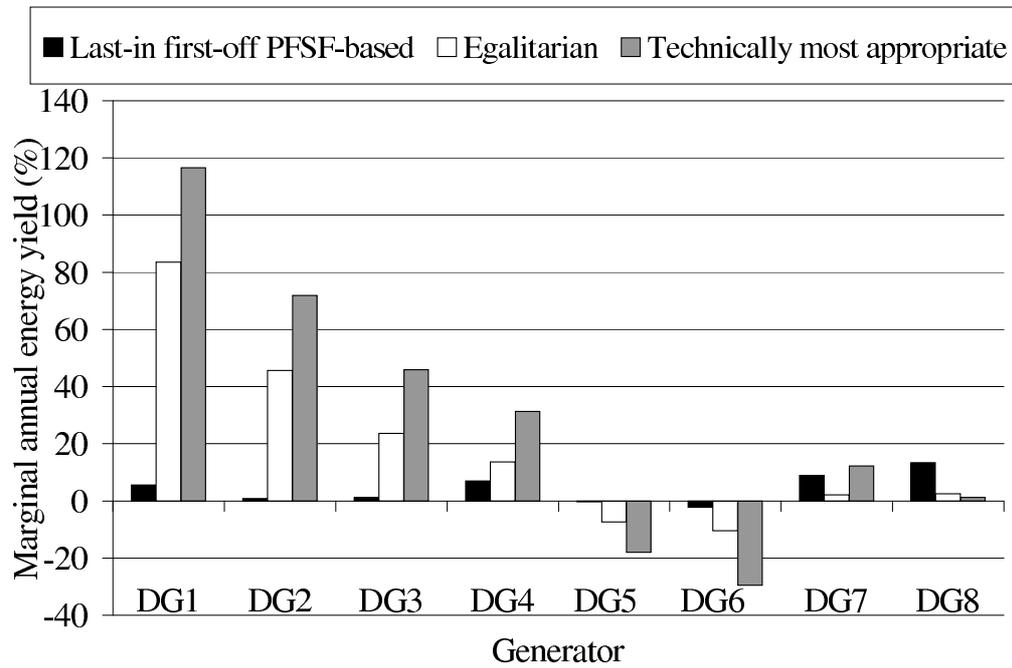
Figure 12.8: Individual DG marginal annual energy yields resulting from candidate control strategy deployments with component static thermal ratings
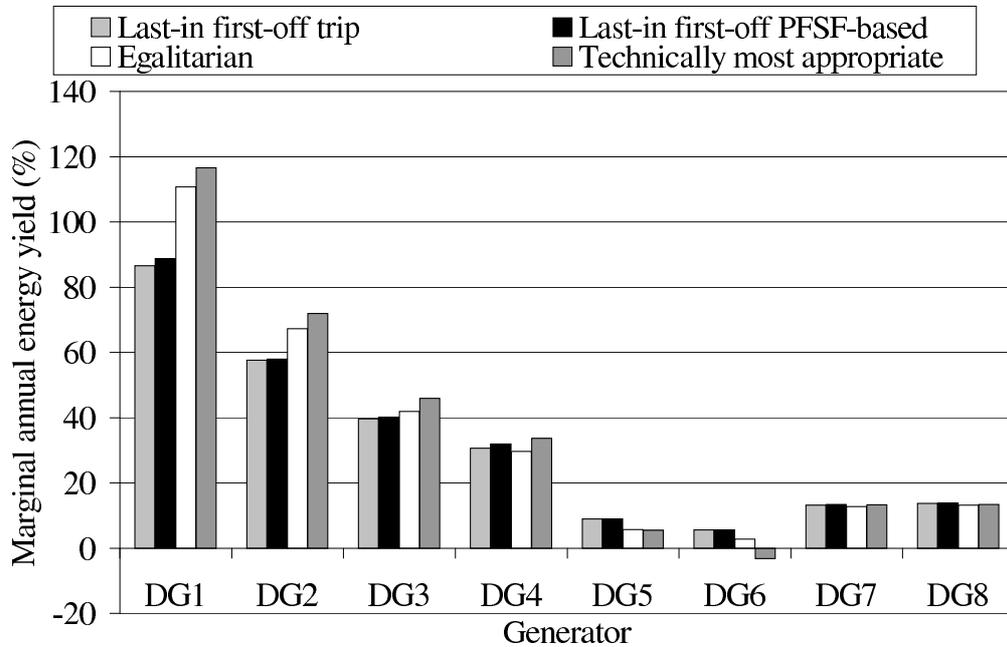
Figure 12.9: Individual DG marginal annual energy yields resulting from candidate control strategy deployments with component real-time thermal ratings

Table 12.3: Marginal aggregated DG annual energy yields (%)

Control strategy	Static	Seasonal	Real-time
LIFO Trip	0.0	12.1	20.1
LIFO PFSF-based	6.5	13.6	20.5
Egalitarian	7.1	13.9	20.5
TMA	11.0	15.8	21.0

Considering Figure 12.8, the egalitarian control strategy deployed with component static ratings facilitates increased annual energy yields for DG1–4 by 25.8 GWh, 21.3 GWh, 16.9 GWh and 12.0 GWh respectively, through the reduction in annual energy yields of DG5 and DG6 by 8.4 GWh and 11.9 GWh respectively. The TMA control strategy facilitates increased annual energy yields for DG1–4 by 36.0 GWh, 33.6 GWh, 32.8 GWh and 27.5 GWh respectively, through the reduction in annual energy yields of DG5 and DG6 by 20.6 GWh and 33.6 GWh respectively.

Considering Figure 12.9, with the exception of the annual energy yield of DG6 resulting from the TMA control strategy (110.2 GWh in absolute terms), every DG scheme sees an energy yield gain and hence revenue stream enhancement. As seen in (12.2), DG5 and DG6 have higher power flow sensitivity factors, relative to DG1, DG2, DG3 and DG4, therefore they are, technically, the most appropriate generators to constrain in order to manage power flows within C9.

The marginal aggregated DG annual energy yields are summarised in Table 12.3. Considering Table 12.3, based on the datum value of 943.8 GWh/annum, by inspection of the data in each column it is possible to observe the aggregated annual energy yield gains that may be achieved by the adoption of more sophisticated candidate power flow sensitivity factor-based control strategies, deployed with the specified component thermal rating system. Similarly, by inspection of each row it is possible to observe the aggregated annual energy yield gains that may be achieved by adopting a more sophisticated component thermal rating system, deployed with the specified control strategy.

Respective aggregated annual energy yield gains of 6.5%, 7.1%, and 11.0% may be achieved by adoption of LIFO PFSF-based, egalitarian and TMA control strategies deployed with component static thermal ratings. The latter control system deployment represents an increased aggregated energy yield of 104.2 GWh/annum. The impact that coordinated power output control approaches have on individual DG scheme revenue streams could mean that, even if the 'first-in' DG schemes are remunerated for curtailing their power

output at certain times of the year, there is an overall revenue gain for all the DG schemes.

Respective aggregated annual energy yield gains of 12.1% and 20.1% may be achieved by the adoption of a basic DG tripping control strategy deployed with component seasonal and real-time thermal ratings. The latter deployment represents an increased aggregated energy yield of 190.1 GWh/annum. Combining the TMA control strategy with a sophisticated component real-time thermal rating system, results in an aggregated annual energy yield gain of 21.0%. This represents an increase of 198 GWh/annum beyond the datum value. As the component thermal rating system becomes more sophisticated the distinction between aggregated energy yields for the different candidate control strategies becomes less pronounced. However, the increased power transfer capacity that may be unlocked through component real-time thermal rating systems could lead to the accommodation of larger DG installed capacities [84]. Therefore the adoption of coordinated DG power output control strategies could allow a greater percentage of the additional power transfer headroom to be realised.

12.6.2 Losses

The energy losses in C3 were apportioned directly to DG7, the losses in C5 were apportioned directly to DG8, and the losses in C9 can be apportioned directly to DG1–DG6, based on (9.16)–(9.17) in Chapter 9. This is because these components are the feeder connections for the wind farms as seen in Figure 12.1.

Considering Figure 12.10, DG1–4 are apportioned additional annual energy losses of 291 MWh, 252 MWh, 219 MWh and 177 MWh respectively when the egalitarian control strategy is adopted. Additional annual energy losses of 421 MWh, 409 MWh, 423 MWh and 380 MWh are attributed to DG1–4 respectively in deploying the TMA control strategy. Inspection of Figure 12.11 shows that further additional annual energy losses are apportioned to all the DG schemes in deploying the candidate control strategies with component real-time thermal ratings. The increase in losses resulting from coordinated control strategies are a direct result of increased power transfers and hence increased energy yields of the DG schemes.
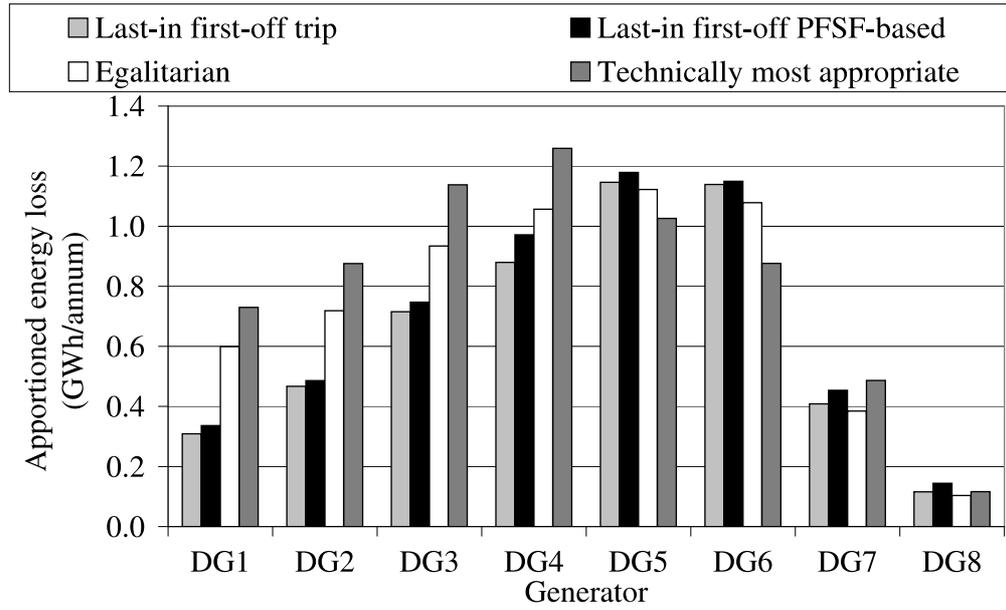
Figure 12.10: DG apportioned annual energy losses resulting from candidate control strategy deployments with component static thermal ratings
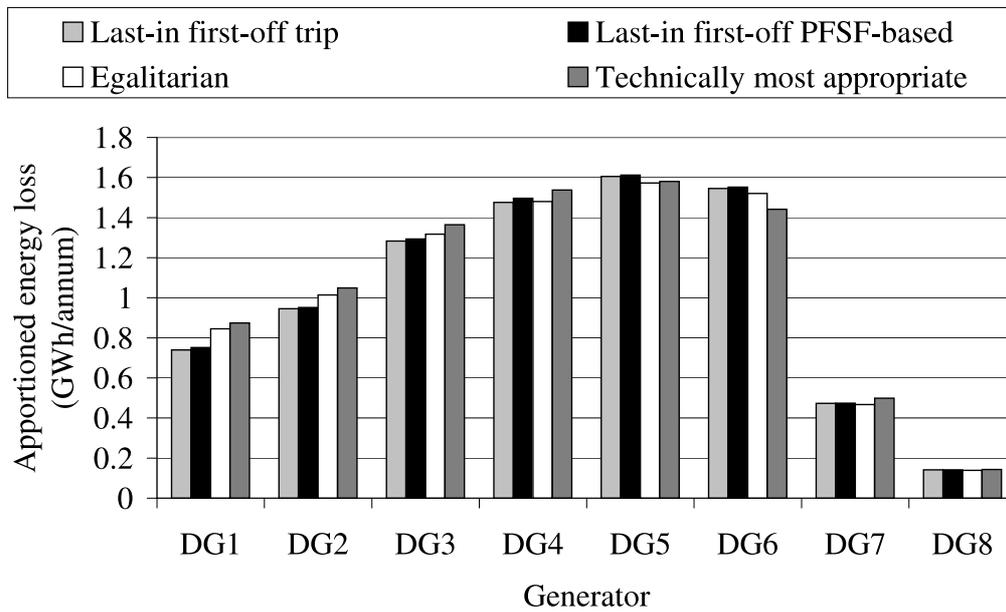
Figure 12.11: DG apportioned annual energy losses resulting from candidate control strategy deployments with component real-time thermal ratings

12.6.3 Financial performance

Tables 12.4 and 12.5 summarise DG investment NPVs and PIs for the candidate control strategies deployed with component static and real-time thermal ratings respectively. An NPV ≤ 0 indicates an investment is not financially viable. Moreover, in evaluating the impact of candidate control strategies on the financial performance of the DG developments, a PI ≥ 1 could be specified as the investment criterion. This indicates that the investor will recover at least double the cost of the initial investment over the project lifetime.

Considering the results presented in Table 12.4 for the LIFO DG tripping control strategy, it can be seen that if this approach is adopted then the investment would not be viable for DG1 since the NPV of the development is £-0.9M. This is because DG1 represents the last DG scheme to connect to the network and therefore the first DG scheme to be disconnected to manage network power flows. The resulting impact on the annual energy yield of the DG scheme means that insufficient revenue is earned over the project lifetime to justify the initial investment cost. In general, the power flow sensitivity factor-based control strategies facilitate improved financial benefits for all the DG developers. The LIFO PFSF-based approach is most preferable for DG5–8, in terms of revenue stream enhancement (with respective NPV gains of £34.4M, £33.8M, £105.8M and £151.6M), since they are the 'first-in' generators. The egalitarian strategy enhances the revenue streams and hence increases the profitability indices of DG1–4 and DG7. The respective NPV gains for these DG schemes are £41.4M, £42.3M, £45.7M, £42.3M and £112.2M. The TMA control strategy resulted in the greatest enhancement to the revenue streams of DG1–4 (with respective NPVs of £49.2M, £58.6M, £76.2M and £85.5M), due to the coordinated power output control of DG5–8 at times of power flow management.

Considering Table 12.5, it can be observed that the candidate control strategies deployed with component real-time thermal ratings all display a similar financial performance (the largest NPV difference being £8.6M for DG6 without remuneration). The LIFO PFSF-based strategy is marginally favourable for DG5–8 (with respective profitability indices of 1.9, 2.4, 1.8 and 1.8) and the TMA strategy is marginally favourable for DG1–4 (with respective PIs of 2.4, 2.3, 2.4 and 2.6).

12.6.4 Power transfers

The impact of the control strategy deployments with component static ratings on power transfers through component C9 are given in Figure 12.12.

Table 12.4: Wind farm financial evaluation (static thermal ratings)

Parameter	Control strategy	DG1	DG2	DG3	DG4	DG5	DG6	DG7	DG8
NPV	LIFO Trip	-0.9	5.9	16.9	29.9	34.6	46.5	49.0	64.4
(£M)	LIFO PFSF-based	19.8	30.2	48.9	67.2	79.0	80.3	154.8	216.0
	Egalitarian	40.5	48.2	62.6	72.2	72.1	72.3	161.2	190.4
	TMA	49.2	58.6	76.2	85.5	61.7	53.6	150.9	187.4
PI	LIFO Trip	-	0.2	0.5	0.9	0.8	1.3	0.5	0.5
	LIFO PFSF-based	1.0	1.2	1.5	2.0	1.7	2.2	1.7	1.8
	Egalitarian	2.0	1.9	1.9	2.2	1.6	2.0	1.8	1.6
	TMA	2.4	2.3	2.4	2.6	1.3	1.4	1.7	1.6

Table 12.5: Wind farm financial evaluation (real-time thermal ratings)

Parameter	Control strategy	DG1	DG2	DG3	DG4	DG5	DG6	DG7	DG8
NPV	LIFO Trip	22.0	28.9	41.2	52.9	43.3	51.8	72.4	96.7
(£M)	LIFO PFSF-based	41.8	53.0	72.7	85.8	88.0	87.8	162.6	217.0
	Egalitarian	47.6	56.7	73.8	84.2	84.8	85.1	162.2	215.5
	TMA	49.2	58.6	76.2	87.2	84.6	79.2	161.5	215.9
PI	LIFO Trip	1.1	1.2	1.3	1.6	0.9	1.4	0.8	0.8
	LIFO PFSF-based	2.1	2.1	2.3	2.6	1.9	2.4	1.8	1.8
	Egalitarian	2.4	2.3	2.3	2.5	1.9	2.3	1.8	1.8
	TMA	2.4	2.3	2.4	2.6	1.8	2.1	1.8	1.8

The clear distinction between power transfers through component C9 due to the simulation of the different candidate control strategies may be observed. The LIFO trip strategy allows the least amount of power to be transferred (465.5 GWh/annum) and therefore utilises the capacity of component C9 the least. The candidate power flow sensitivity factor-based control strategies improve the utilisation of the component and thus allow more power to be transferred. The TMA strategy facilitates the greatest power transfer (541.1 GWh/annum), followed by the egalitarian strategy (521.2 GWh/annum), and followed by the LIFO PFSF-based strategy (471.7 GWh/annum). The control of DG scheme power outputs and hence the control of power flows through the component is apparent due to the capping of the profiles for the candidate power flow sensitivity factor-based strategies. The flat parts of the curves in the region of 3–20% of the year represent the constraint of power flows through the component to match the desired utilisation target of 95% of the component rating.

Considering Figure 12.13, three discrete capping intervals occur in the profiles of the candidate power flow sensitivity factor-based strategies in the region of 0–20% of the years duration. These represent the regions of power flow control in order to achieve a 95% utilisation target of the respective seasonal ratings. The overall utilisation of the component, in terms of power transfers, is improved since the peak power flow has increased from 120 MVA to 136 MVA. The respective power transfers are 525.5 GWh/annum, 529.9 GWh/annum, 553.3 GWh/annum, and 561.5 GWh/annum for the LIFO DG tripping, LIFO PFSF-based, egalitarian, and TMA control strategies.

Considering Figure 12.14, the peak power flow is increased to 242.6 MVA and the power transfer is increased to 591.0 GWh/annum, 593.3 GWh/annum, 596.9 GWh/annum and 600.0 GWh/annum for the LIFO DG tripping, LIFO PFSF-based, egalitarian and TMA control strategies respectively. Since there is an increase in the overall power transfer this demonstrates that the component is being utilised more effectively. However, there is a minimal distinction (1.5%) between the candidate power output control strategies in terms of power transfers and hence DG constraint. For this particular case study it can be concluded that the sophistication of the control system, in terms of the implementation of power flow sensitivity factor-based control strategies, in less beneficial when real-time thermal ratings are deployed. This is attributed to the strong correlation between the power output of wind-based generators and the positive cooling effect that the wind has on overhead lines, thus unlocking power flow transfer capacity. However, in situations where the generation is not wind-sourced and there is not a strong correlation between the output

of DG schemes and the transfer capacity of components, there are potential advantages to the deployment of the candidate power flow sensitivity factor-based control strategies.
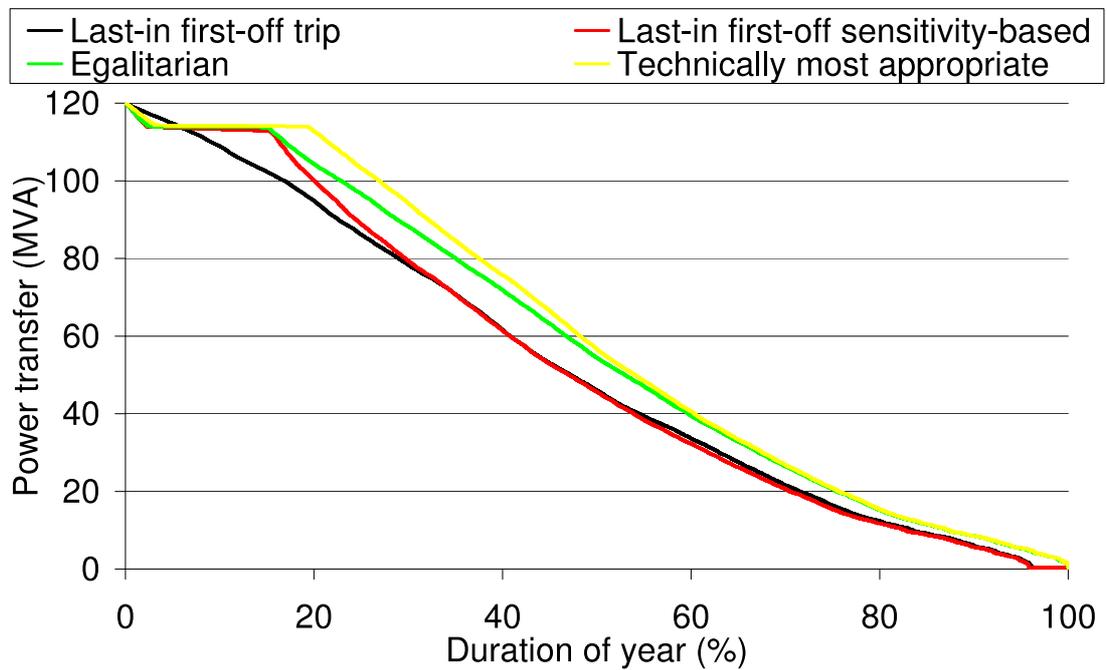
Figure 12.12: Power transfer through component C9 due to candidate strategy deployments with component static thermal rating.
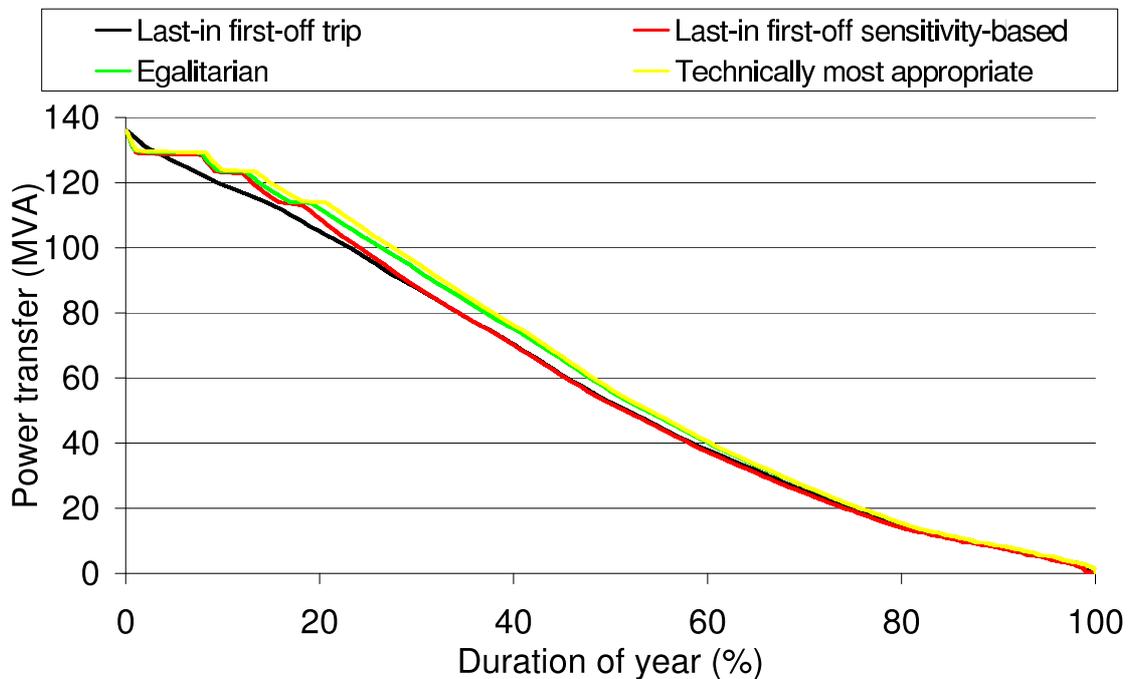
Figure 12.13: Power transfer through component C9 due to candidate strategy deployments with component seasonal thermal rating.
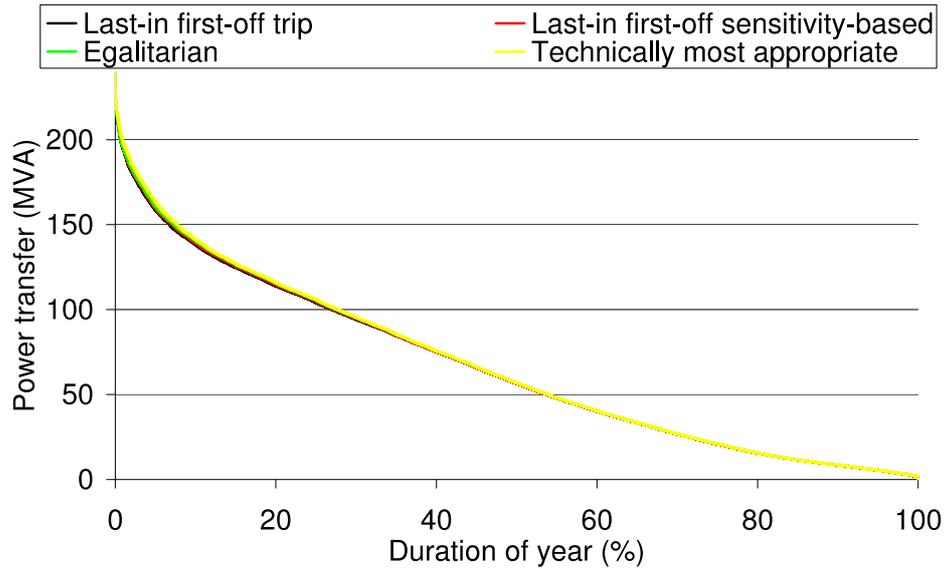
Figure 12.14: Power transfer through component C9 due to candidate strategy deployments with component real-time thermal rating.

12.6.5 Busbar voltages

This section quantifies the impact of the candidate control strategies deployed with the different component thermal rating systems on busbar voltages. In all cases the busbar voltages conformed to the statutory UK requirements specified in [15]. Furthermore, the voltage profiles of the busbars at the GSPs represented the extremities of voltage excursions and all other busbar voltages lay within these bounds. Due to the variation in powers transferred through component C9, the most significant variation in busbar voltages occurred at node B9. The impact of the candidate control strategies with static thermal ratings is shown in Figure 12.15, with an enlargement in Figure 12.16. The impact of the TMA control strategy with different thermal rating systems is shown in Figure 12.17, with an enlargement in Figure 12.18.

Considering Figures 12.15 and 12.16, the increased power transfer through component C9, as a result of the candidate power flow sensitivity factor-based control strategies, leads to a marginal increase in the voltage at B9. The maximum per unit voltage difference between the LIFO DG tripping approach and the TMA strategy was found to be 0.4%. This was attributed to a voltage rise effect along the feeder [48]. As seen in Figures 12.17 and 12.18, the voltage rise effect is more pronounced due to the increased power transfers resulting from the deployment of the TMA control strategy with different component thermal rating systems. A maximum per unit voltage difference between control system deployments with component static and real-time thermal ratings was found to be 0.9%.
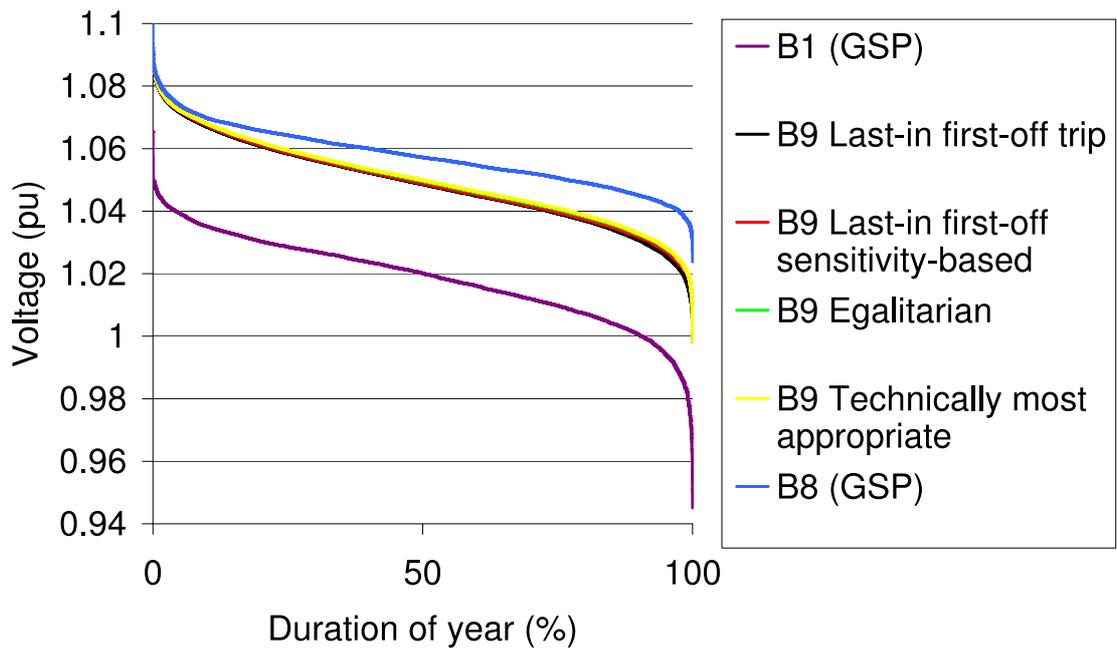
Figure 12.15: Busbar voltages due to candidate strategy deployments with component static thermal ratings
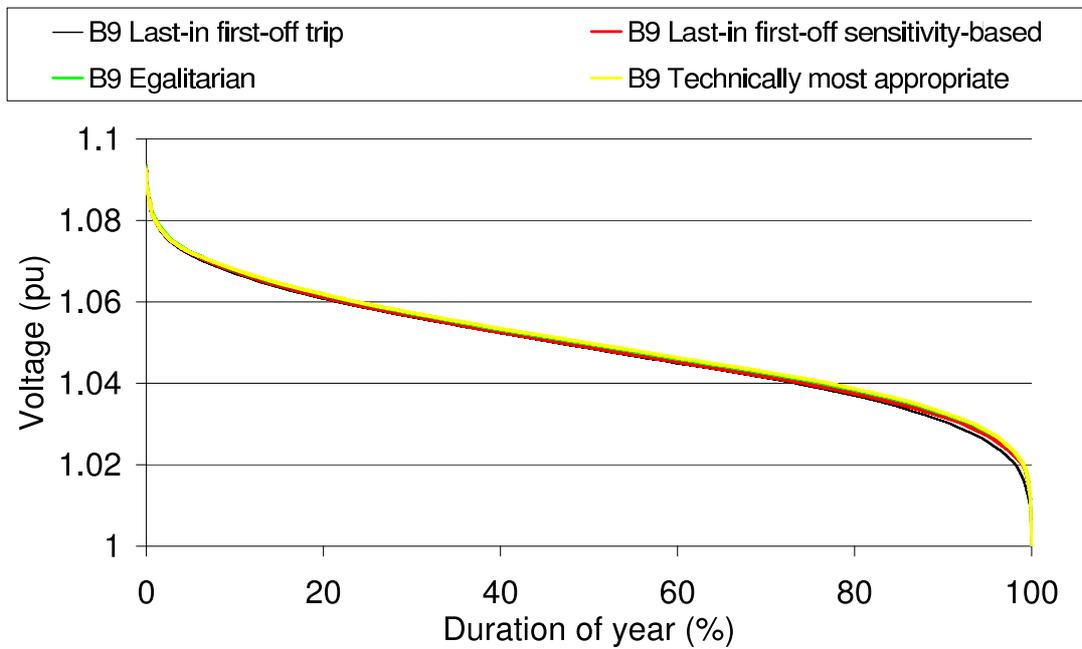
Figure 12.16: Zoomed-in representation of busbar voltage at B9 due to candidate strategy deployments with component static thermal ratings
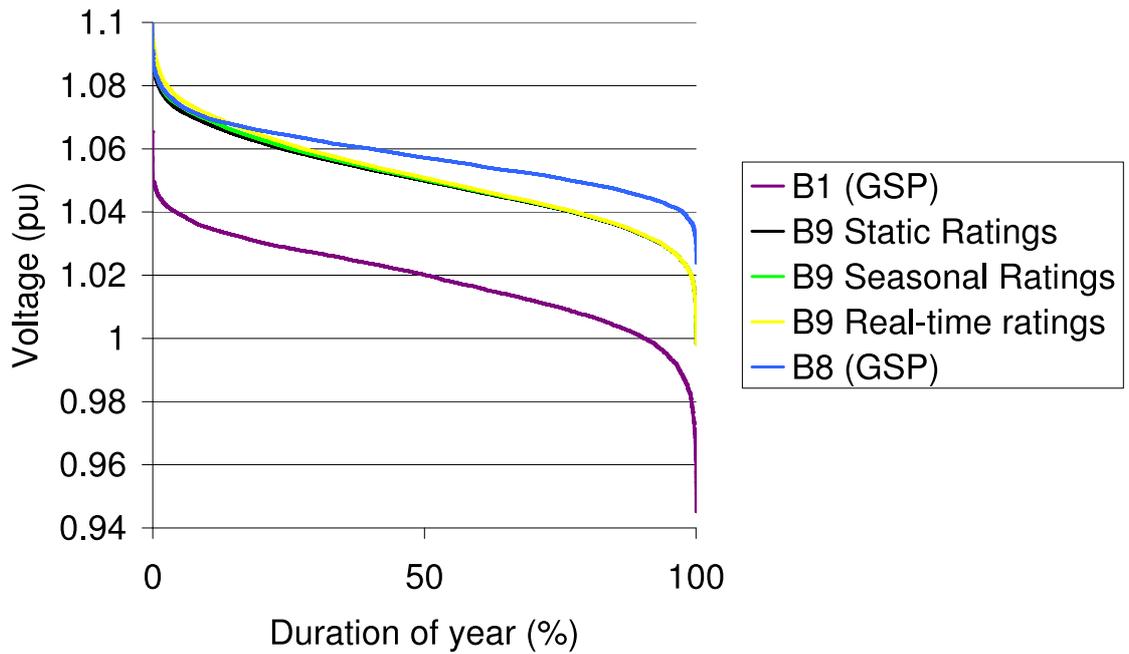
Figure 12.17: Busbar voltages due to TMA DG control with component static, seasonal and real-time thermal ratings
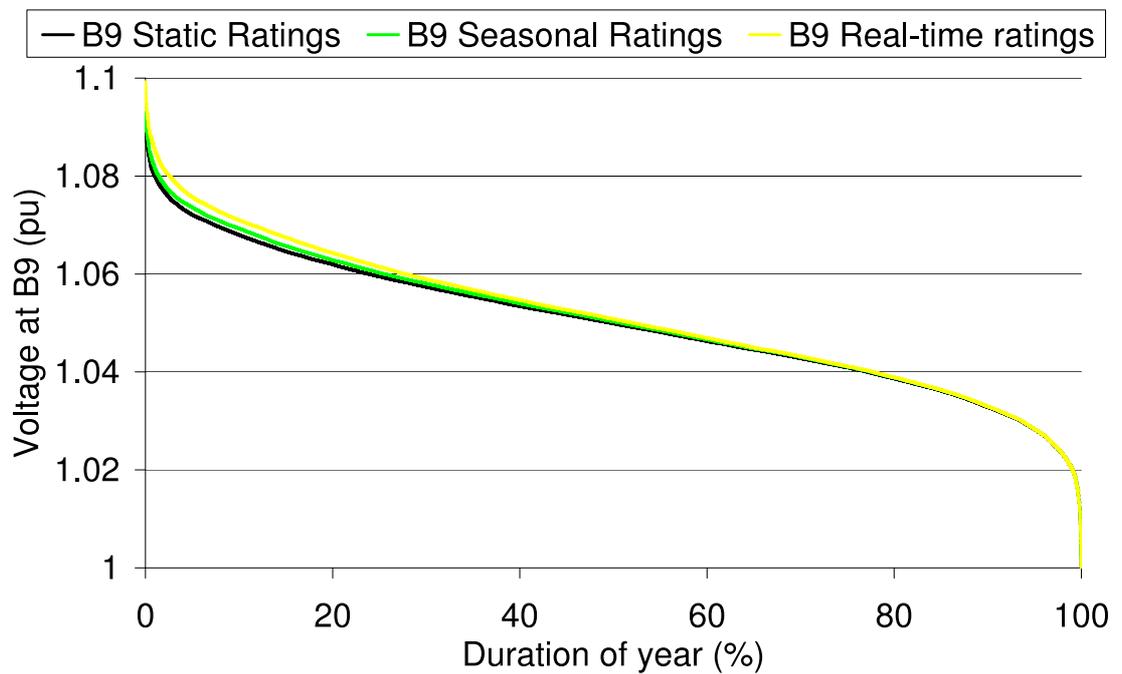
Figure 12.18: Zoomed-in representation of busbar voltages due to TMA DG control deployment with different component thermal ratings systems

12.7   Discussion

The LIFO DG output control strategy represents the present UK practice whereby 'last-in' DG schemes bear responsibility for managing network power flow issues. If network power flow management requirements become more widespread 'last-in' DG schemes may not be, technically, the most appropriate to constrain. Moreover, there is an increased complexity for DNOs in terms of dispatching constraint signals. The egalitarian broadcast strategy overcomes signal dispatching complexities. All technically relevant DG schemes bear the responsibility for managing network power flows which has the potential to facilitate aggregated annual energy gains. The TMA strategy utilises DG schemes with the best technical ability to manage network power flows. This has the potential to lead to the greatest aggregated annual energy yield gains of the proposed power flow sensitivity factor-based strategies. However, there is an associated signal dispatching complexity as DG proliferates and network power flow management requirements become more widespread.

Clearly, it can be seen from (9.4)–(9.5) that the control action, $\Delta G_{P,m}$, and ultimately the annual energy yields resulting from the control strategy implementations are a function of a number of factors: The utilisation target, U_{Tar}, the thermal limits of the power system, S_{lim}, the apparent power flowing in the thermally vulnerable components as a result of DG installed capacities, DG types and reactive power flow, and the magnitude of power flow sensitivity factors.

It is anticipated that the utilisation target, U_{Tar}, would be defined by the DG developer or DNO to represent the factor of safety, or risk, that the DNO is prepared to accommodate in terms of operating the relevant power system component. With particular reference to Figure 12.12 it follows that, as the utilisation target tends to 1, the capped power transfer limit will tend to the actual capacity limit of the component (in the particular case highlighted this would be 120 MVA). As a result, the aggregated annual energy yield of the DG schemes would be marginally increased. In order to reduce the risk of power flow excursions beyond the transfer capacity of components, and thus to ensure the safe and secure operation of the distribution network, it is expected that the candidate control strategies would be deployed with an auxiliary trip system [50]. With the functionality to incorporate the same component rating systems as the primary control system, the auxiliary system acts as a backup in the case of control system operation failure, communications failures or the failure of DG schemes to match the updated set points within the required time frame.

The adoption of sophisticated component thermal rating systems within the proposed candidate control strategies is application specific. Clearly there are advantages in deploying DG power output control systems with real-time thermal ratings for the connection of wind farms to the power system through overhead lines. This is because high power flows resulting from wind generation at high wind speeds could be accommodated since the same wind speed has a positive effect on component cooling mechanisms. As the rating tends towards its theoretical maximum value, the annual energy yield of multiple DG schemes is increased. Since the frequency of control actions reduces, the distinction between the control strategies in terms of their marginal aggregated annual energy yields diminishes.

The apparent power flow through thermally vulnerable components is a function of the installed capacity of the DG and the intermittency of the generation. As DG proliferates and the capacity of networks to accept new DG connections reduces, the energy yield (and hence economic viability of new DG connections) reduces if LIFO constraint regimes continue to be adopted. However, in situations where generation is highly intermittent, there is capacity to accept new DG connections with the adoption of alternative DG output control strategies such as egalitarian or TMA approaches. DG schemes with highly intermittent outputs, such as wind farms, would be expected to have lower energy yields than CHP plants for the same installed capacity. Therefore the un-utilised power transfer capacity of components would be significantly greater.

The magnitude of power flow sensitivity factors affects the extent to which DG schemes are constrained in order to manage network power flows. Power flow sensitivity factors are a function of the complex impedances of components within the electrical network as embodied in the Jacobian matrix. The connection of DG to electrically 'strong' distribution networks with low impedance paths lead to high power flow sensitivity factors. In 'weaker' electrical networks, such as those found in rural parts of the UK, the long electrical feeders result in high electrical impedances. As a result there are greater electrical losses and lower power flow sensitivity factors. In situations where the power flow sensitivity factors are of similar magnitude there is little merit in applying the TMA control strategy. However, the egalitarian strategy has the potential to allow increased installed capacities of intermittent DG thereby impacting on both individual and aggregated annual energy yields. The derived power flow sensitivity factors are network topology and operating condition specific and, in simulating the proposed control strategies it was assumed that the network topology was constant. It is feasible, however, to develop power flow sensitivity factor-based control strategies that make use of alternative sets of the above-mentioned predetermined

power flow sensitivity factors, based on network switch information. Alternatively, power flow sensitivity factors could be calculated in real-time, to account for operating condition changes, and used to update the values in $\boldsymbol{M}_{PFSF}$ (12.2).

12.8   Conclusions

This chapter quantified the potential benefits in adopting candidate power flow sensitivity factor-based strategies for the future coordinated output control of multiple DG schemes. The impact that the proposed strategies have on individual DG scheme revenue streams could mean that, even if the first-in DG schemes are remunerated for curtailing their power output at certain times of the year, there is an overall revenue gain for all the DG scheme developers.

Based on a datum value of 943.8 GWh/annum (corresponding to LIFO DG tripping with component static ratings), non-LIFO-based control strategies led to DG aggregated annual energy yield gains of 7.1% and 11.0%. In addition, gains of 20.5% and 21.0% resulted from non-LIFO-based control strategies deployed with power system real-time thermal ratings.

The increased transparency of distribution network usage, arising from the off-line power transfer analyses, could be used to inform shallow connection charging mechanisms if such mechanisms were to be introduced to UK power systems, at the distribution network level, in the future.

Although the case study presented is UK-based, the strategies, simulation approach and research outcomes are transferable to networks internationally. Whilst, in the UK no mechanisms exist at present to encourage and reward an increase in aggregated energy yield contributions from separately owned DG schemes, there are examples in Europe where this concept is recognized [56, 57].

In light of the results and discussions presented in this chapter, it is recommended that any DNO or DG developer looking to adopt the proposed power flow sensitivity factor-based strategies should conduct an off-line analysis to assess the value of output control of multiple DG schemes. This is because the control strategy implementations are a function of a number of site-specific control variables and therefore the economic value in each case is different.

Chapter 13

Practical implementation of the prototype DG output control system

13.1 Introduction

This chapter describes the practical implementation of the prototype DG output control system, installed within the field trial network. This represents a key deliverable and research outcome from the DIUS Project and was published by the research consortium in [110, 111]. Section 13.2 describes the hardware implementation of the prototype control system. Section 13.3 describes the installation of measurement equipment to provide the minimum signal for the prototype control system to function in open and closed loop trials. Section 13.4 describes the thermal state estimation and control algorithm integration which, together with data harvested from the field trial, can be used for control system open and closed loop performance analyses. Section 13.5 describes the validation of the on-line simulation tool with monitored data from the previous FMC-Tech installation (which over-instrumented the field trial network to provide additional validation measurements) and Section 13.6 describes the simulation of the closed-loop control algorithm and the implementation set points dispatched to the wind farm.

13.2 Hardware implementation

The degree to which a control system is decentralised across an electrical network is driven by the control function and communication constraints. Ultimately, the DG output control system could be integrated within the DNO's network management system. However, the prototype control system has been developed as a stand-alone system, being hosted on a separate platform to that of the network management system for decision support purposes.

In electrical power systems, certain functions require centralised control (for example global voltage control and the coordination of load shedding sequences or multiple generation scheme outputs). ScottishPower EnergyNetworks operate the 'Manweb' area of their distribution network from a centralised location at Prenton, Birkenhead. This gives global visibility of the network and allows the coordinated control of the system to take place at times of network faults which have the potential to have widespread electrical effects. Centralised systems not only provide global control functions but also allow the maintenance and configuration of hardware, software and database facilities to take place in one location. However, a reliable communications infrastructure needs to exist between the central SCADA host and substations where elements of network control take place. Testing of the centralised control system may prove difficult due to physical distances involved and there is the risk of a single point of failure affecting the entire control system [51].

Protection and monitoring systems are decentralised across the network since these functions are related to local component states. Protection relays and inter-tripping equipment monitor local component states and are designed to isolate faults with the minimum amount of disruption to other components in the system. A hierarchical architecture is needed to coordinate this distributed system otherwise a cascading failure may result. The advantages of adopting a decentralised control approach are documented as reducing operational complexity, increasing flexibility in terms of allowing for network changes and increasing the reliability and integrity of the control (or protection) system [112]. However, the drawbacks could be that the decentralised system requires additional software maintenance skills to those needed for a centralised system as well as field visits for decentralised software maintenance and additional staff to facilitate these visits. In both centralised and decentralised systems the response time, in terms of controlling the network, is limited by the speed of the communications infrastructure. The communications infrastructure between substations and SCADA host network management systems are low bandwidth (based on historical development of the network).

The adoption of a service oriented architecture with the associated platform independence benefits, as described in Chapter 4, allows the DG output control system services to be located on one hardware platform or distributed across a number of hardware platforms. Therefore it was decided that control functions relating to individual components of the network would be decentralised and located on AREVA's MiCOM relay platforms. This included individual component thermal modelling, component monitoring and component protection functions. However, it was perceived that a fully decentralised architecture

in this project would not facilitate the global coordination of multiple DG schemes since distributed controllers would only be able to control local DG outputs based on local conditions. As a consequence the controller would not be able to monitor the effect of power set point dispatches on the wider network which is of critical importance in meshed topologies, such as ScottishPower EnergyNetworks' distribution network, when power flows cannot be intuitively predicted. Furthermore, it was anticipated that the topology of the 132kV and 33kV infrastructure was not likely to undergo vast rapid change in the lifetime of this research project. Therefore the decision was taken to locate the thermal state estimation and control algorithms on a more centralised hardware platform for coordinated DG output control.

The DG output control system will produce a small number of recommended actions which will be communicated back to the network management system. The prototype control system layout is shown in Figure 13.1. The relays will convert the readings to digital format and communicate with the DG output control system host using the IEC 61850 protocol [113]. Under normal operation, the DG output control system and the relay will run the same algorithm predicting the thermal limits of the component. If, for some reason, the network management system and DG output control system fail to stop power flows violating power system thermal limits, the relay will trip circuit breakers, thus protecting power system components. It will be possible for the network management system to inhibit this function of the relay in circumstances where it is not required.

13.3   Network instrumentation for prototype control system

This section explains the minimum set of measurements, required as inputs to the prototype DG output control system installed within the field trial network. The instrumentation for the prototype control system was categorised into 'electrical', 'environmental condition' and 'weather station' requirements.

Electrical requirements:

(i) Real and reactive power (directional) at Transformer T1 at Rhyl substation; (ii) real and reactive power (directional) at Transformer T2 at Rhyl substation; and (iii) voltage magnitude at St Asaph substation (132kV side).
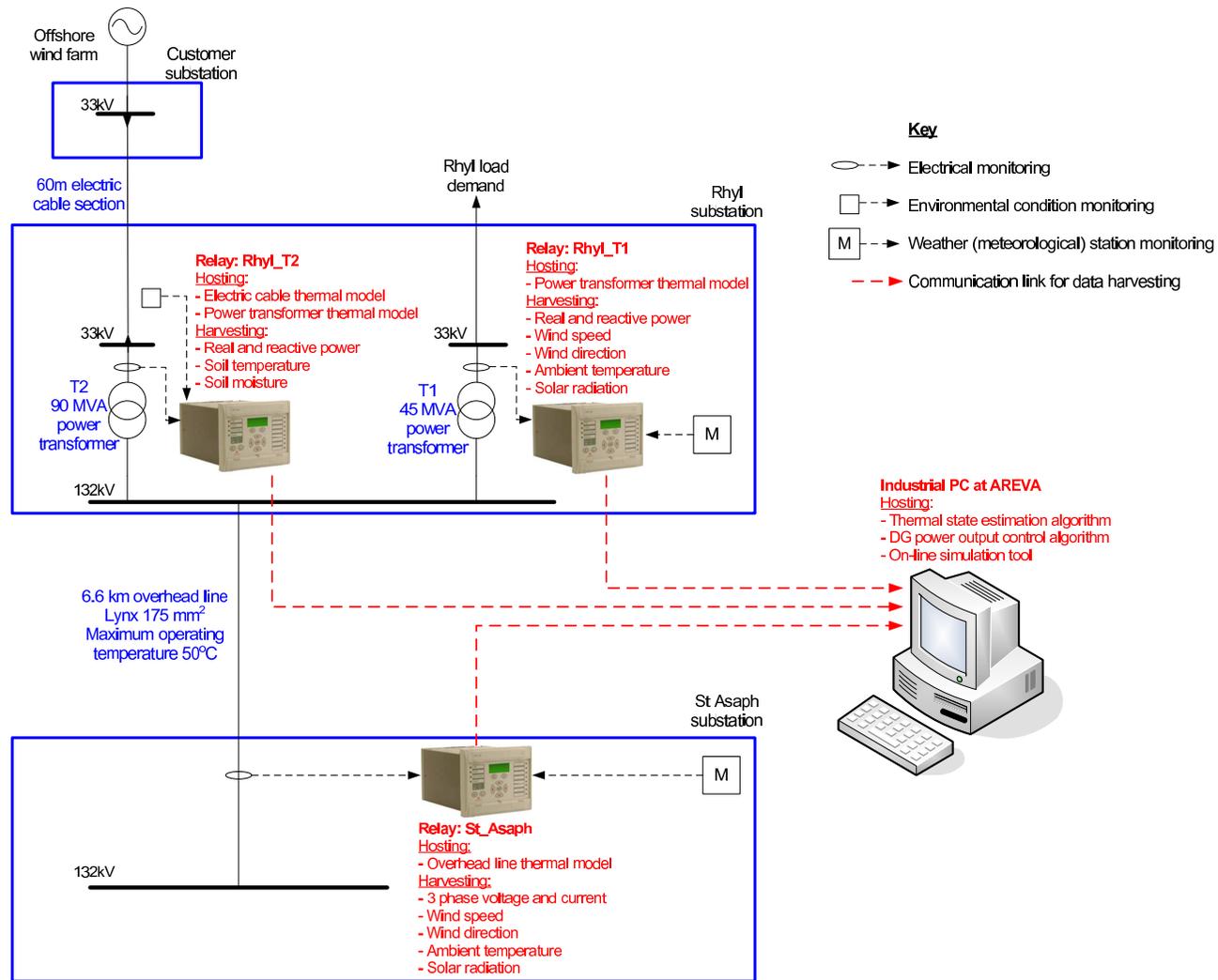
Figure 13.1: Hardware representation of DG output control system

Environmental condition requirements:

(i) Soil thermal resistivity surrounding cable from North Hoyle customer (wind farm) substation to ScottishPower EnergyNetworks' substation at Rhyl; and (ii) soil temperature surrounding cable from North Hoyle customer (wind farm) substation to ScottishPower EnergyNetworks' substation at Rhyl.

Weather station requirements:

(i) At St Asaph substation; and (ii) at Rhyl substation. Each weather station measures the following parameters: (i) Wind speed; (ii) wind direction; (iii) ambient temperature; and (iv) solar radiation.

Based on the network instrumentation requirements specified by Durham University, ScottishPower EnergyNetworks commissioned AREVA T&D to install the necessary monitoring equipment. Figure 13.2 displays the meteorological condition monitoring equipment installed on the side of a building in the Rhyl substation compound. Figure 13.3 displays the MiCOM relay cubicle in the substation panel at St Asaph. Figure 13.4 shows the communication links from the monitoring equipment into the back of the MiCOM relay cubicle.

Figure 13.2: Meteorological sensors installed in the Rhyl substation compound
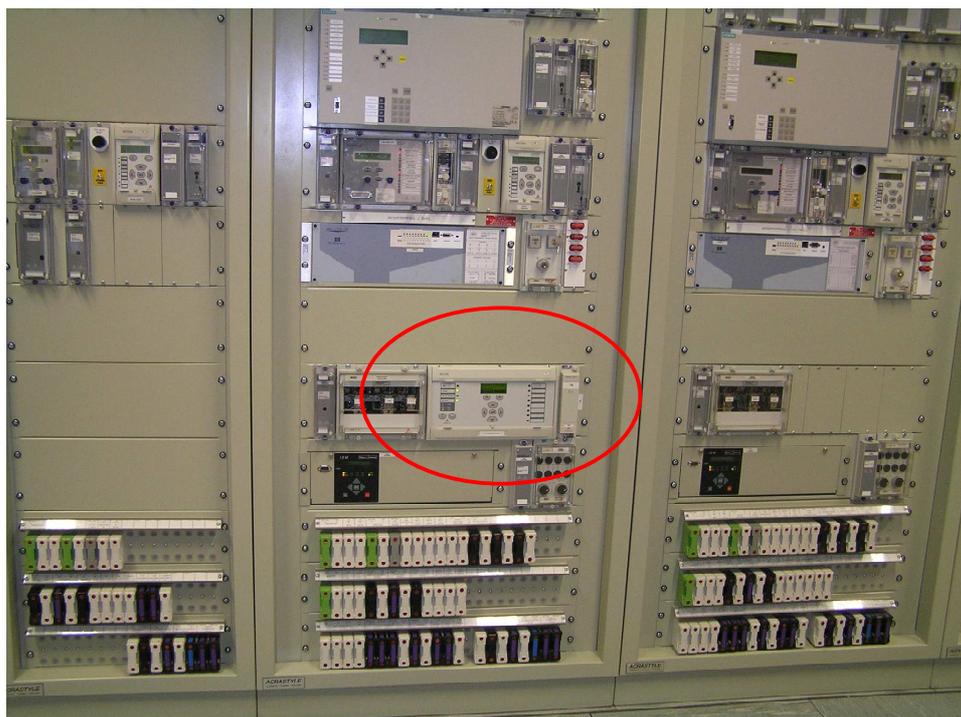
Figure 13.3: MiCOM relay installed in the panel of St Asaph substation
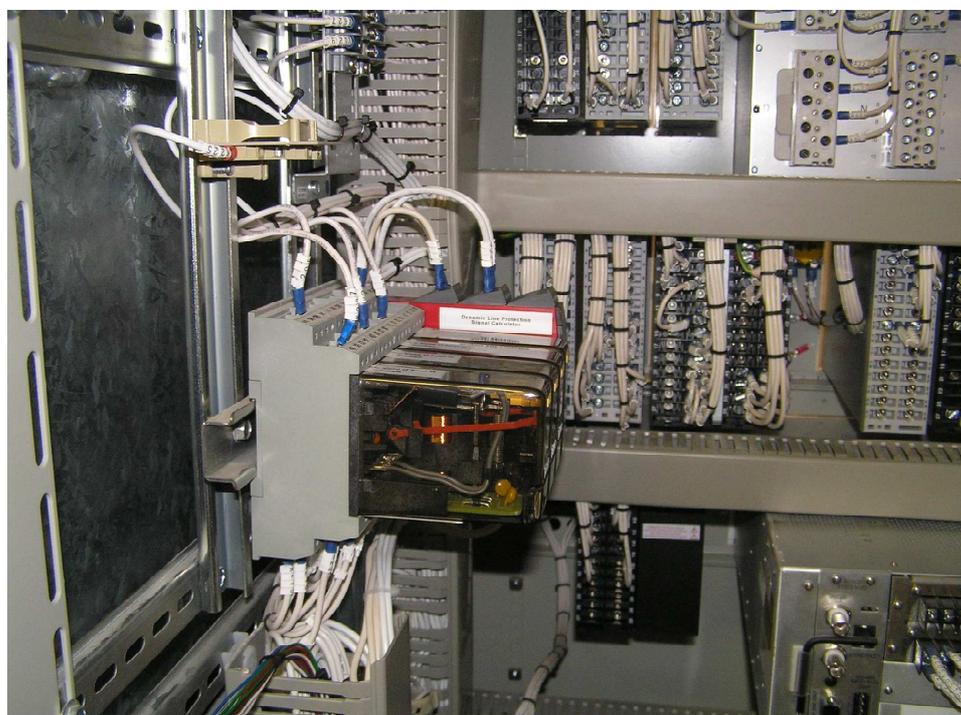
Figure 13.4: Communication links into the back of the MiCOM relay cubicle

13.4 Algorithm integration within the DG output control system

This section describes the software integration of the algorithms. This occurred in two stages. Firstly, the thermal state estimation and control algorithm services were integrated together. Secondly, the thermal state estimation and control algorithms were integrated with a MySQL database (used to store the monitored data, harvested from the field trial network). For developmental and testing purposes the ETR 124-based load demand-following control algorithm, as described in Chapters 8–10, was adopted for implementation within the prototype control system. Practical aspects of the control algorithm were refined as the end-to-end commissioning of the DG output control system took place, such as methods to deal with input measurement uncertainties. The source code and software support documentation for the control algorithm was delivered to the DIUS Project consortium for the prototype DG output control system installation.

Since the thermal state estimation algorithm was written in the Visual Basic programming language and the control algorithm was written in Java, it was necessary to make the thermal state estimation algorithm available as a service to the control algorithm. Using web-based protocols the control algorithm could then pass a time-stamp and component name to the thermal state estimation algorithm and the real-time thermal rating corresponding to that particular time-stamp was then returned.

Harvested electrical and thermal data from the monitoring equipment, installed for the prototype control system, was written into a MySQL database. Rather than developing two separate interfaces for the thermal state estimation algorithm and control algorithm to query the database, one interface was written between Visual Basic and MySQL, and a second web service was created in Visual Basic to allow the control algorithm to access the necessary electrical data. It was then necessary to map the MySQL fields to the corresponding variables within the thermal state estimation and control algorithms.

13.5 Validation of on-line simulation tool and dealing with monitored data errors

Throughout the off-line open-loop simulations of the DG output control system (as presented in Chapters 10–12, a simulation tool has been employed to validate the control actions and ensure the safe and secure operation of the distribution network. This section

investigates the validity of the simulation tool against monitored data, by comparing modelled and monitored electrical currents. In order to conduct the investigation a time period was selected $(1/6/09 - 8/6/09)$ when both SCADA datasets and FMC-Tech monitoring datasets were available for direct comparison. The monitored datasets from SCADA were used together with IPSA to simulate power flows in the overhead line that is the component of most interest to the research consortium in the prototype DG output control system installation. This allowed the electrical current in the overhead line to be modelled and compared with monitored data from the FMC-Tech installation for network characterisation. The modelled and monitored currents are plotted in Figure 13.5.

Considering Figure 13.5, the possible sources of error between the modelled and monitored currents were identified as:

- The time-stamping difference between the data monitored by SCADA and the data monitored by the FMC-Tech equipment;

- the accuracy of the SCADA monitoring equipment;

- the accuracy of the FMC-Tech monitoring equipment; and

- assumptions made by the IPSA package in solving the load flow algorithm.

These sources of error were investigated further in an attempt to quantify the errors and understand the extent to which the simulation tool is a valid representation of power system.

Errors related to time-stamps could result from (i) the propagation delay between the signal being monitored and time taken for the signal to be logged in the relevant database; (ii) a mismatch of timestamps resulting from Greenwich Mean Time and British Summer Time zone assumptions; and (iii) whether the signal recorded by SCADA represents an instantaneous sampling of power flows or power flows averaged over the previous 30 minutes of power system operation. Based on these potential sources of error, and by inspection of Figure 13.5, the apparent 1-hour misalignment of the data (resulting from time zone timestamps) was corrected and the updated data plots are given in Figure 13.6. This produced an average error between the modelled and monitored currents of 6 A, with the model generally under-predicting the current with respect to the monitored data.
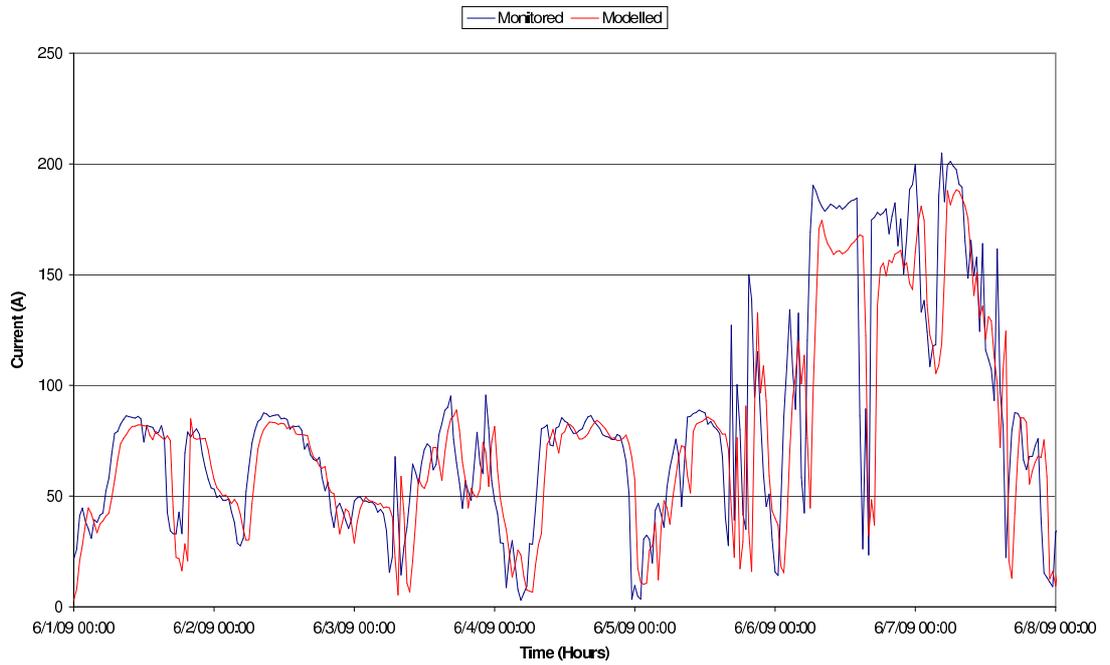
Figure 13.5: Validation of simulation tool model
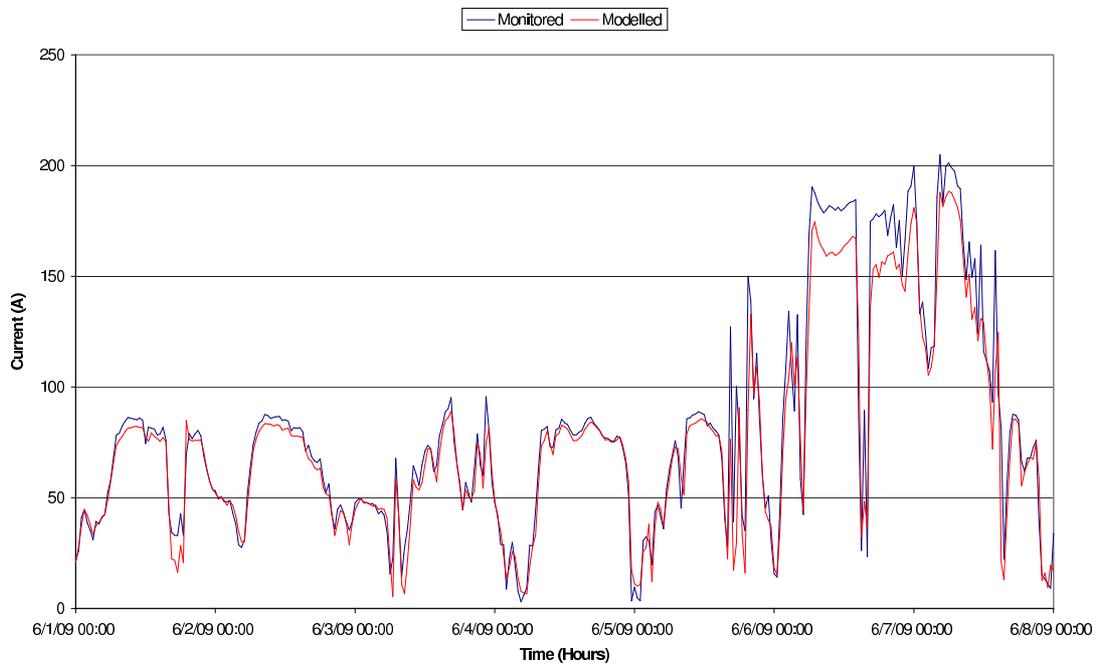
Figure 13.6: Validation of simulation tool model, accounting for monitored data timestamps

Regarding errors associated with SCADA measurements, a typical $\pm 5\%$ deviation in monitored values is quoted in [9]. On this basis the inputs to the simulation tool were corrected in the following manner, and used to re-simulated the electrical current flow: If the monitored output of the DG scheme is overestimated by 5% and the monitored load demands are underestimated by 5%, overall this would lead to the greatest overestimation of power flows in the line, relative to the actual flow. If the monitored output of the DG scheme is underestimated by 5% and the monitored load demands are overestimated by 5%, overall this would lead to the greatest underestimation of power flows in the line, relative to the actual flow. These error bands were plotted together with the monitored current as in Figure 13.7.

Considering Figure 13.7 it can be seen that the monitored current generally lies within the bands of the potential monitoing errors of SCADA, introduced into the IPSA model. Exceptions to this occur, for example, during 08:30-11:30 on 6/6/09 and 16:30–19:30 on 6/6/09. In the former of the mentioned time periods the greatest difference between measured and monitored currents is $5\,\text{A}$. In the latter of the mentioned time periods the greatest deviation in current is $10\,\text{A}$. Since the accuracy of the monitored current was quoted by FMC-Tech as being $\pm 1\%$ of the readings, this error band was plotted together with the modelled error band as in Figure 13.8.

Considering Figure 13.8, and neglecting short-term current spikes, the monitored current tolerances lie within the modelled tolerances for significant periods of the simulated week. There is a cumulative 10 hour period during the entire week of simulation when the monitored current lies outside the tolerance bands of the modelled current. This means that for 94.1% of the simulated time period the modelled and monitored currents are in agreement, when possible measurement errors are taken into account. This suggests that the IPSA model provides an acceptable basis for power flow validation and that the majority of errors between monitored and modelled currents could be attributed to the errors in monitoring equipment rather than the model itself. Clearly errors are also likely to exist between the monitored and modelled currents based on assumptions that are embedded within IPSA, such as a balanced three-phase power system for load flow solutions. It is likely that these errors are minimal relative to the errors introduced by the monitoring equipment but could account for the cumulative 10-hour period of errors.
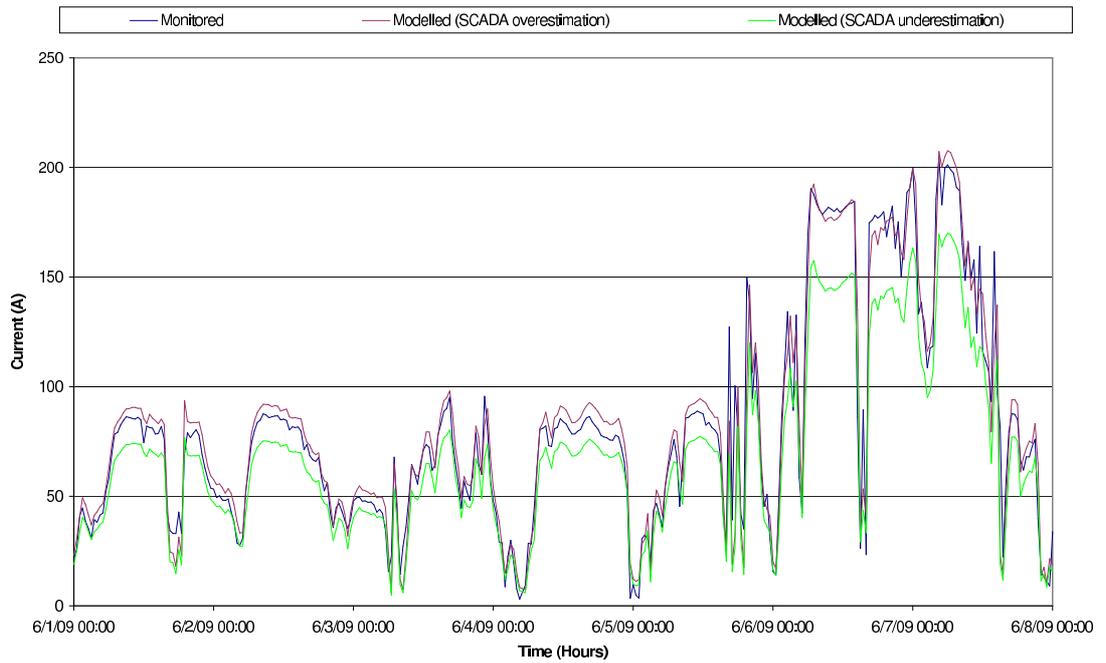
Figure 13.7: Validation of simulation tool model, accounting for monitored data errors from SCADA
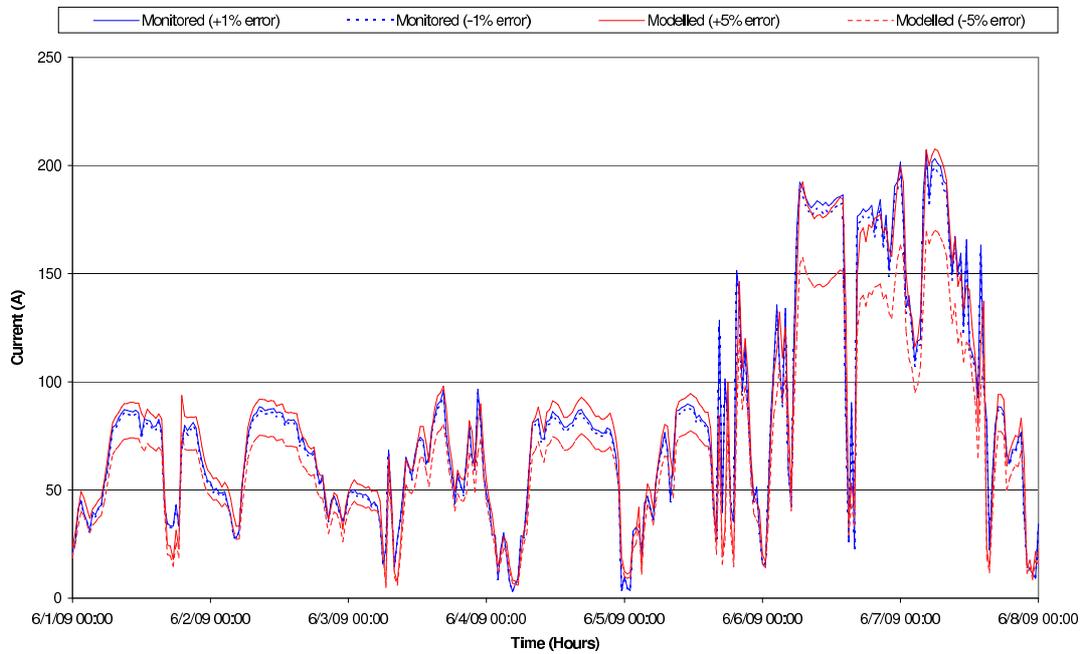
Figure 13.8: Validation of simulation tool model, accounting for monitored data errors from SCADA and FMC-Tech

In practice it is better for the model to over-predict currents relative to monitored operational currents as this would lead to a more conservative operation of the DG output control system, in terms of dispatching set points to the DG scheme(s), than if the model under-predicts the currents. Correction factors for the errors in monitored data could be taken into account at the 'front end' of the control algorithm by introducing error margins into the monitored SCADA data to ensure that the worst case (i.e. highest) distribution network power flow scenarios are reflected.

13.6 Closed loop control and DG set point implementation

This section discusses the off-line time-series closed loop simulation of the control algorithm with historical data and the potential methods of implementing the DG set points, identified by the control algorithm to be dispatch to the DG scheme(s).

13.6.1 Closed loop control

Figure 13.9 represents the unconstrained output of a DG scheme, with a non-firm connection and installed capacity of 120 MW. The output of the DG scheme has been simulated in the field trial network with static thermal ratings for an illustrative 24-hour period. With no power output control there are two extended periods (from time step 6 to time step 10 and from time step 18 to time step 25) when the line utilisation exceeds the upper utilisation limit. Closed-loop demand-following DG output control was simulated, as given in Figure 13.10, with an upper utilisation limit of 1, a target utilisation of 0.9 and a lower utilisation limit of 0.7. (This relates to the inference engine described in Figure 8.3, Chapter 8.) When the line utilisation exceeds the upper utilisation limit, the DG output is constrained (by adjusting the peak capacity output of the DG scheme) in order to reduce the line utilisation and bring power flows back within limits. This action occurs at time steps 5, 17 and 41. Reflecting the closed-loop control of the DG scheme, the DG peak capacity remains at a reduced level (since the line utilisation lies between the upper and lower utilisation bounds) until the power output of the DG scheme reduces (or the load demand at the DG connection bus increases) and, as a result, the line utilisation drops below the lower utilisation target. At this point the constraint on the DG scheme is relaxed to allow a potential 90% capacity utilisation of the overhead line. The introduction of real-time thermal ratings would result in utilisation bounds that also vary in real-time, rather than remaining static according to a component static thermal rating.
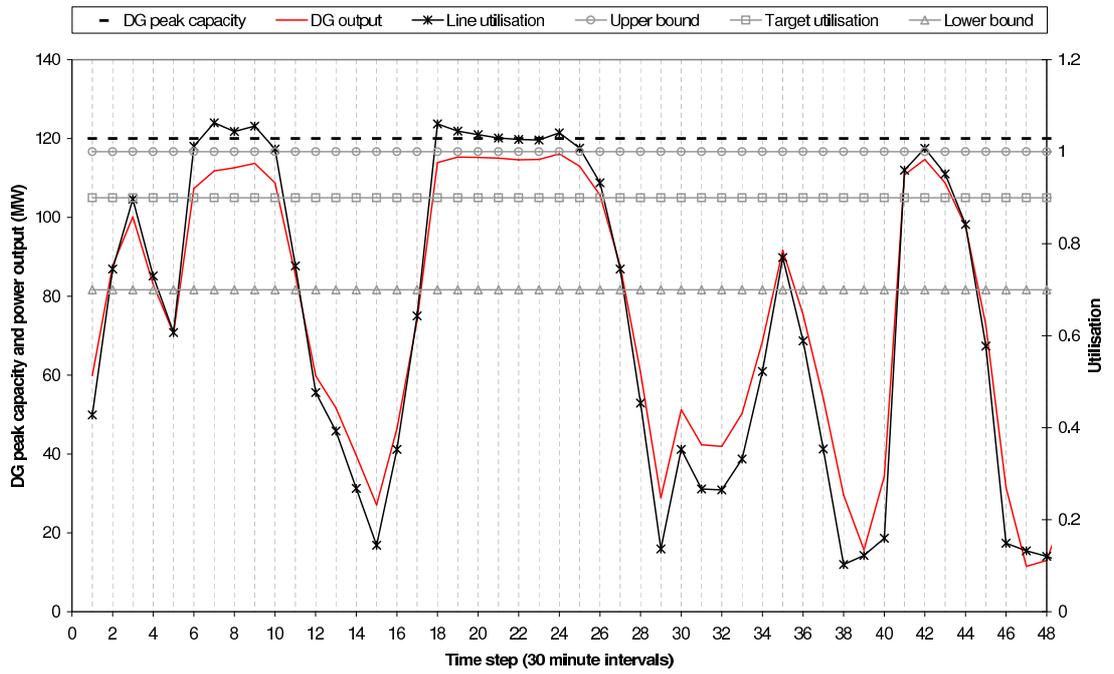
Figure 13.9: Unconstrained DG output violating utilisation limits
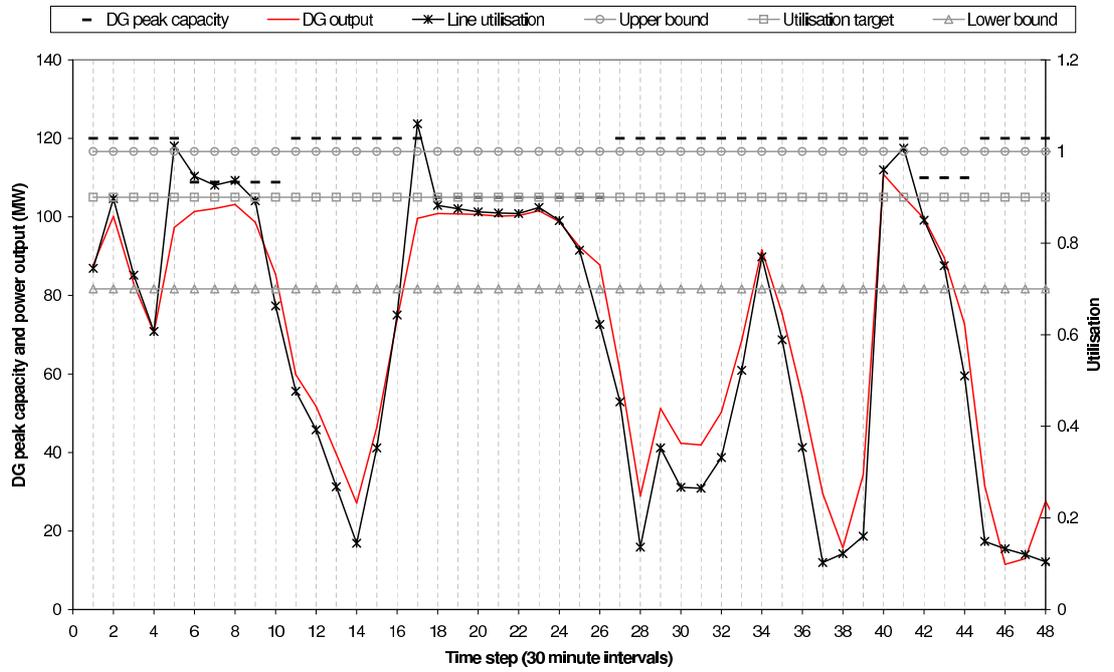
Figure 13.10: Off-line closed loop DG output control

13.6.2   Set point implementation

The Wind Energy Handbook [100] provides detailed descriptions of the methods that may be used in order to regulate the power output of wind-based DG to achieve dispatched set points. Active pitch control systems adjust (or feather) the wind turbine blades in order to capture a desired amount of energy from the wind. Power limitation above rated wind speeds is achieved by rotating each turbine blade about its axis and hence reducing the angle of attack of the wind. Pitch systems are designed to act rapidly (e.g. changes of $5\,°/s$) such that the power output is limited as a result of sudden gusts of wind. A variety of pitch actuation systems exists and can be broadly categorised in those where each blade has its own actuator and those where a single actuator pitches all three blades. Software-based closed loop control systems allow the DG power output to be regulated in order to achieve a desired operational performance.

13.7   Conclusion

This chapter described the practical implementation of the prototype DG output control system for field trials within the DIUS Project. The control algorithm used in the prototype control system was discussed along with the network instrumentation phases. A description of the integration of the control system services within the host platform and data harvesting from the field trial network was given and the results of open and closed loop system testing were presented which led to the validation of the on-line simulation tool within DG output control system. The adoption of a service-oriented architecture with web-service interfaces and the associated platform independence benefits allow the DG output control system services to be located on one hardware platform or distributed across a number of hardware platforms. Therefore it was decided that control system functions relating to individual components of the network would be decentralised and located on AREVA's MiCOM relay platforms. However, it was perceived that a fully decentralised architecture in this project would not facilitate the global coordination of multiple DG schemes since distributed controllers would only be able to control local DG outputs based on local conditions. Therefore the thermal state estimation and control algorithms were located on a more centralised 'host' hardware platform.

During December 2009 the thermal state estimation and control algorithms were installed on an industrial PC at AREVA T&D in preparation for DG output control in open and closed loops, with the data harvested from field trial network.

Chapter 14

Research evaluation

14.1 DG output control system evaluation against user and functional requirements

This section evaluates the DG output control system against the user and functional requirements which were identified in Chapter 1 as being specific to the research presented in this thesis. Where the control system functionality fulfils a number of user and functional requirements, these requirements have been combined together.

- *Increase the thermal exploitation of the power system through the intelligent management of constrained DG connections in non-contingent [electrical] situations without violating voltage requirements and equipment thermal ratings:* As proposed in Chapters 8 and 9, the thermal exploitation of the power system was increased through the implementation of a demand-following output control technique for a single DG scheme based on Engineering Technical Recommendation (ETR) 124 and the development of candidate strategies for the coordinated output control of multiple DG schemes based on power flow sensitivity factors. The control system was designed to utilise an on-line simulation tool to validate the integrity of control actions (in not violating voltage requirements and equipment thermal ratings) before dispatch to the DG scheme(s).

- *Provide decision support for the DNO control room engineers in determining real power set points for single and multiple DG schemes connected to the network under control:* As above, the control algorithms within the DG output control system were developed to recommend real power set points for dispatch to the DG schemes (as proposed in Chapters 8 and 9).

- *Provide a method for selection of measured thermal quantities and locations:* A DG output control system development methodology was proposed in Chapter 4, the first stage of which is the identification of thermally vulnerable component locations within distribution networks (as outlined in Chapter 5). Once the thermally vulnerable component locations have been identified, the thermal quantities relevant to the particular component type and required for measurement may be assessed, as detailed in Chapter 7.

- *Be cost effective with respect to network reinforcement and present constrained connection techniques:* A framework for the quantification of DG development net present values and profitability indices was proposed in Chapter 9. Through time-series electro-thermal simulations (detailed in Chapters 10 and 12) the DG output control system was found to be cost effective with respect to network reinforcement and present constrained connection techniques for the case study networks considered.

- *Obtain electrical measurements through the integration of the control system with power system components and SCADA, minimising interruptions to supply:* The control algorithms presented in this thesis were developed to make use of existing electrical signals from SCADA and thus limit the number of additional electrical measurements required. This served to facilitate the integration of the DG output control system with power system components by limiting the required circuit outages in order to install additional monitoring equipment.

- *Utilise transparent decision making processes to facilitate performance evaluation:* The control algorithms developed for use within the DG output control system utilised transparent rule-based decision-making techniques coupled with recognised DG output control techniques emerging from the literature review in Chapter 2.

- *Be self-diagnostic and tolerant of communication faults, degrading in a graceful manner:* Rather than tripping-off the DG scheme(s) if communications failures occur, the 'front-end' of the control algorithm within the DG output control system is configured with default values to allow continued operation, and graceful degradation, in the event of communication signal losses. If a partial dataset is input to the control system, the control algorithm makes a diagnosis and uses default parameters to allow continued operation. This was demonstrated in Chapter 10.

- *Ensure safe power system operation:* In order to ensure the safe and secure operation of the power system, the DG output system is designed with an auxiliary trip system, which calculates the same ratings as the DG output control system, to act as a backup in the case of control system operation failure. This was discussed in Chapters 10 and 13.

- *Utilise power system static, seasonal or real-time thermal ratings:* The control techniques that are described in Chapters 8 and 9 have been developed to utilise component thermal properties in making control decisions. Those thermal properties could be based on fixed meteorological assumptions or could be supplied by more sophisticated real-time thermal rating systems where they are available. Therefore the control techniques within the DG output control system may be deployed, equally applicably, with power system static, seasonal or real-time thermal ratings.

- *Utilise load flow routines based on electrical network models and a power systems equipment database:* As demonstrated in Chapter 8, the DG output control system makes use of the IPSA load flow package for three specific purposes: (i) For 'front end' parameter estimation whereby limited real and reactive power flow measurements from SCADA can be used to establish a complete set of network power flows; (ii) for the off-line calculation of power flow sensitivity factors; and (iii) as an off-line and on-line simulation tool to validate control actions of the DG output control system. The IPSA network model contains the power systems equipment database.

- *Utilise an appropriate software architecture, allowing for modularity, flexibility, maintainability and openness:* The overall DG output control system, as detailed in Chapter 4, was designed with a service oriented architecture and implemented using web service protocols. This provided modularity and flexibility in terms of DG output control system components, as well as hardware platform independence. The languages selected for control algorithm development (Java and Python) are both open source, platform independent, mature and well-documented programming languages. By developing the control algorithm with modular components, this facilitated the maintainability of the software code.

14.2   Evaluation of research against original objectives

The original research objectives, as given in Chapter 1 were:

1. The proposal of a methodology for the development of DG output control systems;

2. The development of techniques for the on-line output control of single and multiple DG schemes, based on power system static, seasonal and real-time thermal ratings;

3. The validation of the techniques and assessment of gains through simulation; and

4. The development of control algorithms for use in field trials of a prototype DG output control system.

The research which aimed to fulfil each of the research objectives is outlined below:

1. *The proposal of a methodology for the development of DG output control systems:*

   A methodology was proposed in Chapter 4 for the development of DG output control systems, the off-line aspects of which may be used for the planning of distribution networks and on-line aspects of which may be used for the operation of DG based on component thermal properties.

   It is anticipated that distribution networks will see a proliferation of DG in coming years. In some cases, this will result in network power flow management requirements with thermally vulnerable components restricting the connection capacity and annual energy yield of DG. Therefore a system that can be developed for the management of power flows within distribution networks, through the power output control of DG schemes, could be of great benefit. The development stages of such a system were illustrated using UKGDSs and applied to a field trial network in the UK. These included: (i) the identification of thermally vulnerable components through an assessment of thermal vulnerability factors that relate power flow sensitivity factors to component thermal limits; (ii) the strategic investment in thermal monitoring equipment and the targeted development of component thermal models for the thermal characterisation of the distribution network (informed by the assessment in the previous stage); (iii) the development of a real-time thermal rating system that would allow component steady-state thermal models to be populated with real-time data from thermal monitoring equipment installed in the previous phase; and (iv) the use of real-time thermal ratings together with DG output control techniques (such as the

power flow sensitivity factors assessed in the first stage of the methodology) for the on-line management of network power flows.

The first stage of the methodology was validated through simulation of the field trial network and resulted in the strategic investment of thermal monitoring equipment for the thermal characterisation of that section of the UK power system. The power flow sensitivity factors have the potential to be embedded within an on-line control system with a view to managing the power output of multiple DG schemes, based on the real-time knowledge of the thermal and electrical status of the distribution network.

As discussed in Chapter 8, the proposed methodology provides a framework for accommodating network topology changes (such as network reconfiguration, network extensions and new DG connections) in the development of DG output control systems. In the case of network extensions and new DG connections, it is anticipated that these changes to the distribution network topology will be planned by the DNO many months in advance which would allow time for the DG output control system to be adapted.

Whilst power flow sensitivity factors may be used to fulfil stages (i) and (iv) of the proposed methodology, clearly the methodology could be implemented with totally different techniques. If different techniques are used to implement the stages in the methodology to those proposed in this thesis, this would demonstrate the potential flexibility (and hence value) of the methodology in providing a framework for the development of DG output control systems.

2. *The development of techniques for the on-line output control of single and multiple DG schemes, based on power system static, seasonal and real-time thermal ratings:*

Techniques for the on-line operational control of single and multiple DG schemes were proposed in Chapters 8 and 9 as a means of managing distribution network power flows. This required the development of control algorithms which have the capability of utilising real-time information about the thermal status of the network and, in reaching a control decision, guarantee that the secure operation of the distribution network is maintained. Techniques based on concepts given in ETR 124 were developed for the control of single DG schemes. Strategies based on power flow sensitivity factors were proposed for the coordinated output control of multiple DG schemes informed by power system static, seasonal or real-time thermal ratings.

The candidate multiple DG scheme control strategies were developed to manage power flows in single and multiple components of the power system. This is of relevance in situations where individual DG schemes may cause power flow congestion in individual components but of particular relevance where the aggregation of power flows from multiple DG schemes may cause more widespread power flow management issues. Therefore, with the expected proliferation of DG the resulting power flows are likely to affect many components and it is important to take a holistic view of power flow congestion within the power system. Last-in first-off (LIFO) control strategies for multiple DG schemes were developed to reflect the present regulatory framework of the UK. Two additional strategies were developed for the coordinated output control of multiple DG schemes: (i) an egalitarian strategy where a single broadcast signal is dispatched to all the relevant DG scheme operators to adjust the outputs of the DG schemes as an equal percentage proportion of the present power output; and (ii) a technically most appropriate strategy whereby the DG scheme with the best technical ability to manage power flows is selected to be constrained first. In such circumstances the coordinated output control of DG schemes could enhance the revenue streams of last-in' DG schemes to an extent that the investment in the installation is economically viable. Moreover, cross-payments could be set-up between DG schemes to ensure that those DG schemes that constrain their power output to manage network power flows, facilitating an aggregated annual energy yield gain, are remunerated.

The rapid processing time, reduced memory requirements and robustness associated with embedding predetermined power flow sensitivity factors in a DG power output control system make it attractive for substation installations and on-line decision-making applications for DNOs. This is strengthened further by the ability of the DG power output control system to readily integrate component real-time thermal ratings in the management of network power flows. The control system described in this thesis has been developed with algorithms that may give a sub-optimal solution in the real-time decision-making environment but are robust to errors in data input. For this particular industrial application these features are preferable to an optimal solution which may not be reached within the required time-frame and may, on occasion, not converge to a solution.

3. *The validation of the techniques and assessment of gains through simulation:*

In Chapter 9, a number of techniques were proposed to evaluate the control algorithms and quantify the benefits of DG output control system development. The proposed evaluation parameters and techniques for assessment included: (i) numerical integration to calculate annual energy yields and annual energy losses; (ii) a loss apportioning technique to attribute energy losses to particular DG schemes; (iii) the financial quantification of DG development net present values and profitability indices; and (iv) the summarising of component power transfers and busbar voltages through duration curves.

Through time-series electro-thermal simulations, the evaluation parameters were quantified for the single DG scheme and multiple DG control algorithms deployed with power system static, seasonal and real-time thermal ratings. The validity of the control algorithms was assessed through the off-line analysis of evaluation parameters, as quantified through the electro-thermal simulations. The electro-thermal simulation tools were developed to return exception reports to capture any thermal limit and voltage violations after the simulated implementation of the candidate control strategies. The simulations were described in Chapters 10, 11 and 12.

Considering single DG scheme output control, the technical considerations and economics of a number of solutions that would allow a greater installed capacity of DG to be connected to, and managed within, the distribution network were presented and compared. The simulation of alternative solutions, reflecting current practices, included (i) the disconnection of the DG scheme; and (ii) the reinforcement of the network to relieve power flow congestion. These solutions were compared to the DG output control system deployed with component static, seasonal and real-time thermal ratings. Disconnecting the DG scheme at times of thermal overloads was shown to impact, significantly, on the annual energy yield and hence revenue stream of the DG developer. The reinforcement option had the potential to allow the DG scheme to operate without constraints through a 'fit and forget' DG connection policy. However, the energy yield from the DG output control system deployed with component real-time thermal ratings was found to be only slightly lower than the network reinforcement option, for the case study network considered. The DG output control system option is likely to have significantly lower capital cost than the network reinforcement option and avoids other drawbacks such as lengthy planning delays and

environmental objections.

The benefits in adopting the candidate power flow sensitivity factor-based strategies for the future coordinated output control of multiple distributed generators were quantified. It was shown that, in certain circumstances, there are significant benefits to individual DG schemes in terms of energy yields and hence revenue streams by moving away from 'last-in first-off' control strategies. As a result the aggregated annual energy yield of separately owned DG schemes is considerably improved. The impact that coordinated power output control approaches have on individual DG scheme revenue streams could mean that, even if the 'first-in' DG schemes are remunerated for curtailing their power output at certain times of the year, there is an overall revenue gain for all the DG schemes. In addition, the increased transparency of distribution network usage, arising from the off-line power transfer analyses, could be used to inform shallow connection charging mechanisms if such mechanisms were to be introduced to UK power systems, at the distribution network level, in the future.

4. *The practical implementation of a prototype DG output control system:*

In Chapter 13 the practical implementation of a prototype DG output control system within a section of the UK power system was described. The control algorithm described in Chapters 8 and 9, and simulated, evaluated and validated in Chapter 10 was delivered to the research consortium of the DIUS Project. Practical aspects of the algorithm, such as methods to deal with communications failures and data measurement errors were discussed, as well as the validation of the on-line simulation tool with monitored data. The algorithms display graceful degradation in terms of dealing with communications failures whereby the behaviour of the control system becomes increasingly conservative as an increasing number of signal failures occur. The control algorithm delivered to the research consortium was integrated with a real-time thermal rating system for the open and closed loop control of a DG scheme.

14.3   Generality of the research

Considering the spectrum of electrical voltage levels, this research is generally applicable to transmission and sub-transmission systems where electrical monitoring equipment has matured, is widely installed across the power system and is in operation for network management systems. In addition, the power flow sensitivity factors of generators are likely to exhibit a greater variation (as a result of a meshed power system topology or high impedance

radial lines, as found in rural parts of the UK) and the network topology is not frequently evolving.

At lower voltage levels, for example 11kV and below, the frequency of the distribution network topology evolution has the potential to impact on the continued operation of the DG output control system particularly if the magnitude of power flow sensitivity factors is affected. The network management system of DNOs in the UK extends down only as far as the 33/11kV transformers. Therefore the applicability of this research to voltage levels at the 11kV and below is, at present, limited since the implementation of the control system would require the (costly) investment in electrical monitoring equipment.

The derived sensitivity factors are network topology and network configuration specific and, in simulating the proposed control strategies in the case study networks considered in this thesis, it was assumed that the network topology was constant. It is feasible, however, to develop PFSF-based control strategies that make use of alternative sets of the above-mentioned predetermined PFSFs, based on network switch information. For each configuration a new offline analysis would be required to determine the sensitivity factors. Alternatively, PFSFs could be calculated in real-time and used to update values within the control matrix M_{PFSF}.

At the transmission and sub-transmission voltage level, network extensions and new generation connections are planned by the power system operator many months in advance. The offline methodology required to adapt the DG output control system to deal with these network topology changes is provided in Chapter 4.

An overview of the required control system modification is outlined below:

1. Modify the topology of the network, as appropriate, in the off-line analysis software and on-line simulation tool;

2. Conduct an new off-line study to identify any new thermally vulnerable components within the distribution network

3. Develop, as appropriate, a new real-time thermal rating system to incorporate new thermally vulnerable components

4. Specifically related to the control algorithm, each control strategy would require updating in the following manner:

   (a) Determining updated power flow sensitivity factors

(b) Modifying the rule-base in the inference engine to achieve desired control functions

(c) Incorporate additional terms in the DG set point calculator equations

(d) Update the on-line simulation tool to maintain the integrity of the power flow and voltage validation tasks.

It should be noted that some network topology changes may have a negligible impact on the magnitude of the sensitivity factors and therefore control system modifications may not be necessary.

Regarding the communications necessary for DNOs to implement the proposed strategies for controlling distributed generation, the control system uses the DNO's SCADA signals for electrical monitoring and DG output control. Therefore, moving from LIFO-based to non-LIFO-based control strategies has no added communication requirements when deployed with static thermal ratings. The step which would entail extra communication links is the implementation of RTTR systems. In research, also carried out Durham University as part of this project, thermal state estimation techniques have been developed and validated to estimate RTTRs in wide areas of the distribution network based on limited monitoring equipment and communication link installations [85].

Clearly, the figures relating to financial assessments vary with time and location. Variations in wind farm installation and operating costs would impact on the net present values and profitability indices of the DG scheme developments, and hence the investment decision. If these values were to differ from the costs used in this thesis, the principle of the analysis would still remain valid. The proposed methodology may be used with figures that are most appropriate to the particular situation being considered.

Chapter 15

Conclusions and further work

15.1 Conclusions

In conclusion, the following key outcomes resulted from this research:

- It is anticipated that distribution networks will see a proliferation of distributed generation (DG) in coming years. In some cases this will result in power flow congestion with thermally vulnerable components restricting the connection capacity and annual active energy yield of DG. Therefore a system that can be developed for the management of power flows within distribution networks, through the power output control of DG schemes, could be of great benefit. The development stages of such a system were proposed using a novel methodology which entailed the following stages:

    1. The identification of thermally vulnerable components within distribution networks.

    2. The installation of monitoring equipment and thermal modelling of components for the off-line assessment of power system rating gains.

    3. The development of a real-time thermal rating systems for the on-line exploitation of power system ratings.

    4. The use of real-time ratings together with control techniques for DG output control to manage distribution network power flows.

- The first stage of the methodology was realised in an innovative manner by calculating thermal vulnerability factors which combined power flow sensitivity factors with component thermal ratings. The thermal vulnerability factor assessments presented in this thesis were designed to complement previous network characterisation practices by first identifying the type (overhead line, electric cable, power transformer)

and geographical location of thermally vulnerable components. In addition, the assessments add to the state of knowledge in this area since they may be used to give a holistic network view of the impact of multiple DG schemes in concurrent operation on accumulated power flows and hence vulnerable component locations. The thermal vulnerability factor assessment was applied to UKGDSs and a section of the UK power system selected for prototype DG output control system field trials. The perceived benefits are summarised below:

– It was demonstrated that the thermal vulnerability factor assessment was not confined to a specific topology type and could be used by distribution network operators (DNOs) and DG developers to identify the thermal impacts of planned individual DG schemes or, in a more strategic way, to assess longer term and more widespread DG growth scenarios;

– The thermal vulnerability factor assessment was used to inform instrumentation investment decisions for the installation of monitoring equipment in thermally vulnerable sections of the field trial network. This led to the development and testing of a real-time thermal rating system; and

– The power flow sensitivity factors that have been derived off-line for thermally vulnerable component identification may be used in an on-line manner for the coordinated output control of multiple DG schemes.

- Through a comprehensive literature review and evaluation against user and functional requirements, candidate techniques for DG output control based on component thermal properties were identified as:

– Tripping (disconnection) [for single and multiple DG scheme control];

– demand-following [for single DG scheme control];

– discrete interval adjustments [for multiple DG scheme control];

– ranked lists to prioritise the constraint order of DG schemes [for multiple DG scheme control];

– proportional adjustments [for multiple DG scheme control]; and

– power flow sensitivity factors [for multiple DG scheme control].

For the first time, the above mentioned techniques were combined with a rule-based inference engine and an on-line simulation tool. This allowed DG output control to be

achieved that was not only based on static thermal ratings (as is the present industry practice) but that also allowed seasonal and real-time thermal ratings to be utilised, in a safe manner, in future on-line power system operation applications.

- Rather than approximating the behaviour of the power system at the generation and loading extremes, the candidate techniques were simulated, in a rigorous manner using a time-series analysis (for an entire operational year with a half-hourly data resolution), to manage the power output of a single DG scheme within the field trial network. The demand-following DG output control technique with real-time thermal ratings resulted in a marginal annual energy yield gain of 10.75% when compared to 418.1 GWh/annum resulting from a present industry practice of DG tripping based on static thermal ratings. Despite increasing electrical losses, the demand-following DG output control technique was found to have a marginal net present value to the DG developer of £38.46M, compared to £36.97M resulting from a network reinforcement option. The cost of capital for the DG developer is likely to make DG output control systems, with lower upfront costs, a more attractive investment.

- Three candidate strategies were proposed for multiple DG scheme output control using power flow sensitivity factors, which added to the prior art of DG output control: (i) Last-in first-off; (ii) egalitarian; and (iii) technically most appropriate. This is of relevance in situations where individual generators may cause power flow excursions in individual components but of particular relevance in situations where the aggregation of power flows from multiple generators may cause more widespread power flow management issues. Therefore, with the expected proliferation of DG the resulting power flows are likely to affect many components within the distribution network and it is important to take a holistic view of power flow management. Using a UKGDS and the field trial network it was demonstrated through simulation that the DG output control strategies could be combined with static, seasonal or real-time thermal ratings to manage power flows resulting from a single thermal constraint or multiple thermal constraints within distribution networks.

- Using a time-series analysis for an entire operational year with a half-hourly data resolution, the following parameters were quantified to evaluate the potential benefits of the DG output control system: (i) DG scheme individual and aggregated annual energy yields; (ii) DG-apportioned losses; (iii) DG development net present values and profitability indices; (iv) component power transfers; and (v) busbar voltages. In

addition, an on-line simulation tool was developed to validate the control actions of the DG output control system and, for the first time, to calculate specific values and figures of merit for a variety of DG control strategies. It was found that:

- In the UKGDS, based on a datum value of 525.48 GWh/annum (corresponding to LIFO discrete-interval DG output control with static thermal ratings), non-LIFO-based control strategies led to DG aggregated annual energy yield gains of 7.7% and 9.0%. In addition, gains of 12.3% and 13.1% resulted from non-LIFO-based control strategies with component real-time thermal ratings.

- In the field trial network, based on a datum value of 943.8 GWh/annum (corresponding to LIFO DG tripping with component static ratings), non-LIFO-based control strategies led to DG aggregated annual energy yield gains of 7.1% and 11.0%. In addition, gains of 20.5% and 21.0% resulted from non-LIFO-based control strategies deployed with power system real-time thermal ratings.

- Although the case studies presented in this thesis are UK-based, the control techniques, simulation approach and research outcomes are transferable to distribution networks internationally. It is recommended that any DNO or DG developer looking to adopt the proposed strategies should conduct an off-line analysis to assess the value of the DG output control system. This is because the control strategy implementations are a function of a number of site-specific variables and therefore the economic value in each case is different.

- The impact that the proposed strategies have on individual DG revenue streams could allow DG schemes greater access to the distribution network in a non-firm manner and, even if the first-in DG schemes are remunerated for curtailing power outputs, there could be an overall revenue gain for all the DG scheme developers.

- The DG output control algorithms were delivered to the DIUS Project consortium and the demand-following control algorithm was installed on an industrial PC for open and closed loop trials of the prototype control system with monitored data from the field trial network. This process required further innovative refinements to the control algorithms to provide graceful degradation functionality, allowing the control system to continue to operate with increasingly conservative signals dispatched to the DG scheme as an increasing number of communication signals to the control system are lost.

In summary, it appears that, if suitable contractual and regulatory mechanisms are in place, the active management of DG based on component thermal properties is a viable option for facilitating future renewable energy penetration gains through non-firm DG access to the distribution network.

15.2   Further work

A number of avenues for further research were identified as:

- The use of real-time power flow sensitivity factors within the control algorithms;

- the development of a DG output control system to function in electrical contingency scenarios;

- the development of a proactive DG output control system that makes use of load forecasts and real-time thermal rating forecasts;

- the development of a DG output control system utilising fuzzy logic to deal with decision-making uncertainties;

- the development of a DG output control system that allows provision of ancillary services such as voltage control;

- the development of a DG output control system that makes use of alternative multiple DG output control strategies such as an equal MW reduction signal dispatched to all DG schemes or the use of flow-tracing techniques with power flow sensitivity factors;

- the dynamic modelling and analysis of DG set point changes;

- the active management of generators based on component thermal properties at the transmission level; and

- the potential adaptation of the power flow sensitivity factor techniques for future demand-side management scenarios.

References

[1] G. Strbac, "Electric power systems research on dispersed generation," *Electr. Power Syst. Res.*, vol. 77, no. 9, pp. 1143–1147, Jul. 2007.

[2] N. Jenkins, R. Allan, P. Crossley, D. Kirschen, and G. Strbac, *Embedded Generation*, Power and Energy Series 31 ed. London, UK: IEE, 2000, pp. 1-9.

[3] UK Department of Trade and Industry, "Meeting the energy challenge - A white paper on energy," DTI, Tech. Rep., 2007.

[4] P. S. Fox-Penner, "Easing gridlock on the grid - electricity planning and siting compacts," *The Electricity Journal*, vol. 14, no. 9, pp. 11–30, Nov. 2001.

[5] A. Neumann, P. C. Taylor, S. C. E. Jupe, A. Michiorri, A. Goode, D. Curry, and D. A. Roberts, "Dynamic thermal rating and active control for improved distribution network utilization," in *Proc. PowerGrid*, Milan, Italy, 2008.

[6] PB Power (Parsons Brinckerhoff Ltd.), "Active management of distributed generators based on component thermal properties," DTI funding application, Tech. Rep., 2005, Original proposal.

[7] R. Allan, G. Strbac, P. Djapic, and K. Jarrett, "Developing the P2/6 methodology," DTI, Tech. Rep., Contract No. DG/CG/00023/00/00.

[8] *Security of supply*, ENA Std. ER P2/6, 2006.

[9] Energy Networks Association, "Application guide for assessing the capacity of networks containing distributed generation," Tech. Rep., 2006, Engineering Technical Report 130.

[10] CIGRÉ WG C6.11. (2002) Development and operation of active distribution networks. [Online]. Available: http://www.cigre-c6.org

[11] C. D'Adamo, S. C. E. Jupe, and C. Abbey, "Global survey on planning and operation of active distribution networks - update of CIGRÉ C6.11 working group activities," in *Proc. 20th International Conference on Electricity Distribution*, Prague, CZ, 2009.

[12] G. Ault, C. E. T. Foote, and J. R. McDonald, "UK research activities on advanced distribution automation," in *Power Engineering Society General Meeting*, 2005.

[13] UK Department of Trade and Industry, "Register of active management pilots, trials, research, development and demonstration activities," University of Strathclyde, Tech. Rep., 2001, contract no. DG/CG/00079/00/00.

[14] SP transmission and distribution, "Distribution long term development statement for SP Manweb PLC for the years 2005/6 to 2009/10," SP Manweb plc., Prenton, Tech. Rep., 2005.

[15] UK Department of Trade and Industry, "The electricity safety, quality and continuity regulations," London, Tech. Rep., 2002.

[16] D. A. Douglass, D. C. Lawry, A. A. Edris, and E. C. Bascom III, "Dynamic thermal ratings realize circuit load limits," *IEEE Comput. Appl. Power*, pp. 38–44, 2000.

[17] J. A. Nuijten, A. Greschiere, J. C. Smit, and G. J. Frijmersum, "Future network planning and grid control," in *Proc. International Conference on Future Power Systems*, 2005.

[18] H. T. Yip, C. An, M. Aten, and R. Ferris, "Dynamic line rating protection for wind farm connections," in *Proc. 9th International Conference on Developments in Power System Protection*, Glasgow, UK, 2008.

[19] A. Collinson, F. Dai, A. Beddoes, and J. Crabtree, "Solutions for the connection and operation of distributed generation," UK Department for Trade and Industry, Tech. Rep., 2003.

[20] R. Stephen, "Description and evaluation of options relating to the uprating of overhead transmission lines," *Electra*, vol. B2-201, pp. 1–7, 2004.

[21] S. P. Hoffmann and A. M. Clark, "The approach to thermal uprating of transmission lines in the UK," *Electra*, vol. B2-317, pp. 1–8, 2004.

[22] F. Soto, J. Lattore, and M. Wagensberg, "Increasing the capacity of overhead lines in the 400kV Spanish transmission network: real time thermal ratings," *Electra*, vol. 22-211, pp. 1–6, 1998.

[23] (2008) Wind atlas analysis and application program. [Online]. Available: http://www.wasp.dk

[24] D. A. Douglass and A. A. Edris, "Real-time monitoring and dynamic thermal rating of power transmission circuits," *IEEE Trans. Power Deliv.*, vol. 11, no. 3, pp. 1407–1418, 1996.

[25] D. A. Douglass, A. A. Edris, and G. A. Pritchard, "Field application of a dynamic thermal circuit rating method," *IEEE Trans. Power Deliv.*, vol. 12, no. 2, pp. 823–831, 1997.

[26] M. Helmer, "Optimized size of wind power plant transformer and parallel operation," in *Proc. Wind Power for the 21st Century*, Kassel, Germany, 2000.

[27] P. B. Belben and C. D. Ziesler, "Aeolian uprating: how wind farms can solve their own transmission problems," in *Proc. World Wind Energy Conference*, Berlin, Germany, 2002.

[28] H. E. House and P. D. Tuttle, "Current carrying capacity of ACSR," *IEEE Trans. Power Appar. Syst.*, vol. 78, no. 3, pp. 1169–1177, 1959.

[29] V. T. Morgan, "The thermal rating of overhead-line conductors. 1. The steady-state thermal mode," *Electr. Power Syst. Res.*, vol. 5, no. 2, pp. 119–139, 1982.

[30] *Overhead electrical conductors - calculation methods for stranded bare conductors*, IEC Std. TR 1597, 1995.

[31] WG 22.12, "The thermal behaviour of overhead line conductors," *Electra*, vol. 144, no. 3, pp. 107–125, 1992.

[32] *Standard for calculating the current-temperature relationship of bare overhead conductors*, IEEE Std. 738, 1993.

[33] *Current rating guide for high voltage overhead lines operating in the UK distribution system*, ENA Std. ER P27, 1986.

[34] J. H. Neher and M. H. McGrath, "The calculation of the temperature rise and load capability of cable systems," *AIEE Trans.*, vol. 76, no. 3, pp. 752–772, 1957.

[35] *Electric cables - calculation of the current rating*, IEC Std. 60 287, 1994.

[36] *IEEE standard power cable ampacity tables*, IEEE Std. 835, 1994.

[37] *Current rating for distribution cables*, ENA Std. ER P17, 2004.

[38] M. L. D. Susa and H. Nordman, "Dynamic thermal modelling of power transformers," *IEEE Trans. Power Deliv.*, vol. 20, no. 1, pp. 197–204, 2005.

[39] *Power transformers - part 7: loading guide for oil-immersed power transformers*, IEC Std. 60 076-7, 2008.

[40] *Guide for loading mineral oil-immersed power transformers up to and including 100 MVA with 55ºC or 65ºC average winding rise*, IEEE Std. C57.92, 1981.

[41] *Transformers loading guide*, ENA Std. ER P15, 1971.

[42] M. J. C. Berende, J. G. Slootweg, and G. J. M. B. Clemens, "Incorporating weather statistics in determining overhead line ampacity," in *Proc. International Conference on Future Power Systems*, 2005.

[43] N. Dinic, D. Flynn, L. Xu, and A. Kennedy, "Increasing wind farm connection capacity," *IEE Proc. GTD*, vol. 153, no. 4, pp. 493–498, Jul. 2006.

[44] R. A. F. Currie, G. W. Ault, and J. R. McDonald, "Methodology for determination of economic connection capacity for renewable generator connections to distribution networks optimised by active power flow management," *IEE Proc. GTD*, vol. 153, no. 4, pp. 456–462, Jul. 2006.

[45] P. N. Vovos, G. P. Harrison, A. R. Wallace, and J. W. Bialek, "Optimal power flow as a tool for fault level-constrained network capacity analysis," *IEEE Trans. Power Syst.*, vol. 20, no. 2, pp. 734–741, May. 2005.

[46] V. H. Mendez Quezada, J. R. Abbad, and G. T. San Romain, "Assessment of energy distribution losses for increasing penetration of distributed generation," *IEEE Trans. Power Syst.*, vol. 21, no. 2, pp. 533–540, May. 2006.

[47] G. P. Harrison and A. R. Wallace, "Optimal power flow evaluation of distribution network capacity for the connection of distributed generation," *IEE Proc. GTD*, vol. 152, no. 1, pp. 115–122, Jan. 2005.

[48] C. L. Masters, "Voltage rise: The big issue when connecting embedded generation to long 11kV overhead lines," *Power Eng. J.*, vol. 16, no. 1, pp. 5–12, Feb. 2002.

[49] P. Smart, A. Dinning, A. Maloyd, A. Causebook, and S. Cowdroy, "Accommodating distributed generation," UK Department for Trade and Industry, Tech. Rep., 2006, econnect project no: 1672.

[50] Energy Networks Association, "Guidelines for actively managing power flows associated with the connection of a single distributed generation plant," Tech. Rep., 2004, Engineering Technical Report 124.

[51] D. A. Roberts, "Network management systems for active distribution networks - a feasibility study," SP Power Systems Ltd., Scottish Power Plc., Tech. Rep., 2004.

[52] S. N. Liew and T. Moore, "Design and commissioning of active generator constraint for an offshore wind farm," in *Proc. 18th International Conference on Electricity Distribution*, Turin, Italy, 2005.

[53] Scottish Hydro-Electric Power Distribution Limited, "Facilitate generation connections on Orkney by automatic distribution network management," UK Department for Trade and Industry, Tech. Rep., 2004, Contract Number: K/EL/0031/00/00.

[54] R. A. F. Currie, G. W. Ault, C. Foote, and J. R. McDonald, "Active power-flow management utilising operating margins for the increased connection of distributed generation," *IET Proc. GTD.*, vol. 1, no. 1, pp. 197–202, Jan. 2007.

[55] M. J. Dolan, E. M. Davidson, G. W. Ault, and J. R. McDonald, "Techniques for managing the power flows in active distribution networks within thermal constraints," in *Proc. 20th International Conference on Electricity Distribution*, Prague, CZ, 2009.

[56] J. Kabouris and C. D. Vournas, "Application of interruptible contracts to increase wind-power penetration in congested areas," *IEEE Trans. Power Syst.*, vol. 19, no. 3, pp. 1642–1649, Aug. 2004.

[57] E. Castronuovo, J. Martinez-Crespo, and J. Usaola, "Optimal controllability of wind generators in a delegated dispatch," *Electr. Power Syst. Res.*, vol. 77, no. 10, pp. 1442–1448, Aug. 2007.

[58] Y. V. Makarov, C. Loutan, J. Ma, and P. de Mello, "Operational impacts of wind generation on California power systems," *IEEE Trans. Power Syst.*, vol. 24, no. 2, pp. 1039–1050, May. 2009.

[59] EA Technology, "Overcoming barriers to scheduling embedded generation," Crown, Tech. Rep., 2000, ETSU K/EL/00217/REP.

[60] J. L. Rodriguez-Amenedo, S. Arnalte, and J. C. Burgos, "Automatic generation control of a wind farm with variable speed control," *IEEE Trans. Energy Convers.*, vol. 17, no. 2, pp. 279–284, Jun. 2002.

[61] B. Weedy and B. Cory, *Electric power systems*, 4th ed. Chichester, UK: John Wiley & Sons, Ltd, 1998, pp. 61-90.

[62] R. E. de Almeida, E. D. Castronuovo, and J. A. P. Lopes, "Optimum generation control in wind parks when carrying out system operators requests," *IEEE Trans. Power Syst.*, vol. 21, no. 2, pp. 718–725, May. 2006.

[63] B. Strah, O. Kujaca, and Z. Vukic, "Speed and active power control of hydro turbine unit," *IEEE Trans. Energy Convers.*, vol. 20, no. 2, pp. 424–434, Jun. 2005.

[64] S. W. Director and R. A. Rohrer, "The generalized adjoint network and network sensitivities," *IEEE Transactions on Circuit Theory*, vol. 16, no. 3, pp. 318–323, Aug. 1968.

[65] G. C. Ejebe and B. F. Wollenberg, "Automatic contingency selection," *IEEE Trans. Power Apparatus and Systems*, vol. PAS-98, no. 1, pp. 97–104, Jan/Feb. 1979.

[66] A. J. Wood and B. F. Wollenberg, *Power generation, operation and control*, 4th ed. New York, NY: Wiley, 1996, pp. 421-427.

[67] W. Y. Ng, "Generalized generation distribution factors for power system security evaluations," *IEEE Transactions on Power Apparatus and Systems*, vol. PAS-100, no. 3, pp. 1001–1005, Mar. 1981.

[68] M. Huneault and F. D. Galiana, "A survey of optimal power flow literature," *IEEE Trans. Power Syst.*, vol. 6, no. 2, pp. 762–770, 1991.

[69] D. Grgic and F. Gubina, "Congestion management approach after deregulation of Slovenian power system," *Power Engineering Society Summer Meeting*, vol. 3, pp. 1661–1665, Jul. 2002.

[70] M. Noroozian and G. Andersson, "Power flow control by use of controllable series components," *IEEE Trans. Power Deliv.*, vol. 8, no. 3, pp. 1420–1429, Jul. 1993.

[71] Q. Zhou and J. W. Bialek, "Generation curtailment to manage voltage constraints in distribution networks," *IET Proc. GTD*, vol. 1, no. 3, pp. 492–498, May. 2007.

[72] A. Keane, Q. Zhou, J. Bialek, and M. O'Malley, "Planning and operating non-firm distributed generation," *IET Proc. Renew. Power Gener.*, vol. 3, no. 4, pp. 455–461, Dec. 2009.

[73] Y.-H. Song, *Modern optimisation techniques in power systems.* Dordrecht, The Netherlands: Kluwer academic publishers, 1999, pp. 63-89, 113-139, 247-260.

[74] H. Singh, S. Hao, and A. Papalexopoulos, "Transmission congestion management in competitive electricity markets," *IEEE Trans. Power Syst.*, vol. 13, no. 2, pp. 672–680, May. 1998.

[75] G. P. Harrison, A. Piccolo, P. Siano, and A. R. Wallace, "Exploring the tradeoffs between incentives for distributed generation developers and DNOs," *IEEE Trans. Power Syst.*, vol. 22, no. 2, pp. 821–828, May. 2007.

[76] P. Siano, L. F. Ochoa, G. P. Harrison, and A. Piccolo, "Assessing the strategic benefits of distributed generation ownership for DNOs," *IET Proc. GTD.*, vol. 3, no. 3, pp. 225–236, May. 2009.

[77] J. W. Bialek, "Tracing the flow of electricity," *IET Proc. GTD*, vol. 143, pp. 313–320, 2007.

[78] D. Kirschen and G. Strbac, "Tracing active and reactive power between generators and loads using real and imaginary currents," *IEEE Trans. Power Syst.*, vol. 14, no. 4, pp. 1312–1318, Nov. 1999.

[79] Office of the Gas and Electricity Markets, "2005/06 Electricity Distribution Quality of Service Report," London, Tech. Rep., 2006.

[80] Office of the Gas and Electricity Markets, "Electricity Distribution Price Control Review, Final Proposals," London, Tech. Rep., 2004.

[81] C. Foote, P. Djapic, G. Ault, J. Mutale, G. Burt, and G. Strbac. (2006) United Kingdom Generic Distribution Systems - Summary of EHV networks. [Online]. Available: http://monaco.eee.strath.ac.uk/ukgds/php/file.php?id=91

[82] A. Kaw and E. Kalu, "Bisection method of solving a non-linear equation," in *Numerical methods with applications*. Florida, USA: Brooks/Cole, 2008, ch. 3, pp. 03.1–03.9.

[83] S. C. E. Jupe and P. C. Taylor, "Distributed generation output control for network power flow management," *IET Proc. Renew. Power Gener.*, vol. 3, no. 4, pp. 371–386, Dec. 2009.

[84] A. Michiorri, P. C. Taylor, S. C. E. Jupe, and C. J. Berry, "An investigation into the influence of environmental conditions on power system ratings," *Proc. IMechE - Part A: J. Power and energy*, vol. 227, no. A7, pp. 743–757, Nov. 2009.

[85] A. Michiorri, P. C. Taylor, and S. C. E. Jupe, "Overhead line real-time rating estimation algorithm: description and validation," *Proc. IMechE - Part A: J. Power and energy*, In press 2009.

[86] S. C. E. Jupe and P. C. Taylor, "Strategies for the control of multiple distributed generation schemes," in *Proc. 20th International Conference on Electricity Distribution*, Prague, CZ, 2009.

[87] S. C. E. Jupe, A. Michiorri, and P. C. Taylor, "Increasing the energy penetration of generation from new and renewable energy resources," in *Renewable energy*. Vienna, Austria: IN-TECH, 2009, ch. 4, pp. 37–62.

[88] S. C. E. Jupe and P. C. Taylor, "Coordinated output control of multiple distributed generation schemes," *IET Proc. Renew. Power Gener.*, accepted, 2010.

[89] "Service oriented architecture," Olsen Software, Tech. Rep., 2006.

[90] D. Shepard, "A two-dimensional interpolation function for irregularly-spaced data," in *Proc. 23rd ACM National Conference*, New York, 1968.

[91] L. M. Cipcigan and P. C. Taylor, "Investigation of the reverse power flow requirements of high penetrations of small scale embedded generation," *IET Proc. RPG.*, vol. 1, no. 3, pp. 160–166, Sep. 2007.

[92] M. Pantos and F. Gubina, "A flow-tracing method for transmission networks," *Energy*, vol. 30, pp. 1781–1792, 2005.

[93] TNEI. (2008) IPSA Software Package. [Online]. Available: http://www.ipsa-power.com

[94] *Planning limits for voltage fluctuations caused by industrial, commercial and domestic equipment in the UK*, ENA Std. ER P28, 2003.

[95] M. Hird, N. Jenkins, and P. C. Taylor, "An active 11kV voltage controller: Practical considerations," in *Proc. 17th International Conference on Electricity Distribution*, Barcelona, Italy, 2003.

[96] J. Jantzen, *Foundations of Fuzzy Control.* Chichester, UK: John Wiley & Sons, Ltd, 2007, pp. 35-36, 57-61.

[97] M. Lutz, *Learning Python*, 3rd ed. Sebastopol, CA: O'Reilly Media Inc, 2007.

[98] S. C. E. Jupe, P. C. Taylor, and C. J. Berry, "Assessing the value of active constrained connection managers for distribution networks," in *Proc. CIRED Seminar 2008: SmartGrids for Distribution*, Frankfurt, Germany, 2008.

[99] S. Payyala and T. C. Green, "Sizing of distributed generation plant through techno-economic feasibility assessment," in *Power Engineering Society General Meeting*, 2006.

[100] T. Burton, D. Sharpe, N. Jenkins, and E. Bossanyi, *Wind Energy Handbook.* Chichester, UK: John Wiley & Sons, Ltd, 2001.

[101] S. C. E. Jupe, P. C. Taylor, A. Michiorri, and C. J. Berry, "An evaluation of distributed generation constrained connection managers," in *Proc. 6th Mediterranean Conference on Generation, Transmission and Distribution*, Thessaloniki, Greece, 2008.

[102] UK Meteorological Office. (2008) Data for the valley area of the uk. [Online]. Available: http://www.metoffice.gov.uk

[103] Mott McDonald, "The Carbon Trust and DTI Renewables Network Impact Study, Annex 3: Distribution Network Topography Analysis," London, Tech. Rep., 2003.

[104] European Commission, "Quarterly Review of European Gas and Electricity Prices," Luxembourg, Tech. Rep., 2005.

[105] Office of the Gas and Electricity Markets, "Renewables Obligation: Annual Report 2006 - 2007," London, Tech. Rep., 2008.

[106] Department for Business Enterprise and Regulatory Reform. (2004) Strategic Environmental Assessment, Wind Background - Cost of Wind Power Generation. [Online]. Available: http://www.offshore-sea.org.uk

[107] British Wind Energy Association. (2008) UK Wind Energy Database. [Online]. Available: http://www.bwea.com/index.html

[108] UK Department of Trade and Industry, "Offshore wind energy - wind energy factsheet 1," London, Tech. Rep., 2001.

[109] UK Department of Energy and Climate Change, "Cost of and financial support for offshore wind," London, Tech. Rep., URN 09D/534.

[110] H. T. Yip, C. An, G. Lloyd, P. C. Taylor, S. C. E. Jupe, A. Michiorri, and M. Bartlett, "Dynamic thermal rating and active control for improved distribution network utilisation," in *Proc. 10th International Conference on Developments in Power System Protection*, Manchester, UK, 2010.

[111] H. T. Yip, C. An, G. Lloyd, P. C. Taylor, S. C. E. Jupe, A. Michiorri, and M. Bartlett, "Dynamic thermal rating and active control for improved distribution network utilisation," in *Protection, Automation and Control World Conference*, Dublin, Ireland, 2010.

[112] B. Stedall, *The hierarchical control and protection of power systems*. Bath, UK: University of Bath, 1994.

[113] *Communication networks and systems in substations - Part 1: Introduction and overview*, IEC Std. 61 850, 2003.

Appendix A

Journal publications

www.ietdl.org

Distributed generation output control for network power flow management

S.C.E. Jupe   P.C. Taylor

School of Engineering, Durham University, South Road, Durham DH1 3LE, UK
E-mail: s.c.e.jupe@durham.ac.uk

Abstract: The development stages in the output control of distributed generation (DG) for network power flow management are illustrated. The first stage requires an assessment of the location of thermally vulnerable components within the distribution network. This is achieved through the offline calculation of thermal vulnerability factors that relate component power flow sensitivity factors to component thermal limits. This directly informs Stage 2 – the installation of meteorological stations and component temperature monitoring equipment for network thermal characterisation. In Stage 3, steady-state component rating models are populated with real-time environmental information from the meteorological stations to generate component real-time thermal ratings. In Stage 4, the power flow sensitivity factors calculated in Stage 1 are embedded within a network power flow management system which, together with the component real-time thermal ratings calculated in Stage 3, is used to control the power output of DG schemes.

1 Introduction

There is an expectation that distribution networks within the United Kingdom (UK), and internationally, will continue to see expanding levels of distributed generation (DG) because of the drive by respective Governments to promote electricity generation from renewable sources [1, 2]. Incentives are in place in the UK to encourage and reward investment in such schemes. However, incentives for distribution network operators (DNOs) to accommodate DG are only just emerging through the regulatory framework from Ofgem and the financial gain for DNOs is capped [3]. The UK has viable renewable resources and has seen increased growth in the wind-related DG sector for both onshore and offshore connections [4].

When a developer seeks to connect a DG scheme of significant capacity, the DNO may offer a firm connection on the condition that the developer pays for any necessary network reinforcements. In parts of the UK, for example areas of outstanding natural beauty, an environmental constraint exists that prevents the building of infrastructure to reduce the detrimental impact of the power system on the landscape. Furthermore, the developer may not be able to justify the expense of the required reinforcement and

negotiates a non-firm or 'constrained' connection agreement, whereby the DG will be tripped off or constrained back under certain network operating conditions. These types of connections are expected to occur more frequently as network power flow congestion occurs and thus may require the power output of DG to be controlled in a manner outlined in this paper.

With a geographically dispersed portfolio of assets, the reinforcement issues highlighted above and developers seeking to connect greater levels of DG, it is in the interest of DNOs to increase asset utilisation in a safe manner, potentially allowing latent capacity to be used under strictly controlled conditions. In order to effectively utilise capacity headroom, it is important to understand the electro-thermal behaviour of the network, both in terms of power flows and the identification of components that could be thermally at risk of damage.

AREVA T&D, Imass, PB power, ScottishPower EnergyNetworks (SPEN) and Durham University have formed a research consortium, part sponsored by the Department for Innovation, Universities and Skills (DIUS), in a project entitled 'Active management of distributed generators based on component thermal properties' [5].

www.ietdl.org

Through field trials, the project will monitor environmental and meteorological conditions which, together with component steady-state thermal models, will be used to give greater visibility to the DNO control room of the real-time thermal ratings of network assets. This information, together with power flows, could potentially act as a decision support tool for DG control. If proven in open-loop, the concept may be trialled to automatically control multiple DG schemes. It is hoped that this system will increase the annual energy yield of DG schemes, helping the UK to move towards low-carbon economy targets.

The purpose of this paper is to outline the development stages in the power output control of DG schemes for the management of network power flows and, in particular, to highlight the role of power flow sensitivity factors in this process. The main development stages are summarised below:

Stage 1: Conduct an offline assessment to identify areas of the distribution network that are thermally vulnerable to the penetration of DG. This may be achieved through the calculation of component thermal vulnerability factors by aggregating power flow sensitivity factors and component thermal ratings.

Stage 2: Thermally characterise the vulnerable sections of the distribution network to quantify headroom gains that may be exploited through the use of a real-time thermal rating system. This may be achieved by the offline analysis of directly monitored conductor operating temperatures or by monitoring meteorological conditions that are then used to populate component steady-state thermal models.

Stage 3: In situations where it is assessed to be viable, a system needs to be developed to allow the real-time exploitation of component thermal ratings.

Stage 4: The component real-time thermal rating system could then be used to inform the power output control of DG for network power flow management through the use of power flow sensitivity factors.

To reflect the key aspects of these development stages the paper is structured in the following way: Section 2 provides a survey of work relating to the offline assessment of DG connection capacities and the present use of real-time thermal ratings in the electrical industry. It also sets out the theoretical principles that underpin this research, including the relationship of sensitivity factors to governing alternating current (AC) power flow equations and the steady-state component rating equations that would be used in Stages 2 and 3. These principles are then used in Section 3 to formulate thermal vulnerability factors and to develop equations for the output control of DG. A procedure for assessing power flow sensitivity factors and thermal vulnerability factors is also given. Section 4 illustrates development Stages 1 and 4 through the use of United

Kingdom Generic Distribution Systems (UKGDSs) and Section 5 illustrates these stages applied to the field trial network being considered in the 'Active management of distributed generators based on component thermal properties' project. Through system simulations, in conjunction with SPEN, the components identified through the assessment of thermal vulnerability factors were validated. This formed the basis for instrumentation investment decisions that will characterise the thermal behaviour of the field trial network (as suggested in development Stage 2) and provide information for the real-time assessment of component thermal ratings in Stage 3. Section 6 outlines further work regarding strategies for the online control of multiple DG schemes and Section 7 discusses the wider benefits and limitations of utilising power flow sensitivity factors in the output control of DG for network power flow management.

2 Background

2.1 Related work

DG connection capacity assessments are the current research focus of numerous institutions in order to determine the impact of voltage regulations, operational economics, fault levels, losses and thermal limits as constraining parameters. Dinic *et al.* [6] consider voltage limitations and installed DG capacity, relative to the system fault level, in 33 kV networks and conclude that capacitive compensation can allow capacity maximisation within operational limits. The economics of DG connections are considered by Currie *et al.* [7] with a methodology that facilitates greater DG access for multiple generators by exploiting operating margins with an active power flow management technique termed 'trim then trip'. Vovos *et al.* [8] develop an optimal power flow (OPF) technique along with an iterative procedure to calculate generation allocations at nodes based on fault-level limitations. Mendez Quezada *et al.* [9] examine the impact of increased DG penetration on electrical losses within the IEEE 34-node test network and conclude that losses follow a U-shaped trajectory when plotted as a function of DG penetration. Harrison and Wallace [10] present an OPF formulation to determine the maximum connection capacity of DG based on thermal limits and statutory voltage regulation. The 'reverse load-ability' methodology coupled with OPF software modelled generators as loads with a fixed power factor and created an analysis tool that could allow additional constraints (such as fault-level limitations) to be incorporated into the formulation if necessary. It was also suggested that Langrangian relaxation of constraint coefficients may be developed to simulate changes in component ratings although this was not demonstrated.

It is acknowledged that technical barriers such as voltage rise [11] and fault levels [12] may inhibit DG connection capacities. However, this paper focuses on the thermal limit of power system components. Real-time thermal ratings are the present focus of research for the following institutions:

EPRI in the USA [13] for increased security and capacity of transmission networks, NUON in the Netherlands [14] for coping with load growth and delaying infrastructure investment, E.ON and Central Networks in the UK to facilitate the constrained connection of DG [15] and the Energy Networks Strategy Group within the UK, as a solution for the accommodation of DG from the DG Co-ordinating Group in Work Stream 3 [16]. A technique for identifying the thermally vulnerable span of an overhead line is given by Berende *et al.* in [17]. In contrast to the desk-study simulations presented in this paper, the team from the Netherlands used imagery from helicopter flights to record and time-stamp the sag of overhead lines. This was done for a specific operating condition and then, together with an offline algorithm, used to simulate the sag for other conditions. The technique was appropriate for that particular application because the vulnerable section of the network had been predetermined through operational experience.

The work detailed in this paper moves beyond the offline assessment of DG connection capacities that are presented above to outline the development stages in the online control of DG power output for network power flow management. This requires the development of a system that has the capability of utilising real-time information about the thermal status of the network and, in reaching a control decision, guarantees that the secure operation of the distribution network is maintained. Assessments of the power flow sensitivity factors are designed to inform the development process and aid in assessing the perceived benefits of installing a real-time thermal rating system. Although OPF is acknowledged as a powerful tool for the offline planning of electrical networks, there is an emerging requirement to manage non-firm DG connections in an online manner. The rapid processing time, reduced memory requirements and robustness associated with embedding predetermined power flow sensitivity factors in a DG power output control system make it attractive for substation installations and online applications. This is strengthened further by the ability of the DG power output control system to readily integrate component real-time thermal ratings in the management of network power flows.

The assessments of the thermal vulnerability factors presented in this paper complement network characterisation, such as that carried out in [17] by first identifying the type (overhead line, underground cable, power transformer) and geographical location of thermally vulnerable components. The assessments may be used to give a holistic network view of the impact of multiple DG schemes in concurrent operation on accumulated power flows and hence vulnerable component locations. This could then inform investment decisions relating to thermal monitoring equipment, particularly in the development stages of real-time thermal rating systems. As seen in the development of the DG power output control system for the field trial network in Section 5,

the power flow sensitivity factors may result in counter-flow relationships where the increased output of a particular DG scheme allows the output of another DG scheme to be increased.

2.2 Existing principles

Power flow sensitivity factors are integral to the work presented in this paper and are related to the governing power flow equations for AC electrical networks in Section 2.2.1. The steady-state thermal limit of electrical distribution network assets is discussed in Section 2.2.2 and it is demonstrated how the current carrying capacity of assets are a function of time-variant meteorological conditions.

2.2.1 Power flow sensitivity factors: Once the inverse Jacobian has been evaluated in the full AC power flow solution, perturbations about a given set of system conditions may be calculated as in (1) [18]. This gives the changes expected in bus voltage angles and voltage magnitudes because of injections of real or reactive power

$$
\begin{bmatrix} \Delta\theta_i \\ \frac{\Delta|E_i|}{|E_i|} \\ \Delta\theta_k \\ \frac{\Delta|E_k|}{|E_k|} \\ \vdots \end{bmatrix} = [J]^{-1} \begin{bmatrix} \Delta P_i \\ \Delta Q_i \\ \Delta P_k \\ \Delta Q_k \\ \vdots \end{bmatrix} \tag{1}
$$

where θ_i and θ_k (rad) represent voltage angles at nodes i and k, respectively; $|E_i|$ and $|E_k|$ (kV) represent nodal voltages; J is the Jacobian matrix; P_i and P_k (MW) represent real power injections at nodes i and k, respectively; and Q_i and Q_k (MVAr) represent reactive power injections at nodes i and k, respectively.

The work presented in this paper is specifically concerned with calculating the effect of a perturbation of ΔP_m — that is an injection of power at unity power factor (real power) into node m. Since the generation shifts, the reference (slack) bus compensates for the increase in power. The $\Delta\theta$ and $\Delta|E|/|E|$ values in (2) are, thus, equal to the derivative of the bus angles and voltage magnitudes with respect to a change in power at bus m

$$
\begin{bmatrix} \Delta\theta \\ \frac{\Delta|E|}{|E|} \end{bmatrix} = [J]^{-1} \begin{bmatrix} \Delta P_m \\ \Delta Q_m \\ \vdots \\ \Delta P_{\text{ref}} \\ \Delta Q_{\text{ref}} \end{bmatrix} \tag{2}
$$

Thus, the sensitivity factors for a real power injection at node m

www.ietdl.org

are given in (3–6)

$$f(\theta): \frac{\mathrm{d}P_{i,k}^c}{\mathrm{d}G_{P,m}} = \left(\frac{\partial P}{\partial \theta}\right)_{i,k}\left(\frac{\mathrm{d}\theta_k}{\mathrm{d}G_{P,m}} - \frac{\mathrm{d}\theta_i}{\mathrm{d}G_{P,m}}\right) \quad (3)$$

$$f(|E|): \frac{\mathrm{d}P_{i,k}^c}{\mathrm{d}G_{P,m}} = \left(\frac{\partial P}{\partial |E|/|E|}\right)_{i,k}\left(\frac{\mathrm{d}|E_k|/|E_k|}{\mathrm{d}G_{P,m}} - \frac{\mathrm{d}|E_i|/|E_i|}{\mathrm{d}G_{P,m}}\right) \quad (4)$$

$$f(\theta): \frac{\mathrm{d}Q_{i,k}^c}{\mathrm{d}G_{P,m}} = \left(\frac{\partial Q}{\partial \theta}\right)_{i,k}\left(\frac{\mathrm{d}\theta_k}{\mathrm{d}G_{P,m}} - \frac{\mathrm{d}\theta_i}{\mathrm{d}G_{P,m}}\right) \quad (5)$$

$$f(|E|): \frac{\mathrm{d}Q_{i,k}^c}{\mathrm{d}G_{P,m}} = \left(\frac{\partial Q}{\partial |E|/|E|}\right)_{i,k}\left(\frac{\mathrm{d}|E_k|/|E_k|}{\mathrm{d}G_{P,m}} - \frac{\mathrm{d}|E_i|/|E_i|}{\mathrm{d}G_{P,m}}\right) \quad (6)$$

where $f(\theta)$ and $f(|E|)$ represent functions of voltage angles and voltage magnitudes, respectively, $(\partial P/\partial \theta)_{i,k}$, $(\partial P/(\partial |E|/|E|))_{i,k}$, $(\partial Q/\partial \theta)_{i,k}$ and $(\partial Q/(\partial |E|/|E|))_{i,k}$ represent elements within the Jacobian matrix and $\mathrm{d}\theta_k/\mathrm{d}G_{P,m}$, $\mathrm{d}\theta_i/\mathrm{d}G_{P,m}$, $(\mathrm{d}|E_k|/|E_k|)/\mathrm{d}G_{P,m}$ and $(\mathrm{d}|E_i|/|E_i|)/\mathrm{d}G_{P,m}$ represent elements corresponding to the vector $\begin{bmatrix}\Delta\theta \\ \frac{\Delta|E|}{|E|}\end{bmatrix}$ evaluated in (2).

This gives an overall power flow sensitivity factor (SSF$_{i,k,m}^c$) of component c, from node i to node k, because of an injection of real power, at node m, as in (7)

$$\mathrm{SSF}_{i,k,m}^c = \left[\left(\left(\frac{\partial P}{\partial \theta}\right)_{i,k}\left(\frac{\mathrm{d}\theta_k}{\mathrm{d}G_{P,m}} - \frac{\mathrm{d}\theta_i}{\mathrm{d}G_{P,m}}\right)\right) \right.$$
$$+ \left(\left(\frac{\partial P}{\partial |E|/|E|}\right)_{i,k}\left(\frac{\mathrm{d}|E_k|/|E_k|}{\mathrm{d}G_{P,m}} - \frac{\mathrm{d}|E_i|/|E_i|}{\mathrm{d}G_{P,m}}\right)\right)\right]$$
$$+ j\left[\left(\left(\frac{\partial Q}{\partial \theta}\right)_{i,k}\left(\frac{\mathrm{d}\theta_k}{\mathrm{d}G_{P,m}} - \frac{\mathrm{d}\theta_i}{\mathrm{d}G_{P,m}}\right)\right)\right.$$
$$+ \left(\left(\frac{\partial Q}{\partial |E|/|E|}\right)_{i,k}\left(\frac{\mathrm{d}|E_k|/|E_k|}{\mathrm{d}G_{P,m}} - \frac{\mathrm{d}|E_i|/|E_i|}{\mathrm{d}G_{P,m}}\right)\right)\right] \quad (7)$$

Simplified versions of the power flow sensitivity factor theory (focusing on the P-θ sensitivity) are used at the transmission level for real power flow sensitivity analyses. The generation shift factor technique proposed by Wood and Wollenburg [18] is acceptable for use in DC representations of AC systems where the network behaviour is approximated by neglecting MVAr flow and assuming the voltage to be constant. However, in distribution networks those assumptions do not always hold since, in some cases, the ratio of $X/R \simeq 1$ and reactive power flow may contribute to a significant portion of the resultant power flowing in components. Thus, it is important that both real and reactive power flows are considered when assessing the locations of

thermally vulnerable components and developing techniques for the online power output control of DG.

The phenomenon of bi-directional power flow is becoming increasingly more common in distribution networks, particularly in situations when installed DG capacity meets the local load demand and begins to export power in the opposite direction through feeders or back through transformers into higher voltage levels. Thus, it is important to understand the reverse power flow capability of transformers [19]. Since the connection of DG may cause power flows to reverse through components under certain load-generation patterns, a frame of reference must be established whereby power flow sensitivities can be related to power flow directions and directional limits. Only by doing this, is it possible to assess whether the power flow sensitivities of components to concurrent nodal injections will cause power flows to aggregate through the components or oppose one another, creating counter-flows and finding different impedance routes through the network. Pantos and Gubina describe this phenomenon in a simple diagram that displays the four possible power flow combinations of real and reactive power flow flowing to and from nodes in the same reference frame [20].

2.2.2 Thermal limits: Thermal limits within power systems are a well known phenomenon with static limits applied to power system components in the formulation of OPFs to solve a variety of problems from economic dispatch [21] at the transmission level to more recent voltage rise issues at the distribution level [22]. The work describing voltage rise issues is of particular relevance to the research presented in this paper as it is concerned with the control of DG power output as determined by the voltage sensitivity factors. At present, the thermal limit applied by DNOs tends to be based on fixed or assumed meteorological conditions that are not always an accurate representation of the actual operating conditions [23], the result of which is potentially a conservative constraint on power flows.

For the purpose of this research, real-time thermal ratings are defined as a time-variant rating, which can be practically exploited without damaging components or reducing their lifetime. Actual environmental parameter measurements are used as the input to steady-state thermal models. In order to calculate and exploit the real-time thermal rating, it is assumed that local environmental parameters are available and that there are no outages (planned or unplanned) present within the electrical power system. Short-term transients, taking into account the thermal capacitance of power system assets are not included within the real-time thermal rating assessment. It is felt that this would not affect the MWh/annum throughput of energy within the electrical power system.

The steady-state current carrying capacity of an overhead line conductor is related to meteorological parameters as given in (8) [24]. Similar equations may be found in [25]

for electrical cables and [26] for power transformers

$$I_{max} = \sqrt{\frac{P_{rad} + P_{conv} - P_{sol}}{R}} \qquad (8)$$

where I_{max} (A) is the steady-state current carrying capacity, P_{rad} (W/m) the heat loss by radiation of the conductor, P_{conv} (W/m) the convective heat loss through wind cooling, P_{sol} (W/m) the solar heat gain by the conductor surface and R (Ω/m) the AC electrical resistance of the conductor at its maximum operating temperature.

The maximum allowable apparent power through a component is a function of the current and voltage and can be described by (9) [27]

$$S_{lim} = |P + jQ|_{lim} = \sqrt{3}EI_{max} \qquad (9)$$

where S_{lim} (MVA) is the maximum allowable apparent flow or thermal limit of a component, $|P + jQ|_{lim}$ represents the real and reactive components of the maximum apparent power flow, E (kV) represents the voltage of the component and I_{max} (A) is the steady-state current carrying capacity of the conductor.

3 Network power flow management through power flow sensitivity factors

In a generalised manner, this section demonstrates how the power flow sensitivity factors may be assessed and used in Stages 1 and 4 of the proposed network power flow management process to formulate the thermal vulnerability factors and for the online control of DG power output coupled with real-time thermal ratings resulting from Stages 2 and 3.

3.1 Formulation of thermal vulnerability factors

Equation (7) may be combined with (9) and the resulting thermal vulnerability factors, as seen in (10), is standardised by conversion to a per unit term on the base MVA

$$\text{TVF}_{i,k,m}^c = \left(\frac{\text{SSF}_{i,k,m}^c}{S_{lim}^c}\right) \text{ on } S_{base} \qquad (10)$$

where $\text{TVF}_{i,k,m}^c$ represents the thermal vulnerability factor of component c, from node i to node k because of a real power injection at node m; $\text{SSF}_{i,k,m}^c$ represents the power flow sensitivity factor of component c, from node i to node k, because of a real power injection at node m; S_{lim}^c (MVA) represents the thermal limit of component c; and S_{base} is a predefined MVA base.

This gives a consistent measure of component thermal vulnerabilities, relative to one another and accounts for

different nodal real power injections, for a particular network operating condition. It can also be seen in (11) that the sensitivity factor relative to the component rating is equivalent to the change in utilisation of a particular component c from node i to node k, because of an injection of real power at node m

$$\left(\frac{\text{SSF}_{i,k,m}^c}{S_{lim}^c}\right) = \left(\frac{\Delta S_{i,k}^c}{\Delta G_{P,m} \times S_{lim}^c}\right) \equiv \left(\frac{\Delta U_{i,k}^c}{\Delta G_{P,m}}\right) \qquad (11)$$

where $\text{SSF}_{i,k,m}^c$ represents the power flow sensitivity factor of component c, from node i to node k, because of a real power injection at node m; S_{lim}^c (MVA) represents the thermal limit of component c; $\Delta S_{i,k}^c$ (MVA) represents the change in apparent power flow in component c, from node i to node k; $\Delta G_{P,m}$ (MW) represents the change in real power injection at node m; and $\Delta U_{i,k}^c$ represents the change in capacity utilisation of component c, from node i to node k.

Power flow sensitivity factors indicate the extent to which the power flow changes within components because of nodal power injections. However, a large change in the power flow, indicated by high sensitivity, does not necessarily mean a component is thermally vulnerable unless its rating is taken into account. A large power flow change in a component with a large thermal rating (S_{lim}^c) could be less critical than a small power flow change in a component with a small rating. By calculating the apparent power sensitivity relative to the rating for each component, the thermally vulnerable components are identified and can be ranked for single nodal power injections or accumulated for multiple injections.

The physical meaning of the thermal vulnerability factor has been described as the change in a component capacity utilisation because of a per unit DG injection at a particular node. Depending on the status of the original power flow before DG is connected, an excursion relative to the rating of 100% (or $\text{TVF}_{i,k,m}^c = 1$), does not necessarily mean a component is thermally overloaded. By definition, the maximum possible $\text{TVF}_{i,k,m}^c$ without overload occurring could be just below 200%, recognising that a power flow utilising almost 100% of thermal capacity in one direction may be reversed by a DG injection to become a 100% utilisation with power flowing in the opposite direction.

3.2 DG power output control through power flow sensitivity factors

Although DG may, at times, be requested to operate in a voltage control mode, it is in the interest of DG operators to maximise the real power output and, hence, maximise the annual exported active energy (MWh) as that directly relates to the revenue of the DG owner. Thus, it is assumed that the network power flow management system outlined in this paper is utilised with DG schemes exporting real power at a unity power factor. An online assessment of the real power output adjustment required by a generator may be calculated in (12) and (13), relating to the component power flow

www.ietdl.org

sensitivity factor and the real-time thermal rating of the component as

$$\Delta G_{P,m} = \frac{\Delta P^c_{i,k}}{(\mathrm{d}P^c_{i,k}/\mathrm{d}G_{P,m})} \qquad (12)$$

where $\Delta G_{P,m}$ (MW) is the required change in the real power output of the generator at node m; $\Delta P^c_{i,k}$ (MW) is the required change in real power flow through component c, from node i to node k, in order to bring the resultant power flow back within thermal limits; $\mathrm{d}P^c_{i,k}/\mathrm{d}G_{P,m}$ is the power flow sensitivity factor that relates the change in nodal real power injection at m with the change in the real power flow seen in component c, from node i to node k and

$$\Delta P^c_{i,k} = \sqrt{((\alpha S^c_{\mathrm{lim}})^2 - (''Q^c_{i,k})^2)} - \sqrt{(('S^c_{i,k})^2 - ('Q^c_{i,k})^2)} \quad (13)$$

where $'S^c_{i,k}$ (MVA) is the apparent power flow in component c before control actions are implemented; $'Q^c_{i,k}$ (MVAr) is the reactive power flow in component c from node i to node k before the control actions are implemented; α is the target utilisation limit of component c after the control actions have been implemented; S^c_{lim} (MVA) is the real-time thermal rating of component c; and $''Q^c_{i,k}$ (MVAr) is the reactive power flow in component c from node i to node k after the control actions have been implemented. Rather than neglecting the MVAr flow, it may be assumed constant for a particular operating condition. Thus, $\mathrm{d}P^c_{i,k}/\mathrm{d}G_{P,m} \gg \mathrm{d}Q^c_{i,k}/\mathrm{d}G_{P,m}$ and a simplification can be made to (13) that $''Q^c_{i,k} \simeq 'Q^c_{i,k}$.

3.3 Assessment of power flow sensitivity and thermal vulnerability factors

The procedure used to assess power flow sensitivity factors and generate lists of thermally vulnerable components for different network topologies is shown in Fig. 1. Initially a 'base case' AC load flow was run in the power system simulation package, IPSA [28], to establish the initial real, reactive and apparent power flows for each component. The procedure iterated by injecting 1 pu of real power at each node of interest and recording the new component power flows. In the UKGDSs, new DG connections have been assumed at existing nodes in the network. However, in the field trial application, the two nodes selected for thermal vulnerability assessments (and resulting DG power output control) correspond to existing DG connection points where DG may be re-planted with larger installed capacities because of future planning applications. The initial flow, final flow and thermal rating of each component were used to relate component power flow sensitivity factors to nodal injections and ratings. The resulting power flow sensitivity factors and thermal vulnerability factors were efficiently stored in matrix form and, with the thermal vulnerability factors represented graphically, a visual identification of the most thermally vulnerable components was given. Assessments were made

at maximum generation – maximum loading and maximum generation – minimum loading conditions to identify the worst-case operating scenario for the critical components. The voltage limits in accordance with [29, 30] were not directly formulated as constraints within the assessments but were constantly monitored in simulation runs through the functionality in IPSA to 'colour'-code the network diagram according to per unit voltage excursions.

4 Development stages for the power output control of DG illustrated by UKGDSs

With the use of UKGDSs, this section of the paper illustrates Stages 1 and 4 in the development of a DG power output control system. UKGDS 'EHV3' was divided into three case study networks for analysis simplification. UKGDS A displays a predominantly meshed topology, whereas UKGDS B and UKGDS C are both predominantly radial in topology. For simulation purposes, the tie-lines between the sub-networks were modelled using IPSA with a load-equivalent to the power flow seen in the line during the full network simulation. The electrical parameters for the case studies, including maximum and minimum loading conditions are given in [31].

4.1 Assessment of thermal vulnerability factors in generic networks

The assessment of the thermal vulnerability factors, described in Section 3 was applied to UKGDS A and UKGDS B to determine the location of thermally vulnerable components for both meshed and radial network topologies because of single-nodal and multiple-nodal real power injections. In validating the assessments, a full AC power flow simulation also yielded the DG capacity that could be connected before thermal issues arose. In each case, it was found that the first technical limit met was a thermal constraint, with voltages close to nominal and within the regulations prescribed in [29].

4.1.1 Thermally vulnerable components resulting from single DG injections in UKGDS A: The assessment of the thermal vulnerability factors, applied to UKGDS A, has been used to establish the relationship between single DG real power injections and the location of thermally vulnerable components. Illustrative vulnerability correlations are shown in Fig. 2 and the simulated DG connection capacities at these nodes have been summarised in Table 1. Fig. 2 is interpreted by relating the magnitude of component thermal vulnerability factors to nodal locations via the network diagram. The DG connection capacities given in Table 1 correspond to a summer minimum loading condition. This is because for a given quantity of DG, for example at node 317, the power exported through feeder
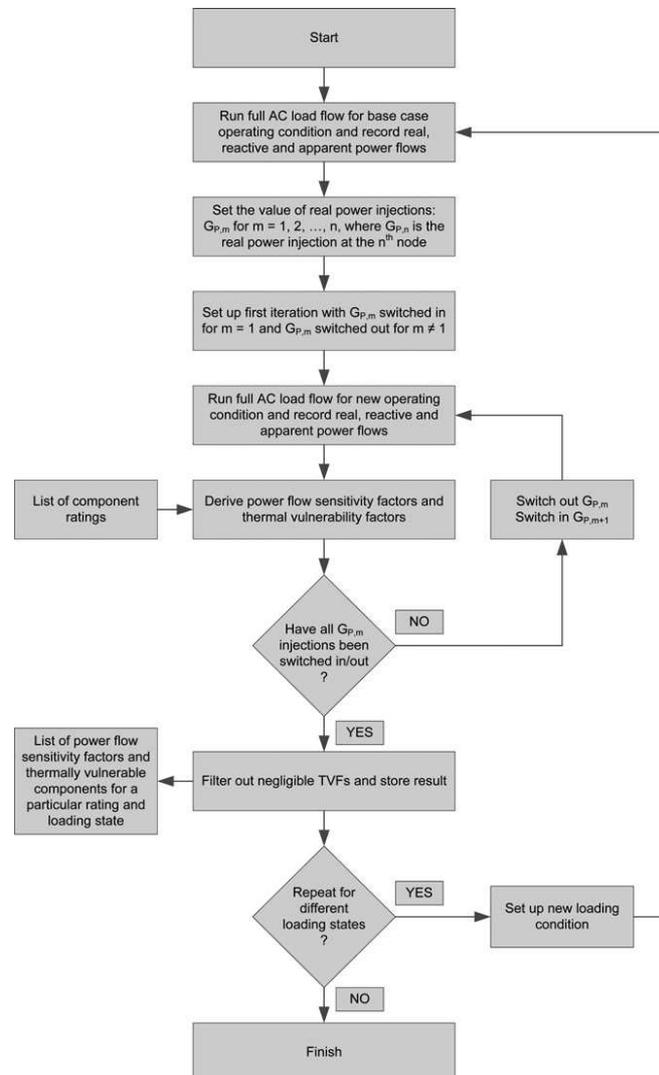
Figure 1 *Flow chart for the assessment of power flow sensitivity factors and thermal vulnerability factors*

C13 to the rest of the network would be greater in summer when the demand through T13 is at a minimum.

Inspecting the results, it can be seen that single DG injections at nodes 317, 318, 352 and 354, each have a vulnerable component local to the point of injection. Topologically, these nodes are in a more radial portion of the distribution system. However, power injection at the meshed node, 314, causes component C15 and then C18

to become thermally vulnerable, which are non-local to the point of DG injection.

4.1.2 Thermally vulnerable components resulting from multiple DG injections in UKGDS B: This section demonstrates how the assessment of the thermal vulnerability factors may be applied to UKGDS B to identify accumulated power flows because of the widespread injection of real power from DG. The graph, together with

www.ietdl.org
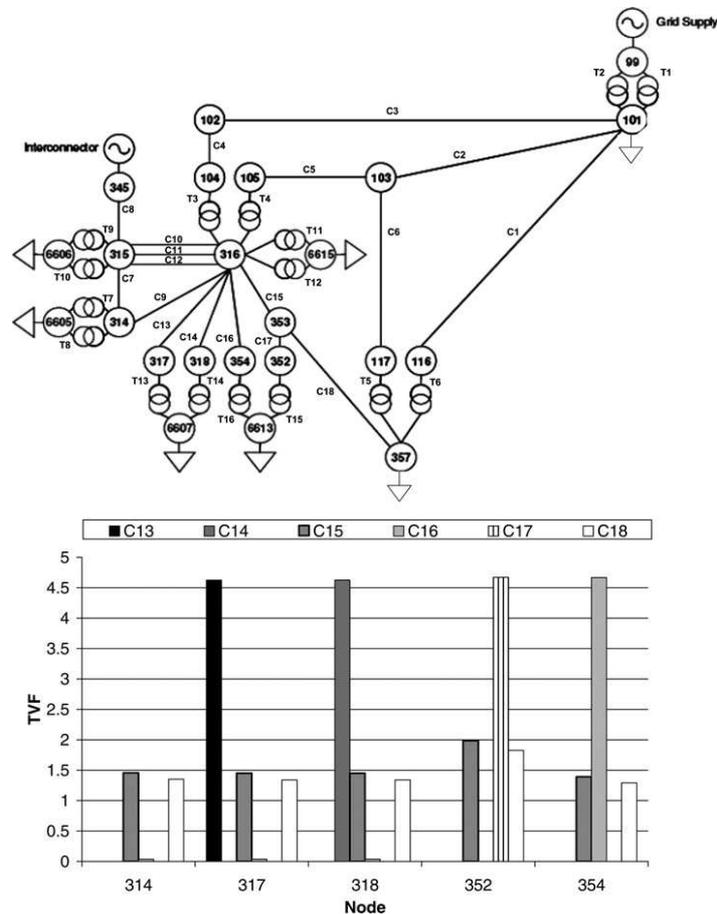
Figure 2 *Vulnerable component identification for single DG injections in UKGDS A*

the network diagram in Fig. 3, shows that, although strong local-overload correlations do exist for some nodes, if small contributions from nodes 324, 327, 328, 329 and 348 are accumulated, then transformers T3 and T4 could potentially be at risk. Table 2 illustrates six cases with a generation scheme switched out in turn (Cases 1–5) and all the generation schemes switched in (Case 6). In the last case, transformer T4 is thermally vulnerable from the accumulation of power flows.

4.2 DG power output control in a generic network

Through a full AC power flow simulation, an assessment was made of the maximum connection capacity of DG that could be individually accommodated at each 33 kV node in UKGDS C (Fig. 4) under the worst-case summer minimum

load demand conditions. DG capacities in excess of these thermal limits (but still within voltage and fault-level limits) were installed to emulate the management of non-firm generation connections. It was assumed that the circuits in the network were overhead lines with the potential to be up-rated by at least 50% – this is not unreasonable given that Aeolian (wind) cooling of the line could produce increased capacities from 20% to as much as 100% [32]. With components up-rated individually (representing an incremental investment in meteorological station installations) and with target utilisation of 100% (i.e. $\alpha = 1$), the maximum possible adjustment in DG real power output was calculated, at each node, using (12) and (13) and validated with a full AC power flow simulation. A comparison was made of the increased DG output that could be achieved because of the increased component rating, and a summary of these findings is given in Table 3.

Table 1 Vulnerable component hierarchies at different nodes in UKGDS A (All values are given in per unit form on 100 MVA base)

DG injection node	Simulated DG connection capacity (at unity power factor)	Thermally vulnerable component	Standard rating
314	0.511	C15	0.2
	0.567	C18	0.2
317	0.236	C13	0.2
318	0.236	C14	0.2
352	0.226	C17	0.2
	0.390	C15	0.2
	0.414	C18	0.2
354	0.228	C16	0.2
	0.466	C15	0.2
	0.501	C18	0.2

4.3 Discussion of generic distribution system results

By analysing thermal vulnerability factors for single and multiple DG power injections, strategic locations for meteorological stations and conductor temperature monitoring equipment may be chosen. In the case of single DG injections at radial nodes, it was found that components local to the point of DG injection may become thermally vulnerable. However, in the case of a single DG injection at a meshed node, it was found that components non-local to the point of injection may become thermally vulnerable. In the case of multiple DG injections, it was observed that widespread power injections may lead to an accumulation of power flows, causing thermal problems on a more global scale.

From the full AC load flow assessments of technical DG connection capacities in UKGDS C, (as shown in Table 3) it can be seen that the greatest DG capacity could be accommodated at nodes 331 and 330. Furthermore, the components that thermally limit the DG power output at these nodes (C7 and C6, respectively) would also facilitate the greatest increase in DG power output for a 50% up-rating of the lines. A comparison of increased line rating against increased DG power output shows that a 50% increase in rating will not necessarily facilitate a 50% increase in DG power output to be achieved. This is a topology-specific conclusion and relates to the magnitude of the power flow sensitivity factors.

Through the constant monitoring of maximum nodal voltage excursions, the analysed networks were found to reach thermal limits before voltage constraints for both the meshed and radial topologies when considering static thermal ratings and, in the illustration of the DG power output control system, with the assets up-rated by 50%. The DG power output control system under development at Durham University has the capability of validating that voltage limits are not violated through the use of an online simulation tool. This tool simulates the real-time electrical status of the distribution network through an electrical model populated with real-time electrical signals. If voltage limits were to become a constraining factor, this would currently need to be dealt with outside the jurisdiction of the DG power output control system, using active voltage measures such as demonstrated in [33].

In making the assumption that $dP_{i,k}^c/dG_{P,m} \gg dQ_{i,k}^i/dG_{P,m}$ and the simplification in (13) that $''Q_{i,k}^i \simeq {}'Q_{i,k}^i$, the largest percentage error between the DG power output adjustment from the control system and the validated DG power output adjustment from the full AC load flow was found to be 1.12% at node 331. In this case, $|\partial P/\partial Q| = 6.8$. The slight discrepancies between adjustments will be accommodated in the control system by designing an error margin into the target utilisation limit, α.

5 Development stages for the control of DG power output applied to a UK field trial network

5.1 Network description

The field trial network to be used in the 'Active management of distributed generators based on component thermal properties' project has a meshed topology with a mixture of overhead line and underground cable infrastructure at 132 kV and 33 kV. Indoor and outdoor transformers convert the voltage between these levels. A schematic diagram of the network is shown in Fig. 5. A 60 MW DG project is connected at B5 and a further 90 MW DG is expected to be connected at B3, teeing into a 132 kV overhead line feeder. The static ratings together with minimum and maximum network loading levels supplied by SPEN from their Long-Term Development Statement [34] and Engineering Recommendations [35–37] were utilised together with current operational practices. The network was simplified by reducing substations to a single node with power flows and nodal voltages validated against those in the original model. A full list of network parameters may be found in the Appendix.

5.2 Assessment of thermal vulnerability factors in the field trial network

The assessment of the thermal vulnerability factors were applied to the field trial network at nodes B3 and B5. The purpose of examining the thermal vulnerability factors for node B5 was to assess the implications of the DG being re-planted with a greater installed capacity in the future. It

www.ietdl.org
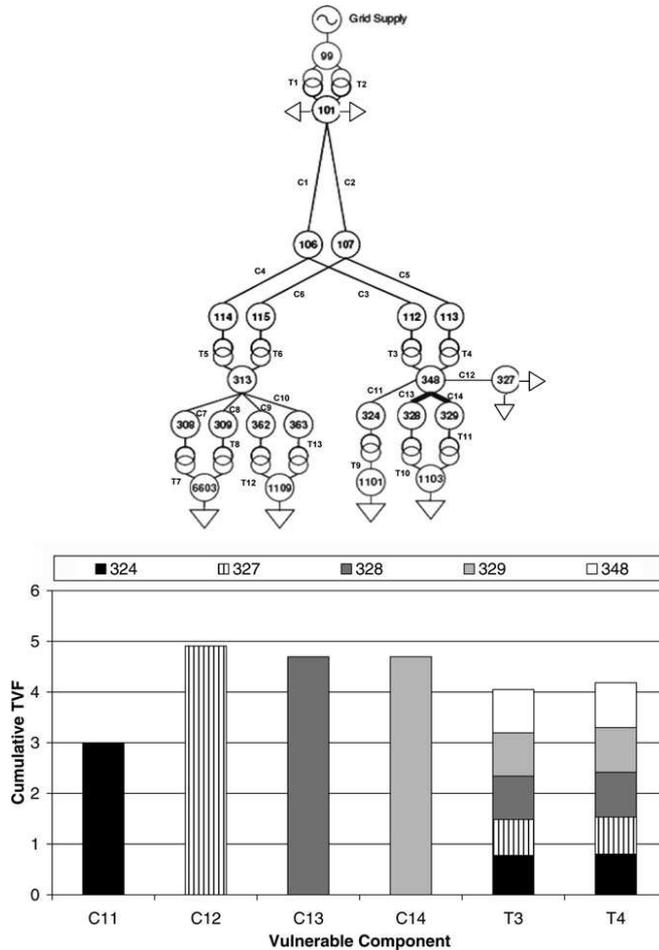
Figure 3 *Assessing the location of vulnerable components through cumulative thermal vulnerability factors in UKGDS B*

Table 2 Accumulation of DG injections that produce an overload in UKGDS B (All values are given in per unit form on 100 MVA base)

	Size and nodal locations of generators (at unity power factor)						T4 rating	T4 power flow
	$G_{P,324}$	$G_{P,327}$	$G_{P,328}$	$G_{P,329}$	$G_{P,348}$	$G_{P,Total}$		
Case 1	–	0.15	0.25	0.25	0.20	0.85	0.45	0.26
Case 2	0.40	–	0.25	0.25	0.20	1.10	0.45	0.37
Case 3	0.40	0.15	–	0.25	0.20	1.00	0.45	0.33
Case 4	0.40	0.15	0.25	–	0.20	1.00	0.45	0.33
Case 5	0.40	0.15	0.25	0.25	–	1.05	0.45	0.36
Case 6	0.40	0.15	0.25	0.25	0.20	1.25	0.45	0.47

Figure 4 *Topological representation of UKGDS C*

Table 3 Application of DG power output control system to UKGDS C (All values are given in per unit form on 100 MVA base unless otherwise stated)

Node	Power flow constraining component	Rating	$dP^c_{i,k}/dG_{P,m}$	$dQ^c_{i,k}/dG_{P,m}$	$\lvert\partial P/\partial Q\rvert$	Simulated DG connection capacity (at unity power factor)	ΔDG output through power output control system, %	ΔDG output through full AC load flow simulation, %
361	C14	0.20	0.983	0.057	17.3	0.288	35.4	35.4
360	C13	0.20	0.981	0.044	22.2	0.288	35.5	35.5
347	C12	0.20	0.992	0.061	16.3	0.265	38.2	38.2
346	C11	0.20	0.991	0.021	46.3	0.265	38.3	38.3
340	C9	0.20	0.999	0.001	>100	0.283	36.0	36.0
339	C8	0.20	0.999	0.001	>100	0.283	36.1	36.1
331	C7	0.30	0.933	0.137	6.8	0.355	45.1	44.6
330	C6	0.30	0.939	0.127	7.4	0.355	45.1	44.8
341	C10	0.20	0.959	0.065	14.7	0.335	31.8	31.5
306	C5	0.20	0.947	0.093	10.2	0.270	39.1	38.8
305	C4	0.20	0.955	0.079	12.0	0.268	38.6	38.2

can be seen in Fig. 5 that circuit C4 is the most thermally vulnerable to a DG injection at node B5, whereas component C3 is the most thermally vulnerable to a DG injection into node B3. The assessment also revealed a counter-flow sensitivity relationship in component C3 where real power injection at node B5 caused a power flow increase from B4 to B3, and real power injection at node B3 caused a power flow increase from B3 to B4. The net effect is that in certain situations, DG injected at B5 could be used to allow greater power export from the DG scheme at B3 through component C3. In this particular case, the phenomenon exists because injection at B5 meets more of

www.ietdl.org

Figure 5 *Thermal vulnerability factor analysis of the field trial network of SPEN*

the local demand in the 'right-hand' portion of the network and, thus, the power from B3 is diverted into component C2. In conjunction with SPEN, a series of full AC power flow simulations demonstrated that potentially up to 115 MW of generation, at a unity power factor, could be accepted at node B5 in the wintertime, reducing to 100 MW in the summertime. Similarly, a generation of 113 MW, at a unity power factor, could potentially be accepted at node B3, reducing to 100 MW during the

summer months. These results are summarised in Table 4 together with the power flow sensitivity factors.

5.3 DG power output control in the field trial network

To illustrate the application of the DG power output control system in the field trial network, it was assumed that DG was installed in excess of the winter values, simulated in Table 4,

Table 4 Simulated DG connection capacities in the field trial network of SPEN (All values are given in per unit form on 100 MVA base unless otherwise stated)

Node	Component	Loading condition	$dP^c_{i,k}/dG_{P,m}$	$dQ^c_{i,k}/dG_{P,m}$	$|\partial P/\partial Q|$	Simulated DG connection capacity (at unity power factor)
B5	C4	winter peak	0.947	−0.001	>100	1.155
B5	C4	summer minimum	0.954	0.003	>100	1.005
B3	C3	winter peak	0.778	−0.018	52.3	1.134
B3	C3	summer minimum	0.778	0.003	>100	1.001

in order to emulate non-firm generation connections. As before, (12) and (13) were used to predict potential DG power output adjustments for a 50% increase in the real-time thermal rating of the power flow-constraining components. In conjunction with SPEN, the predicted power output adjustments were validated through a full AC power flow and a comparison of the results is given in Table 5. In this case, the control system slightly under-predicted the potential power output adjustments. This is attributed to a negative $dQ_{i,k}^c/dG_{P,m}$, which indicates that an increase in real power injection reduces the MVAr flow.

5.4 Discussion of field trial network results

The assessment of the thermal vulnerability factors effectively identified components C3 and C4 as potentially being the power flow-constraining components in the field trial network in the future. From Table 4, the validated results demonstrate that potentially a generation up to 115 MW, at a unity power factor, could be accepted at node B5 in the wintertime, reducing to 100 MW in the summertime. Similarly, a generation of 113 MW, at a unity power factor, could potentially be accepted at node B3, reducing to 100 MW during the summer months. Considering both the DG schemes concurrently, the net result of the vulnerability factors in C3 is lower when the DG at B5 is exporting than when it is not. This result is based on counter-flow sensitivity factors that show that a greater amount of power could be exported from the DG at B3 when the DG at B5 is exporting.

Considering Table 5, a 50% up-rating of component C4 could provide as much as 40.9% of increased DG real power output at node B5 and a 50% up-rating of component C3 could facilitate 50.7% of increased DG access at node B3, within voltage limits. These conclusions were taken forward to an instrumentation meeting with SPEN engineers and resulted in the decision to thermally instrument components C3 and C4 to provide more detailed thermal characterisation, as suggested in Stages 2 and 3 of the development of the DG power output control system.

6 Strategies for the power output control of multiple DG schemes

The power flow sensitivity factors that have underpinned the steps in developing a DG power output control system may be readily incorporated into strategies for the management of multiple DG schemes. A current management strategy adopted by DNOs is a 'last-in, first-off' (LIFO) approach. This requires knowledge of the historical order in which DG schemes were connected to the distribution network. It is assumed that each generation scheme has a separate contractual agreement with the DNO, specifying the network conditions under which the DG may be requested to be constrained or disconnected. If a power flow excursion occurs, which can be attributed to the power output of the DG schemes, the most recently connected generation scheme is requested to constrain its output. This may be achieved through the use of power flow sensitivity factors, requiring a DG real power output change as calculated in (12) and (13). The LIFO strategy aims to ensure that the DG schemes already operating within the distribution network are not penalised, in terms of their power export, by the connection of new generation schemes. If a more holistic view is adopted for the management of multiple DG connections, candidate strategies could include:

1. An egalitarian constraint of DG schemes, where each scheme is requested to effect an equal percentage reduction in its current power output

2. Constraint of DG schemes in accordance with a power flow tracing algorithm [38, 39] that relates the contribution of each DG injection to the power flowing through the thermally vulnerable components

3. Constraint of DG schemes in accordance with their contribution to the total injection of DG at the time of constraint, as illustrated in (14)

$$\Delta G_{P,m} = \frac{\Delta P_{i,k}^c \times (G_{P,m}/G_{P,\text{total}})}{(dP_{i,k}^c/dG_{P,m})} \qquad (14)$$

where $\Delta G_{P,m}$ (MW) is the required change in the real power output of the generator at node m; $\Delta P_{i,k}^c$ (MW) as defined in (13) is the required change in real power flow through component c, from node i to node k in order to bring the resultant power flow back within thermal limits; $G_{P,m}$ (MW) is the measured injection of real power at node m before constraints are implemented; $G_{P,\text{total}}$ (MW) is the measured total injection of real power from the DG schemes before constraints are implemented; and
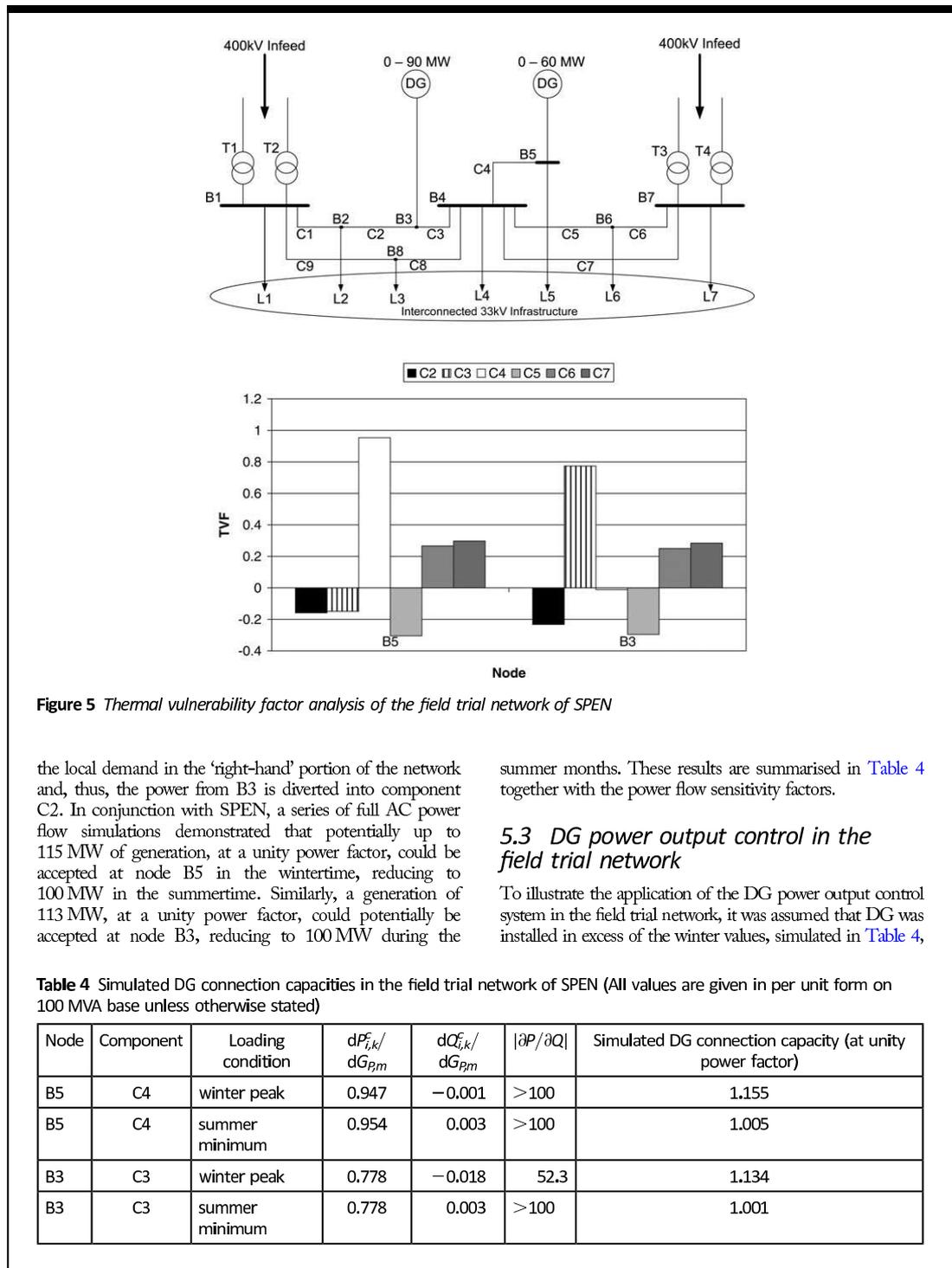
Table 5 Application of DG power output control system to the field trial network (All values are given in per unit form on 100 MVA base unless otherwise stated)

Node	Power flow constraining component	Rating	Simulated DG connection capacity (at unity power factor)	ΔDG output through power output control system, %	ΔDG output through full AC load flow simulation, %
B5	C4	0.89	1.155	40.9	41.0
B3	C3	0.89	1.134	50.7	50.8

www.ietdl.org

$dP^c_{i,k}/dG_{P,m}$ is the power flow sensitivity factor that relates the change in the nodal real power injection at m with the change in real power flow seen in component c, from node i to node k.

7 Discussion

The aim of this research was to outline the development stages required in the power output control of DG for network power flow management and, in particular, to illustrate the role of power flow sensitivity factors.

The purpose of the assessment of the thermal vulnerability factors was to identify thermally vulnerable components within distribution networks. As demonstrated through the UKGDS applications, the assessment of the thermal vulnerability factors is not confined to a specific topology type. It can be applied to predominantly radial, predominantly meshed or mixed topologies with equally valid results. It has been shown that the assessment of the thermal vulnerability factors is appropriate for use in identifying the thermal impacts of planned individual DG schemes or, in a more strategic way, to assess longer term and more widespread DG growth scenarios. Therefore the procedure for the assessment of the thermal vulnerability factors would be valuable for DNOs aiming to develop long-term DG accommodation strategies for the areas of their network.

Instrumentation investment decisions have been made to thermally and electrically characterise the field trial network based on components identified through the assessment of the thermal vulnerability factors. Furthermore, the assessment of the thermal vulnerability factors identifies those components that would most benefit from being thermally monitored to unlock the latent power flow capacity through a real-time thermal rating system, the offline analysis of which may be used for sizing the installed capacity of non-firm DG connections.

The derived power flow sensitivity factors are network configuration-specific and assume that the network configuration will not be frequently changing. It is feasible, however, to develop an online control system that makes use of alternative sets of the above-mentioned predetermined power flow sensitivity factors based on network switch status information.

8 Conclusions

It is anticipated that distribution networks will see a proliferation of DG in the coming years. In some cases, this will result in power flow congestion with the thermally vulnerable components restricting the connection capacity and annual active energy yield of DG. Therefore a system that can be developed for the management of power flows

within distribution networks, through the power output control of DG schemes, could be of great benefit. The development stages of such a system were illustrated using UKGDSs and applied to a field trial network in the UK. These included: (i) the identification of thermally vulnerable components through an assessment of the thermal vulnerability factors that related power flow sensitivity factors to component thermal limits, (ii) the strategic investment in meteorological and conductor temperature monitoring equipment for the thermal characterisation of the network, informed by the assessment in the previous stage, (iii) the development of a real-time thermal rating system that would allow component steady-state thermal models to be populated with real-time data from the monitoring equipment installed in the previous phase and (iv) the use of the real-time thermal ratings together with power flow sensitivity factors to control the power output of DG for the online management of network power flows. The key development stages were validated through simulation on the field trial network and resulted in the strategic investment of meteorological stations for the thermal characterisation of that section of the UK power system. The application of the control system development stages to that section of the network also yielded a counter-flow finding based on opposing power flow sensitivity factors, highlighting the fact that increasing the output of one DG scheme could enable the increased output of an entirely separate DG scheme. The power flow sensitivity factors have the potential to be embedded in an online control system with a view to managing the output of multiple DG schemes, based on real-time knowledge of the thermal and electrical status of the distribution network.

9 Acknowledgments

10 References

[1] STRBAC G.: 'Electric power systems research on dispersed generation', *Electr. Power Syst. Res.*, 2007, **77**, pp. 1143–1147

[2] JENKINS N., ALLAN R., CROSSLEY P., KIRSCHEN D., STRBAC G.: 'Embedded generation' (IEE, 2000), Power and Energy Series 31

www.ietdl.org

[3] Office of gas and electricity markets: 'Electricity distribution price control review, final proposals', November 2004, available at: http://www.ofgem.gov.uk/Networks/ElecDist/PriceCntrls/DPCR4/Pages/DPCR4.aspx, accessed February 2008

[4] http://www.bwea.com/ukwed/index.asp, accessed February 2008

[5] NEUMANN A., TAYLOR P., JUPE S., ET AL.: 'Dynamic thermal rating and active control for improved distribution network utilisation'. Proc. PowerGrid Europe, Milan, Italy, 3–5 June 2008

[6] DINIC N., FLYNN D., XU L., KENNEDY A.: 'Increasing wind farm capacity', IEE Proc., GTD, 2006, 153, (4), pp. 493–498

[7] CURRIE R.A.F., AULT G.W., MCDONALD J.R.: 'Methodology for determination of economic connection capacity for renewable generator connections to distribution networks optimised by active power flow management', IEE Proc. GTD, 2006, 153, (4), pp. 456–462

[8] VOVOS P.N., HARRISON G.P., WALLACE A.R., BIALEK J.W.: 'Optimal power flow as a tool for fault level-constrained network capacity analysis', IEEE Trans. Power Syst., 2005, 20, (2), pp. 734–741

[9] MENDEZ QUEZADA V.H., ABBAD J.R., SAN ROMAIN G.T.: 'Assessment of energy distribution losses for increasing penetration of distributed generation', IEEE Trans. Power Syst., 2006, 21, (2), pp. 533–540

[10] HARRISON G.P., WALLACE A.R.: 'Optimal power flow evaluation of distributed network capacity for the connection of distributed generation'. IEE Proc. GTD, 2005, 152, (1), pp. 115–122

[11] MASTERS C.L.: 'Voltage rise: the big issue when connecting embedded generation to long 11 kV overhead lines', Power Eng. J., 2002, 16, (1), pp. 5–12

[12] SMART P., DINNING A., MALOYD A., CAUSEBROOK A., COWDROY S.: 'Accommodating distributed generation', Econnect Project No: 1672, DTI 2006

[13] DOUGLASS D.A., LAWRY D.C., EDRIS A.-A., BASCOM E.C. III: 'Dynamic thermal ratings realize circuit load limits', IEEE Comput. Appl. Power, 2000, 13, (1), pp. 38–44

[14] NUIJTEN J.A., GRESCHIERE A., SMIT J.C., FRIJMERSUM G.J.: 'Future network planning and grid control'. Proc. Int. Conf. Future Power Systems, 16–18 November 2005

[15] YIP H.T., AN C., ATEN M., FERRIS R.: 'Dynamic line rating protection for wind farm connections'. 9th Int. Conf. Developments Power System Protection, Glasgow, UK, 17–20 March 2008

[16] COLLINSON A., DAI F., BEDDOES A., CRABTREE J.: 'Solutions for the connection and operation of distributed generation'. DTI, July 2003

[17] BERENDE M.J.C., SLOOTWEG J.G., CLEMENS G.J.M.B.: 'Incorporating weather statistics in determining overhead line ampacity'. Proc. Int. Conf. Future Power Systems, 16–18 November 2005

[18] WOOD A.J., WOLLENBERG B.F.: 'Power generation, operation and control' (Wiley, 1996), pp. 421–427

[19] CIPCIGAN L.M., TAYLOR P.C.: 'Investigation of the reverse power flow requirements of high penetrations of small scale embedded generation', IET Proc. RPG, 2007, 1, (3), pp. 160–166

[20] PANTOS M., GUBINA F.: 'A flow-tracing method for transmission networks', Energy, 2005, 30, pp. 1781–1792

[21] HUNEAULT M., GALIANA F.D.: 'A survey of the optimal power flow literature', IEEE Trans. Power Syst., 1991, 6, (2), pp. 762–770

[22] ZHOU Q., BIALEK J.W.: 'Generation curtailment to manage voltage constraints in distribution networks', IET Proc., GTD, 2007, 1, (3), pp. 492–498

[23] ROBERTS D.A.: 'Network management systems for active distribution networks – a feasibility study' (SP Power Systems Ltd, Scottish Power Plc, 2004)

[24] IEC 61597: 'Overhead electrical conductors – calculation methods for stranded bare conductors, '1995

[25] IEC 60287-1-1:1994: 'Electric cables – calculation of the current rating – Part 1: current rating equations (100% load factor) and calculation of losses', 1994

[26] IEC 354: 'Loading guide for oil-immersed power transformers', 1991

[27] WEEDY B., CORY B.: 'Electric power systems' (Wiley, 1967, 4th edn.), 1998

[28] http://www.ipsa-power.com/, accessed February 2008

[29] DTI: 'The electricity safety, quality and continuity regulations, The Stationery Office', 2002

[30] Engineering Recommendation P28-1989: 'Planning limits for voltage fluctuations caused by industrial, commercial and domestic equipment in the UK', 2003

[31] FOOTE C., DJAPIC P., AULT G., MUTALE J., BURT G., STRBAC G.: 'United Kingdom Generic Distribution System (UKGDS) – summary of EHV networks', DTI Centre for

www.ietdl.org

Distributed Generation and Sustainable Electrical Energy, March 2006, http://monaco.eee.strath.ac.uk/ukgds/php/file.php?id=91, accessed February 2008

[32] BELBEN P.B., ZIESLER C.D.: 'Aeolian uprating: how wind farms can solve their own transmission problems'. World Wind Energy Conf. and Exhibition, Berlin, Germany, July 2002

[33] HIRD M., JENKINS N., TAYLOR P.C.: 'An active 11 kV voltage controller: practical considerations'. Proc. from 17th Conf. Electricity Distribution CIRED, Barcelona, 12–15 May 2003

[34] SP transmission and distribution: 'Distribution long term development statement for SP Manweb PLC for the years 2005/6 to 2009/10', SP Manweb plc, November 2005

[35] Engineering recommendation P15 – 1979: 'Transformer loading guide: a guide to the loading of double wound transformers having nominal ratings of 120 MVA and below, Supplying Systems at 66 kV and below from Supergrid and 132 kV systems', 2003

[36] Engineering recommendation P17 – 1976: 'Part 1: current rating guide for distribution cables', 2003

[37] Engineering recommendation P27 – 1986: 'Current rating guide for high voltage overhead lines operating in the UK distribution system', 2003

[38] BIALEK J.W.: 'Tracing the flow of electricity', IET Proc., GTD, 1996, **143**, pp. 313–320

[39] KIRSCHEN D., STRBAC G.: 'Tracing active and reactive power between generators and loads using real and imaginary currents', IEEE Trans. Power Syst., 1999, **14**, (4), pp. 1312–1318

11   Appendix

Unless otherwise stated, all values are given in per unit form on 100 MVA base.

Infeeds

Infeed point	Summer	Winter
T1	$0.47797 - j0.07695$	$1.21042 + j0.35052$
T2	$0.47624 - j0.07675$	$1.206 + j0.34903$
T3	$-0.12812 + j0.12106$	$0.73085 + j0.49021$
T4	$-0.12812 + j0.12106$	$0.73085 + j0.49021$

Nodal voltages

Node	Voltage, kV
B1	132
B2	132
B3	132
B4	132
B5	132
B6	132
B7	132

Component data

Name	Voltage, kV	R	X	Rating
T1	400/132	0.0014	0.0829	2.4
T2	400/132	0.0014	0.0832	2.4
T3	400/132	0.0015	0.0813	2.4
T4	400/132	0.0015	0.0813	2.4
C1	132	0.042176	0.094215	0.89
C2	132	0.01827	0.0407	0.89
C3	132	0.004862	0.013975	0.89
C4	132	0.007	0.0165	0.89
C5	132	0.014772	0.032786	0.89
C6	132	0.01314	0.0326	0.89
C7	132	0.0262	0.0658	0.89
C8	132	0.027341	0.060908	0.89
C9	132	0.024559	0.054979	0.89

Loading

Load	Summer	Winter
L1	$0.52191 + j0.16237$	$1.69525 + j0.54876$
L2	$0.09694 + j0.02983$	$0.34507 + j0.15064$
L3	$0.04624 + j0.00192$	$0.14267 + j0.02349$
L4	$0.06751 + j0.00170$	$0.22313 + j0.10697$
L5	$0.06239 + j0.02601$	$0.21023 + j0.09029$
L6	$0.11822 + j0.03568$	$0.41951 + j0.20115$
L7	$0.60351 + j0.17862$	$2.03067 + j0.59877$

743

Investigation into the influence of environmental conditions on power system ratings

A Michiorri[1]*, P C Taylor[1], S C E Jupe[1], and C J Berry[2]
[1]School of Engineering, Durham University, Durham, UK
[2]ScottishPower EnergyNetworks, Birkenhead, UK

Abstract: This article presents research that seeks to assist distribution network operators in the adoption of real-time thermal rating (RTR) systems. The exploitation of power system rating variations is challenging because of the complex nature of environmental conditions such as wind speed. The adoption of an RTR system may overcome this challenge and offers perceived benefits such as increased distributed generation (DG) accommodation and avoidance of component damage or premature ageing. Simulations, using lumped parameter component models, are used to investigate the influence of environmental conditions on overhead line, electric cable, and power transformer ratings. Key findings showed that the average rating of overhead lines, electric cables, and power transformers ranged from 1.70 to 2.53, 1.00 to 1.06, and 1.06 to 1.10 times the static rating, respectively. Since overhead lines were found to have the greatest potential for rating exploitation, the influence of environmental conditions on four overhead line types was investigated and it was shown that the value of an RTR system is location dependent. Furthermore, the additional annual energy yield from DG that could potentially be accommodated through deployment of an RTR system was found to be 54 per cent for the case considered.

Keywords: overhead lines, electric cables, power transformers, real-time ratings, distributed generation

1 INTRODUCTION

This article describes the offline simulation of power system thermal models populated with historical environmental conditions in order to derive real-time thermal ratings (RTRs). This information is used to quantify (in GWhs) the exploitable headroom that may be achieved by implementing an RTR system within distribution networks. In many cases the current carrying capacity of power system components is limited by a maximum allowable operating temperature. Actual component operating temperatures are determined by the ability of components to dissipate to the environment the heat produced by the Joule effect and by environmental conditions such as ambient temperature and wind speed, which are continuously varying. As a result, the current carrying capacity

of components may be continually assessed and this is proportional to the RTR in MVA. For the purpose of this research, RTRs are defined as a time-variant rating that can be practically exploited without damaging components or reducing their life expectancy. Actual measurements of environmental conditions are used as the input to steady-state thermal models. In order to calculate and exploit the RTR, it is assumed that local environmental condition measurements are available and that there are no outages (planned or unplanned) present within the electrical power system. Short term transients, taking into account the thermal capacitance of power system components, are not included within the RTR assessment. It is felt that this would not materially affect the GWh/annum throughput of energy within the electrical power system. The mechanisms of heat exchange underpinning component ratings are well documented [1–3]. However, the estimation of component operating temperatures (and thus current carrying limits) is a non-trivial task. This is because of the complexity of monitoring and modelling environmental conditions. For this

Corresponding author: School of Engineering, Durham University, South Road, Durham, DH1 3LE, UK.
email: andrea.michiorri@durham.ac.uk

reason component ratings based on fixed assumptions of environmental conditions are often used by distribution network operators (DNOs). The implementation of an RTR system has the potential to give DNOs greater visibility of network operating conditions thus reducing the risk of exceeding the component maximum operating temperature. This could be used both offline, to inform power system planning, and online, within future operational philosophies, in order to increase cautiously the utilization of power system components. However, system implementation requires a number of challenges to be overcome, including the measurement, estimation and communication of real-time component temperatures, and environmental conditions. At the distribution network level these are likely to be dispersed over complex terrains throughout wide geographical areas containing significant numbers of power system components. The research described in this article forms part of a UK Government part-funded project [4] that aims to develop and deploy an online power output controller for distributed generation (DG) based on component RTRs. In this project a DG power output controller compares RTRs with network power flows and produces set points that are fed back to the DG operator for implementation, as shown in Fig. 1. The research consortium includes ScottishPower EnergyNetworks, AREVA T&D, PB Power, and Imass and Durham University.

The article is structured in the following way: section 2 provides an overview of relevant work. In section 3, the models developed for network components and environmental conditions are described. Section 4 describes the component data, the environmental condition data, and the RTR simulation approach and, in section 5, simulation results are presented and discussed.
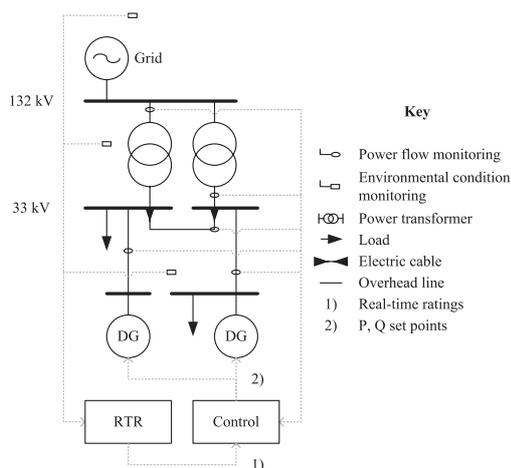
2 RELEVANT WORK

Significant research has been carried out at the transmission level for RTR applications. Research tends to focus on overhead lines, which, because of their exposure to the environment, exhibit the greatest rating variability. A description of the cost and suitability of different uprating techniques for overhead lines is described in reference [5], taking into account different operating conditions. This work shows how RTRs can be a more appropriate solution than network reinforcement when connecting new customers to the network who are able to curtail their generation output or reduce their power demand requirement at short notice. Similarly, experience regarding thermal uprating in the UK is reported in reference [6] where it was suggested that RTRs could give overhead lines an average uprating of 5 per cent for 50 per cent of the year. An example of an RTR application for transmission overhead lines of Red Eléctrica de España is described in reference [7], where a minimal amount of weather stations are used to gather real-time data. The data are then processed using a meteorological model based on the Wind Atlas Analysis and Application Program (WAsP) [8], taking into account the effect of obstacles and ground roughness, and finally the rating is calculated. A similar system was developed in the USA by EPRI in the late 1990s, which considered overhead lines, power transformers, electric cables, and substation equipment. The system is described in reference [9] and preliminary results of field tests are given in reference [10]. A key finding was that up to 12 h of low wind speeds (<0.76 m/s) were observed during the field tests, which therefore suggests that overhead line RTRs may be lower than seasonal ratings for extended periods of time. Furthermore, a strong correlation was found to exist between independent air temperature measurements distributed along the lengths of the overhead lines. At the distribution level, an RTR project carried out by the Dutch companies NUON and KEMA is described in reference [11] that demonstrates the operating temperature monitoring of overhead lines, electric cables, and power transformers.

The advantages of an RTR system for the connection of DG, especially wind power, are reported in various sources, each of which considers only single power system components. It is demonstrated in reference [12] that the rating of transformers positioned at the base of wind turbines may presently be oversized by up to 20 per cent. Moreover, in reference [13] the power flowing in an overhead line close to a wind farm is compared to its RTR using WAsP. In this research, it was highlighted that high power flows resulting from wind generation at high wind speeds could be accommodated since the same wind speed has a positive effect on the line cooling. This observation makes the adoption of RTR systems

Fig. 1 DG power output controller informed by RTRs

relevant in applications where strong correlations exist between the cooling effect of environmental conditions and electrical power flow transfers. Moreover, in references [14] to [16] the influence of component thermal model (CTM) input errors on the accuracy of RTR systems is studied. The application of different state estimation techniques, such as affine arithmetic, interval arithmetic, and Montecarlo simulations was studied for overhead lines, electric cables, and power transformers. Errors of up to ±20 per cent for an operating point of 75 °C, ±29 per cent for an operating point of 60 °C and ±15 per cent for an operating point of 65 °C were found when estimating the operating temperature of overhead lines, electric cables, and power transformers, respectively. This highlights the necessity to have reliable and accurate environmental condition monitoring. The thermal models, used to estimate RTRs for different types of power system components, are fundamental to this research as the accuracy of the models influences significantly the accuracy of RTRs obtained. Particular attention was given to industrial standards because of their wide application and validation both in industry and academia. For overhead lines, the model is described in references [17] and [18] that has been developed into industrial standards [1, 19, 20] by the IEC, CIGRE, and IEEE, respectively. Static seasonal ratings for different standard conductors and for calculated risks are provided by the Electricity Network Association (ENA) in reference [21]. Thermal model calculation methods for electric cable ratings are described in reference [22] and developed into an industrial standard by the IEC in reference [2]. The same models are used by the IEEE in reference [23] and the ENA in reference [24] to produce tables of calculated ratings for particular operating conditions. Power transformer thermal behaviour is described in reference [25] with further models described in the industrial standards [3, 26, 27] by the IEC, IEEE, and ENA, respectively.

The research presented in this article adds to the work described above by modelling the influence of environmental conditions on multiple power system component types simultaneously. This is of particular relevance in situations where the increased power flow resulting from the alleviation of the thermal constraint on one power system component may cause an entirely different component to constrain power flows. Furthermore, with the expected proliferation of DG the resulting power flows are likely to affect many components and it is important to take a holistic view of power system thermal ratings. Since this research project aims to develop and deploy an economically viable real-time system, it is important that algorithms are developed with fast computational speeds using a minimal amount of environmental condition monitoring. Thus an inverse distance interpolation technique is used for modelling environmental conditions across a wide geographical area,

which offers faster computational speeds than applications such as WAsP. Beyond the research described above, this article also aims to quantify the annual energy throughput that may be gained through the deployment of an RTR system.

3 MODELLING APPROACH

3.1 Components

In order to assess, in a consistent manner, component RTRs because of the influence of environmental conditions, thermal models were developed based on IEC standards [1–3] for overhead lines, electric cables, and power transformers, respectively. Where necessary, refinements were made to the models using [19, 24]. Steady-state models have been used in preference to dynamic models since this would provide a maximum allowable rating for long term power system operation. Moreover, the estimation of final steady-state component temperatures after a transient has occurred is influenced by initial conditions, which must also be estimated. It is felt that with the resolution of the available data (comprising hourly averaged environmental conditions) it is extremely difficult to obtain an acceptable precision for dynamic models, particularly for overhead lines with time constants of less than an hour.

3.1.1 Overhead lines

Overhead line ratings are constrained by a necessity to maintain statutory clearances between the conductor and other objects. The temperature rise causes conductor elongation which, in turn, causes an increase in sag. The line sag S depends on the tension H, the weight m applied to the conductor inclusive of the dynamic force of the wind and the length of the span. The sag can be calculated as a catenary or its parabolic approximation, as given in equation (1). To calculate the tension, it is necessary to consider the thermal-tensional equilibrium of the conductor, as shown in equation (2). For calculating the conductor operating temperature at a given current, or the maximum current for a given operating temperature, it is necessary to solve the energy balance between the heat dissipated in the conductor by the current, and the thermal exchange on its surface, as given in equation (3)

$$S = \frac{H}{mg}\left[\cosh\left(\frac{mgL}{2H}\right) - 1\right] \approx \frac{mgL^2}{8H} \tag{1}$$

$$EA\beta\left(T_{c,2} - T_{c,1}\right) + \left(\frac{m_1^2 g^2 L^2 EA}{24 H_1^2}\right) - H_1$$

$$= \left(\frac{m_2^2 g^2 L^2 EA}{24 H_2^2}\right) - H_2 \tag{2}$$

$$q_c + q_r = q_s + I^2 r \tag{3}$$

The formulae proposed in reference [1] were used for the calculation of the contribution of solar radiation q_s, radiative heat exchange q_r, and convective heat exchange q_c. These equations are shown in equations (4) to (6), respectively

$$q_s = \alpha D \, Sr \tag{4}$$

$$q_r = \varepsilon \sigma_{S-B}(T_c^4 - T_a^4)\pi D \tag{5}$$

$$q_c = \pi Nu\lambda(T_c - T_a) \tag{6}$$

The influences of wind direction and natural convection on convective heat exchange are not considered in reference [1]. However, in this research these effects were considered to be important, particularly as a wind direction perpendicular to the conductor would maximize the turbulence around the conductor and hence the heat exchange on its surface whereas a wind direction parallel to the conductor would reduce the heat exchange with respect to perpendicular wind direction. Therefore, the modifications proposed in reference [19] and given in equations (7) and (10) were used. It is possible to calculate the Nusselt number Nu from the Reynolds number Re as shown in equation (8). The Reynolds number can be calculated using equation (9)

$$K_{dir} = K_{dir-1} + K_{dir-2} \sin^{K_{dir-3}}(Wd) \tag{7}$$

$$Nu = K_{dir}(0.65 \, Re^{0.2} + 0.23 \, Re^{0.61}) \tag{8}$$

$$Re = 1.644 \times 10^9 \, Ws \, D \left(\frac{T_c + T_a}{2}\right)^{-1.78} \tag{9}$$

For null wind speeds, the Nusselt number must be calculated as in equation (10) where Gr is the Grashof number, calculated as in equation (11), and Pr is the Prandtl number

$$Nu = K_{nat-1}(Gr \, Pr)^{K_{nat-2}} \tag{10}$$

$$Gr = \frac{D^3(T_c - T_a)g}{[(T_c + T_a)/2]\nu^2} \tag{11}$$

It should be noted that for wind speeds between 0–0.5 m/s the larger of the Nusselt numbers resulting from equations (8) and (10) should be used.

3.1.2 Electric cables

The current carrying capacity of electric cables is limited by the maximum operating temperature of the insulation. Sustained high currents may generate temperatures in exceedance of the maximum operating temperature, causing irreversible damage to the cable. In extreme cases this may result in complete insulation deterioration and cable destruction.

References [2], [22], and [23] were used to model the conductor temperature in steady-state conditions. This accounts for the heat balance between the power

dissipated in the conductor by the Joule effect, and the heat dissipated in the environment through the thermal resistance R_T of the insulation and the soil as shown in equation (12). The electrical current rating may then be calculated, as shown in equation (13)

$$I^2 r = \frac{\Delta T}{R_T} \tag{12}$$

$$I = \sqrt{\frac{\Delta T}{rR_T}} \tag{13}$$

Refinements incorporating dielectric losses q_d, eddy currents and circulating currents in metallic sheaths ($\lambda_{1,2}$), resistance variation with temperature, skin and proximity effects, and the thermal resistance of each insulating layer $R_{T,i}$ lead to the more complex equation (14)

$$I = \sqrt{\frac{\Delta T - q_d[1/2 \, R_{T,1} + n(R_{T,2} + R_{T,3} + R_{T,4})]}{r(T_c)[R_{T,1} + n(1 + \lambda_1)R_{T,2} + n(1 + \lambda_1 + \lambda_2)(R_{T,3} + R_{T,4})]}} \tag{14}$$

Thermal resistances for cylindrical layers are calculated with equation (15) and soil thermal resistance is modelled with equation (16). Other calculation methods [2] have to be utilized when operating conditions differ from those stated above (for example when the cable is in a duct or in open air)

$$R_{T-1,2,3} = \frac{\rho_{s-T}}{2\pi} \ln\left(1 + 2\frac{D-d}{d}\right) \tag{15}$$

$$R_{T-4} = \frac{\rho_{s-T}}{2\pi} \ln \frac{2z_b}{D} + \sqrt{\left(\frac{2z_b}{D}\right)^2 + 1} \tag{16}$$

The model described above requires detailed knowledge of the electric cable installation. However, this information may not always be available and therefore it is difficult to make practical use of the model. In these circumstances an alternative model, described in reference [24] and summarized in equation (17), may be used. The rated current of electric cables I_0 is given in tables depending on the standardized cable cross-sectional area and laying conditions (trefoil, flat formation; in air, in ducts, or directly buried). The dependence of the cable ampacity on external temperature and soil thermal resistivity is made linear through the coefficients ξ_T and ξ_ρ, respectively.

$$I = I_0(A, V, \text{laying})[\xi_T(T_s - T_{s\,\text{rated}})][\xi_\rho(\rho_{s,T} - \rho_{s\,T\,\text{rated}})] \tag{17}$$

Since this research concerns the influence of environmental conditions on component ratings, the effect of the voltage level V, which influences the dielectric loss q_d in equation (14) is not considered. The effect

of the heating given by adjacent components is also neglected as it is assumed that each cable has already been de-rated to take this effect into account.

3.1.3 Power transformers

The model described in reference [3] was used to calculate the winding hot spot temperature for power transformers. This is the most important parameter since hotspot temperature exceedance can damage the transformer in two ways. First, a temperature exceedance of 120–140 °C can induce the formation of bubbles in the coolant oil, which in turn is liable to cause an insulation breakdown because of the local reduction of dielectric insulation strength. Second, high temperatures increase the ageing rate of the winding insulation. For this reason the maximum operating temperature should not exceed the rated value. The thermal model consists of a heat balance between the power dissipated in the winding and iron core, and the heat transferred to the environment via the refrigerating circuit. Considering the thermal resistance between the winding and the oil ($R_{T,W}$), the thermal resistance between the heat exchanger and the air ($R_{T,HE}$) and the power dissipated into the core ($I^2 r_{windings}$), it is possible to calculate the hot spot temperature T_{HS} as in equation (18)

$$T_{HS} = T_a + I^2 r_{windings}(R_{T,W} + R_{T,HE}) \qquad (18)$$

Equation (18) is discussed in reference [25] leading to the IEC standard model for rating oil-filled power transformers as shown in equation (19)

$$T_{HS} = T_a + (T_{TO} - T_a)\left(\frac{1 + RK^2}{1 + R}\right)^x + (T_{HS} - T_{TO})K^y \qquad (19)$$

The maximum rating can be obtained by iteration, once the hot spot temperature has been set, and tabulated values for the parameters can be found in reference [3] for transformers with different types cooling system. Correction factors in reference [3] can be used to model other operating conditions such as transformers operating within enclosures. Transformer cooling systems are classified with an acronym summarizing (a) the coolant fluid: oil (O) or air (A); (b) the convection around the core: natural (N), forced (F) or direct (D); (c) the external refrigerating fluid: air (A) or water (W); and (d) the external convection method: natural (N) or forced (F). Typically distribution transformers have ONAN or ONAF cooling systems.

3.2 Environmental conditions

This section describes the approach adopted to estimate, correct, and interpolate environmental

conditions to represent more accurately the actual environmental operating conditions for sections of the UK power system in different geographical areas.

3.2.1 Environmental condition interpolation

The inverse distance interpolation technique [28] allows environmental conditions to be determined over a wide geographical area using a reduced set of inputs. This is attractive for situations where a large amount of installed measurements may be financially unattractive to the DNO. The technique is also computationally efficient and allows the input locations to be readily adapted. The wind speed correction process is described in section 3.2.2. The soil parameter correction process is described in section 3.2.3. Wind direction, air temperature, and solar radiation values were included within interpolations but did not require the application of a correction factor. At each point in the geographical area k the value of the parameter Z representing the environmental condition can be estimated as a weighted average of the parameter values known at i points. The weighting factor is a function of the distance between the points as shown in equation (20)

$$Z_k = \frac{\sum_i (1/d_{i,k}^2)Z_i}{\sum_i 1/d_{i,k}^2} \qquad (20)$$

3.2.2 Wind speed correction

Ground roughness influences wind speed profiles and may lead to differences between the wind speed recorded by anemometers and the actual wind speed passing across an overhead line, particularly if the anemometer and overhead line are installed at different heights. This may be corrected using the wind profile power law given in equation (21). The wind speed at two different heights is linked with the ground roughness through the exponent Kshear. Values of Kshear for different ground types may be found in reference [29]

$$Ws = Ws_a \left(\frac{z_{ref}}{z_a}\right)^{Kshear_a} \left(\frac{z_c}{z_{ref}}\right)^{Kshear_c} \qquad (21)$$

Using equation (21), the anemometer wind speed Ws_a at the weather station height z_a is extrapolated to a reference height z_{ref} (in this case 100 m) to remove ground roughness dependence represented by the parameter $Kshear_a$. The values from different anemometer locations may then be interpolated, using equation (20) as described in section 3.2.1, to provide a wind speed estimate at the reference height for a particular geographical location. The ground roughness at this location is then taken into account through the coefficient $Kshear_c$ along with the conductor height z_c in equation (21) to estimate the wind speed (Ws) across the overhead line.

3.2.3 Soil parameter estimation

Electric cable ratings are dependent on soil temperature and soil thermal resistivity, as well as cable construction, burial layout, and burial depth (which is typically 0.8–1 m). MetOffice [30] datasets contain information regarding soil temperatures at a depth of 0.3 m. However, no information was available from this source regarding soil thermal resistivity. Depth-dependent soil temperature distributions may be calculated using the Fourier law [31] as shown in equation (22)

$$\frac{\mathrm{d}T_{\mathrm{s}}}{\mathrm{d}t} = \frac{\mathrm{d}}{\mathrm{d}z}\left[\delta_{\mathrm{s-T}}(\theta)\frac{\mathrm{d}T_{\mathrm{s}}}{\mathrm{d}z}\right] \qquad (22)$$

Boundary conditions were set up with a constant temperature of 10 °C at a depth of 2 m for the lower layer and MetOffice soil temperature readings for the upper layer. Soil thermal resistivity $\rho_{\mathrm{s-T}}$, may be calculated from equation (23) using the soil thermal diffusivity $\delta_{\mathrm{s-T}}$, the dry soil density $\rho_{\mathrm{s-density}}$, and the soil thermal capacity $C_{\mathrm{s-T}}$

$$\rho_{\mathrm{s-T}} = (\delta_{\mathrm{s-T}}\,\rho_{\mathrm{s-density}}C_{\mathrm{s-T}})^{-1} \qquad (23)$$

Soil thermal diffusivity $\delta_{\mathrm{s-T}}$ and soil thermal capacity are influenced by soil composition N and water content θ and can be calculated using equations (24) and (25) [32]

$$\delta_{\mathrm{s-T}}(\theta) = -14.8 + 0.209\,N + 4.79\theta \qquad (24)$$

$$C_{\mathrm{s-T}} = -0.224 - 0.00561\,N + 0.753\,\rho_{\mathrm{s-density}} + 5.81\theta \qquad (25)$$

Ground water content may be determined using the closed form of Richard's equation [33] as described in equation (26) after the calculation of the unsaturated hydraulic diffusivity $\delta_{\mathrm{s}-\theta}(\theta)$ and the unsaturated hydraulic conductivity $k_{\mathrm{s}-\theta}(\theta)$ as described in reference [34]

$$\frac{\mathrm{d}\theta}{\mathrm{d}t} = \frac{\mathrm{d}}{\mathrm{d}z}\left[\delta_{\mathrm{s}-\theta}(\theta)\frac{\mathrm{d}\theta}{\mathrm{d}z} + k_{\mathrm{s}-\theta}(\theta)\right] \qquad (26)$$

In order to solve equation (26), boundary and initial conditions must be specified. A constant water content equal to the saturation value was set at a depth of 2.5 m, corresponding to the water table. Furthermore, the ground-level water content was linked to MetOffice rainfall values l_{r} using the model described in equation (27), where Krain_1 and Krain_2 can be calculated using [35]

$$\frac{\mathrm{d}\theta}{\mathrm{d}t} = -\mathrm{Krain}_1\theta t + \mathrm{Krain}_2 lr(t) \qquad (27)$$

3.2.4 Sensitivity analysis

It can be seen from the work presented above that there are many diverse parameters that affect the rating of power system components. These parameters may be categorized into component properties, geographical properties, and environmental conditions. A list of the parameters used in the offline simulations is given in Table 1. For the purposes of the offline simulations, component properties and geographical properties were assumed to be constants of the system. Therefore, the thermal models presented were underpinned by an extensive and rigorous sensitivity analysis that gave an indication of the influence of environmental conditions on power system component ratings. The sensitivity analysis was carried out such that one parameter was varied at a time while all other parameters were maintained at their credible mid range values. A summary of the results of this analysis is presented in Table 2 and shows the percentage variation in component rating for a given percentage variation of environmental conditions from credible mid-range parameter values. Moreover, in the sensitivity analysis, the soil thermal resistance is assumed to take into account the effect of rainfall. It can be seen that the rating of overhead lines is particularly sensitive to the environmental conditions of wind speed, wind direction, and ambient temperature, and that the rating of electric cables is particularly sensitive to the thermal resistance of the surrounding medium.

Furthermore, a series of credible worst case scenarios were selected to give an indication of the minimum component rating that would potentially result from the deployment of a real-time rating system. In this worst case analysis the following values were specified: Ta = 38.5 °C (the maximum temperature registered in England, August 2003) [30]; Ws = 0, Wd = 0, Sr = 0 W/m² (from studies carried out at CERL, the highest conductor temperature excursions are recorded at times of low wind speed where there is negligible solar radiation) [36]; Ts = 20 °C [2] and $\rho_{\mathrm{s-T}}$ = 3 Km/W [24]. The resulting rating multipliers of the standard static component rating were 0.81, 0.86, and 0.78 for overhead lines, electric cables, and power transformers, respectively.

4 SIMULATION APPROACH

In Fig. 2, a general description of the simulation algorithm, with the different software applications, is provided. The algorithm uses three databases to store network component data, weather measurement data, and calculated rating data, respectively. It comprises two main applications: the environmental condition processor for simulating weather data, described in section 3.2 and the CTMs for calculating component ratings, as described in section 3.1. A third application

Table 1 Parameters affecting the rating of power system components

Component type	Component properties			Geographical properties			Environmental conditions		
	Name	Symbol	Unit	Name	Symbol	Unit	Name	Symbol	Unit
Overhead line	Conductor diameter	D	(m)	Ground roughness factor	Kshear	(dimensionless)	Wind speed	Ws	(m/s)
	Conductor resistance per unit length	r	(Ω/m)	Conductor height	z_c	(m)	Wind-conductor angle	Wd	(rad)
	Absorption coefficient	α	(dimensionless)	Weather station height	z_a	(m)	Air temperature	Ta	(°C)
	Emission coefficient	ε	(dimensionless)	Distance between weather station and component	$d_{i,k}$	(m)	Solar radiation	Sr	(W/m^2)
Electric cable	Rated ampacity	I_0	(A)	Sum of sand and clay percentage	N	(dimensionless)	Soil thermal resistivity	R_T	(m K/W)
				Normalized soil water loss	Krain$_1$	(day^{-1})	Soil temperature	Ts	(°C)
	Voltage	V	(V)	Normalized net rainfall coefficient	Krain$_2$	(day^{-1}/mm)			
				Distance between weather station and component	$d_{i,k}$	(m)	Rainfall	l_r	(mm)
Power transformers	Oil exponent	x	(dimensionless)	Distance between weather station and component	$d_{i,k}$	(m)	Air temperature	Ta	(°C)
	Winding exponent	y	(dimensionless)						
	Ratio of windings to core losses	R	(dimensionless)						

Table 2 Environmental condition sensitivity analysis (parameter variation versus rating variation)

Parameter (credible mid-range value)		Overhead lines (Lynx 50)				Electric cables (150 mm^2)		Transformers (ONAN 45)
		Ws (8 m/s)	Wd $\left(\frac{\pi}{4}\text{rad}\right)$	T_a (15 °C)	Sr (500W/m^2)	R_T (1.2WK/m)	T_s (10 °C)	T_a (15 °C)
Variation from mid-range value	−50%	−23.86%	−11.38%	+10.80%	+0.72%	+31.46%	+3.00%	+6.11%
	−25%	−10.73%	−4.97%	+5.52%	+0.36%	+12.36%	+1.50%	+3.09%
	−10%	−4.07%	−1.85%	+2.24%	+0.15%	+6.18%	+0.60%	+1.24%
	10%	+3.84%	+1.66%	−2.29%	−0.15%	−4.49%	−0.60%	−1.25%
	25%	+9.22%	+3.82%	−5.81%	−0.36%	−8.99%	−1.50%	−3.16%
	50%	+17.40%	+6.54%	−11.96%	−0.73%	−16.48%	−3.00%	−6.40%
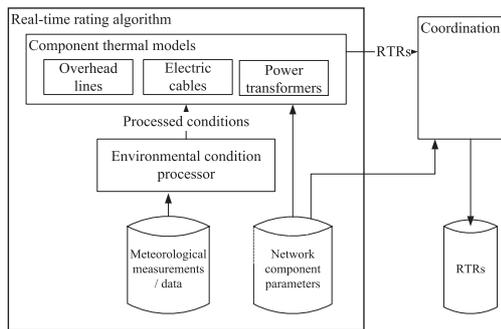
Fig. 2 Simulation scheme

Fig. 4 Air temperature PD

(coordination) was added to supervise the simulation dataflow. The offline simulation algorithm computes component real-time ratings with a temporal resolution of 1 h.

4.1 Weather

MetOffice datasets were used, referring to four British airports: Bishopton (Glasgow), Valley (Anglesey), Woodford (Manchester), and Heathrow (London). The data comprised hourly averages of wind speed, wind direction, air temperature, solar radiation, and soil temperature throughout the calendar year 2005. In Figs 3 to 5, the data from those sites are summarized and compared.

In Fig. 3, it is possible to observe the different site characteristics for the wind speed: Valley, on the west coast of Wales, is the windiest area with the highest
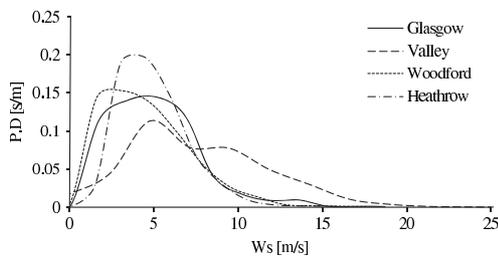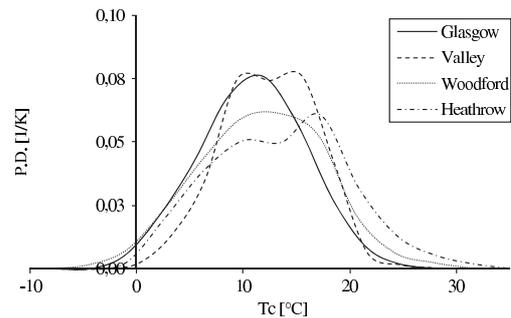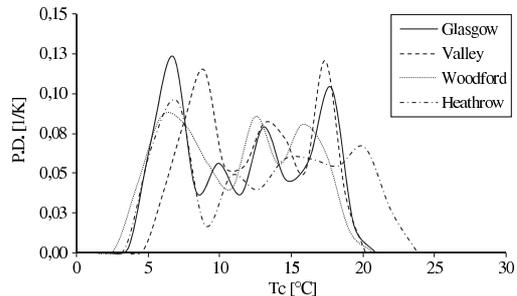
Fig. 5 Soil temperature PD

maximum wind speed values and a probability distribution (PD) with the smallest peak. Heathrow, which is located in an urban environment, has wind speeds that are generally lower and more concentrated in the range between 2–7 m/s. As seen in Fig. 4, air temperature appears to be the least variable parameter. Different sites may be differentiated by average temperature values. In Fig. 5, the behaviour of the soil temperature is illustrated. Whereas the air temperature shows a variation with one peak across the year, soil temperature appears to vary with multiple peaks.

Regarding wind direction, the presence of prevalent winds from the west and the north-west in the range 180–360° was noted for all areas. Some areas also exhibited site-specific prevalent wind directions, for example from the south-west in Woodford and from north-north-west in Bishopton. Regarding solar

Fig. 3 Wind speed PD

radiation, no significant differences between the four sites were found.

4.2 Networks

In order to simulate in a rigorous manner the influence of environmental conditions on power system ratings, three network models were adapted from the United Kingdom Generic Distribution Systems (UKGDSs) [37], each of which contain the three component types considered in this article. Moreover, a portion of the ScottishPower EnergyNetworks distribution network was included in simulations as this will be instrumented in the near future for RTR validation purposes. Voltage levels in the four networks studied vary from 6.6 to 132 kV.

The ScottishPower EnergyNetworks Site network is shown in Fig. 6 and has a meshed topology, with a prevalence of Lynx 175 mm^2 overhead lines. The network also has eleven electric cable circuits of 150 mm^2 at the 33 kV level and 13 power transformers rated at 45 MVA, 60 MVA, 90 MVA, and 240 MVA. Topological representations of the UKGDSs can be found in Appendix 3. Technical characteristics for the overhead lines may be found in reference [21]. UKGDS_A has six overhead line circuits with Zebra and Lynx conductors rated at 50, 65, and 75 °C, 12 electric cables circuits with 150 and 240 mm^2 conductors, and 16 transformers with ratings from 14 to 500 MVA. UKGDS_B consists of six overhead lines with Zebra and Lynx conductors, eight electric cable circuits with 150 mm^2 conductors and 13 power transformers, with ratings from of 21 and 500 MVA. UKGDS_C is characterized by a prevalence of electric cable circuits and power transformers. It comprises two overhead lines with Zebra conductors, 12 electric cable circuits with 150 and 240 mm^2 conductors and 18 power transformers with ratings from 14
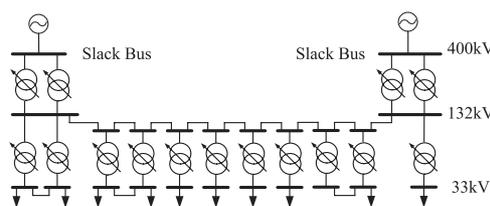
to 500 MVA. Electrical parameters for modelling the UKGDSs may be found in reference [37].

5 RESULTS AND ANALYSIS

In order to quantify the influence of environmental conditions on power system ratings, simulations were carried out on the networks described in section 4.2 subjected to a range of UK climatic conditions. For each scenario the minimum, maximum, and average rating values together with additional potential annual energy throughput (in GWh) were calculated and the results are tabulated in Appendix 3. These data may be summarized as follows: the average rating of overhead lines ranged from 1.70 to 2.53 times the static rating with minimum and maximum ratings of 0.81 and 4.23, respectively. The average rating of electric cables ranged from 1.00 to 1.06 times the static rating with minimum and maximum ratings of 0.88 and 1.23, respectively. The average rating of power transformers ranged from 1.06 to 1.10 times the static rating with minimum and maximum ratings of 0.92 and 1.22, respectively.

Simulations results were analysed in three different ways:

(a) comparing the rating cumulative probabilities of different component types against one another within the same network and environmental conditions;
(b) comparing the GWh headroom of four different overhead line types subjected to four different UK climates;
(c) assessing the increased energy throughput from DG that may be accommodated by using RTRs, as opposed to seasonal ratings, for a single overhead line.

5.1 Rating comparison of different component types

In Table 3, the simulation results for the site network exposed to the Valley climatic scenario are given. For each component type the average, minimum, and maximum RTRs are given, and the additional headroom theoretically obtainable with RTRs (as opposed to seasonal ratings) is quantified. The additional headroom was calculated by summing the difference

Fig. 6 Site trial

Table 3 Simulation results for SITE network components exposed to the Valley climatic scenario

Component	Static rating (MVA)	RTR average (MVA)	RTR minimum (MVA)	RTR maximum (MVA)	Additional RTR headroom (GWh/year)
Electric cable (150 mm^2)	21	21	19	23	1.83
Power transformer (ONAN 45)	45	48	44	52	30.7
Power transformer (OFAN 240)	240	257	235	276	149.1
Overhead line (Lynx 50)	89	253	107	419	1342

between the RTR and the seasonal ratings across the year in hourly intervals. For overhead lines, the seasonal ratings reported in reference [21] were used for this calculation. In Fig. 7(a), the rating cumulative probabilities for the four components described in Table 3 are shown. RTRs have been normalized using the static component rating. From inspection of Fig. 7(a) it is evident that overhead lines show the greatest potential for rating exploitation. As seen in Fig. 7(b), electric cable and power transformer ratings have a limited variability. This is because soil temperature, soil thermal resistivity, and air temperature are much less variable than wind speed and direction and it is these latter parameters that greatly influence the rating of overhead lines. This is in agreement with the analysis in section 4.1. By representing component ratings as cumulative probabilities, the potential comparison with power transfer duty (PTD) curves

is facilitated. Moreover, DNOs are able to specify a probability with which they are comfortable to operate a particular component and an assessment of the corresponding rating may be made.

5.2   Rating comparison of overhead line types

It was shown in Fig. 7 and Table 3 that overhead lines exhibit the greatest potential for RTR exploitation. Therefore, in Fig. 8 the average headroom for different overhead line types, exposed to different climatic scenarios, is compared. For each case, the average headroom is given along with the minimum and maximum headroom. Headroom variations exist since differences in component orientation and component location result in rating variations. Variation bars are representative of the possible headroom ranges simulated. The size of the variation band is determined by the number of components existing within each case study network. A large variation band represents a frequently occurring component. By inspecting the position of the lower variation band it is evident that the additional headroom is greater for conductors with a greater initial static rating, and this effect is accentuated by conductor rated temperature. This is because the conductor temperature rise above ambient temperature multiplies the heat exchange coefficient as seen in equation (6).

Regarding the influence of the climates, Valley exhibits the highest average wind speed values and Bishopton the lowest average temperatures as seen in Figs 3 and 4. Since overhead line ratings are more sensitive to wind speed than air temperature the climate of Valley leads to the greatest overhead line power transfer headroom. Clearly from this evidence the value of adopting an RTR system is dependent on geographical location. Therefore, any utility interested in deploying an RTR system should conduct a site specific study to assess the value of RTRs as the output varies according to climate, and therefore the economic value is
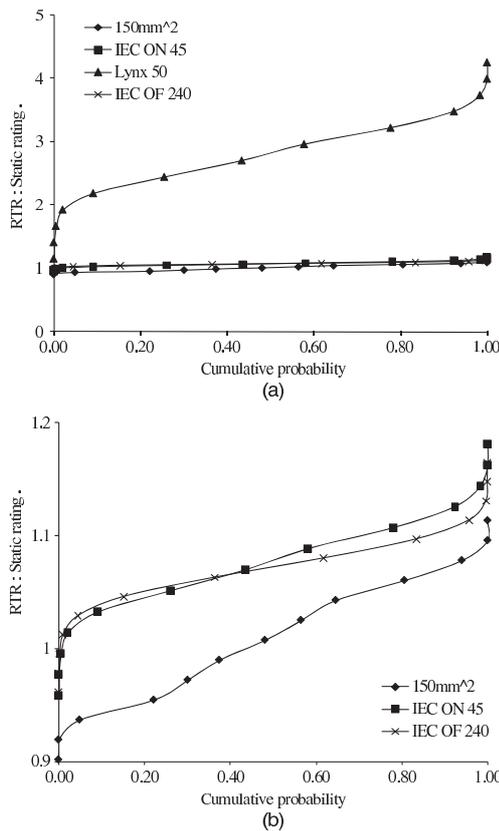
Fig. 7   (a) Rating cumulative probability for SITE network components exposed to the Valley climatic scenario and (b) magnified rating cumulative probability for SITE network components exposed to the Valley climatic scenario
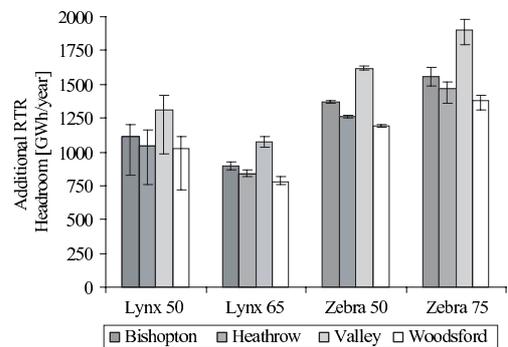
Fig. 8   Influence of different UK climates on overhead lines power transfer headroom

different. Furthermore, the quantification assessment presented in Fig. 8 allows a conservative approach to be adopted in developing RTR systems since an investor may choose to utilize the rating seen at the bottom of the variation band.

5.3 Power transfer accommodation assessment

This section presents a methodology for quantifying the practically exploitable headroom for the specific case of a 132 kV Lynx overhead line conductor with a maximum operating temperature of 50 °C subjected to the Valley climate in the site network. This location was selected since it is an area attractive to prospective wind farm development. The practically exploitable headroom was quantified as follows: meteorological wind data from the Valley site were used together with the GE 3.6 MW wind turbine power curve [**38**] to assess the power generated throughout the year and transferred through the overhead line conductor. Clearly the exposure of the overhead line conductor to environmental conditions varies as a function of line orientation and ground roughness. Therefore, when making an assessment of the RTR, the overhead line was divided into sections to represent the variation in these parameters. The section of overhead line with the lowest rating represents the weakest point of the overhead line system and therefore this lowest rating was adopted as the RTR for the entire overhead line. By comparing the power transfer across the year with the overhead line rating, for both seasonal and RTR regimes, the wind farm installed capacity was sized to correspond to a line cumulative overload probability of 1/1000 (8.76 h/annum). Results are summarized in Fig. 9, where the line RTR cumulative probability,

along with the inverse cumulative probability for two different PTDs, seasonal and switchgear ratings are represented. The cumulative probability curve (the RTR distribution) may be interpreted by selecting an acceptable probability at which the component may be operated, e.g. 0.1 (10 per cent). This corresponds to a rating of 149 MVA. Therefore, there is the probability of 10 per cent that during the course of the year the rating is ⩽149 MVA (conversely there is a 90 per cent probability that the rating is >149 MVA). Similarly the inverse cumulative probability (PTD curves 1 and 2) may be interpreted by selecting a PTD value, e.g. 76 MVA on PTD 2 curve. This corresponds to a probability of 10 per cent. Therefore there is a probability of 10 per cent that during the course of the year PTD 2 is ⩾76 MVA (conversely there is a 90 per cent probability that the PTD is <76 MVA). For the seasonal rating regime an installed capacity of 89 MW (25 turbines) could be accommodated and an annual energy yield from the wind farm of 245 GWh could be attained. For the RTR regime, an installed capacity of 137 MW (38 turbines) could be accommodated and an annual energy yield from the wind farm of 377 GWh could be attained. This represents an increase in installed capacity and annual energy yield of 54 per cent, which is specific to the weather data used, the type of conductor, the risk at which the DNO is prepared to operate the asset and the type of turbine selected. An annual energy yield increase of 54 per cent would significantly enhance the revenue stream of a wind farm developer, demonstrating the value of an RTR approach. However, this is only 10 per cent of the theoretical average additional headroom for this type of overhead line conductor exposed to the Valley climate, as seen in Fig. 8. Installing a larger capacity of DG together with the adoption of an online power output
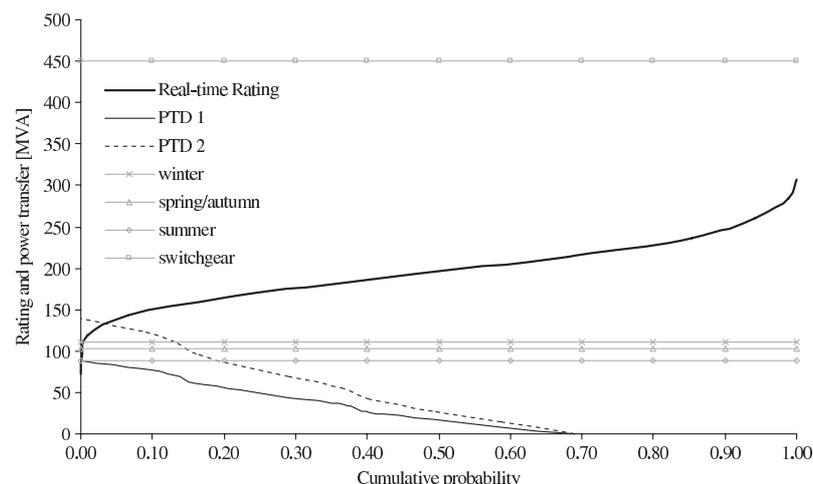

Fig. 9 Cumulative probability comparison for a Lynx conductor in the Valley scenario

controller [39] could allow a greater percentage of the theoretical average additional headroom to be realized while maintaining an acceptable level of risk to the DNO.

An estimation of the losses associated with the two PTD curves was carried out in the following way: from the average environmental conditions at the Valley site and from the average value of the power transfer, the average conductor temperature was calculated. From this, the average conductor resistance was calculated and, using the hourly values of the power transfer, it was possible to obtain the losses arising from Joule effect for the whole year. Loss values of 0.12 and 0.19 per cent of the entire annual energy throughput were obtained for PTD 1 and PTD 2, respectively.

6   CONCLUSIONS

This article described the offline simulation of power system thermal models populated with historical environmental conditions in order to derive RTRs. This information was used to quantify (in GWhs) the exploitable headroom that may be achieved by implementing an RTR system within distribution networks. Power system component models were developed based on IEC standards and environmental conditions were corrected and interpolated to represent, as closely as possible, actual network operating conditions. Component data and environmental condition data were used to populate the models in simulation to derive component RTRs. For a wide number of power system components and environmental conditions the minimum, maximum, and average ratings were quantified together with the additional power transfer headroom. This information is likely to be of use to DNOs in planning and operating future distribution networks that may be reaching a level of power transfer saturation. It was found that overhead lines exhibit the greatest potential RTR exploitation since they exhibit the greatest rating variability. Furthermore, it was found that power transformers and electric cables have a slight RTR exploitation potential relative to overhead lines. The value of adopting an RTR system is dependent on geographical location. Therefore any utility interested in deploying an RTR system should conduct a site specific study to assess the value of RTRs as the output varies according to climate, and therefore the economic value is different.

The increase in power transfer from DG that could be accommodated through an RTR system implementation was investigated. For a Lynx overhead line conductor with a maximum operating temperature of 50 °C it was found that a GWh energy throughput increase of 54 per cent could be accommodated by operating the line with an RTR regime as opposed to a seasonal rating regime. Work is continuing in this area to realize the potential of RTR system implementations.

REFERENCES

1 IEC TR 1597. Overhead electrical conductors – calculation methods for stranded bare conductors, 1995.
2 IEC 60287. Electric cables – calculation of the current rating, 1994.
3 IEC 60076-7. Power transformers – part 7: loading guide for oil-immersed power transformers, 2008.
4 **Neumann, A., Taylor, P., Jupe, S., Michiorri, A., Goode, A., Curry, D.,** and **Roberts, D.** Dynamic thermal rating and active control for improved distribution network utilisation. In PowerGrid 08, Milan, Italy, 2008.
5 **Stephen, R.** Description and evaluation of options relating to uprating of overhead transmission lines. *Electra*, 2004, **B2-201**, 1–7.
6 **Hoffmann, S. P.** and **Clark, A. M.** The approach to thermal uprating of transmission lines in the UK. *Electra*, 2004, **B2-317**, 1–8.
7 **Soto, F., Latorre, J.,** and **Wagensberg, M.** Increasing the capacity of overhead lines in the 400 kV Spanish transmission network: real time thermal ratings. *Electra*, 1998, **22–211**, 1–6.
8 Available at http://www.wasp.dk, accessed January 2008.
9 **Douglass, D. A.** and **Edris A. A.** Real-time monitoring and dynamic thermal rating of power transmission circuits. *IEEE Trans. Power Deliv.*, 1996, **11**(3), 1407–1418.
10 **Douglass D. A., Edris A. A.,** and **Pritchard G. A.** Field application of a dynamic thermal circuit rating method. *IEEE Trans. Power Deliv.*, 1997, **12**(2), 823–831.
11 **Nuijten, J. M. A.** and **Geschiere, A.** Future network planning and grid control. In Proceedings of the International Conference on *Future power systems*, Amsterdam, The Netherlands, 16–18 November, 2005.
12 **Helmer, M.** Optimized size of wind power plant transformer and parallel operation. In Wind Power for the 21st century, Kassel, Germany, 25–27 September 2000.
13 **Belben, P. D.** and **Ziesler, C. D.** Aeolian uprating: how wind farms can solve their own transmission problems. In Proceedings of the World Wind Energy Conference and Exhibition, Berlin, July 2002.
14 **Piccolo, A., Vaccaro, A.,** and **Villacci, D.** Thermal rating assessment of overhead lines by Affine arithmetic. *Electr. Power Syst. Res.*, 2004, **71**(3), 275–283.
15 **Villacci, D.** and **Vaccaro, A.** Transient tolerance analysis of power cables thermal dynamic by interval mathematic. *Electr. Power Syst. Res.*, 2007, **77**, 308–314.

16 Ippolito, L., Vaccaro, A., and Villacci, D. The use of affine arithmetic for thermal state estimation of substation distribution transformers. *COMPEL, Int. J. Comput. Math. Electr. Electron. Eng.*, 2004, **23**(1), 237–249.

17 House, H. E. and Tuttle, P. D. Current carrying capacity of ACSR. *IEEE Trans. Power Appar. Syst.*, 1959, **78**(3), 1169–1177.

18 Morgan, V. T. The thermal rating of overhead-line conductors. 1. The steady-state thermal mode. *Electr. Power Syst. Res.*, 1982, **5**(2) 119–139.

19 WG 22.12. The thermal behaviour of overhead conductors – section 1. *Electra*, 1992, **144**(3), 107–125.

20 IEEE 738. Standard for calculating the current-temperature relationship of bare overhead conductors, 1993.

21 ENA ER P27. Current rating guide for high voltage overhead lines operating in the UK distribution system, 1986.

22 Neher, J. H. and McGrath, M. H. The calculation of the temperature rise and load capability of cable systems. *AIEE Trans.*, 1957, **76**(3), 752–772.

23 IEEE 835. IEEE Standard Power Cable Ampacity Tables, 1994.

24 ENA ER P17. Current rating for distribution cables, 2004.

25 Susa, D., Lehtonen, M., and Nordman, H. Dynamic thermal modelling of power transformers. *IEEE Trans. Power Deliv.*, 2005, **20**(1), 197–204.

26 ANSI/IEEE, C57.92. Guide for loading mineral oil-immersed power transformers up to and including 100 MVA with 55 °C or 65 °C average winding rise, 1981.

27 ENA ER P15. Transformers loading guide, 1971.

28 Shepard D. A two-dimensional interpolation function for irregularly-spaced data. In Proceedings of the 23rd ACM National Conference, 1968, pp. 517–524.

29 IEC 60826. Loading and strength of overhead transmission lines, 1991.

30 Available at www.metoffice.gov.uk, accessed January 2008.

31 Nairen, D., Qinyun, L., and Zhaohong, F. Heat transfer in ground heat exchangers with groundwater advection. *Int. J. Therm. Sci.*, 2004, **43**, 1203–1211.

32 Abu–Hamdeh, N. H. Thermal properties of soil as affected by density and water content. *Biosyst. Eng.*, 2003, **86**(1), 97–102.

33 Celia, M., Boulotas, E., and Zarba, R. A general mass-conservative numerical solution for the unsaturated flow problem. *Water Resour. Res.*, 1990, **26**(7), 1483–1496.

34 Van Genuchten, M. A closed for equation for predicting the hydraulic conductivity of unsaturated soils. *Soil Sci. Soc. Am. J.*, 1980, **44**, 892–898.

35 Rodríguez-Iturbe, I., Isham, V., Cox, D. R., Manfreda, S., and Porporato, A. Space-time modelling of soil moisture: stochastic rainfall forcing with heterogeneous vegetation. *Water Resour. Res.*, 2006, **42**, 1–11.

36 Price, C. and Gibbon, R. Statistical approach to thermal rating of overhead lines for power transmission and distribution. *IEE Proc.*, 1983, **130**(5), 245–256.

37 Available at http://www.sedg.ac.uk/ukgds.htm, accessed January 2008.

38 Energy, G. E. 3.6 MW Offshore Series Wind Turbine, 2005.

39 Jupe, S. C. E., Taylor, P. C., Michiorri, A., and Berry, C. J. An evaluation of distributed generation constrained

connection managers. In Proceedings of the MedPower 2008 – 6th Mediterranean Conference and Exhibition on *Power generation, transmission and distribution*, Thessaloniki, Greece, 2–5 November 2008.

APPENDIX 1

Notation

A	conductor cross-sectional area (m²)
C_{s-T}	soil thermal capacitance (J/kg/K)
d	internal diameter (m)
d_{i-k}	distance from weather station to component (m)
D	external diameter (m)
E	Young's modulus of conductor (Pa)
g	gravitational acceleration (m/s²)
Gr	Grashof number
H	tension (N)
i	index
I	current (A)
I_0	electric cable rated current (A)
k	number of weather stations
$k_{s-\theta}$	soil unsaturated hydraulic conductivity (m/s)
K	load ratio
K_{dir}	wind direction influence coefficient
$K_{dir-1,2,3}$	wind direction coefficient constants
$K_{nat-1,2}$	natural convection coefficients
$Krain_1$	normalized soil water loss (day⁻¹)
$Krain_2$	normalized net rainfall coefficient (day⁻¹/mm)
$Kshear_a$	ground roughness factor at the weather station
$Kshear_c$	ground roughness factor at the conductor
l_r	rainfall (mm)
L	span (m)
m	mass per unit length (kg/m)
n	number of conductors in the cable
N	sum of sand and clay percentage
Nu	Nusselt number
P	real power set point dispatched to generator (MW)
Pr	Prandtl number
q_c	heat exchanged per unit length by convection (W/m)
q_d	dielectric loss per length unit (W/m)
q_r	heat exchanged per unit length by irradiation (W/m)
q_s	heat gained per unit length by solar radiation (W/m)
Q	reactive power set point dispatched to generator (MVAr)

r	conductor resistance per length unit (Ω/m)
$r_{windings}$	transformer windings resistance (Ω)
R	ratio between windings and core losses
R_T	thermal resistance (m K/W)
$R_{T,HE}$	transformer heat exchanger thermal resistance (m K/W)
$R_{T,W}$	windings to oil thermal resistance (m K/W)
Re	Reynolds number
S	sag (m)
Sr	solar radiation (W/m)
t	time (s)
T_a	air temperature (K)
T_c	conductor temperature (K)
T_{HS}	hot spot temperature (K)
T_s	soil temperature (K)
T_{TO}	top oil temperature (K)
V	voltage (V)
Wd	wind conductor angle (rad)
Ws	wind speed (m/s)
x	transformer oil exponent
y	transformer winding exponent
z_b	cable burial depth (m)
$z_{c,ref,a}$	conductor, reference, and weather station heights for wind correction (m)
Z_k	generic environmental condition parameter
α	absorption coefficient
β	conductor thermal expansion coefficient (K^{-1})
δ_{s-T}	soil thermal diffusivity (m^2/s)
$\delta_{s-\theta}$	soil unsaturated hydraulic diffusivity (m^2/s)
ΔT	temperature difference (K)
ε	emission coefficient
θ	gravimetric water content
λ	air thermal conductivity (W/m/K)
$\lambda_{1,2}$	ratio between metal sheath losses and total losses
ν	kinematic viscosity (m^2/s)
ξ_T	electric cables rating temperature correction factor (K^{-1})
ξ_ρ	electric cables rating thermal resistivity correction factor (W/m/K)
$\rho_{s-density}$	dry soil density (kg/m^3)
ρ_{s-T}	soil thermal resistivity (m K/W)
σ_{S-B}	Stephen–Boltzmann constant (W/m^2/K^4)

APPENDIX 2

UKGDS networks

In Figs 10 to 12, a description of the UKGDS networks used is given.
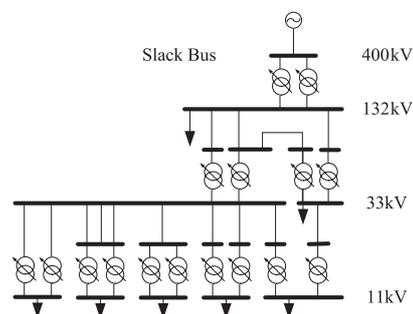
Fig. 10 UKGDS_A
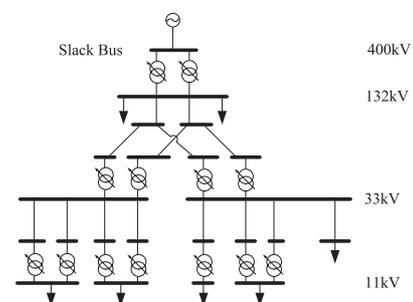
Fig. 11 UKGDS_B
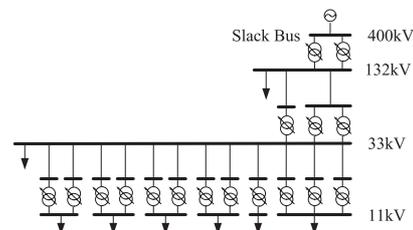
Fig. 12 UKGDS_C

APPENDIX 3

Simulation results

This section provides a summary of the simulation results. For each climate and each network, the average, minimum, and maximum calculated ratings are given in Table 4, along with the static rating and the average annual headroom for each component type. Overhead lines are described with their conductor codes and rated temperature, electric cables with the

Table 4 Simulation results, component ratings, and theoretical headroom

Component	Static rating (MVA)	RTR average (MVA)	RTR minimum (MVA)	RTR maximum (MVA)	RTR headroom (GWh/year)
Overhead line (Lynx 50)	89	213	84	419	988.48
Overhead line (Lynx 65)	108	220	94	390	898.94
Overhead line (Zebra 50)	154	328	125	595	1359.66
Overhead line (Zebra 75)	206	402	178	731	1576.20
Electric cable (150 mm^2)	21	21	18	25	2.94
Electric cable (240 mm^2)	30	32	27	37	13.33
Power transformer (ODAF 500)	500	532	469	580	282.41
Power transformer (OFAF 240)	240	258	223	284	154.75
Power transformer (ONAN 100)	100	108	92	120	70.80
Power transformer (ONAN 90)	90	97	83	108	63.72
Power transformer (ONAN 60)	60	65	55	72	42.48
Power transformer (ONAN 45)	45	49	41	54	31.87
Power transformer (ONAN 23)	23	25	21	28	16.28
Power transformer (ONAN 21)	21	23	19	25	14.87
Power transformer (ONAN 14)	14	15	13	17	10.80

conductor cross-sectional area, and power transformers with the cooling method and the rating. In Table 5, a list of the components within each network is given.

Table 5 Network components

Network	Component	Number of components
SITE	Overhead line (Lynx 50)	11
SITE	Electric cable (150 mm^2)	11
SITE	Power transformer (OFAF 240)	5
SITE	Power transformer (ONAN 45)	5
SITE	Power transformer (ONAN 60)	2
SITE	Power transformer (ONAN 90)	1
UKGDS_A	Overhead line (Lynx 50)	1
UKGDS_A	Overhead line (Lynx 65)	3
UKGDS_A	Overhead line (Zebra 75)	2
UKGDS_A	Electric cable (150 mm^2)	4
UKGDS_A	Electric cable (240 mm^2)	10
UKGDS_A	Power transformer (ODAF 500)	1
UKGDS_A	Power transformer (ONAN 23)	1
UKGDS_A	Power transformer (ONAN 60)	6
UKGDS_A	Power transformer (ONAN 90)	2
UKGDS_A	Power transformer (ONAN 14)	2
UKGDS_B	Overhead line (Lynx 65)	4
UKGDS_B	Overhead line (Zebra 75)	2
UKGDS_B	Electric cable (150 mm^2)	7
UKGDS_B	Electric cable (240 mm^2)	1
UKGDS_B	Power transformer (ODAF 500)	2
UKGDS_B	Power transformer (ONAN 100)	1
UKGDS_B	Power transformer (ONAN 21)	2
UKGDS_B	Power transformer (ONAN 23)	5
UKGDS_B	Power transformer (ONAN 45)	2
UKGDS_B	Power transformer (ONAN 90)	1
UKGDS_C	Overhead line (Zebra 50)	2
UKGDS_C	Electric cable (150 mm^2)	1
UKGDS_C	Electric cable (240 mm^2)	9
UKGDS_C	Power transformer (ODAF 500)	1
UKGDS_C	Power transformer (ONAN 60)	1
UKGDS_C	Power transformer (ONAN 14)	1
UKGDS_C	Power transformer (ONAN 23)	10
UKGDS_C	Power transformer (ONAN 60)	1
UKGDS_C	Power transformer (ONAN 14)	2
UKGDS_C	Power transformer (ONAN 23)	1

WG C6.11 REPORT

Active Distribution Networks:
general features, present status of implementation and operation practices

Update of WG C6.11 Activities

Members:
C. D'Adamo, Convenor, (IT) P. Taylor (GB),
S. Jupe (GB), B. Buchholz (DL),
F. Pilo (IT), C. Abbey, Secretary, (CA),
J. Marti (ES).

Abstract

This paper presents the progress of WG C6.11: development and operation of active distribution networks (ADNs). It gives the definition of ADNs, as well as the results of a global survey involving 27 utilities and research bodies worldwide: general features of ADNs, current status of their implementation, operating practices, and limits/barriers are discussed.

Foreword

The proliferation of distributed generation (DG) together with load growth, energy storage technology advancements and increased consumer expectations have significantly changed the approach to planning, design and operation of distribution networks. Around the globe, distribution companies, equipment manufacturers, electrical engineering consultants, research institutions, regulators and stakeholders are dealing with these issues.

Several organisations worldwide are addressing these issues (e.g. IntelliGrid in the US, Smart Grids Technology Platform and Microgrids in the EU) and promoting collaborative projects on the electricity networks of the future. Part of this new paradigm includes the possibil-

ity for distribution system operators (DSOs) to control, operate and thereby integrate distributed energy resources (DER) into the network under their responsibility. This vision sees the evolution of electricity distribution from passive to active distribution networks.

The CIGRÉ C6 Study Committee [1] considers the different aspects of integration of distributed generation. In this context, the C6.11 Working Group (WG) is specifically focused on "Development and operation of active distribution networks". The WG has 27 members, experts and observers, representing 14 different countries. This WG aims to assess the various requirements to facilitate the transition towards active distribution networks (ADNs).

Specifically, the WG scope includes:
✓ Assessment of network and generators requirements for the operation of DG and DER (islanding criteria, protection, ancillary services);
✓ Identification of enabling technologies both for demand and generators;
✓ Definition of limits/barriers (costs, infrastructures, investment remuneration); and
✓ Evolution in the regulatory framework.

To assess the state-of-the-art, identify the enablers, and provide a shared global definition of ADN, the WG submitted a questionnaire through its members to national CIGRÉ committees, distribution compa- ● ● ●

WG **C6.11**
REPORT

nies, research organizations and other stakeholders. This paper provides a summary of the survey results and WG analyses. Probably the most important outcomes of this exercise are the shared definition and main features. In the following section the different sections of the survey results are discussed in turn.

Active Distribution Networks Industry Survey

The industry survey was circulated by WG members within each of their countries and 27 responses were received during 2007. The questionnaires have been analysed by 5 sub-WGs during 2007 and the first half 2008, and key results were presented to the C6 study committee at the meeting in August 2008. Here the key findings are provided, organized according to the different sections of the survey.

Definition, Main Features and SWOT Analysis

Within sub-WG 1, the questionnaire responses were analysed from three perspectives:
1. The definition of active distribution networks
2. The main features of active distribution networks

3. The strengths, weaknesses, development opportunities and threats to active distribution networks

Defining Active Distribution Networks

It is important to define the term *active distribution networks* as this leads to a standardisation of the concept which, in turn, facilitates the sharing of experience, the communication of ideas and allows appropriate technologies to be developed and transferred. Within the questionnaire distributed by WG C6.11, a number of candidate definitions for active distribution networks were proposed. Considering the comments received on these definitions and subsequent discussions during the 2008 WG C6.11 meeting, the WG reached a consensus on one that would be sufficiently generic but capture the salient features of this concept. This shared global definition of ADN is as follows:

Active distribution networks (ADNs) are distribution networks that have systems in place to control a combination of distributed energy resources (generators, loads and storage). Distribution system operators (DSOs) have the possibility of managing the electricity flows using a flexible network topology. DERs take some degree of responsibility for system support, which will depend on a suitable regulatory environment and connection agreement.

Key Features of Active Distribution Networks

From the survey responses and the alternate definitions supplied, the main features of active distribution networks were ascertained. These are summarized in Table 1.

Strengths, Weaknesses, Opportunities, and Threats Analysis

This section analyses active distribution networks in terms of their potential advantages and disadvantages when compared to passive distribution networks. In

Table 1: Main features of active distribution networks

Infrastructure Needs / Specifications	Applications	Driver/Benefit
• Protection	• Power flow congestion management	• Improved reliability
• Communication	• Data collection and management	• Increased asset utilization
• Integration into existing systems	• Voltage management	• Improved access for DG
• Flexible network topology	• DG and load control	• Alternative to network reinforcement
	• Fast reconfiguration	• Network stability

WG **C6.11**
REPORT

doing so, the opportunities arising from, and the potential threats to, the development of active distribution networks are identified. The full "SWOT" (strengths, weaknesses, opportunities, threats) analysis, gleaned from questionnaire responses, is appended:

Strengths:
- ✓ Economic alternative to network reinforcement
- ✓ Increased operational reliability, including power delivery
- ✓ Electrical loss reduction
- ✓ Automation and control leading to improved network access for DG / load customers

Weaknesses:
- ✓ Maintenance issues
- ✓ Present lack of experience
- ✓ DNOs are not incentivised to take risks
- ✓ Existing communications infrastructure

Opportunities:
- ✓ Ageing assets could be replaced with active management capable equipment
- ✓ Development and implementation of smart metering technologies
- ✓ Development of communications infrastructure
- ✓ Movement towards a low-carbon economy through the accommodation of distributed renewable energy sources

Threats:
- ✓ Regulatory issues impede the development of active distribution networks
- ✓ DG continues to grow in size and is connected to the transmission network
- ✓ Security of information on the communication infrastructure
- ✓ Active networks are not compatible with existing passive networks ● ● ●

WG C6.11
REPORT

Current level of implementation

The main feedback related to the current level of implementation was that the present level of development is quite low. Nonetheless, there were a number of pilot installations that were mentioned including those in: Australia, Denmark, the Netherlands, Spain and the UK. Also, a number of pilots known to the WG experts were not mentioned in the questionnaire responses, suggesting that there is a need to disseminate this information. As such, the WG decided to pursue documentation of these existing pilots and collate information related to technologies and applications.

On the issue of factors that would help facilitate future deployment of ADNs, a number of suggestions were received. These included (in level of priority, from highest to lowest): new investment remuneration / regulatory frameworks to foster utility adoption; research and development (including publicly funded demonstration projects); standardization. Demand growth and environmental factors were perceived to be only minor factors in the adoption of ADN.

The communication medium used by the companies surveyed varied greatly. Table 2 summarizes the technologies mentioned in the responses received. Only a limited number of companies cited the use of communication for remote operation of DER, with an even smaller percentage of cases cited where the control extended down to low voltage networks.

Review of actual operating procedures

Section 4 of the questionnaire addressed the operational procedures currently implemented, identifying the barriers to a widespread diffusion of distributed intelligence in the networks.

Rules for parallel to the network

There is no general agreement as to the rules for operation in parallel with the network for MV and LV generators. The rules are mandated by National legislation, are published in the Grid Codes, or prescribed by the local utility. As a general rule the DG should not degrade the

Table 2: Communication technologies used by surveyed utilities

Method	Wireless	Hard wired
• Voice only (telephone to local operator)	• Microwave	• Copper pilot table
• Remote control	• Radio, UHF radio, radio links	• Optical fibre
• Connection to SCADA systems	• Satellite	• Power line carrier (PLC)
		• GSM
		• GPRS

WG C6.11
REPORT

power quality of the network. In case of a fault or loss of the main grid islanding is generally prohibited and in most cases automatic disconnection is performed, either based on local signals or remotely from the substation.

Fault clearing

Fault clearing procedures are the same as for feeders without DG in 60% of the interviewed DSOs. Dedicated settings for feeders with DG are used by 40% of the respondents but no coordination is granted in the case of embedded MV and LV generation.

Remote control

Only 41% of the interviewed DSOs have the possibility of remotely controlling the DG at the MV and LV level. Few DSOs have the responsibility (or capability) to dispatch or regulate the output power produced by the DG. Most DSOs are obliged to accommodate all DG power injections and as mentioned in the section 2.4.1

the interface protections disconnect the DG in case of voltage transients or faults.

Voltage control

The only experience cited in the responses related to coordination of voltage regulation for MV feeders with DG is done with the adjustable setting of the tap changer of MV/LV transformers. The situation is even less common at the LV in which no contribution of DG to voltage control was mentioned.

Intentional islanding

Presently there is very limited application of intentional islanding; 22% of DSOs interviewed perform intentional islanding of DG under certain conditions. In most cases this represents islanding of the DG owner's load (generally an industrial load) only and consequently the island does not include any utility infrastructure. However, 14% of the DSOs interviewed may per- ● ● ●

WG C6.11
REPORT

form intentional islanding that includes the utility system, in emergency cases.

Future operating practices

Present operating procedures reveal that ADN applications are applied in only a limited number of cases. The interviewed DSOs indicated development of the following areas, in order of priority (from highest to lowest) as critical for the success of ADNs: protection approaches, safety, fault management, communications, intentional islanding and ancillary services. This suggests that further development of these different areas is a necessary precursor to widespread implementation.

These responses indicate the utility's position vis-à-vis this technology and the steps required for its adoption. There seems to be a perception that safe operation of a number of DER in a distribution network still requires further consideration. Also, it seems that communications are required before some of the ADN applications (ancillary services, intentional islanding) can be taken advantage of. This supports the view from the previous section that presently there are only a few cases of remote control of DER, something that most probably needs to change in order for ADN to become adopted more universally.

Regulatory barriers to ADN

Although the survey did not specifically focus on regulatory and contractual issues, the responses from DSOs interviewed indicated that these aspects will likely be the determining factor as to whether ADNs are adopted or not. Even more so than in the connection of single DERs, these can pose significant barriers to ADNs, in that a fundamental prerequisite for ADNs is that DER be integrated and not simply interconnected.

To implement the ADN concept a DSO must be allowed to control and regulate the output of at least the major DG units. A DER that relinquishes some level of control to the DSO will require different contracting and remuneration than those that simply inject real power into the network. Implicit is the varying degrees of responsibility associated with each. Intentional islanding requires an additional level of complexity as, during islanding, participating generators become the sole mechanism for ensuring the reliability and quality of the energy supplied. As such, this will warrant supplemental regulatory and contractual considerations.

Market models, regulations and responsibilities of different actors (TSO, DSO, generators, etc) will likely vary

according to the operational procedures of the ADN. Successful treatment of these issues will require an integrated approach including utilities, DG owners and the regulator. Ultimately the system should be optimized in terms of overall energy usage, which would include the use of electricity, heating, and cooling. As examples of this level of integration do exist at present, these should be used as starting points for the discussion.

Future developments

Relevant research consortiums

Although not highlighted in the surveys, there are a number of international research initiatives that are conducting R&D and implementing pilots in ADNs or related fields. Many have only recently been initiated but others already have significant results.

In an effort to identify gaps and improve coordination, in 2006 the Electric Power Research Institute (EPRI) conducted a mapping exercise of existing programs, [2]. The organizations profiled included: Intelligrid, CEC-PIER, CERTS, Smart Grid Platform, GridWise, NYSERDA, PSERC, Galvin Electricity Initiative, NETL. While there were a number of overlaps in terms of visioning, functional requirements and demonstration, the analysis revealed that a need existed in terms of addressing standards, user groups and integration of different products.

The analysis was recently updated but there were a number of relevant research programs not included in the original report. These include: European initiatives such as ADDRESS, ADINE, FENIX and Microgrids [5]; the Distribution Vision 2010 and the Smart Grid Demonstrations in the US; as well as other more modest national programs such as those from Australia, Austria, Japan and Canada. While this supplemental list is also not exhaustive, it suggests that there is a great deal of effort being invested in this area that could serve as sources of information for the C6.11 working group.

Standardization

Standardization is a fundamental cornerstone of any successful industry and the power industry is no exception. While it is debatable as to when it is appropriate to begin the process of standardization for emerging technologies, ADNs will benefit from some of the efforts already underway as a result of DG integration.

WG C6.11
REPORT

Communication and information exchange, as with the Smart Grid, is perhaps the most important enabling technology. To this end, the work of the IEC TC 57 is paramount in facilitating the implementation of information and communication technology (ICT). Objectives of this technical committee can be summarized as:

✓ Extension of IEC 61850 to DER and feeder equipment
✓ WG 17 – object models for DER
✓ Common information models (CIM) for distribution automation
✓ Promoting interoperability (near-term) and plug-and-play (long-term)

In North America the IEEE 1547 has been widely adopted as the interconnection standard for distributed generation. Of perhaps greater relevance to the development of active distribution networks is the series of application guides that accompany the standard. The relevant IEEE 1547 series of guides published and under development (denoted by 'P') include:

✓ IEEE 1547.2 – Application guide on the use of IEEE 1547
✓ IEEE 1547.3 – Information exchange and communication protocols for distributed generation
✓ IEEE P1547.4 – Design and operation of DER Islands
✓ IEEE P1547.6 – DG in secondary or spot networks

Future working group activities

ADNs entail two technologies: DERs and advanced distribution automation, including ICT. To better understand ways to coordinate the implementation of these technologies with ADN applications, future efforts of the working group will focus on documentation and analysis of identified pilot projects.

The WG will follow two strategies for identifying and gathering information on promising projects. The first will be to follow-up with questionnaire respondents who cited applications of ADN and request more specific information on the pilot installations. The second will be acquisition of information through the WG's involvement in two different workshops—one that was held in conjunction with the IRED conference, [3], and the second to be held in the spring of 2009 at CIRED. This should yield a good library of case studies from which general conclusions can be extracted.

The final WG technical brochure will document the analysis of the case studies and develop a map of the different applications of ADN, the necessary enabling technologies, and barriers encountered in their implementation. It is hoped that this will serve as useful reference information for future planners and help fuel the implementation of this technology.

Conclusions

This paper has presented survey results and working group analyses relating to active distribution networks. A globally accepted definition for this concept was reached and main features were outlined. Communications equipment emerged as a key enabler for the transition towards ADNs; however, there is no consensus regarding the most appropriate technologies and techniques for their integration into existing networks. A number of interrelated technical, regulatory and contractual issues must be resolved before significant deployment of active distribution networks can become a reality. With only modest implementation of this new concept to date, future working group activities will focus on classifying the range of applications, identifying enabling technologies and charting future development, based on experience from practical case studies taken from industry.

References

[1] C6 Study Committee website: http://www.cigre-c6.org/

[2] *Profiling and Mapping of Intelligent Grid R&D Programs*. EPRI, Palo Alto, CA and EDF R&D, Clamart, France: 2006. 1014600.

[3] EPRI Active Distribution Network Workshop, list of presentations. Available: http://sites.google.com/site/smartgridresourcecenter/Home/public-documents/epri-active-distribution-network-workshop—nice-france—dec-2008

[4] Microgrids and More Microgrids projects: overview, consortium and reports. Available : http://www.microgrids.eu ■

Appendix B

Field trial network electrical parameters

B.1   Parameters used in TVF study

Unless otherwise stated, all values are given in per unit form on 100MVA base.

Table B.1: Infeeds

Infeed point	Summer	Winter
T1	0.47797 j0.07695	1.21042 + j0.35052
T2	0.47624 j0.07675	1.206 + j0.34903
T3	-0.12812 + j0.12106	0.73085 + j0.49021
T4	-0.12812 + j0.12106	0.73085 + j0.49021

Table B.2: Nodal voltages

Node	Voltage (kV)
B1	132
B2	132
B3	132
B4	132
B5	132
B6	132
B7	132

Table B.3: Component data

Name	Voltage (kV)	R	X	Rating
T1	400/132	0.0014	0.0829	2.4
T2	400/132	0.0014	0.0832	2.4
T3	400/132	0.0015	0.0813	2.4
T4	400/132	0.0015	0.0813	2.4
C1	132	0.042176	0.094215	0.89
C2	132	0.01827	0.0407	0.89
C3	132	0.004862	0.013975	0.89
C4	132	0.007	0.0165	0.89
C5	132	0.014772	0.032786	0.89
C6	132	0.01314	0.0326	0.89
C7	132	0.0262	0.0658	0.89
C8	132	0.027341	0.060908	0.89
C9	132	0.024559	0.054979	0.89

Table B.4: Loads

Infeed point	Summer	Winter
L1	0.52191 + j0.16237	1.69525 + j0.54876
L2	0.09694 + j0.02983	0.34507 + j0.15064
L3	0.04624 + j0.00192	0.14267 + j0.02349
L4	0.06751 + j0.00170	0.22313 + j0.10697
L5	0.06239 + j0.02601	0.21023 + j0.09029
L6	0.11822 + j0.03568	0.41951 + j0.20115
L7	0.60351 + j0.17862	2.03067 + j0.59877

Appendix C

UKGDS electrical parameters

C.1   Parameters used in UKGDS studies

Unless otherwise stated, all values are given in per unit form on $100\,\mathrm{MVA}$ base.

Table C.1: Nodal voltages

Node	Voltage (kV)
99	275
101	132
102	132
103	132
104	132
105	132
106	132
107	132
108	132
109	132
110	132
111	132
112	132
113	132
114	132
115	132
116	132
117	132
301	33
303	33
305	33
306	33
307	33
308	33
309	33
311	33
312	33
313	33

Node	Voltage (kV)
314	33
315	33
316	33
317	33
318	33
319	33
320	33
321	33
322	33
324	33
325	33
326	33
327	33
328	33
329	33
330	33
331	33
332	33
333	33
334	33
335	33
336	33
337	33
338	33
339	33
340	33
341	33
342	33
343	33
344	33

Continued on next page

Node	Voltage (kV)
345	33
346	33
347	33
348	33
350	33
351	33
352	33
353	33
354	33
355	33
356	33
357	33
358	33
359	33
360	33
361	33
362	33
363	33
1101	11
1102	11
1103	11
1104	11
1105	11
1106	11
1107	11
1108	11
1109	11
6601	6.6
6602	6.6
6603	6.6

Continued on next page

Node	Voltage (kV)
6604	6.6
6605	6.6
6606	6.6
6607	6.6
6608	6.6
6609	6.6
6610	6.6
6611	6.6
6612	6.6
6613	6.6
6614	6.6
6615	6.6
6616	6.6
6617	6.6

Table C.2: Component data

From node	To node	Voltage (kV)	R	X	Rating
101	102	132	0.004564	0.022781	1.900
101	103	132	0.004067	0.020296	1.900
101	106	132	0.017095	0.037430	1.000
101	107	132	0.014924	0.032644	1.000
101	108	132	0.000364	0.000818	1.300
101	109	132	0.000432	0.000969	1.300
101	110	132	0.006169	0.013279	1.000
101	111	132	0.006503	0.013986	1.000
101	116	132	0.012188	0.027453	1.000
102	104	132	0.000876	0.001226	1.000
103	105	132	0.000768	0.001081	1.000

From node	To node	Voltage (kV)	R	X	Rating
103	117	132	0.002139	0.004865	0.700
106	112	132	0.000335	0.000754	1.000
106	114	132	0.006463	0.022041	1.900
107	113	132	0.000330	0.000741	1.000
107	115	132	0.006869	0.023424	1.900
307	341	33	0.017766	0.021981	0.300
313	308	33	0.057083	0.054039	0.200
313	309	33	0.079069	0.107759	0.200
313	362	33	0.001023	0.001279	0.200
313	363	33	0.000641	0.001182	0.200
314	315	33	0.018691	0.017724	0.300
315	345	33	0.070712	0.062393	0.200
316	314	33	0.034026	0.034219	0.300
316	315	33	0.069053	0.048957	0.200
316	317	33	0.005534	0.005148	0.200
316	318	33	0.005619	0.004905	0.200
316	353	33	0.032158	0.029616	0.200
316	354	33	0.039416	0.020025	0.200
327	326	33	0.083931	0.086985	0.300
332	325	33	0.019861	0.018063	0.200
334	327	33	0.042027	0.081161	0.300
334	332	33	0.022549	0.019765	0.300
336	332	33	0.033351	0.037060	0.300
337	333	33	0.033351	0.037060	0.300
337	336	33	—	0.000100	0.200
338	305	33	0.045306	0.077399	0.200
338	306	33	0.057065	0.089944	0.200
338	330	33	0.102503	0.127480	0.300
338	331	33	0.111052	0.139716	0.300
338	334	33	0.062959	0.103335	0.300

From node	To node	Voltage (kV)	R	X	Rating
338	331	33	0.111052	0.139716	0.300
338	334	33	0.062959	0.103335	0.300
338	339	33	0.000826	0.001105	0.200
338	340	33	0.000472	0.000651	0.200
338	341	33	0.043377	0.071572	0.200
338	346	33	0.018128	0.016164	0.200
338	347	33	0.016821	0.014892	0.200
338	360	33	0.040269	0.037007	0.200
338	361	33	0.035162	0.032313	0.200
342	319	33	0.016932	0.016005	0.300
342	320	33	0.012286	0.012501	0.300
342	335	33	0.043167	0.034897	0.300
342	336	33	0.039394	0.047223	0.300
342	337	33	0.065757	0.081714	0.300
342	343	33	0.009937	0.009219	0.200
342	344	33	0.007715	0.007088	0.200
342	350	33	0.014976	0.010769	0.200
342	351	33	0.013056	0.009365	0.200
348	324	33	0.107692	0.107409	0.300
348	327	33	0.273013	0.371732	0.200
348	328	33	—	0.000100	0.200
348	329	33	—	0.000100	0.200
353	352	33	0.028663	0.024380	0.200
353	357	33	0.014894	0.012959	0.200
357	301	33	0.033273	0.031276	0.200
357	303	33	0.035057	0.031145	0.200
357	311	33	0.01781	0.015729	0.200
357	312	33	0.019458	0.017318	0.200
357	321	33	0.008119	0.009733	0.300
357	322	33	0.009055	0.010849	0.300

From node	To node	Voltage (kV)	R	X	Rating
357	355	33	0.024342	0.023032	0.200
357	356	33	0.036877	0.038044	0.200
357	358	33	0.001456	0.001393	0.200
357	359	33	0.001475	0.001411	0.200
99	101	275/132	—	0.100000	5.000
99	101	275/132	—	0.100000	5.000
104	316	132/33	0.005563	0.171987	0.900
105	316	132/33	0.005380	0.170619	0.900
108	338	132/33	0.009160	0.194580	0.600
109	338	132/33	0.008975	0.194858	0.600
109	338	132/33	0.009160	0.198374	0.600
110	342	132/33	0.010704	0.223500	0.600
111	342	132/33	0.010704	0.224570	0.600
112	348	132/33	0.013165	0.302382	0.450
113	348	132/33	0.013165	0.294631	0.450
114	313	132/33	0.006896	0.235117	1.000
115	313	132/33	0.006140	0.237100	0.900
116	357	132/33	0.010789	0.228085	0.600
117	357	132/33	0.010789	0.225280	0.600
301	6601	33/6.6	0.037376	0.971779	0.140
303	6601	33/6.6	0.037376	0.971779	0.140
305	6602	33/6.6	0.043849	1.096230	0.230
306	6602	33/6.6	0.043849	1.096230	0.230
307	6602	33/6.6	0.043849	1.096230	0.230
308	6603	33/6.6	0.037154	0.928840	0.230
309	6603	33/6.6	0.037154	0.928840	0.230
311	6604	33/6.6	0.041118	1.027950	0.230
312	6604	33/6.6	0.041118	1.027950	0.230
314	6605	33/6.6	0.039312	1.022120	0.140
314	6605	33/6.6	0.039312	1.022120	0.140

From node	To node	Voltage (kV)	R	X	Rating
315	6606	33/6.6	0.040651	1.016270	0.230
315	6606	33/6.6	0.040651	1.016270	0.230
316	6615	33/6.6	0.038145	0.991776	0.230
316	6615	33/6.6	0.038145	0.991776	0.230
317	6607	33/6.6	0.043217	1.080420	0.230
318	6607	33/6.6	0.043217	1.080420	0.230
319	6608	33/6.6	0.037279	0.931982	0.230
320	6608	33/6.6	0.037279	0.931982	0.230
321	6609	33/6.6	0.042804	1.070110	0.230
322	6609	33/6.6	0.042804	1.070110	0.230
324	1101	33/11	0.042555	1.063870	0.230
325	1102	33/11	0.040077	1.042000	0.125
326	1102	33/11	0.040077	1.042000	0.125
328	1103	33/11	0.042227	1.055670	0.210
329	1103	33/11	0.042227	1.055670	0.210
330	1104	33/11	0.038733	0.968323	0.230
331	1104	33/11	0.038733	0.968323	0.230
332	1105	33/11	0.040500	1.012500	0.230
333	1105	33/11	0.040500	1.012500	0.230
336	1106	33/11	0.037728	0.980926	0.140
337	1106	33/11	0.037728	0.980926	0.125
339	6610	33/6.6	0.043526	1.088150	0.230
340	6610	33/6.6	0.043526	1.088150	0.230
341	6611	33/6.6	0.038321	0.996347	0.140
341	6611	33/6.6	0.038321	0.996347	0.140
343	6612	33/6.6	0.038563	0.964073	0.230
344	6612	33/6.6	0.038563	0.964073	0.230
346	1107	33/11	0.039257	0.981416	0.230
347	1107	33/11	0.039257	0.981416	0.230
350	1108	33/11	0.041460	1.077970	0.125

From node	To node	Voltage (kV)	R	X	Rating
351	1108	33/11	0.041460	1.077970	0.125
352	6613	33/11	0.037538	0.975993	0.140
354	6613	33/6.6	0.037538	0.975993	0.140
355	6614	33/6.6	0.036398	0.946356	0.140
356	6614	33/6.6	0.036398	0.946356	0.140
358	6616	33/6.6	0.040595	1.014880	0.230
359	6616	33/6.6	0.040595	1.014880	0.230
360	6617	33/6.6	0.041927	1.048170	0.230
361	6617	33/6.6	0.041927	1.048170	0.230
362	1109	33/11	0.041597	1.039940	0.230
363	1109	33/11	0.041597	1.039940	0.230

Table C.3: Loads

Infeed point	Summer	Winter
1101	0.04666 + j0.02526	0.15554 + j0.10103
1102	0.04695 + j0.00995	0.15649 + j0.03981
1103	0.06027 + j0.00822	0.20090 + j0.03286
1104	0.02353 + j0.02325	0.07844 + j0.09301
1105	0.04507 + j0.00820	0.15024 + j0.03279
1106	0.03110 + j0.00518	0.10368 + j0.02072
1107	0.03800 + j0.00813	0.12666 + j0.03253
1108	0.01573 + j0.00239	0.52420 + j0.09560
1109	0.05344 + j0.02443	0.17814 + j0.09771
6601	0.04622 + j0.01245	0.15407 + j0.04981
6602	0.05221 + j0.01680	0.17403 + j0.06718
6603	0.05381 + j0.01194	0.17936 + j0.04774
6604	0.05313 + j0.01472	0.17711 + j0.05887
6605	0.04635 + j0.01081	0.15451 + j0.04324

Continued on next page

Infeed point	Summer	Winter
6606	0.06438 + j0.01347	0.21461 + j0.05386
6607	0.07055 + j0.01808	0.23516 + j0.07230
6608	0.04665 + j0.02160	0.15549 + j0.08640
6609	0.00753 + j0.00134	0.25110 + j0.05370
6610	0.05249 + j0.01797	0.17498 + j0.07188
6611	0.02288 + j0.00723	0.76280 + j0.02892
6612	0.06907 + j0.02138	0.23023 + j0.08552
6613	0.04523 + j0.01206	0.15075 + j0.04823
6614	0.04756 + j0.01435	0.15852 + j0.05741
6615	0.02006 + j0.01081	0.66860 + j0.04322
6616	0.04569 + j0.01583	0.15230 + j0.06330
6617	0.04927 + j0.00085	0.16423 + j0.03380

Appendix D

DG output control

D.1 Control equation derivations using ETR 124

Figure D.1 represents the constrained connection of a single DG scheme to the distribution network. The constrained connection exists between node i and node k and means that the power flow in this component will require the power output constraint of the DG scheme attached to node i.
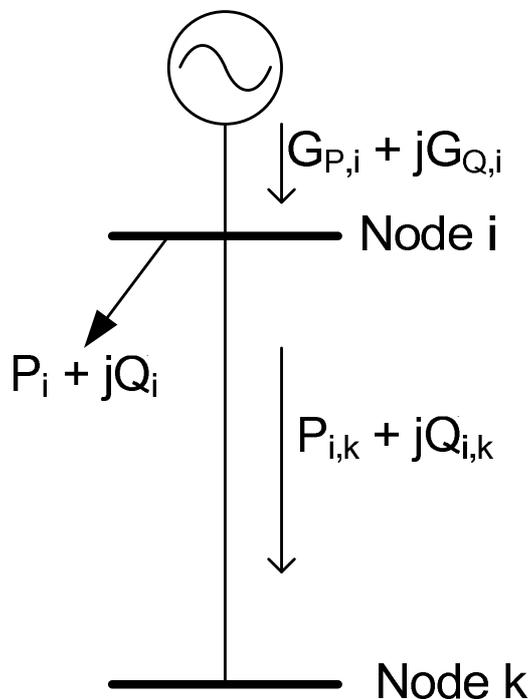

Figure D.1: Single DG output control with local constraint

Using an algebraic summation of the power flows at node i [50] the net flow from node i to node k is given in (D.1.1)-(D.1.3)

$$P_{i,k} = G_{P,i} - P_i \tag{D.1.1}$$

$$Q_{i,k} = G_{Q,i} - Q_i \tag{D.1.2}$$

$$S_{i,k} = |P_{i,k} + jQ_{i,k}| = |(G_{P,i} - P_i) + j(G_{Q,i} - Q_i)| \tag{D.1.3}$$

where $P_{i,k}$, $Q_{i,k}$ and $S_{i,k}$ represent the real, reactive and apparent power flows from node i to node k, $G_{P,i}$ and $G_{Q,i}$ represent the real and reactive power outputs of the DG scheme and P_i and Q_i represent the real and reactive load demands at node i. Therefore the real power output of the DG scheme in terms of the other parameters is given in (D.1.4)

$$G_{P,i} = \sqrt{S_{i,k}^2 - (G_{Q,i} - Q_i)^2} + P_i \tag{D.1.4}$$

When the power flow is at the thermal limit, $S_{i,k(lim)}^c$, of the component (between node i and node k) the maximum real power output of the DG scheme, $G_{P,i-max}$ is given in (D.1.5)

$$G_{P,i-max} = \sqrt{(S_{i,k(lim)}^c)^2 - (G_{Q,i} - Q_i)^2} + P_i \tag{D.1.5}$$

If there is a target utilisation of the component, U_{Tar} the modification to (D.1.5) may be made as in (D.1.6).

$$G_{P,i-max} = \sqrt{(U_{Tar} \times S_{i,k(lim)}^c)^2 - (G_{Q,i} - Q_i)^2} + P_i \tag{D.1.6}$$

D.2   Control equation derivations using PFSFs

If the power flow constraint exists deeper into the distribution network, as given in Figure D.2, the relationship between the change of real power output of the DG scheme at node m, $\Delta G_{P,m}$ and the change in real power flow in the thermally vulnerable component between node i and node k, $\Delta P_{i,k}$ is given by the real power flow sensitivity factor, $\frac{dP_{i,k}}{dG_{P,m}}$ as in (D.2.7).

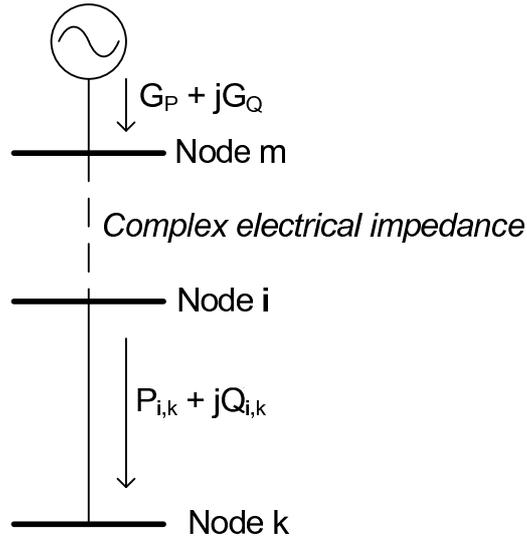$$\Delta P_{i,k} = \frac{dP_{i,k}}{dG_{P,m}} \times \Delta G_{P,m} \tag{D.2.7}$$

Figure D.2: Single DG output control with non-local constraint

In this case the value of $\Delta P_{i,k}$, calculated based on the required power flow management and the thermal limit of the thermally vulnerable component is given in (D.2.8)

$$
\begin{aligned}
\Delta P_{i,k} &= \sqrt{(U_{Tar} \times S^c_{i,k(lim)})^2 - (''Q_{i,k})^2} - \sqrt{(S_{i,k})^2 - ('Q_{i,k})^2} \\
&\equiv \sqrt{(U_{Tar} \times S^c_{i,k(lim)})^2 - (''Q_{i,k})^2} - {}'P_{i,k}
\end{aligned}
\tag{D.2.8}
$$

where $'P_{i,k}$ and $'Q_{i,k}$ represent the real and reactive power flows in the component before power flow management takes place and $''Q_{i,k}$ represents the reactive power flow in the component after power flow management has taken place.

D.3 Egalitarian broadcast signal derivation

This section derives the equation used to provide an egalitarian broadcast signal to multiple DG schemes. The aim was to provide a single signal that would manage distribution network power flows by adjust the power outputs of multiple DG schemes by the same percentage of their present power output.

The total real power adjustment required to manage network power flows in the thermally vulnerable component is given in (D.2.8). Each DG scheme may be apportioned an amount of the total real power adjustment as given in (D.3.9)

$$\Delta P_{i,k-Total} = \Delta P_{i,k-G_{P,1}} + \Delta P_{i,k-G_{P,2}} + ... + \Delta P_{i,k-G_{P,m_T}} \tag{D.3.9}$$

where $\Delta P_{i,k-Total}$ is the total real power adjustment in the thermally vulnerable component to manage network power flows and $\Delta P_{i,k-G_{P,1 \ to \ m_T}}$ represents the real power adjustment apportioned to the DG schemes at nodes 1, 2... m_T respectively. The total real power adjustment to manage network power flows may be written in terms of DG scheme present power outputs and power flow sensitivity factors by substituting (D.2.7) into (D.3.9) as in (D.3.10).

$$\Delta P_{i,k-Total} = \Delta G_{P,1}\frac{dP_{i,k}}{dG_{P,1}} + \Delta G_{P,2}\frac{dP_{i,k}}{dG_{P,2}} + ... + \Delta G_{P,m_T}\frac{dP_{i,k}}{dG_{P,m_T}} \tag{D.3.10}$$

The change in power output of each DG scheme, $\Delta G_{P,m}$, may be written in terms of the percentage reduction, Φ, of the present power output, $G_{P,m}$, as in (D.3.11).

$$\Delta P_{i,k-Total} = \Phi G_{P,1}\frac{dP_{i,k}}{dG_{P,1}} + \Phi G_{P,2}\frac{dP_{i,k}}{dG_{P,2}} + ... + \Phi G_{P,m_T}\frac{dP_{i,k}}{dG_{P,m_T}} \tag{D.3.11}$$

Equation (D.3.11) may be written, generically, as in (D.3.12), which, making Φ the subject of the equation, gives the egalitarian broadcast signal as in (D.3.13).

$$\Delta P_{i,k} = \Phi \sum_{m=1}^{m=m_T} G_{P,m}\frac{dP_{i,k}}{dG_{P,m}} \tag{D.3.12}$$

$$\Phi = \frac{\Delta P_{i,k}}{\sum_{m=1}^{m=m_T}\left(G_{P,m} \times \left(\frac{dP_{i,k}}{dG_{P,m}}\right)\right)} \tag{D.3.13}$$

Appendix E

Field trial network evaluation parameter results

E.1   Real-time changes in DG outputs

Illustrative graphs of real-time changes in DG outputs for multiple DG control strategies simulated with component static thermal ratings in the field trial network case study are presented in Figures E.1–E.4.

E.2   Results analysis: Component seasonal thermal ratings

The marginal annual energy yields for each wind farm development resulting from the each candidate control strategy simulation with component seasonal thermal rating systems are given in Figure E.5, based on datum values in Table 12.1. As a general observation the marginal annual energy yield of each DG scheme is increased for each control strategy deployment with component seasonal thermal ratings as opposed to component static thermal ratings. This is because the increased component thermal ratings that result from a seasonal thermal rating system lead to greater power transfer capacities within components of the power system during the spring, autumn and winter months. Therefore power flow management is required less frequently and/or the thermal violation of components is less severe.
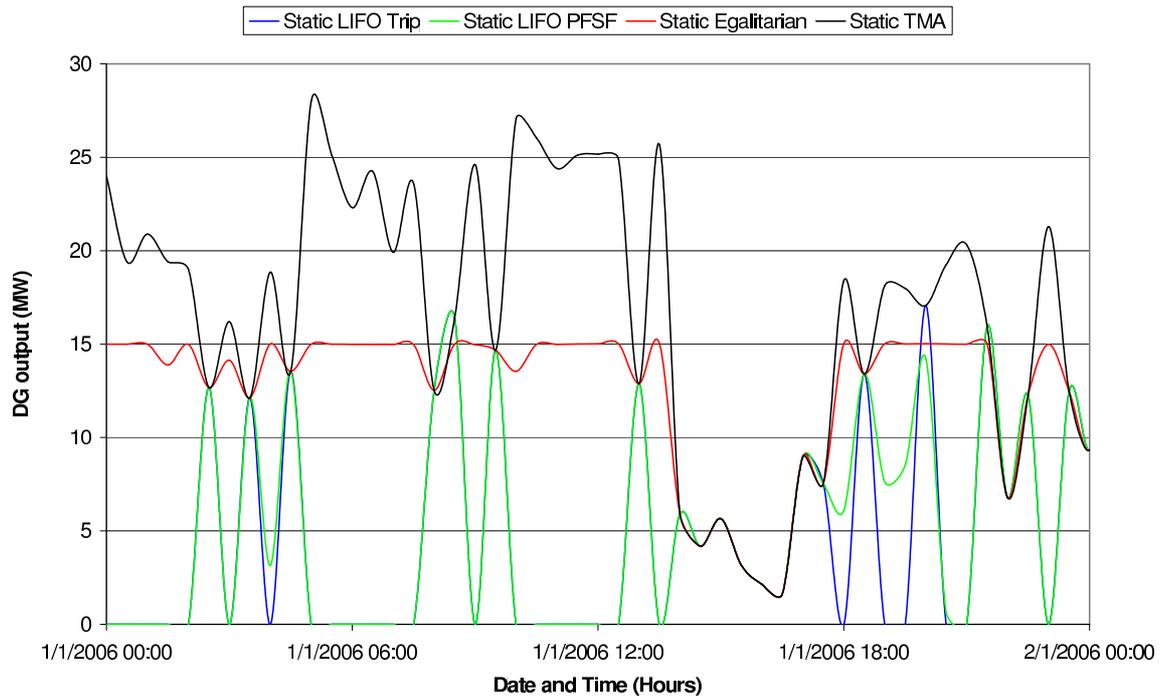
Figure E.1: Illustration of real-time changes in DG2 output for candidate control strategy simulations
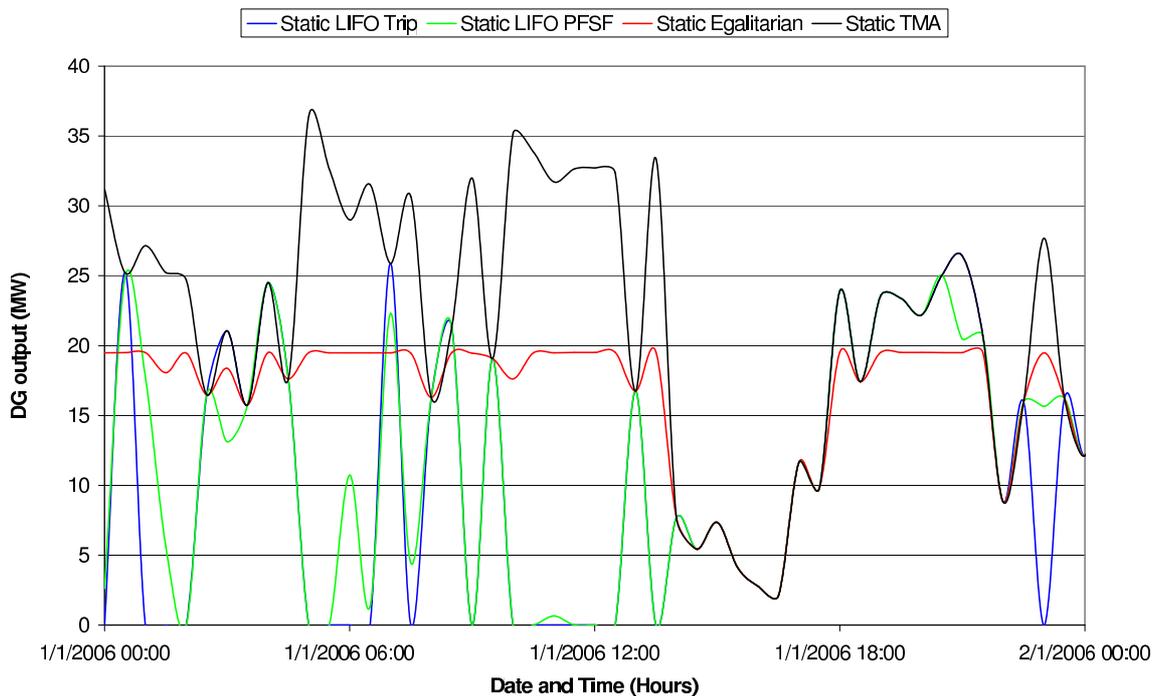

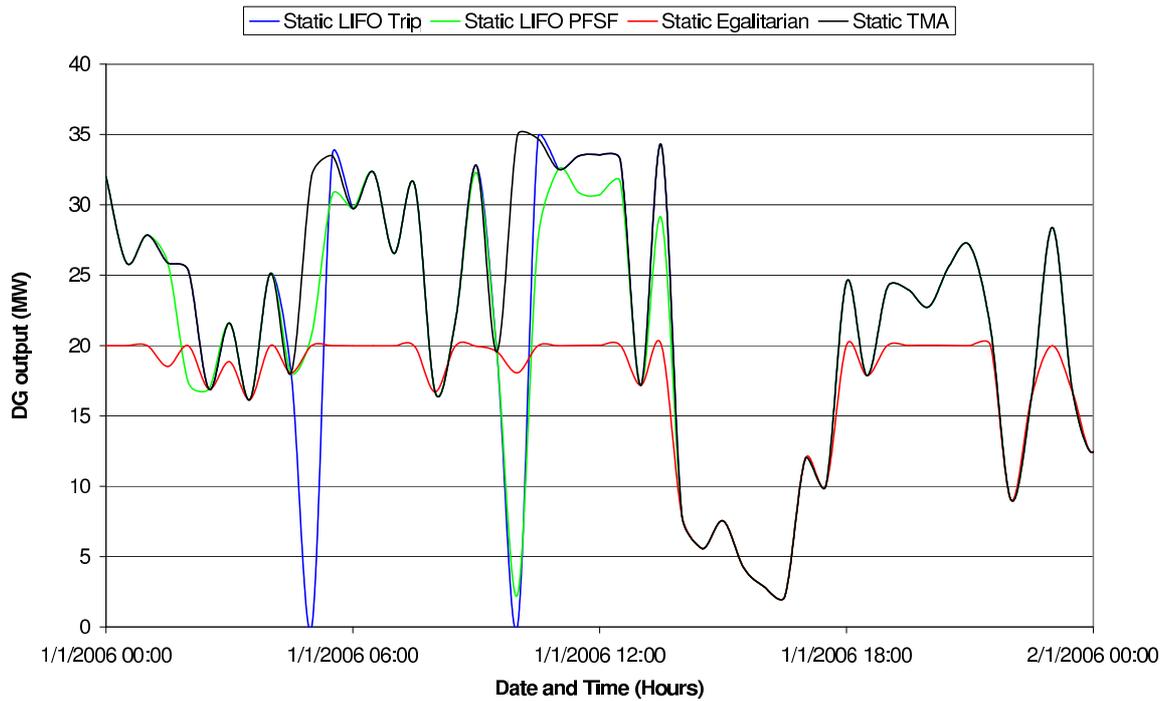Figure E.2: Illustration of real-time changes in DG3 output for candidate control strategy simulations

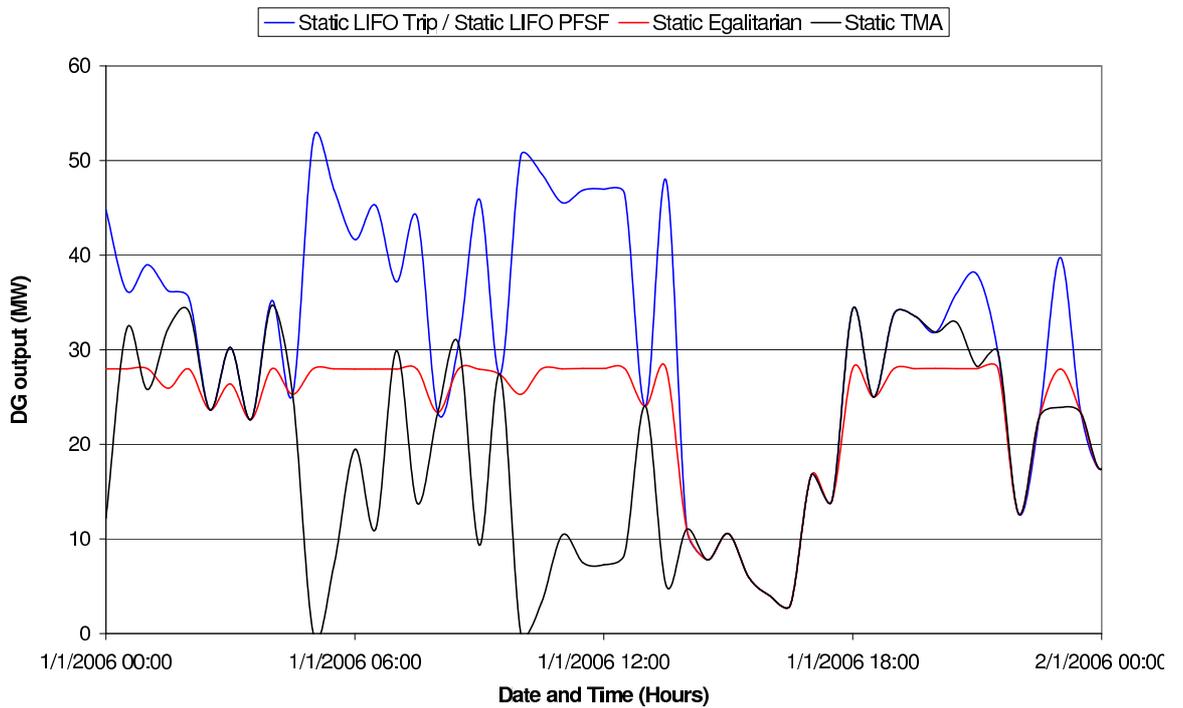Figure E.3: Illustration of real-time changes in DG4 output for candidate control strategy simulations

Figure E.4: Illustration of real-time changes in DG5 output for candidate control strategy simulations
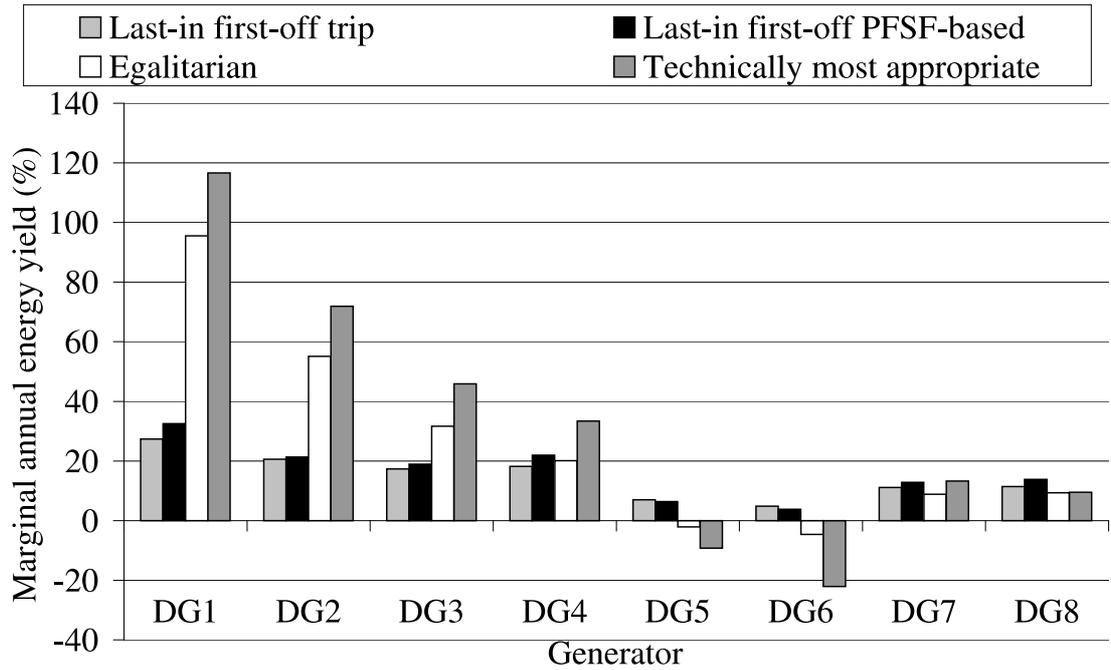
Figure E.5: Individual DG marginal annual energy yields resulting from candidate control strategy deployments with component seasonal thermal ratings

Consequently, the requirement to constrain DG schemes occurs less frequently, the magnitude of the constraint is smaller and the net result is improved DG annual energy yields. However, from an operational perspective there are difficulties associated with the maintenance of an accurate database of component seasonal ratings. Moreover, the seasonal rating approach bears the latent risk of an anomalous 'hot day' where the prevailing meteorological conditions could result in components being rated higher than they should be.

As expected, the losses are increased (relative to the static thermal rating simulations) in those individual components that, as a result of increased ratings, facilitate increased power transfers. Component marginal losses are increased by the greatest amount when the TMA strategy is adopted. C6, C8, and C9 represent a subset of components (C3–C9) in which the greatest losses occur. Marginally, increases in losses of 35.7%, 34.2%, and 39.2% occur in components C6, C8 and C9 respectively. This represents losses of 4.5 GWh/annum, 6.4 GWh/annum and 6.5 GWh/annum in the respective components in absolute terms.

A summary of losses apportioned to individual DG schemes due to the implementation of the candidate control strategies with component seasonal rating systems is given in Figure E.6. Due to greater individual component energy losses the DG apportioned losses are increased relative to the values presented in Figure 12.10. Considering the LIFO DG tripping control approach, DG4–DG6 are apportioned the greatest amount of losses:
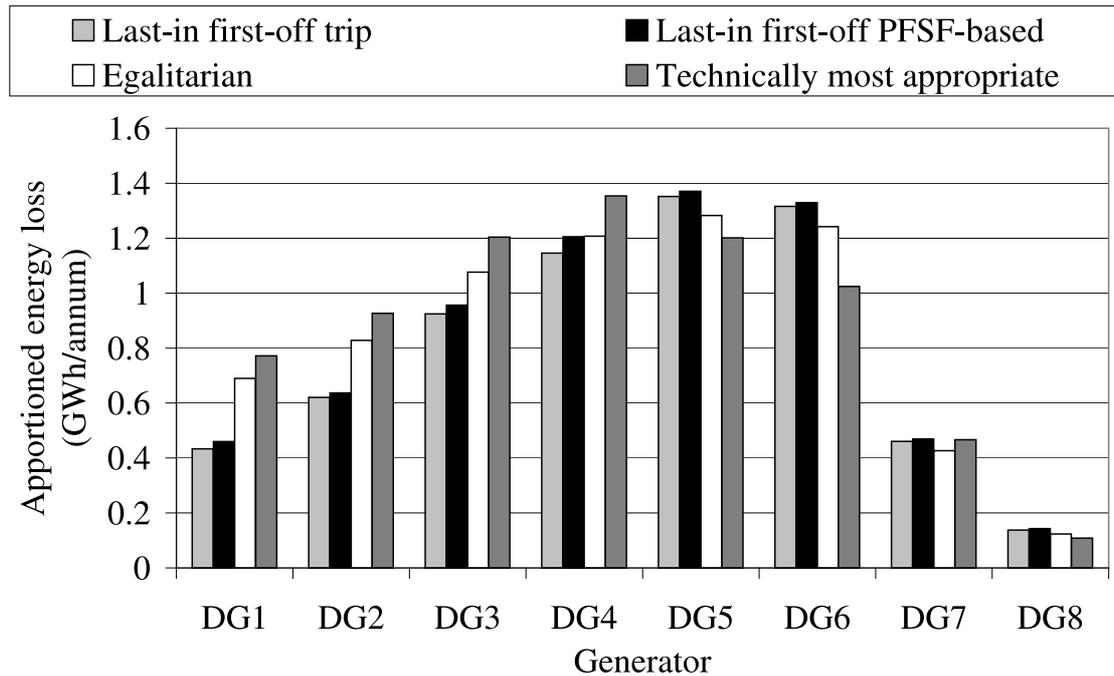
Figure E.6: DG apportioned annual energy losses resulting from candidate control strategy deployments with component seasonal thermal ratings

1.14 GWh/annum, 1.35 GWh/annum, and 1.31 GWh/annum respectively. The same observation may be made for the LIFO PFSF-based approach and the egalitarian control approach. However, considering the technically most approach control strategy, DG3–DG5 are apportioned the greatest amount of losses: 1.20 GWh/annum, 1.35 GWh/annum, and 1.20 GWh/annum respectively. This reflects a shift in the magnitude of DG annual energy yields brought about by adopting a coordinated control approach.

The NPVs and PIs for each wind farm development are summarised in Table E.1. Relative to the values in Table 12.4, it can be seen that greater NPVs and hence PIs occur for all the DG schemes with LIFO tripping, LIFO PFSF-based and egalitarian control strategies. Moreover, for DG1–DG3 the same NPVs (£49.2M, £58.6M, and £76.2M respectively) and PIs (2.4, 2.3, and 2.4 respectively) result from the TMA control strategy deployed with both static and seasonal thermal ratings. This indicates that with the TMA control strategy the above mentioned DG schemes are operating with unconstrained outputs. This is because the PFSFs of the DG schemes DG1–DG3, as given in (12.2), are lower than the DG schemes DG4–DG8 and therefore it is the latter DG schemes that are constrained, in a coordinated manner, to manage network power flows.

Table E.1: Wind farm financial evaluation (seasonal thermal ratings)

Parameter	Control strategy	DG1	DG2	DG3	DG4	DG5	DG6	DG7	DG8
NPV	LIFO Trip	6.4	14.1	27.5	43.6	41.5	51.2	68.7	91.3
(£M)	LIFO PFSF-based	26.9	38.4	59.7	78.4	85.6	86.2	161.7	217.0
	Egalitarian	43.6	51.9	67.5	77.0	77.2	77.9	160.9	206.4
	TMA	49.2	58.6	76.2	87.1	70.2	60.8	154.6	206.8
PI	LIFO Trip	0.3	0.6	0.9	1.3	0.9	1.4	0.8	0.8
	LIFO PFSF-based	1.3	1.5	1.9	2.4	1.9	2.3	1.8	1.8
	Egalitarian	2.2	2.1	2.1	2.3	1.7	2.1	1.8	1.7
	TMA	2.4	2.3	2.4	2.6	1.5	1.6	1.7	1.7